

Durham E-Theses

Two-loop helicity amplitudes in QCD

Garland, Lee W.

How to cite:

Garland, Lee W. (2003) *Two-loop helicity amplitudes in QCD*, Durham theses, Durham University.
Available at Durham E-Theses Online: <http://etheses.dur.ac.uk/4122/>

Use policy

The full-text may be used and/or reproduced, and given to third parties in any format or medium, without prior permission or charge, for personal research or study, educational, or not-for-profit purposes provided that:

- a full bibliographic reference is made to the original source
- a [link](#) is made to the metadata record in Durham E-Theses
- the full-text is not changed in any way

The full-text must not be sold in any format or medium without the formal permission of the copyright holders.

Please consult the [full Durham E-Theses policy](#) for further details.

Two-Loop Helicity Amplitudes in QCD

A thesis presented for the degree of

Doctor of Philosophy

by

Lee W. Garland

The copyright of this thesis rests with the author.

No quotation from it should be published without
his prior written consent and information derived
from it should be acknowledged.

Institute for Particle Physics Phenomenology

Physics Department

University of Durham

January 2003



18 JUN 2003



University
of Durham

Two-Loop Helicity Amplitudes in QCD

A thesis presented for the degree of

Doctor of Philosophy

by

Lee W. Garland

Abstract

We compute the $\mathcal{O}(\alpha_s^3)$ virtual QCD corrections for the process $e^+e^- \rightarrow q\bar{q}g$ arising from the interference of the two-loop and tree amplitudes and from the self-interference of the one-loop amplitude. The results are presented in the form of both matrix elements and helicity amplitudes.

The calculation of the matrix elements is performed by the direct evaluation of the Feynman diagrams and corresponding loop integrals. The helicity amplitudes are derived in a scheme-independent way from the coefficients appearing in the general expression for the tensorial structure of this process. The tensor coefficients are then extracted from the Feynman diagrams by means of projectors.

The one- and two-loop integrals appearing in the amplitudes are reduced to a small set of known master integrals by means of integration-by-parts identities. This reduction has been automated by construction of an algorithm based on that proposed by Laporta.

The infrared pole structure of both the matrix elements and helicity amplitudes is shown to agree with the predictions made by the infrared factorisation formula of Catani. The analytic results for the finite terms, regularised in conventional dimensional regularisation and renormalised in the $\overline{\text{MS}}$ scheme, are presented, expressed in terms of one- and two-dimensional harmonic polylogarithms.

Acknowledgements

Firstly, and perhaps most importantly, I would like to thank my supervisor, *Nigel Glover*, for his continuous support, guidance and seemingly endless patience throughout the past three years. The project which we have worked on has been a source of education, challenge and sometimes frustration, but nevertheless I thank him for finding such a rewarding problem.

During this work I have had the fortune of collaborating with *Thanos Koukout-sakis*. I thank him for many insightful discussions, his willingness to share ideas, and of course, the *hot chocolate*.

I am grateful to *Babis Anastasiou* and *Maria Elena Tejeda Yeomans* for their invaluable help as members of the ‘Two-Loop Group’.

A special mention must go to *Kate Adamson* for always being there to talk, to *Neil Pomeroy* for his endless supply of humour and cartoons and to *Jeppe Andersen* for all his help and discussions. Life in the office and in Durham would not have been the same without you.

I thank *James Gregory* for being a great housemate and providing all of those memorable moments at GradSoc.

To everybody else at the IPPP, in particular *Jon Levell*, *David Howe* and *Pete Williams* for all of your help and for making the group such a friendly place to work.

To *Mel*, a special thanks for being there over the past months, for helping me through the write-up and for making the end of life in Durham such a fantastic time.

Finally, to my *family*, I thank them for all the support and encouragement they have provided, not only during the PhD, but also throughout my time in Durham—I couldn’t have made it without you!

This work was supported by a PPARC studentship which is gratefully acknowledged.

Declaration

I declare that no material presented in this thesis has been previously submitted for a degree at this or any other University.

The research described in this thesis has been carried out between October 1999 and September 2002 under the supervision of Professor E. W. N. Glover^a and in collaboration with T. Gehrmann^b, A. Koukoutsakis^a and E. Remiddi^c.

This work is based on the following publications:

- L. W. G., T. Gehrmann, E. W. N. Glover, A. Koukoutsakis and E. Remiddi, “*The Two-Loop QCD Matrix Element for $e^+e^- \rightarrow 3$ Jets*,” Nucl. Phys. B **627** (2002) 107 [arXiv:hep-ph/0112081].
- L. W. G., T. Gehrmann, E. W. N. Glover, A. Koukoutsakis and E. Remiddi, “*Two-Loop QCD Helicity Amplitudes for $e^+e^- \rightarrow 3$ Jets*,” Nucl. Phys. B **642** (2002) 227 [arXiv:hep-ph/0206067].

^a *Department of Physics, University of Durham, Durham DH1 3LE, England*

^b *Theory Division, CERN, CH-1211 Geneva 23, Switzerland*

^c *Dipartimento di Fisica, Università di Bologna and INFN, Sezione di Bologna, I-40126 Bologna, Italy*

© The copyright of this thesis rests with the author. No quotation from it should be published without their prior written consent and information derived from it should be acknowledged.

Contents

Abstract	ii
Acknowledgements	iii
Declaration	iv
Preface	1
1 QCD Beginnings	2
1.1 From Hadrons to Quarks	2
1.2 The QCD Lagrangian	5
1.3 The Feynman Rules of QCD	10
1.4 Regularisation	12
1.5 Renormalisation	15
1.6 Renormalisation Group Equations	16
1.7 The Running Coupling	17
1.8 From NLO to NNLO	20
1.8.1 Scale Dependence	21
1.8.2 Jets and Event Shapes	23
1.8.3 Power Corrections	24
1.9 Summary	25

2	Matrix Elements	29
2.1	Introduction	29
2.2	Infrared Divergences	30
2.2.1	$e^+e^- \rightarrow q\bar{q} + X$ at Leading Order	32
2.2.2	$e^+e^- \rightarrow q\bar{q} + X$ at Next-to-Leading Order	35
2.2.3	Cancellation of IR Divergences	40
2.3	Matrix Elements in Colour Space	42
2.4	Singular Behaviour	45
2.4.1	Ultraviolet Renormalisation	47
2.4.2	$I^{(1)}(\epsilon)$ for $e^+e^- \rightarrow q\bar{q}$	48
3	Loop Integrals	51
3.1	Introduction	51
3.2	Basic Notation / Generalities	53
3.2.1	Auxiliary Diagrams	56
3.2.2	Symmetries	58
3.3	Parameterisation	60
3.3.1	Schwinger Parameterisation	60
3.3.2	Feynman Parameterisation	64
3.3.3	Direct Approaches to Integration	66
3.4	Tensor Reduction	66
3.4.1	Dimensional Shift	69
3.5	Integration-by-Parts	71
3.5.1	Construction of the IBP Identities	71
3.5.2	IBP Identities for the Planar Auxiliary Diagram	74
3.5.3	Example Application of IBP to a Reducible Integral	77
3.5.4	Example Application of IBP to an Irreducible Integral	80
3.6	The Laporta Algorithm	85

3.6.1	The Algorithm Explained	86
3.6.2	The Algorithm	87
3.7	Master Integrals	91
3.7.1	Calculating Master Integrals	91
3.7.2	Differential Equations for Master Integrals	92
3.7.3	The Master Integrals	96
4	The NNLO Matrix Element for $e^+e^- \rightarrow q\bar{q}g$	99
4.1	Notation	100
4.2	Ultraviolet Renormalisation	103
4.3	Infrared Factorisation	104
4.3.1	One-Loop Pole Structure	105
4.3.2	Two-Loop Pole Structure	106
4.3.3	$\mathbf{I}^{(1)}(\epsilon)$ for $e^+e^- \rightarrow q\bar{q}g$	108
4.3.4	$\mathbf{H}^{(2)}(\epsilon)$ for $e^+e^- \rightarrow q\bar{q}g$	110
4.3.5	$\langle \mathcal{M}^{(0)} \mathcal{M}^{(1)} \rangle$ for $e^+e^- \rightarrow q\bar{q}g$	111
4.4	Method	113
4.5	Diagrams	117
4.6	The Finite Contributions	124
4.6.1	One-Loop Contribution to $\mathcal{T}^{(6)}$	125
4.6.2	Two-Loop Contribution to $\mathcal{T}^{(6)}$	126
5	NNLO Helicity Amplitude for $e^+e^- \rightarrow q\bar{q}g$	127
5.1	Notation	130
5.2	The General Tensor	131
5.3	Projectors for Tensor Coefficients	133
5.4	Expansion of Tensor Coefficients	135
5.5	Relation to Matrix Elements	138
5.6	Ultraviolet Renormalisation	139

CONTENTS

5.7	IR Behavior of Tensor Coefficients	140
5.8	Helicity Amplitudes	142
5.9	The Finite Contributions	145
5.9.1	One-Loop Contribution to Ω	145
5.9.2	Two-Loop Contribution to Ω	146
5.9.3	Summary	147
6	Conclusions and Outlook	150
6.1	Summary	150
6.2	Outlook	152
A	One-Loop Contribution to $\mathcal{T}^{(6)}$	154
B	Two-Loop Contribution to $\mathcal{T}^{(6)}$	167
C	One-Loop Contribution to Ω	197
D	Two-Loop Contribution to Ω	199
E	One-Loop Master Integrals	209
F	Harmonic Polylogarithms	212
F.1	1dHPLs	212
F.2	2dHPLs	215
G	Weyl–van der Waerden Spinor Calculus	219
	Bibliography	230

List of Figures

1.1	The one-loop correction to the gluon self-energy.	12
1.2	Renormalisation scale dependence of the single jet ($p\bar{p} \rightarrow \text{jet}$) inclusive distribution with transverse jet energy $E_T = 100$ GeV at different orders in the perturbative series.	22
1.3	CDF data for the coupling constant α_s as a function of the transverse energy displaying the uncertainty represented by the renormalisation scale μ	22
1.4	Schematic representation of how higher order calculations allow more partons to be used in the construction jet cones, thus giving a more accurate perturbative jet description.	24
1.5	The average value of $\langle 1 - T \rangle$ showing the NLO prediction (red), the NLO prediction with a power correction of $\lambda = 1$ GeV (green) and an NNLO prediction with $A_3 = 3$ and $\lambda = 0.6$ GeV (blue).	26
2.1	Feynman diagram for $e^+e^- \rightarrow q\bar{q}$ at leading order.	33
2.2	Virtual emission contribution to $e^+e^- \rightarrow q\bar{q}$ at NLO.	35
2.3	Real gluon emission contribution to $e^+e^- \rightarrow q\bar{q}$ at NLO.	38
2.4	The configurations whereby the gluon is either soft or collinear are kinematically degenerate to the virtual gluon contribution and cannot be distinguished experimentally — the jet structure is identical. . . .	42
3.1	The generic loop integrals.	54

LIST OF FIGURES

3.2	Example Feynman diagrams contributing to $e^+e^- \rightarrow q\bar{q}g$	54
3.3	The two-loop planar auxiliary diagram	57
3.4	The two-loop non-planar auxiliary diagram with the off-shell leg inside.	57
3.5	The two-loop non-planar auxiliary diagram with the off-shell leg outside.	57
3.6	The two-scale planar triangle topology.	78
3.7	Pictorial representation of the action of the IBP equations on the two-scale triangle integral.	78
3.8	Pictorial representation of a pinching of the two-scale triangle integral.	79
3.9	The Cbox ₁ topology	80
4.1	The general procedure for calculating matrix elements.	116

Preface

The aim of this thesis is to present the calculation of the matrix element and helicity amplitudes for $e^+e^- \rightarrow q\bar{q}g$ which until now has remained the missing component for a full NNLO calculation of $e^+e^- \rightarrow 3$ jets.

Before the presenting the main results in Chapters 4 and 5 we aim to provide an overview of the necessary tools for such a calculation. We begin in Chapter 1 with a basic introduction to Quantum Chromodynamics (QCD). We discuss some of the key ideas and techniques which we use throughout the thesis. In particular we introduce the idea of perturbative calculations and motivate the importance of higher order corrections.

In Chapter 2 we present, by way of example, the calculation of $e^+e^- \rightarrow q\bar{q} + X$ matrix element highlighting the important features of the calculation. We are led to discuss the treatment of infrared divergences and introduce the technique of Catani and Seymour for predicting the infrared structure of matrix elements in general.

Having introduced the tools for calculating matrix elements we turn in Chapter 3 to the methods for calculating loop integrals. The main focus of this chapter is on the technique of integration-by-parts. Here we present an algorithm based on the work of Laporta for the automated solution of the integration-by-parts identities.

The matrix elements and helicity amplitudes, regularised in conventional dimensional regularisation and renormalised in the $\overline{\text{MS}}$ scheme are presented in Chapters 4 and 5.8. They are expressed in terms of one- and two-dimensional harmonic polylogarithms.

Finally in Chapter 6 we provide a summary of results and discuss the remaining steps to be carried out before a full Next-to-Next-to-Leading Order (NNLO) calculation of $e^+e^- \rightarrow 3$ jets can be made.

CHAPTER 1

QCD Beginnings

In this Chapter we discuss the theory of QCD¹. We begin in Section 1.1 by briefly introducing the quark model, outlining a crucial property of the quarks which gives rise to the structure of QCD, namely *colour*. With the key ideas in place we move in Section 1.2 to a more rigorous description, the Lagrangian of QCD. After introducing the idea of perturbative calculations and consequently Feynman diagrams, we present the corresponding Feynman rules in Section 1.3. In Sections 1.4–1.7 we cover the regularisation and renormalisation of QCD which leads naturally to the discussion of the *running coupling*. Finally in Section 1.8 we discuss higher order corrections and the motivation for such calculations within QCD.

1.1 From Hadrons to Quarks

QCD is the theory of the strong interactions. All particles which undergo the strong interaction are called *hadrons*. Hadrons fall into two classes, *baryons* and *mesons*. Baryons exhibit fermionic behaviour whilst mesons are bosonic. The spectrum of hadrons is a broad one, spanning many hundreds of particles with varying lifetimes

¹This introduction is meant to serve as an overview of the important topics in QCD which will be used throughout this thesis. For more detailed discussions of these topics the reader is referred to one of the many text books. For example, [1, 2, 3, 4, 5, 6] provide excellent overviews of QCD and field theory.

and decay modes [7]. Historically, the large number of hadrons was seen as a clear indication for the possibility of underlying structure. Indeed, it was discovered that the hadrons are not fundamental, but can be constructed from a much *smaller group* of *fundamental* particles, the *quarks* [8, 9]. Quarks are spin $1/2$ (fermionic) point-like particles carrying fractional electric charge. The full observed hadronic spectrum can be completely constructed with *six flavours* of quark (and their corresponding antiparticles):

$$Q_{\text{electric}} = +2/3 \quad u - \text{up}, \quad c - \text{charm}, \quad t - \text{top},$$

$$Q_{\text{electric}} = -1/3 \quad d - \text{down}, \quad s - \text{strange}, \quad b - \text{bottom}.$$

The correct fermionic and bosonic behaviour of the baryons and mesons can be reproduced if they are constructed in the following way: mesons to be composed of a quark and antiquark, $M = q\bar{q}$, and baryons from three (anti)quarks, ($B = \bar{q}\bar{q}\bar{q}$) $B = qqq$. By this construction, all hadrons carry integer electric charge, consistent with the experimental fact that no free, fractionally electric charged particle has been observed.

In this incomplete form, the quark model gives rise to a contradiction with the Fermi-Dirac statistics of its constituents. To construct, for example, the $\Delta^{++}(J = 3/2)$, a baryonic state, we must combine three up-type quarks. The resulting wave function must contain three identical fermions with aligned spins

$$\Delta^{++} = |u^\uparrow u^\uparrow u^\uparrow\rangle,$$

which is clearly symmetric under the exchange of two u -quarks. This problem was solved by the proposal, and subsequent verification, of a new quantum number carried by quarks, called *colour charge* [10]. By assigning each quark a new colour quantum number an antisymmetric wave function can be constructed:

$$\Delta^{++} = \frac{1}{\sqrt{6}} \epsilon^{ijk} |u_i^\uparrow u_j^\uparrow u_k^\uparrow\rangle,$$

providing, of course, there are *at least three* unique colours. It has been verified through experiment, by measuring quantities like the $R^{e^+e^-}$ ratio [11, 12, 13] (see Section 2.2) that *exactly three* colours are required. They are labelled *red*, *green* and *blue*. It is also an experimental fact that no isolated quark has ever been observed. This evidence led to the idea that the observed hadrons must be *colourless*, that is, in combinations like red- $\overline{\text{red}}$ and red-green-blue. *Confinement*, as this phenomena is known, is believed to be a dynamical property of the quarks which, at present, is not fully understood. The full baryonic and mesonic states in terms of coloured quarks is then

$$B = \frac{1}{\sqrt{6}} \epsilon^{ijk} |q_i q_j q_k\rangle \quad \text{and} \quad M = \frac{1}{\sqrt{3}} \delta^{ij} |q_i \bar{q}_j\rangle,$$

where it is understood that the colour indices i , j and k must form a colourless combination.

Since its discovery, the theory of colour has been put on a more rigorous mathematical footing. The resulting theory, which describes the interactions of coloured objects, Quantum Chromodynamics (QCD), is based upon the premise that hadrons are colourless and invariant under the exchange of colour of the constituent quarks. This local (gauge) symmetry is described by a *non-Abelian* gauge group, SU(3). Postulating the invariance of hadrons under rotations of this group leads to the prediction of eight colour-force carrying particles, the *gluons*. The non-Abelian nature of the theory leads to the gluons themselves carrying colour. This gives rise to the phenomena of gluon self interaction (see the Feynman rules in Section 1.3) which has fundamental consequences for the theory, and will be explained in Section 1.7. Gluons are the particles responsible for binding quarks together into hadrons and ultimately hadrons into bound states like the nucleus.

1.2 The QCD Lagrangian

The full Lagrangian density of QCD has many component parts, we therefore arrange it into the following terms

$$\mathcal{L}_{\text{QCD}} = \mathcal{L}_{\text{classical}} + \mathcal{L}_{\text{gauge-fixing}} + \mathcal{L}_{\text{ghost}}. \quad (1.1)$$

We will study the structure of each of the three terms in (1.1) and try to broadly interpret and motivate them. Let us begin with the classical Lagrangian, $\mathcal{L}_{\text{classical}}$. It reflects very closely the structure of the Quantum Electrodynamics (QED) Lagrangian (see for example [1]), let us further decompose this

$$\mathcal{L}_{\text{classical}} = \mathcal{L}_{\text{quark}} + \mathcal{L}_{\text{gluon}}. \quad (1.2)$$

The first term, $\mathcal{L}_{\text{quark}}$, describes the dynamical and mass properties of the quark fields

$$\mathcal{L}_{\text{quark}} = \sum_q \bar{\psi}_q^i (i \not{D} - m_q)_{ij} \psi_q^j, \quad (1.3)$$

where ψ_q^i represents a quark field with flavour q and colour charge $i = 1, 2, 3$, that is, a triplet representation of the colour group $\text{SU}(3)$, m_q is the quark mass, the covariant derivative² \not{D} will be explained shortly. The full structure of QCD is illuminated when we require that the quark fields be invariant under local gauge transformations. As previously explained, experimental evidence leads us to believe that physical states (the hadrons) are colour singlet combinations. We are led to impose the condition that performing a redefinition of the component colour fields of the quarks at every point in space and time should leave physical states unchanged. This so-called gauge invariance is enforced by making the triplet quark

²We will make use the common ‘slashed’ notation, $\not{a} = a_\mu \gamma^\mu$, where γ^μ are the gamma matrices satisfying the Clifford algebra, $\{\gamma^\mu, \gamma^\nu\} = 2g^{\mu\nu}$.

fields invariant under rotations of the $SU(3)$ group. An $SU(3)$ transformation can be parameterised by

$$\Omega(x) = \exp(i\alpha_a(x)t^a), \quad (1.4)$$

where the $\alpha_a(x)$ is the local (x dependent) transformation parameter and t^a are 3×3 matrices which are the generators of $SU(3)$ in the fundamental representation. They satisfy the commutation relation

$$[t^a, t^b] = if^{abc}t^c, \quad (1.5)$$

where f^{abc} are the structure constants of $SU(3)$. There are eight such t^a matrices, $a = 1, \dots, 8$. One representation of them which is commonly used is

$$t^a = \frac{1}{2}\lambda^a, \quad (1.6)$$

where λ^a are the Gell-Mann matrices [2].

Under the action of the local gauge transformation (1.4) the quark fields transform as

$$\psi_q^i(x) \rightarrow \psi_q'^i(x) = \Omega_{ij}(x)\psi_q^j(x). \quad (1.7)$$

In order for the Lagrangian (1.3) to remain invariant under the gauge transformation the covariant derivative must have the following structure in the fundamental representation

$$(D_\mu)_{ij} = \partial_\mu \delta_{ij} - ig_s A_\mu^a t_{ij}^a, \quad (1.8)$$

where g_s is the QCD *strong coupling* and A_μ^a are eight vector gauge fields — the gluons. Thus, the covariant derivative satisfies the commutation relation

$$[D_\mu, D_\nu] = -ig_s G_{\mu\nu}^a t^a, \quad (1.9)$$

where $G_{\mu\nu}^a$ is the gluon field strength tensor. It is constructed from the gluon fields A_μ^a and the structure constants f^{abc}

$$G_{\mu\nu}^a = \partial_\mu A_\nu^a - \partial_\nu A_\mu^a + g_s f^{abc} A_\mu^b A_\nu^c. \quad (1.10)$$

It is the final term in (1.10) which separates QCD from QED and gives rise to its unique features. The extra term represents the self-coupling of the gluon fields, that is, since the gluons carry the colour charge they can interact with themselves producing new vertices not present in QED (shown in Section 1.3). The self interaction terms lead to an amazing feature of QCD known as *asymptotic freedom* which will be discussed in Section 1.7.

The second piece of the classical Lagrangian, $\mathcal{L}_{\text{gluon}}$ can now be constructed. In an analogous way to QED, a dynamic term for the gluon fields A_μ^a is generated from $G_{\mu\nu}^a$, but we cannot create a gauge invariant mass term for the gluon, they remain as massless fields. We construct

$$\mathcal{L}_{\text{gluon}} = -\frac{1}{4} G_{\mu\nu}^a G_a^{\mu\nu}. \quad (1.11)$$

Combining $\mathcal{L}_{\text{quark}}$ and $\mathcal{L}_{\text{gluon}}$ gives the complete form of the classical Lagrangian

$$\mathcal{L}_{\text{classical}} = \sum_q \bar{\psi}_q^i (i\not{D} - m_q)_{ij} \psi_q^j - \frac{1}{4} G_{\mu\nu}^a G_a^{\mu\nu}. \quad (1.12)$$

The Lagrangian is not complete at this point. Unfortunately when imposing the gauge transformation the *canonical quantisation* of the theory is spoilt. By allowing the gauge fields A_μ^a the freedom of gauge transformations we are faced with vanishing canonical momentum, consequently the canonical commutation relation, essential for quantisation cannot be made consistent. The problem lies with trying to describe the two physical polarisations of the spin-1 gluon with a four-component Lorentz vector. The solution to the problem is to eliminate the freedom of the

gauge transformation by constraining the field A_μ^a . This can be done for example by imposing the Lorentz condition

$$\partial^\mu A_\mu^a = 0. \quad (1.13)$$

This constraint is imposed explicitly in the Lagrangian by adding a new gauge-fixing term

$$\mathcal{L}_{\text{gauge-fixing}} = -\frac{1}{2\xi}(\partial^\mu A_\mu^a)^2, \quad (1.14)$$

where ξ is called the *gauge parameter*. By adding this term to the Lagrangian we have spoilt its gauge invariance, however, a physical prediction made with the Lagrangian *is gauge invariant* and independent of the gauge parameter. Due to the arbitrariness of ξ several choices for this parameter exist. The Landau gauge $\xi = 0$, the Feynman gauge³ $\xi = 1$ and the Unitary gauge $\xi \rightarrow \infty$.

There still remain unphysical degrees of freedom for the gluon fields which we need to eliminate since we require the gluon to have only two physical polarisations. To achieve this it is necessary to introduce unphysical anticommuting scalar fields η^a which live in the adjoint representation of SU(3). These fields and their particles have the wrong spin statistics to be physical particles but must be included in the Feynman diagrams (see Section 1.3) when we apply perturbation theory to cancel the unphysical polarisations of the gluon. To describe these so called *Faddeev-Popov ghosts* we add a ghost term to the Lagrangian

$$\mathcal{L}_{\text{ghost}} = -\bar{\eta}^a(\partial^\mu(D_\mu)_{ab})\eta^b. \quad (1.15)$$

In the adjoint representation the covariant derivative takes the form

$$(D_\mu)_{ab} = \partial_\mu\delta_{ab} - ig_s A_\mu^c T_{ab}^c, \quad (1.16)$$

³The Feynman gauge will be adopted in the following work.

where T^a are 8×8 matrices and satisfy an analogous commutation relation to (1.5)

$$[T^a, T^b] = i f^{abc} T^c. \quad (1.17)$$

The structure constants f^{abc} may be used as a representation of the T^a

$$T_{bc}^a = i f^{abc}. \quad (1.18)$$

In this form Eq. (1.17) is just the Jacobi identity. Using (1.16) and (1.18) the ghost Lagrangian (1.15) can be written as

$$\begin{aligned} \mathcal{L}_{\text{ghost}} &= -\bar{\eta}^a (\partial^\mu (D_\mu)_{ab}) \eta^b \\ &= -\bar{\eta}^a (\partial^2 \delta_{ab} - i g_s \partial^\mu A_\mu^c T_{ab}^c) \eta^b \\ &= -\bar{\eta}^a (\partial^2 \delta_{ab} + g_s \partial^\mu A_\mu^c f^{abc}) \eta^b. \end{aligned} \quad (1.19)$$

We now have all the terms in the full Lagrangian (1.1) — this is the basis for all theoretical QCD calculations.

The experiments which probe the behaviour of QCD and its particles, which we would like to make theoretical predictions of, are typically scattering experiments. The likelihood of finding some final state after the interaction (scattering) of two initial states is determined by the *cross section*. The scheme for calculating the cross section is clear, one calculates the *matrix elements* \mathcal{M} of the corresponding *scattering matrix* or *S-matrix*. However, in an *interacting* theory, such as QCD, this is not easily done. In fact, there are very few *exactly* solvable interacting field theories. Instead, we have to solve the theory *approximately*, the interaction terms of the Lagrangian are treated as *perturbations* of the free theory. An expansion of \mathcal{M} , the *perturbation series*, is made in the coupling constant. If the coupling constant is small enough then we might expect the perturbative series to be a reasonable

approximation to the exact result⁴. Use of Wick's theorem allows the terms in the perturbation series to be represented diagrammatically as *Feynman diagrams*. The approach therefore, when making a perturbative calculation of the matrix element, is to construct all possible appropriate Feynman diagrams up to some specific order in the coupling and sum their contributions. Appropriate factors corresponding to the lines and vertices, derived from the Lagrangian in the form of *Feynman rules*, are used to decorate each diagram with its algebraic contribution.

1.3 The Feynman Rules of QCD

As already mentioned, the Feynman rules are used to associate analytic expressions with Feynman diagrams. The rules are derived from the expansion of the interacting terms of the Lagrangian (1.1). Each interaction term in the Lagrangian corresponds to a vertex. There are also the external states and the internal propagating states.

The Feynman rules for QCD are set out below. Applying these rules to the sum of all appropriate Feynman diagrams will construct $i\mathcal{M}$, the matrix element. We denote colour indices of quarks with i and j taking values 1, 2, 3 and those of gluons and ghosts with a, b, c and d taking values 1, \dots , 8. The Lorentz indices are μ, ν, ρ and σ . We begin with the external lines

$$\text{Incoming quark: } \text{---}\nearrow = u(p), \quad \text{Outgoing quark: } \nearrow = \bar{u}(p), \quad (1.20)$$

$$\text{Incoming antiquark: } \text{---}\nwarrow = \bar{v}(p), \quad \text{Outgoing antiquark: } \nwarrow = v(p), \quad (1.21)$$

$$\text{Incoming gluon: } \text{---}\text{oooo}\text{---} = \varepsilon_\mu(p), \quad \text{Outgoing gluon: } \text{oooo}\text{---} = \varepsilon_\mu^*(p). \quad (1.22)$$

⁴The applicability of the perturbation series with regard to the size of the coupling will be discussed in Section 1.7, for now we assume that we can make the appropriate expansion.

Next the propagator rules

Quark propagator: $i \longrightarrow j = \frac{i(p + m_q)}{p^2 - m_q^2 + i0} \delta^{ij}, \quad (1.23)$

Gluon propagator: $a, \mu \text{ } \text{-----} \text{ } b, \nu = \frac{-i}{p^2 + i0} \left(g^{\mu\nu} - (1 - \xi) \frac{p^\mu p^\nu}{p^2} \right) \delta^{ab}, \quad (1.24)$

Ghost propagator: $a \text{ } \text{-----} \text{ } b = \frac{i}{p^2 + i0} \delta^{ab}. \quad (1.25)$

And finally the interaction vertices

Three-gluon vertex: $\begin{array}{c} b, \nu \\ \text{-----} \\ \text{-----} \\ c, \rho \end{array} \text{ } a, \mu = \begin{array}{l} g_s f^{abc} [(p_1 - p_2)^\rho g^{\mu\nu} \\ + (p_2 - p_3)^\mu g^{\nu\rho} \\ + (p_3 - p_1)^\nu g^{\mu\rho}], \end{array} \quad (1.26)$

Four-gluon vertex: $\begin{array}{c} c, \rho \\ \text{-----} \\ \text{-----} \\ d, \sigma \end{array} \text{ } \begin{array}{c} b, \nu \\ \text{-----} \\ \text{-----} \\ a, \mu \end{array} = \begin{array}{l} -i g_s^2 [f^{abe} f^{cde} (g^{\mu\rho} g^{\nu\sigma} - g^{\mu\sigma} g^{\nu\rho}) \\ + f^{ace} f^{bde} (g^{\mu\nu} g^{\rho\sigma} - g^{\mu\sigma} g^{\nu\rho}) \\ + f^{ade} f^{bce} (g^{\mu\nu} g^{\rho\sigma} - g^{\mu\rho} g^{\nu\sigma})], \end{array} \quad (1.27)$

Quark-gluon vertex: $\begin{array}{c} j \\ \text{-----} \\ \text{-----} \\ i \end{array} \text{ } a, \mu = i g_s \gamma^\mu t_{ij}^a, \quad (1.28)$

Ghost-gluon vertex: $\begin{array}{c} c \\ \text{-----} \\ \text{-----} \\ b \end{array} \text{ } a, \mu = g_s f^{abc} p^\mu. \quad (1.29)$

These must be applied together with the following rules:

- i. Integrate over the unconstrained momentum p appearing in each closed loop

with the measure $\int \frac{d^4 p}{(2\pi)^4},$

- ii. Impose momentum conservation at each vertex,
- iii. Multiply by a factor of (-1) for every quark and ghost loop,
- iv. Multiply by an appropriate symmetry factor to allow for permutations of fields in a diagram.

Some remarks are necessary. The gluon propagator contains the gauge parameter ξ . As already discussed, a theoretical prediction should not depend on this parameter. We have chosen to use the Feynman gauge $\xi = 1$, however, this parameter can be left arbitrary, and indeed its cancellation serves as a strong check on the gauge independence of a calculation.

Also, each of the propagators contain an $i0$ term. This is known as the *Feynman prescription* and is a tool to help deal with the divergences caused by the momentum in the denominator becoming zero. The issue of divergent diagrams is discussed in the next Section.

1.4 Regularisation

As soon as we start to apply the Feynman rules to the calculation of physical amplitudes we run into an extremely serious problem, and one that plagues field theories in general, namely that of *divergences*. The origins of the problem lie in Feynman rules which, in particular, require the integration over the *unconstrained* momenta appearing in loop diagrams. For clarity, consider, for example, the diagram of Figure 1.1, the self-energy of the gluon, $\Pi_{ab}^{\mu\nu}(p^2)$.

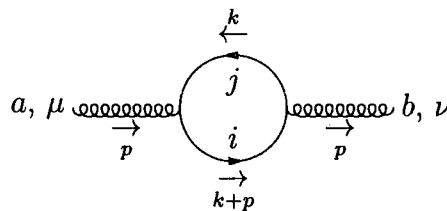


Figure 1.1: The one-loop correction to the gluon self-energy.

Applying the Feynman rules of the previous section we find

$$i\Pi_{ab}^{\mu\nu}(p^2) = -g_s^2 t_{ij}^a t_{ji}^b \int \frac{d^4 k}{(2\pi)^4} \frac{\text{tr}[\gamma^\mu(\not{k} + m_q)\gamma^\nu(\not{k} + \not{p} + m_q)]}{(k^2 - m_q^2)((k+p)^2 - m_q^2)}. \quad (1.30)$$

This integral displays a clear divergence in the limit $k \rightarrow \infty$, known as an *Ultraviolet* (*UV*) divergence. In this limit it can be seen that the integral diverges quadratically. In more general integrals, for example, the vertex integral, another type divergence appears when we consider massless quarks⁵ ($m_q \rightarrow 0$). This type, called *Infrared* (*IR*), appear in the limit $k \rightarrow 0$. Notice that the IR divergences only occur in the massless limit or in situations where the propagating particles are massless (i.e. the same divergences occur for gluon and ghost loops). Keeping a finite mass would render the integral finite in the $k \rightarrow 0$ limit, the mass would *regulate* the integral. In this sense IR divergences are sometimes referred to as *mass singularities*.

The issue of the divergent behaviour of QCD and field theories in general has historically been a huge problem with regard to making meaningful predictions. Fortunately, much work has been done to recover finite results from such calculations. The solutions to removing the two types of divergences are very different. As we shall see in Section 1.5, the UV divergences are removed by the process of *renormalisation*. IR divergences, on the other hand, have the peculiar property that for appropriately defined observables, they cancel between each other⁶. This will be demonstrated more clearly in Section 2.2. The end result of the systematic removal and cancellation of divergences is that the theoretical calculation of a physical observable is finite, as one might expect from a meaningful theory! The establishment of renormalisation and theorems which guarantee the cancellation of IR divergences⁷ was key to the success of not only QCD but field theories in general.

Having identified the problem of divergences, and with the realisation that they

⁵We consider the massless quark limit here since it will be adopted in the following work.

⁶Observables for which the IR divergences cancel are straightforwardly called IR safe.

⁷The Kinoshita–Lee–Nauenberg [14, 15] and Bloch–Nordsieck theorems [16].

must be cancelled carefully, a tool is required to deal with then a well defined way. The technique of manipulating and extracting divergences is called *regularisation*. Several prescriptions for the regularisation of integrals have been developed, each with its own advantages. It is the disadvantages which usually determine the choice, since many of the prescriptions break the invariances upon which field theory is constructed.

One such simple scheme is to introduce a *cut-off*, Λ in the integration such that only momentum scales smaller than Λ are integrated over. This does not respect the gauge invariance of the theory, and of course, breaks Lorentz invariance, thus is not suitable for perturbative calculations based on Feynman diagrams.

By far the most commonly used scheme in QCD calculations today is Dimensional Regularisation (DR) [17, 18, 19]. The idea is very simple but perhaps not as intuitive as that of cut-off regularisation. The Feynman diagrams are treated as analytic functions of space-time dimensionality, D . In lower dimensions the divergent integrals will in fact converge. The regularisation procedure is then to introduce $D = 4 - 2\epsilon$ with ϵ small, make a calculation, and in the final result take the limit $\epsilon \rightarrow 0$. The divergent behaviour becomes evident as poles in ϵ . The beauty of DR is that it respects both gauge and Lorentz invariance. For consistency of the theory however, we are forced to introduce some additional modifications. Perhaps, most obviously, is that the measure of integration becomes D -dimensional, not only in the Feynman integrals but also the phase space integrals. The Lorentz vectors become D -dimensional, $g^{\mu\nu}g_{\mu\nu} = D$, as well as the gamma matrices. More subtly, the dimensionality of the Lagrangian needs to be fixed. By using the dimension as a regulator, we are forced to introduce an arbitrary mass scale μ — the regularisation scale, made effective by the replacement $g_s \rightarrow \mu^\epsilon g_s$. In Conventional Dimensional Regularisation (CDR) no distinction is made between real and virtual particles, additionally, quarks have two helicity states and gluons $D - 2$.

1.5 Renormalisation

Having been regulated, the perturbative expression for an observable explicitly displays the divergent dependence on the regulating parameter, which for CDR will be manifest as poles in ϵ . Renormalisation is the process whereby we extract the divergences due to the UV behaviour of the theory. A theory in which UV divergences can be removed by renormalisation is therefore called a *renormalisable theory*. QCD is one such theory [17].

The principle idea of renormalisation is that the Lagrangian and ultimately the Feynman rules are derived in terms of so-called *bare parameters*, these parameters are just the fields, couplings and masses (and also the non-physical gauge parameter). The bare parameters are not physically observable and are hence subject to possible rescaling. Using the freedom to rescale the unobservable parameters enables us to reconstruct the Lagrangian with *physical parameters*, that is, those which are experimentally observable. This is achieved by rewriting all bare parameters in the Lagrangian as *renormalised* parameters with an appropriate multiplicative factor

$$\begin{aligned}
 \psi_{0q}^i &= Z_\psi^{1/2} \psi_q^i, \\
 A_{0\mu}^a &= Z_A^{1/2} A_\mu^a, \\
 g_{0s} &= Z_g g_s, \\
 m_0 &= Z_m m, \\
 &\vdots
 \end{aligned}
 \tag{1.31}$$

Each term on the left-hand side represents a bare parameter whilst those on the right represent renormalised parameters. The renormalisation constants, Z , absorb the UV divergences and hence represent infinite quantities. If the UV divergences can be absorbed into the renormalisation constants order by order in the perturbative series, then the theory is renormalisable. The divergences of a renormalisable

field theory will not remain in observable quantities. In practise, the multiplicative renormalisation constants do not affect the perturbative expansion of the action (it is effectively a rescaling of parameters) we therefore find that the Feynman rules survive unchanged — except that they should now be considered functions of the physical parameters.

The prescription for renormalisation is not uniquely defined. As well as absorbing the singular structure into the multiplicative factors, it is also equally valid to absorb some of the finite structure as well. This arbitrariness leads to different *renormalisation schemes*. For example, in the Minimal Subtraction (MS) scheme (when using CDR) the $1/\epsilon$ poles are simply removed. We usually find though, that the poles in $1/\epsilon$ are accompanied by finite terms in the following combination

$$(4\pi)^\epsilon \frac{\exp(-\epsilon\gamma_E)}{\epsilon} = \frac{1}{\epsilon} + \ln(4\pi) - \gamma_E + \mathcal{O}(\epsilon). \quad (1.32)$$

where $\gamma_E = 0.5772\dots$ is the Euler–Mascheroni constant. In the modified Minimal Subtraction scheme ($\overline{\text{MS}}$) we remove the $1/\epsilon$ poles as well as all the finite terms appearing in the right-hand side of (1.32).

The dependence of physical observables on renormalisation scheme is slightly more subtle and leads us to discuss the *renormalisation group equations*.

1.6 Renormalisation Group Equations

Recall that CDR requires the introduction of an artificial mass scale, μ to maintain the correct dimensions of the Lagrangian. As a consequence, every physical quantity \mathcal{R} depends not only on the coupling g_s ⁸ and the masses m_q , but also on the scale μ . In general, $\alpha_s(g_s)$ and m_q will also depend on μ . If \mathcal{R} is a dimensionless observable

⁸Since the ratio $g_s^2/4\pi$ appears in many calculations it is conventional to define $\alpha_s = g_s^2/4\pi$.

measured at an energy scale Q then it will have the following form

$$\mathcal{R} = \mathcal{R}(\alpha_s(\mu^2), m_q(\mu^2), Q^2/\mu^2). \quad (1.33)$$

Since the scale μ is entirely arbitrary, it cannot be related to any physical observable, hence physical observables should be invariant under the exchange $\mu \rightarrow \mu'$. This invariance can be imposed by the following condition

$$\begin{aligned} \mu^2 \frac{d\mathcal{R}(\alpha_s, m_q, Q^2/\mu^2)}{d\mu^2} &= 0 \\ \left[\beta(\mu^2) \frac{\partial}{\partial \alpha_s} - \gamma_{m_q}(\mu^2) m_q \frac{\partial}{\partial m_q} + \mu^2 \frac{\partial}{\partial \mu^2} \right] \mathcal{R}(\alpha_s, m_q, Q^2/\mu^2) &= 0, \end{aligned} \quad (1.34)$$

which defines the renormalisation coefficients β and γ_{m_q} , the β function and *anomalous dimension*. These coefficients take the form

$$\beta(\mu^2) = \mu^2 \frac{\partial \alpha_s}{\partial \mu^2}, \quad \gamma_{m_q} = -\mu^2 \frac{1}{m_q} \frac{\partial m_q}{\partial \mu^2}. \quad (1.35)$$

These equations represent the *Renormalisation Group Equations (RGE)*. The solution of the differential equations (1.35) reveal two fundamental properties of QCD — the *running coupling*, $\alpha_s = \alpha_s(Q^2)$ and *running masses*, $m_q = m_q(Q^2)$. Since we shall be considering massless quarks in further discussions we will ignore the mass dependence for now and concentrate on the β function and its consequences for the running coupling.

1.7 The Running Coupling Constant $\alpha_s(Q^2)$

The renormalisation group equation for the running coupling constant (1.35) leads to the following differential equation

$$\mu^2 \frac{\partial \alpha_s}{\partial \mu^2} = \frac{\partial \alpha_s}{\partial \ln \mu^2} = \beta(\alpha_s). \quad (1.36)$$

It is easier to consider the equation in its integral form

$$\ln \left(\frac{Q^2}{\mu^2} \right) = \int_{\alpha_s(\mu)}^{\alpha_s(Q)} \frac{d\alpha}{\beta(\alpha)}. \quad (1.37)$$

This equation governs the evolution of the coupling constant from one scale μ to another scale Q . The solution to this equation can be approximately found when the QCD β function is expanded as a perturbative series in α_s

$$\frac{\beta(\alpha_s)}{2\pi} = -\beta_0 \left(\frac{\alpha_s}{2\pi} \right)^2 - \beta_1 \left(\frac{\alpha_s}{2\pi} \right)^3 - \mathcal{O}(\alpha_s^4), \quad (1.38)$$

where

$$\beta_0 = \frac{11C_A - 4T_R N_F}{6}, \quad (1.39)$$

$$\beta_1 = \frac{17C_A^2 - 10C_A T_R N_F - 6C_F T_R N_F}{6}, \quad (1.40)$$

with N_F (active) quark flavours and QCD colour factors

$$C_A = N, \quad C_F = \frac{N^2 - 1}{2N} \quad \text{and} \quad T_R = \frac{1}{2}. \quad (1.41)$$

If we solve Equation (1.37) to first order (i.e. keeping only the first β_0 term in (1.38)) we get

$$\alpha_s(Q^2) = \frac{\alpha_s(\mu^2)}{1 + \alpha_s(\mu^2) (\beta_0/2\pi) \ln(Q^2/\mu^2)}. \quad (1.42)$$

This result, defining the *running coupling* $\alpha_s(Q^2)$ has important consequences for QCD. The parameter β_0 given in Equation (1.39) is positive for $N_F \leq 16$, this means that for QCD (with no more than 6 possible active quark flavors) the value of α_s *decreases* as Q increases. This property, whereby the coupling is decreasing with increasing energy is known as *asymptotic freedom*. Also importantly, this equation makes no prediction for the value of α_s . α_s must be measured at some energy scale,

typically the Z boson mass $\alpha_s(M_Z)$, then the running equation (1.42) enables the coupling to be *evolved* to a different scale.

It is convenient to re-express the definition of the running coupling $\alpha_s(Q^2)$ in terms of a dimensionful parameter, Λ which is the constant of integration defined by

$$\ln \left(\frac{Q^2}{\Lambda^2} \right) = - \int_{\alpha_s(Q)}^{\infty} \frac{d\alpha}{\beta(\alpha)}. \quad (1.43)$$

Λ represents the scale at which the coupling would diverge if extrapolated too far beyond the perturbative regime. The running coupling becomes

$$\alpha_s(Q^2) = \frac{1}{(\beta_0/2\pi) \ln(Q^2/\Lambda^2)}. \quad (1.44)$$

This notation is generally disfavoured since the value of Λ is scheme dependent and depends on the number of active quark flavours. In the $\overline{\text{MS}}$ scheme with five active quarks we find $\Lambda_{\overline{\text{MS}}}^5 \sim 208 \text{ MeV}$ [7]. We are now able to comment on the applicability of applying perturbation theory to make meaningful QCD predictions. With the running coupling decreasing with increasing energy we expect that perturbative calculations will be applicable in the *high energy* regime. Note that this is in complete contrast to QED for which the β function has the opposite sign [1]. For QED perturbative calculations are only applicable in the low energy regime. We expect the perturbative expansion to become less reliable as the energy decreases and approaches Λ , i.e. energies of the order of several hundred MeV.

Finally, we can define the full relation between the bare coupling α_0 and the renormalised coupling $\alpha_s \equiv \alpha_s(\mu^2)$, evaluated at the renormalisation scale μ^2 . The relation between the two couplings just comes from Equation (1.31)

$$g_0 s \mu_0^\epsilon = Z_g g_s \mu^\epsilon \quad \Rightarrow \quad \alpha_0 \mu_0^{2\epsilon} = Z_g^2 \alpha_s \mu^{2\epsilon}, \quad (1.45)$$

where we have now included the scales μ_0 and μ which are required in the DR

procedure to give the Lagrangian the correct dimensions. Thus, to find the relation between the couplings we see from (1.45) that we need to make a perturbative calculation of the renormalisation coefficient, Z_g . In the $\overline{\text{MS}}$ scheme we find

$$\alpha_0 \mu_0^{2\epsilon} S_\epsilon = \alpha_s \mu^{2\epsilon} \left[1 - \frac{\beta_0}{\epsilon} \left(\frac{\alpha_s}{2\pi} \right) + \left(\frac{\beta_0^2}{\epsilon^2} - \frac{\beta_1}{2\epsilon} \right) \left(\frac{\alpha_s}{2\pi} \right)^2 + \mathcal{O}(\alpha_s^3) \right], \quad (1.46)$$

where

$$S_\epsilon = (4\pi)^\epsilon e^{-\epsilon\gamma_E} \quad (1.47)$$

and β_0 and β_1 are the first two coefficients of the QCD β -function defined by Equations (1.39) and (1.40). To avoid confusing notation we take $\mu_0 = \mu$ unless otherwise mentioned.

1.8 Higher Order Corrections — from NLO to NNLO

So far we have indicated that theoretical calculations in QCD can be carried out perturbatively for small coupling corresponding to the high energy regime. In principle there are an infinite number of terms in the perturbative expansion, in practise, we can only calculate a finite number of them. This computational limit has important consequences when it comes to matching theoretical predictions to physical observations.

The most obvious consequence of ignoring higher orders is that the theoretical prediction has some uncertainty due to these missing higher orders. We need to have some idea of how large the missing orders are, in order that we can safely ‘ignore’ them, or determine an uncertainty due to them. This problem is important when, for example, measuring parameters of the theory. In QCD the strong coupling α_s is a free parameter and must be determined by comparing experimentally measured

quantities to their predictions. To determine α_s as accurately as possible we would thus like to know as many of the higher order terms as possible. Uncertainties in higher orders are directly reflected as an uncertainty in α_s .

1.8.1 Scale Dependence

A slightly more subtle effect of truncating the perturbative series is that of *scale dependence*. Scale dependence is a consequence of the coupling constant α_s and the perturbative coefficients being functions of the unphysical scale μ . This idea led to the RGEs (Section 1.6) by imposing that physical observables should be independent of this scale. Consider the perturbative expansion of a general observable

$$\mathcal{R}(\alpha_s(\mu^2), Q^2/\mu^2) = \sum_{n=1}^{\infty} r_n(Q^2/\mu^2) \alpha_s(\mu^2)^n. \quad (1.48)$$

We can consider the effect of truncation of the perturbative series (to say, N terms) by calculating its μ dependence

$$\frac{d}{d \ln \mu^2} \sum_{n=1}^N r_n(Q^2/\mu^2) \alpha_s(\mu^2)^n = -\frac{d}{d \ln \mu^2} \sum_{n=N+1}^{\infty} r_n(Q^2/\mu^2) \alpha_s(\mu^2)^n \sim \mathcal{O}(\alpha_s^{N+1}), \quad (1.49)$$

where we have employed the RGE (1.34). It can be seen that the truncated series (on the l.h.s. of (1.49)) is *dependent on the scale* μ as determined by the absent higher order terms on the r.h.s. of (1.49). In other words, truncation of the perturbative series destroys the cancellation of the scale dependence between different orders. This unphysical dependence decreases as more terms are added to the truncated series ($N \rightarrow \infty$). Figure 1.2 shows the scale dependence at Leading Order (LO), Next-to-Leading Order (NLO) and NNLO of the differential cross-section for single jet production ($p\bar{p} \rightarrow \text{jet}$), where each jet has transverse momentum $E_T = 100$ GeV. For renormalisation scales up to twice the transverse energy the effect of the higher orders is to reduce the uncertainty from around 20% to 9% to 1%. Figure 1.3 is

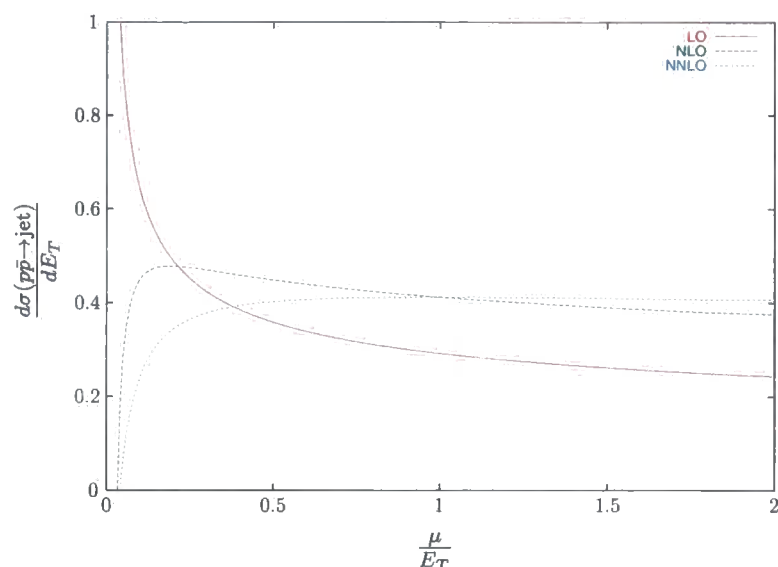


Figure 1.2: Renormalisation scale dependence of the single jet ($p\bar{p} \rightarrow \text{jet}$) inclusive distribution with transverse jet energy $E_T = 100$ GeV at different orders in the perturbative series.

CDF data showing the coupling constant α_s as a function of transverse jet energy and indicating the dominant uncertainty due to the renormalisation scale.

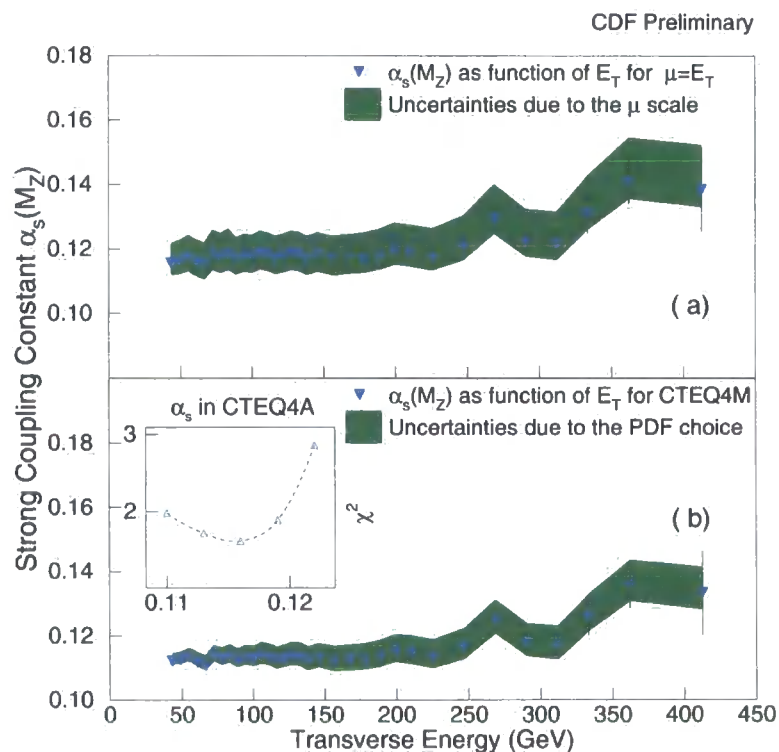


Figure 1.3: CDF data for the coupling constant α_s as a function of the transverse energy displaying the uncertainty represented by the renormalisation scale μ .

1.8.2 Jets and Event Shapes

In typical e^+e^- annihilation experiments a QCD final state will always consist of a discrete number of sprays of hadrons. Within these discrete sprays, the most highly energetic particles are well collimated and separated by only a few tenths of a radian. *Jets*, as these sprays are known, are a direct consequence of *confinement*, that is, the idea based on experimental observation, that no coloured *physical* states exist. The implication of confinement is that the partons in the final states of a perturbative calculation must undergo a *non-perturbative* process known as *hadronisation*. This is the process whereby a coloured parton ‘fragments’ into series of non-coloured hadrons. It is because the produced hadrons remain collimated and reflect the original path of the underlying parton that we can use experimental observations to test perturbative predictions. In fact, the clear observation of two-jet, back-to-back final states at PETRA confirmed the ideas of the parton model developed from deep inelastic scattering.

An accurate description of jet physics and the modelling of jets requires the addition of higher order corrections. After fragmentation there is clearly a mismatch between the number of hadrons and the number of partons in an event. Better jet reconstruction can be achieved at higher orders where more partons can be combined to construct jets. As Figure 1.4 demonstrates, as we move to higher orders the perturbative structure of a jet is refined. At LO an individual parton models a jet giving no prediction for the size of the jet. At NLO two partons may be combined to form a jet, giving some sensitivity to the shape and size of the jet. NNLO will help to better improve the sensitivity allowing three partons to be combined to form a single jet.

Many techniques have been developed to quantify and describe jet structure, these jet observables are generically called *event shapes*. A typical example of an event shape is *Thrust*, T . Thrust is essentially a measure of how ‘pencil-like’ an

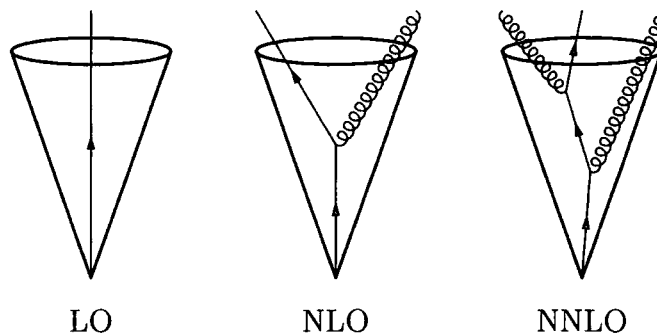


Figure 1.4: Schematic representation of how higher order calculations allow more partons to be used in the construction jet cones, thus giving a more accurate perturbative jet description.

event is, a back to back two jet-event has $T = 1$ and a completely spherical event has $T = 1/2$. Other examples of event shapes are sphericity and the C-parameter [2].

Among jet observables, the three-jet production rate in electron-positron annihilation plays an outstanding role. The experimental observation of three-jet events at PETRA [20], in agreement with the theoretical prediction [21], provided the first evidence for the gluon, interpreted as the result of bremsstrahlung from a quark-antiquark pair. The observation of three-jet events as a departure from the dominant simple two-jet configuration is proportional to the coupling of gluons to quarks, consequently the three-jet rate and related event shape observables have become important experimental tools for the precise determination of strong coupling α_s , see for example [22] for a review. At present, the error on the extraction of α_s from data is dominated by the uncertainty in the NLO calculation [23, 24, 25, 26] of the jet observables.

1.8.3 Power Corrections

At present, comparisons between NLO data and experimental data reveal the need for *power corrections*. In e^+e^- annihilation the NLO prediction of the average value for $1 - \text{Thrust}$ lies well below the experimentally determined data. The difference is accounted for by $1/Q$ power corrections. The general form of the power correction

is theoretically motivated but the magnitude must be extracted from data, and can also be attributed to missing higher orders. The addition of NNLO calculations should reduce the size of the power correction needed to fit data.

To see this slightly more clearly we can construct a model. We assume that the average value of $1 - T$ can be approximated by the series

$$\langle 1 - T \rangle = 0.33\alpha_s(Q) + 1.00\alpha_s(Q)^2 + A_3\alpha_s(Q)^3 + \frac{\lambda}{Q}, \quad (1.50)$$

where λ represents the size of the power corrections. The running coupling is given by Equation (1.44) which for five active quark flavours becomes

$$\alpha_s(Q) = \frac{6\pi}{23 \log(Q/\Lambda)}, \quad (1.51)$$

with $\Lambda \sim 208$ MeV. Figure 1.5 shows the NLO prediction with no power correction $A_3 = 0$, $\lambda = 0$ and the NLO prediction with a power correction $A_3 = 0$, $\lambda = 1$ GeV which we assume to model the actual data. At present the NNLO coefficient A_3 is not known. If we assume that it is positive then this contribution will actually reduce the size of the power correction needed to fit the data. For example, if we assume that $A_3 = 3$ then the NLO prediction with the power correction can be fitted with a power correction of the same form, but $\lambda = 0.6$ GeV. In effect, the power corrections $1/Q$ are being exchanged for a $1/\log^3(Q/\Lambda)$ contribution.

1.9 Summary

We have presented a very brief but broad overview of the basic elements of the theory of QCD. The aim, to introduce some of the more important tools and techniques which will be used in the following work. The main idea is that we can make a perturbative calculation by means of Feynman diagrams. The running coupling for QCD means that these perturbative calculations should be valid in the high energy

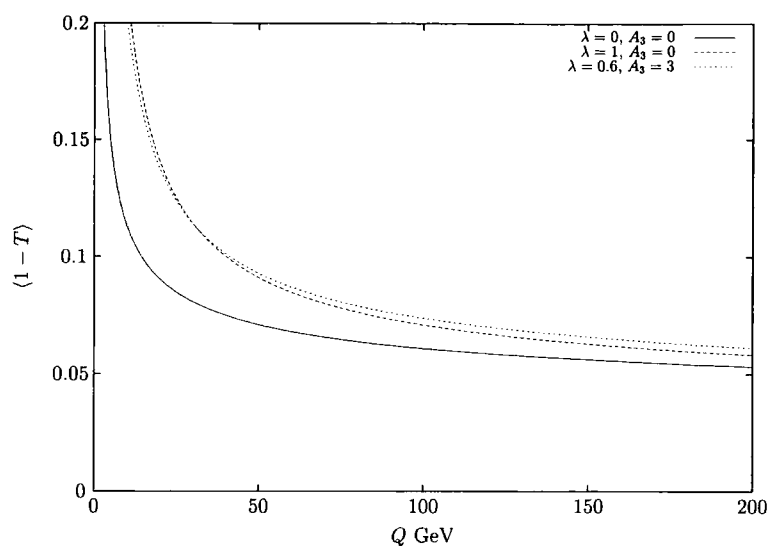


Figure 1.5: The average value of $\langle 1 - T \rangle$ showing the NLO prediction (red), the NLO prediction with a power correction of $\lambda = 1$ GeV (green) and an NNLO prediction with $A_3 = 3$ and $\lambda = 0.6$ GeV (blue).

regime. In general, calculations are usually both IR and UV divergent but by using regularisation and renormalisation these divergences can be brought under control and meaningful predictions made.

Hopefully, the necessity of higher order corrections in perturbative calculations has been demonstrated by the need for increased accuracy, reduction of scale dependence and improved jet description. As we move toward the future, experimental data is set to become more precise as machines improve and statistics increase. Machines like the planned TESLA [27] linear e^+e^- collider will allow precision QCD studies at even higher energies than LEP. The $ep \rightarrow (2 + 1)$ jets and related event shape observables have already reached a level of precision demanding predictions beyond NLO accuracy; further improvement on data is expected from the HERA high luminosity programme.

With these thoughts in mind it is appropriate to introduce the work to be carried out in this thesis. For a long time the evaluation of NNLO corrections to the three-jet rate in e^+e^- annihilation has been considered an important project [28], the reasons for which have just been described. As we shall see in Chapter 4 there are

several components to the full calculation of this process. In this work we focus on one particular contribution, which has for a long time proved an obstacle, namely, we calculate the two-loop (as well as one-loop times one-loop) amplitudes for the $\gamma^* \rightarrow q\bar{q}g$ matrix elements.

The main hurdle has been the evaluation of the many Feynman diagrams and associated loop integrals. This has only become tractable in the past two years due to various technical developments. In particular the systematic application of integration-by-parts relations to reduce the large number of loop integrals to a much smaller basis set of so-called master integrals. In parallel with this we have seen the evaluation of all the master integrals, both planar and non-planar, required for this particular process. This was brought about by the development of techniques for calculating master integrals with differential equations, and the systematic solution of such systems of differential equations. With these two main developments, the necessary tools for the evaluation of the two-loop amplitudes for the $\gamma^* \rightarrow q\bar{q}g$ matrix elements were in place and made such a calculation possible.

We begin in Chapter 2 with an example calculation of the matrix elements for $\gamma^* \rightarrow q\bar{q}$. This provides an overview of the various steps for calculating a matrix element. From the result we obtain the $\mathcal{R}^{e^+e^-}$ ratio and see how higher order corrections improve the accuracy of the perturbative prediction. In particular we see how the IR divergences combine in a physical observable to produce finite predictions. This leads to the general discussion of the singular behaviour of matrix elements and we present the results of Catani and Seymour which predict the IR singular behaviour of one- and two-loop matrix elements.

In Chapter 3 we provide the tools to deal with loop integrals. Among these tools we consider the technique of integration-by-parts to reduce a large number of complicated integrals to a small set of simpler master integrals. Based on the work of Laporta we describe an algorithm for the automated solution of the integration-by-parts identities. We also review the techniques for calculating loop integrals directly

and in particular we show how to construct differential equations for loop integrals and how these can be used to calculate the master integrals.

With the necessary tools in place, we present in Chapter 4 the full matrix element calculation of $\gamma^* \rightarrow q\bar{q}g$. In this Chapter we show all the contributing Feynman diagrams and construct the insertion operator for this process. We present the results for the one-loop times one-loop and two-loop times tree contributions and verify that their pole structure agrees with the prediction of Catani and Seymour. Chapter 5 is complementary to this work and here we present the helicity amplitude for $\gamma^* \rightarrow q\bar{q}g$, again we verify that the pole structure is in agreement with the prediction.

Finally we conclude in Chapter 6 and give an overview of the steps still required to take the matrix element presented in this thesis and make physical predictions for observables at NNLO. We also provide an outlook to future work and other related projects which stem from this thesis.

CHAPTER 2

Matrix Elements

2.1 Introduction

From our basic discussion of QCD we have seen that a perturbative calculation involves the calculation of Matrix Elements (ME) through Feynman diagrams. We begin this chapter on MEs by looking at a simple example calculation of $e^+e^- \rightarrow q\bar{q} + X$. We will introduce NLO corrections to this process in the form of both real and virtual emissions. This will serve as a demonstration of the calculation which we are trying to achieve at NNLO. In particular, we will see the appearance of IR divergences. We will see that the complete calculation is finite, as guaranteed by the KLN and BN theorems. We are naturally led to the concept of an IR safe observable. We begin the discussion of the NNLO ME by considering in more detail the cancellation of the IR divergences. We study the algorithm proposed by Catani and Seymour for predicting the IR singular behaviour of one-loop amplitudes as well as the extension to two-loop amplitudes made by Catani. These tools will serve as an important check for our following calculations. Using the prediction we are able to check the pole structure of our MEs which will enable us to guarantee the cancellation of poles when the total cross section is constructed.

2.2 Infrared Divergences

One of the most straightforward predictions in perturbative QCD is for $R^{e^+e^-}$, the ratio of the total e^+e^- hadronic cross section to the muon pair production cross section. The calculation of the full cross section for $e^+e^- \rightarrow \mu^+\mu^-$ is a simple one. At an energy scale \sqrt{s} far below the Z pole (i.e. $\sqrt{s} \ll M_Z$) one finds [3]

$$\sigma_{e^+e^- \rightarrow \mu^+\mu^-}^0 = \frac{4\pi\alpha^2}{3s}, \quad (2.1)$$

where α is the QED coupling. In e^+e^- annihilation it is also possible to produce hadrons in the final state. However, we know that the formation of the observed hadrons in the final state is not described by perturbation theory. We are able to make a perturbative prediction for this process due to the factorisation of the short-scale physics (the perturbative cross section) and the large-scale physics (the formation of hadrons from partons — hadronisation). In this way we consider the cross section for $e^+e^- \rightarrow \text{hadrons}$ by calculating the inclusive perturbative cross section for $e^+e^- \rightarrow q\bar{q} + X$.

In this Section we begin by showing the perturbative calculation of the cross section for the process $e^+e^- \rightarrow q\bar{q} + X$ by construction of the MEs and the integration over phase space. We extend the calculation to higher orders to demonstrate the appearance and eventual cancellation of IR divergences. To do this will require that we calculate both the *real* and *virtual corrections* to $e^+e^- \rightarrow q\bar{q} + X$ at NLO and show explicitly how the divergences combine to yield a finite result.

The calculation of the total cross section for $e^+e^- \rightarrow q\bar{q} + X$ involves two steps. The first is to calculate the ME for the process, the second is to integrate the ME over all phase-space. We know that the ME can be calculated perturbatively¹ as an expansion in the coupling constant (which for this process is α_s). If we work to

¹We are only interested in performing a perturbative expansion on the final $q\bar{q}$ state, we ignore corrections to the initial state.

$\mathcal{O}(\alpha_s^2)$ then there are two contributions to $e^+e^- \rightarrow q\bar{q} + X$,

$$|\mathcal{M}_{q\bar{q}}\rangle = |\mathcal{M}_{q\bar{q}}^{(0)}\rangle + |\mathcal{M}_{q\bar{q}}^{(1)}\rangle + \mathcal{O}(\alpha_s^2), \quad (2.2)$$

and

$$|\mathcal{M}_{q\bar{q}g}\rangle = |\mathcal{M}_{q\bar{q}g}^{(0)}\rangle + \mathcal{O}(\alpha_s^2). \quad (2.3)$$

The notation $|\mathcal{M}_{q\bar{q}}\rangle$ and $|\mathcal{M}_{q\bar{q}g}\rangle$ leads us to mention a simplification which we will make in this and all following calculations, namely, for practical purposes we will only be calculating the matrix elements for $\gamma^* \rightarrow q\bar{q} + X$ rather than $e^+e^- \rightarrow q\bar{q} + X$. The reason for doing this is so that we can concentrate on the important part of the calculation, the QCD $q\bar{q} + X$ final state. We are able to do this since the initial electron current ($e^+e^- \rightarrow \gamma^*$) factors out of the cross section and ultimately cancels completely when we calculate the $R^{e^+e^-}$ ratio (both $e^+e^- \rightarrow \mu^+\mu^-$ and $e^+e^- \rightarrow q\bar{q} + X$ have exactly the same initial state configuration and kinematic dependence). Thus,

$$R^{e^+e^-} = \frac{\sigma_{e^+e^- \rightarrow \text{hadrons}}}{\sigma_{e^+e^- \rightarrow \mu^+\mu^-}} = \frac{\sigma_{e^+e^- \rightarrow q\bar{q}+X}}{\sigma_{e^+e^- \rightarrow \mu^+\mu^-}} \equiv \frac{\sigma_{\gamma^* \rightarrow q\bar{q}+X}}{\sigma_{\gamma^* \rightarrow \mu^+\mu^-}}. \quad (2.4)$$

With this in mind, one obtains the cross section,

$$\sigma_{q\bar{q}+X} = \mathcal{F} \int \sum_{\text{spin, col}} \langle \mathcal{M}_{q\bar{q}+X} | \mathcal{M}_{q\bar{q}+X} \rangle d\Pi_n, \quad (2.5)$$

and where $d\Pi_n$ is the differential n body phase-space. \mathcal{F} represents a *flux factor* for the incoming particles and integration over the initial state. As we have just explained, this factor ultimately cancels in the final result. Using (2.2) we can expand the $q\bar{q}$ component of the cross section (2.5) in the coupling constant,

$$\sigma_{q\bar{q}} = \sigma_{q\bar{q}}^0 + \sigma_{q\bar{q}}^1 + \mathcal{O}(\alpha_s^2), \quad (2.6)$$

where

$$\sigma_{q\bar{q}}^0 = \mathcal{F} \int \sum_{\text{spin, col}} \langle \mathcal{M}_{q\bar{q}}^{(0)} | \mathcal{M}_{q\bar{q}}^{(0)} \rangle d\Pi_2, \quad (2.7)$$

and

$$\begin{aligned} \sigma_{q\bar{q}}^1 &= \mathcal{F} \int \sum_{\text{spin, col}} \left[\langle \mathcal{M}_{q\bar{q}}^{(0)} | \mathcal{M}_{q\bar{q}}^{(1)} \rangle + \langle \mathcal{M}_{q\bar{q}}^{(1)} | \mathcal{M}_{q\bar{q}}^{(0)} \rangle \right] d\Pi_2 \\ \sigma_{q\bar{q}}^1 &= \mathcal{F} \int \sum_{\text{spin, col}} 2\Re \left[\langle \mathcal{M}_{q\bar{q}}^{(0)} | \mathcal{M}_{q\bar{q}}^{(1)} \rangle \right] d\Pi_2. \end{aligned} \quad (2.8)$$

We can use (2.3) to expand the $q\bar{q}g$ component of the cross section (2.5) in the coupling constant,

$$\sigma_{q\bar{q}g} = \sigma_{q\bar{q}g}^0 + \mathcal{O}(\alpha_s^2), \quad (2.9)$$

where

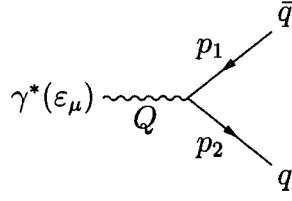
$$\sigma_{q\bar{q}g}^0 = \mathcal{F} \int \sum_{\text{spin, col}} \langle \mathcal{M}_{q\bar{q}g}^{(0)} | \mathcal{M}_{q\bar{q}g}^{(0)} \rangle d\Pi_3. \quad (2.10)$$

In Section 2.2.1 we calculate $\sigma_{q\bar{q}}^0$, in Section 2.2.2 we calculate $\sigma_{q\bar{q}}^1$ and in Section 2.2.2 we calculate $\sigma_{q\bar{q}g}^0$.

2.2.1 $e^+e^- \rightarrow q\bar{q} + X$ at Leading Order

We begin with the lowest order contribution to the process, or LO, that is, $|\mathcal{M}_{q\bar{q}}^{(0)}\rangle$, there is no contribution from $|\mathcal{M}_{q\bar{q}g}^{(0)}\rangle$ since this is one order higher in α_s and contributes to the NLO calculation. At this level only one Feynman diagram contributes, shown in Figure 2.1. Note that we have only shown the $\gamma^* \rightarrow q\bar{q}$ part of the diagram for the reason already mentioned. It is a simple task to calculate the amplitude for this diagram. After simple application of the Feynman rules (Section 1.3) we get

$$i|\mathcal{M}_{q\bar{q}}^{(0)}\rangle = \bar{u}(p_2)(-ie_q\gamma^\mu)\varepsilon_\mu v(p_1), \quad (2.11)$$

Figure 2.1: Feynman diagram for $e^+e^- \rightarrow q\bar{q}$ at leading order.

with e_q the quark charge and ε_μ the photon polarisation. We square the amplitude and sum over spins and colours (and kinematically accessible flavours) giving

$$\sum_{\text{spin, col}} \langle \mathcal{M}_{q\bar{q}}^{(0)} | \mathcal{M}_{q\bar{q}}^{(0)} \rangle = N \sum_{\text{spin}} \sum_q e_q^2 [\bar{u}(p_2) \gamma^\mu v(p_1) \bar{v}(p_1) \gamma^\nu u(p_2) \varepsilon_\mu \varepsilon_\nu^*] \quad (2.12)$$

$$= -N \sum_q e_q^2 \text{tr} [\gamma^\mu \not{p}_1 \gamma_\mu \not{p}_2] , \quad (2.13)$$

where N is the number of colours and the sum over q runs over all quarks which are accessible at a scale Q . Notice that we have taken the massless quark limit, $m_q \rightarrow 0$ in this expression (the mass should appear in the spin sum rules). We have also made use of the following identity

$$\sum_{\text{polarisations}} \varepsilon_\mu \varepsilon_\nu^* \rightarrow -g_{\mu\nu} , \quad (2.14)$$

to sum over the polarisation states of the virtual photon. The trace is easily performed. If we work in CDR then we must apply the Clifford algebra in D dimensions. The squared amplitude becomes

$$\sum_{\text{spin, col}} \langle \mathcal{M}_{q\bar{q}}^{(0)} | \mathcal{M}_{q\bar{q}}^{(0)} \rangle = 2(D-2)sN \sum_q e_q^2 , \quad (2.15)$$

where we have introduced the shorthand notation

$$s = Q^2 = (p_1 + p_2)^2 = 2p_1 \cdot p_2 \quad (\text{for massless particles}) . \quad (2.16)$$

The next step of the calculation is to integrate the ME over phase-space. The integral over the phase-space for two particles is,

$$\int d\Pi_2 = \frac{1}{8\pi} \frac{\Gamma(D/2 - 1)}{\Gamma(D - 2)} \left(\frac{4\pi}{s} \right)^{2-D/2} \int dS \delta(S - s), \quad (2.17)$$

$$= \frac{1}{8\pi} \frac{\Gamma(1 - \epsilon)}{\Gamma(2 - 2\epsilon)} \left(\frac{4\pi}{s} \right)^\epsilon \int dS \delta(S - s). \quad (2.18)$$

Combining all the terms of (2.7) and integrating gives the LO cross section $\sigma_{q\bar{q}}^0$,

$$\sigma_{q\bar{q}}^0 = \mathcal{F} \frac{(D - 2)\Gamma(D/2 - 1)}{\Gamma(D - 2)} \left(\frac{4\pi}{s} \right)^{1-D/2} N \sum_q e_q^2. \quad (2.19)$$

Substituting $D = 4 - 2\epsilon$

$$\sigma_{q\bar{q}}^0 = \mathcal{F} \frac{(2 - 2\epsilon)\Gamma(1 - \epsilon)}{\Gamma(2 - 2\epsilon)} \left(\frac{s}{4\pi} \right)^{1-\epsilon} N \sum_q e_q^2, \quad (2.20)$$

we see that we can safely take the $\epsilon \rightarrow 0$ limit giving the final result,

$$\sigma_{q\bar{q}}^0 = \mathcal{F} \frac{s}{2\pi} N \sum_q e_q^2. \quad (2.21)$$

As we have discussed, it is traditional to present the result in the form of the $R^{e^+e^-}$ ratio

$$R^{e^+e^-} = \frac{\sigma_{e^+e^- \rightarrow q\bar{q}+X}}{\sigma_{e^+e^- \rightarrow \mu^+\mu^-}} \equiv \frac{\sigma_{\gamma^* \rightarrow q\bar{q}+X}}{\sigma_{\gamma^* \rightarrow \mu^+\mu^-}} = N \sum_q e_q^2 (1 + \mathcal{O}(\alpha_s)). \quad (2.22)$$

If we consider energies below the Z exchange threshold $\sqrt{s} \ll M_Z$, and assume that we excite $q = u, d, c, s, b$ then $R^{e^+e^-} = 11/3 = 3.67$. At $\sqrt{s} = 34$ GeV the experimentally determined value is $\mathcal{R}_{\text{exp}}^{e^+e^-} = 3.9^2$. One can also calculate the contribution to the cross section from $Z \rightarrow q\bar{q}$, however the correction is small and our ME result is still some 5% lower than the experimental value. To try to reduce

²As mentioned in Chapter 1, the experimental determination of $R^{e^+e^-}$ is a direct measurement of the number of quark colours N , as seen by Equation (2.22), thus establishing the fact that there are indeed 3 colours.

this discrepancy we must calculate the next order in the perturbative expansion, i.e. the $\mathcal{O}(\alpha_s)$ contribution to (2.22).

2.2.2 $e^+e^- \rightarrow q\bar{q} + X$ at Next-to-Leading Order

We now begin to work at the next order in the perturbative expansion, NLO. We see from expression (2.8) for the cross section $\sigma_{q\bar{q}}^1$ at this order that we need to include the interference of the LO and the one-loop virtual ME. In the next section we look at this contribution.

Virtual Emissions: The One-Loop Correction to $\gamma^* \rightarrow q\bar{q}$

At NLO we get our first contribution from loop-diagrams, for this process we need to calculate a one-loop integral. There is only one type of contribution to virtual emission for the process $e^+e^- \rightarrow q\bar{q}$, corresponding to the emission of a gluon from the outgoing quark which is absorbed by the outgoing anti-quark (and vice-versa)³. This one-loop diagram is shown in Figure 2.2. We apply the Feynman rules as before,

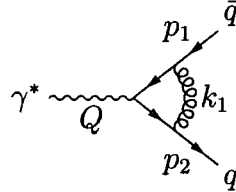


Figure 2.2: Virtual emission contribution to $e^+e^- \rightarrow q\bar{q}$ at NLO.

remembering that we are calculating the interference of LO and virtual diagrams,

$$\sum_{\text{spin, col}} \langle \mathcal{M}_{q\bar{q}}^{(0)} | \mathcal{M}_{q\bar{q}}^{(1)} \rangle = \alpha_s C_F N \sum_q e_q^2 2^{2-D} \pi^{1-D/2} \times \int \frac{d^D k_1}{i\pi^{D/2}} \frac{\text{tr}[\gamma^\mu (\not{k}_1 + \not{p}_2) \gamma^\nu (\not{k}_1 - \not{p}_1) \gamma_\mu \not{p}_1 \gamma_\nu \not{p}_2]}{k_1^2 (k_1 - p_1)^2 (k_1 + p_2)^2}. \quad (2.23)$$

³In fact, there are additional graphs in which the (anti)quark emits and reabsorbs a gluon. These are zero in CDR but must be included in other regularisation schemes.

We can see that this integral is divergent when any factor in the denominator becomes zero. This type of divergence occurs for small values of the loop momenta k_1 and is hence called an *infrared* divergent integral. At first sight these integrals appear to kill our calculation — the result of these integrals will render the prediction for the cross section infinite. As we will see in the next section, we are missing a vital contribution to our calculation which in fact renders the *complete* cross section IR finite. For now we continue to evaluate the expression.

The trace in (2.23) can be calculated and gives rise to terms of the form $k_1 \cdot p_1$, $k_2 \cdot p_2$, k_1^2 etc. The integrals we are faced with calculating have the following structure:

$$\begin{aligned}
 & \int \frac{d^D k_1}{i\pi^{D/2}} \frac{1}{k_1^2 (k_1 - p_1)^2 (k_1 + p_2)^2} && \text{scalar,} \\
 & \int \frac{d^D k_1}{i\pi^{D/2}} \frac{k_1^2}{k_1^2 (k_1 - p_1)^2 (k_1 + p_2)^2} && \text{scalar — pinched,} \\
 & p_{1\mu} \int \frac{d^D k_1}{i\pi^{D/2}} \frac{k_1^\mu}{k_1^2 (k_1 - p_1)^2 (k_1 + p_2)^2} && \text{tensor.} \\
 & p_{1\mu} p_{2\nu} \int \frac{d^D k_1}{i\pi^{D/2}} \frac{k_1^\mu k_1^\nu}{k_1^2 (k_1 - p_1)^2 (k_1 + p_2)^2}
 \end{aligned}$$

At present we do not have the tools to calculate such integrals, these will be discussed in Chapter 3.

The integrations can be performed and the infrared divergences become manifest as poles in the regulating parameter ϵ :

$$\begin{aligned}
 \sum_{\text{spin, col}} \langle \mathcal{M}_{q\bar{q}}^{(0)} | \mathcal{M}_{q\bar{q}}^{(1)} \rangle &= \alpha_s C_F N \sum_q e_q^2 (-1)^{-\epsilon} 2^{1+2\epsilon} \pi^{-1+\epsilon} s^{1-\epsilon} \mu^{2\epsilon} \left(\frac{1-\epsilon}{1-2\epsilon} \right) \\
 &\times \frac{\Gamma(1+\epsilon)\Gamma^2(1-\epsilon)}{\Gamma(1-2\epsilon)} \left[-\frac{1}{\epsilon^2} + \frac{1}{2\epsilon} - 1 \right]. \quad (2.24)
 \end{aligned}$$

In (2.24) we have factored out a combination of gamma functions, these are finite in the $\epsilon \rightarrow 0$ limit

$$\frac{\Gamma(1+\epsilon)\Gamma^2(1-\epsilon)}{\Gamma(1-2\epsilon)} = 1 + \mathcal{O}(\epsilon). \quad (2.25)$$

The next step is to proceed to calculate $\sigma_{q\bar{q}}^1$ by equation (2.8)

$$\sigma_{q\bar{q}}^1 = \mathcal{F} \int \sum_{\text{spin, col}} 2\Re \left[\langle \mathcal{M}_{q\bar{q}}^{(0)} | \mathcal{M}_{q\bar{q}}^{(1)} \rangle \right] d\Pi_2. \quad (2.26)$$

Integrating (2.24) over the two body phase-space given by (2.18) results in

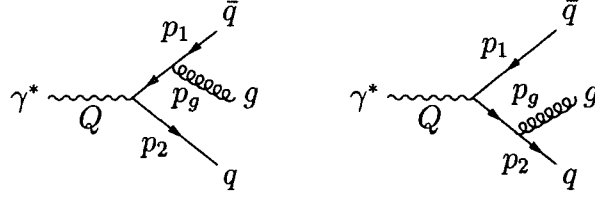
$$\begin{aligned} \sigma_{q\bar{q}}^1 = \sigma_{q\bar{q}}^0 C_F \frac{\alpha_s}{2\pi} \left(\frac{4\pi\mu^2}{s} \right)^\epsilon & \left[-\frac{2}{\epsilon^2} + \frac{(-3 + 2\gamma_E)}{\epsilon} \right. \\ & \left. + (-8 - \gamma_E(\gamma_E - 3) + 7\zeta_2) + \mathcal{O}(\epsilon) \right]. \end{aligned} \quad (2.27)$$

Notice that we have factored out $\sigma_{q\bar{q}}^0$ in (2.27). This expression clearly demonstrates the appearance of infrared divergences in loop calculations. In the next Section we will calculate terms which will ultimately cancel this divergence allowing us to compute a finite cross section.

Real Emissions: The Tree-level $q\bar{q}g$ Contribution

We have seen that the simple calculation of $e^+e^- \rightarrow q\bar{q}$ to NLO with only virtual corrections leads to a divergent result. We know that the cross section must be finite (it is experimentally measurable) so we are clearly not including all effects in our calculation, we do not have a suitably defined inclusive cross section. The missing contribution to the calculation comes from the radiation of real gluons from the quark and antiquark. We will discuss later in section 2.2.3 why it is valid (and necessary) to include these terms in our calculation. For now we assume that they are required and complete the calculation.

At NLO there are two contributions to real emission for the process $e^+e^- \rightarrow q\bar{q}$, each one corresponding to the emission of a gluon from the outgoing quark and antiquark. These are shown in Figure 2.3. Since this process is not a loop-process we label the ME $|\mathcal{M}_{q\bar{q}g}^{(0)}\rangle$. The cross section has a similar structure to that of equation (2.7) except that there are now three particles in the final state and we

Figure 2.3: Real gluon emission contribution to $e^+e^- \rightarrow q\bar{q}$ at NLO.

must use the appropriate phase-space:

$$\sigma_{q\bar{q}g}^0 = \mathcal{F} \int \sum_{\text{spin, col}} \langle \mathcal{M}_{q\bar{q}g}^{(0)} | \mathcal{M}_{q\bar{q}g}^{(0)} \rangle d\Pi_3. \quad (2.28)$$

Applying the Feynman rules and summing over spins and colours gives the squared matrix element

$$\begin{aligned} \sum_{\text{spin, col}} \langle \mathcal{M}_{q\bar{q}g}^{(0)} | \mathcal{M}_{q\bar{q}g}^{(0)} \rangle &= 4\pi\alpha_s\mu^{2e}C_F N \sum_q e_q^2 \left[\frac{\text{I}}{(2p_1 \cdot p_g)^2} + \frac{\text{II}}{(2p_1 \cdot p_g)(2p_2 \cdot p_g)} \right. \\ &\quad \left. + \frac{\text{III}}{(2p_2 \cdot p_g)(2p_1 \cdot p_g)} + \frac{\text{IV}}{(2p_2 \cdot p_g)^2} \right], \end{aligned} \quad (2.29)$$

where **I**, **II**, **III** and **IV** represent trace terms. Note that **I** is the same as **IV** and **II** is the same as **III** under the exchange $p_1 \leftrightarrow p_2$. The traces are:

$$\begin{aligned} \text{I} &= \text{tr} \left[(\not{p}_1 + \not{p}_g) \gamma_\mu \not{p}_1 \gamma^\mu (\not{p}_1 + \not{p}_g) \gamma_\nu \not{p}_2 \gamma^\nu \right] \\ &= 8(D-2)^2 (p_1 \cdot p_g) (p_2 \cdot p_g), \end{aligned} \quad (2.30)$$

$$\begin{aligned} \text{II} &= \text{tr} \left[\gamma^\mu (\not{p}_1 + \not{p}_g) \gamma^\nu \not{p}_1 \gamma_\mu (\not{p}_2 + \not{p}_g) \gamma_\nu \not{p}_2 \right] \\ &= 8(D-2) \left[2(p_1 \cdot p_2)^2 + 2((p_1 \cdot p_g) + (p_2 \cdot p_g))(p_1 \cdot p_2) \right. \\ &\quad \left. + (D-4)(p_1 \cdot p_g)(p_2 \cdot p_g) \right]. \end{aligned} \quad (2.31)$$

For this calculation it is convenient to define energy fractions x_i :

$$x_1 = \frac{2p_1 \cdot Q}{s}, \quad x_2 = \frac{2p_2 \cdot Q}{s}, \quad x_3 = \frac{2p_g \cdot Q}{s}, \quad (2.32)$$

where by energy conservation we must have

$$\sum_{i=1}^3 x_i = 2. \quad (2.33)$$

In terms of the x_i , (2.29) becomes

$$\begin{aligned} \sum_{\text{spin, col}} \langle \mathcal{M}_{q\bar{q}g}^{(0)} | \mathcal{M}_{q\bar{q}g}^{(0)} \rangle &= 8\pi\alpha_s \mu^{2\epsilon} C_F N \sum_q e_q^2 (D-2) \\ &\times \left[(D-2) \left(\frac{1-x_1}{1-x_2} + \frac{1-x_2}{1-x_1} \right) + 4 \frac{x_1+x_2-1}{(1-x_1)(1-x_2)} + 2(D-4) \right]. \end{aligned} \quad (2.34)$$

We have used (2.33) and chosen to eliminate the fraction x_3 , writing the result in terms of x_1 and x_2 . The next step is to integrate over the three body phase-space. In terms of x_i the phase-space is

$$\int d\Pi_3 = \frac{1}{128\pi^3} \frac{s}{\Gamma(2-2\epsilon)} \left(\frac{4\pi}{s} \right)^{2\epsilon} \int \left[\prod_{i=1}^3 dx_i (1-x_i)^{-\epsilon} \right] \delta \left(2 - \sum_{i=1}^3 x_i \right). \quad (2.35)$$

We see in a similar way to which the virtual contribution diverges when we perform the loop integration that the real contribution (2.34) diverges when integrated over phase-space. That is there exist singular regions in phase space. To understand this more clearly, it is more demonstrative to express the momentum fractions x_i in terms of the angle between the quark (antiquark) and gluon, θ_{qg} ($\theta_{\bar{q}g}$):

$$1 - x_1 = \frac{2E_q E_g}{s} (1 - \cos \theta_{qg}) \quad \text{and} \quad 1 - x_2 = \frac{2E_{\bar{q}} E_g}{s} (1 - \cos \theta_{\bar{q}g}). \quad (2.36)$$

We now see the physical origins of the divergences. The factors $1 - x_i$ in the denominator of (2.34) vanish when $E_g \rightarrow 0$ – the gluon becomes *soft* and when $\theta_{qg} \rightarrow 0$

or $\theta_{qg} \rightarrow 0$ – the quark (antiquark) and gluon become *collinear*. Since we have regulated expressions in $D = 4 - 2\epsilon$ these singularities will become manifest as poles in ϵ . The integrations over x_i are easily performed, resulting in the cross section

$$\sigma_{q\bar{q}g}^0 = \sigma_{q\bar{q}}^0 C_F \frac{\alpha_s}{2\pi} \left(\frac{4\pi\mu^2}{s} \right)^\epsilon \left[+ \frac{2}{\epsilon^2} + \frac{(3 - 2\gamma_E)}{\epsilon} + \left(\frac{19}{2} + \gamma_E(\gamma_E - 3) - 7\zeta_2 \right) + \mathcal{O}(\epsilon) \right]. \quad (2.37)$$

We have factored out the LO cross section $\sigma_{q\bar{q}}^0$ just as we did for the virtual contribution.

In the next section we see how the combination of the real and virtual cross sections combine to yield a finite result.

2.2.3 Cancellation of IR Divergences

We have seen that the simple perturbative expansion of the cross section for $e^+e^- \rightarrow q\bar{q}$ yields an infrared divergent result when we start to include higher order contributions, in particular the virtual contributions diverge due to the loop integration.

It was proposed, and shown by example, that the calculation of the cross section is incomplete if only virtual contributions are taken into account, the full, finite cross section is found with the addition of an extra contribution from *real gluon emission*, i.e. we must calculate $e^+e^- \rightarrow q\bar{q} + X$. To finish the calculation we take the results for the two separate divergent contributions, the virtual contribution, $\sigma_{q\bar{q}}^1$ from Equation (2.27) and real contribution $\sigma_{q\bar{q}g}^0$ from Equation (2.37) and we see that the sum of these two contributions is indeed finite in the $\epsilon \rightarrow 0$ limit.

$$\sigma_{q\bar{q}+X}^{tot} = \lim_{\epsilon \rightarrow 0} (\sigma_{q\bar{q}}^0 + \sigma_{q\bar{q}}^1 + \sigma_{q\bar{q}g}^0) + \mathcal{O}(\alpha_s^2), \quad (2.38)$$

$$= \sigma_{q\bar{q}}^0 \left[1 + \frac{\alpha_s}{\pi} + \mathcal{O}(\alpha_s^2) \right]. \quad (2.39)$$

This gives the NLO correction to the $R^{e^+e^-}$ ratio

$$R^{e^+e^-} = N \sum_q e_q^2 \left[1 + \frac{\alpha_s}{\pi} + \mathcal{O}(\alpha_s^2) \right]. \quad (2.40)$$

Taking a value of $\alpha_s = 0.15$ gives $R^{e^+e^-} = 3.84$ which is in better agreement with the experimental measurement $R_{\text{exp}}^{e^+e^-} = 3.9$ taken at an energy $\sqrt{s} = 34$ GeV. This simple example shows how the addition of higher order corrections improve the theoretical prediction of physical observables. One can imagine that adding additional higher orders would yield an even more accurate prediction.

More importantly, we now discuss in more detail the cancellation of the IR divergences. The cancellation of the divergences seems at first sight curious and unmotivated but as one expects it is not. The cancellation of divergences of this form is in fact common to all higher order calculations.

The divergence of the $e^+e^- \rightarrow q\bar{q}$ cross-section shows that we cannot calculate this as an *exclusive process*. To calculate $e^+e^- \rightarrow \text{hadrons}$ we should calculate $e^+e^- \rightarrow q\bar{q} + X$ which is suitably inclusive and finite. We have seen that the divergences of the real amplitude occurred for particular configurations of the partons in phase space — when the gluon and (anti)quark become *collinear* or when the gluon becomes *soft*. We know experimentally about *confinement* which is the observation that no physical states are coloured. In experiments we do not observe the partons but *jets*. Jets are collimated beams of colourless hadrons produced by the *hadronisation* of partons. After the hadronisation process the soft and collinear particles become indistinguishably mixed into the jets — at least at the level of experimental detection which is limited by finite angular and energy resolutions, see Figure 2.4. In other words, when the gluon is very soft or collinear, the $q\bar{q}g$ state is ‘mistaken’ for a $q\bar{q}$ state. What we measure in a detector, the observable cross section is therefore finite and independent of the unphysical singular regions.

The general cancellation of IR divergences between the soft and collinear and

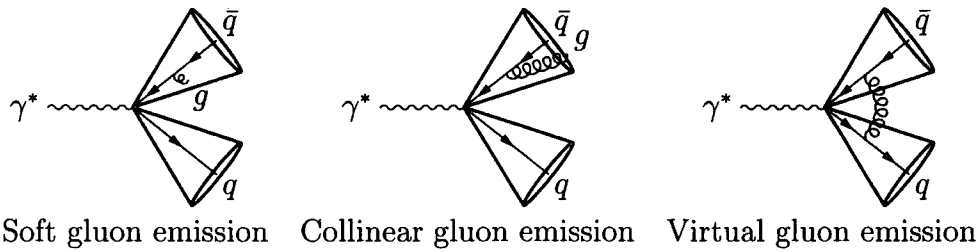


Figure 2.4: The configurations whereby the gluon is either soft or collinear are kinematically degenerate to the virtual gluon contribution and cannot be distinguished experimentally — the jet structure is identical.

the virtual contributions is *guaranteed* by the *Kinoshita–Lee–Nauenberg* [14, 15] and *Bloch–Nordsieck* [16] theorems. These theorems state that for a well defined, suitably inclusive observable, i.e. one which takes into account all degenerate, physically indistinguishable states, will be finite. Quantities for which this true are called *IR safe observables*. We have already calculated on such observable, the inclusive cross-section for $e^+e^- \rightarrow \text{hadrons}$.

The IR divergences cancel order by order in the perturbative series. For this reason their structure is *predictable*. In the following Sections we look at the idea and tools developed by Catani and Seymour to make such a prediction.

2.3 Matrix Elements in Colour Space

Having seen an example of how IR divergences appear in the calculation of ME and how the different components of the calculation ‘conspire’ to cancel these divergences, it is useful to study their structure in a more general way. In this Section we look at an important tool developed by Catani and Seymour [26] which enables us to predict the pole structure of IR divergent amplitudes.

Before the discussion of the IR divergent structure it is necessary to introduce the idea of MEs in *colour space*. In this discussion we follow closely the notation presented in [26].

We begin by considering the tree-level amplitude with m QCD partons in the

*final state*⁴. It has the following structure:

$$\mathcal{M}_m^{c_1, \dots, c_m; s_1, \dots, s_m}(p_1, \dots, p_m) \equiv \mathcal{M}_m^{c_1, \dots, c_m; s_1, \dots, s_m}(\{p\}), \quad (2.41)$$

where $\{c_1, \dots, c_m\}$ are the *colour indices*, $\{s_1, \dots, s_m\}$ are the spins or *helicities* and $\{p_1, \dots, p_m\}$ the momenta. In particular, $c_n = \{i\} = 1, 2, 3$ for (anti)quarks and $c_n = \{a\} = 1, \dots, 8$ for gluons, also, $s_n = 1, 2$ for (anti)quarks and $s_n = 1, \dots, D-2$ for gluons.

Since the amplitude is a function of the colours and helicities we can consider the amplitude living in a colour + helicity space. We introduce a basis $\{|c_1, \dots, c_m\rangle \otimes |s_1, \dots, s_m\rangle\}$ such that

$$\mathcal{M}_m^{c_1, \dots, c_m; s_1, \dots, s_m}(\{p\}) = (\langle c_1, \dots, c_m| \otimes \langle s_1, \dots, s_m|) |\mathcal{M}_m(\{p\})\rangle. \quad (2.42)$$

In general, we would like to calculate colour and spin summed amplitudes, these can be written as

$$|\mathcal{M}_m(\{p\})|^2 = \langle \mathcal{M}_m(\{p\}) | \mathcal{M}_m(\{p\}) \rangle. \quad (2.43)$$

Having established notation, we are now in a position to study the colour structure of an amplitude. Colour interactions are represented by the association of a *colour-charge operator* \mathbf{T}_n with the emission of a gluon from each parton n . If the emitted gluon has colour index c_g then the colour-charge operator is

$$\mathbf{T}_n \equiv T_n^{c_g} |c_g\rangle, \quad (2.44)$$

which acts in colour space as

$$\langle c_1, \dots, c_n, \dots, c_m, c_g | \mathbf{T}_n | b_1, \dots, b_n, \dots, b_m \rangle = \delta_{c_1 b_1} \dots T_{c_n b_n}^{c_g} \dots \delta_{c_m b_m}, \quad (2.45)$$

⁴We consider an e^+e^- type process. The notation can be extended to include a QCD initial state.

where $T_{c_m b_m}^{c_g}$ is a colour-charge matrix. It is given by

$$T_{c_m b_m}^{c_g} = \begin{cases} t_{c_m b_m}^{c_g} & \text{if emitter is quark } (c_m, b_m = 1, 2, 3), \\ -t_{c_m b_m}^{c_g} & \text{if emitter is antiquark } (c_m, b_m = 1, 2, 3), \\ i f^{c_g c_m b_m} & \text{if emitter is gluon } (c_m, b_m = 1, \dots, 8). \end{cases} \quad (2.46)$$

That is, if the emitting particle is a (anti)quark then \mathbf{T}_n is a colour-charge matrix in the fundamental representation, if the emitting particle is a gluon \mathbf{T}_n is a matrix in the adjoint representation (see Section 1.2).

In this language, the state $|\mathcal{M}_m(\{p\})\rangle$ is a colour singlet (all physical states must be), so colour conservation implies

$$\sum_{n=1}^m \mathbf{T}_n |\mathcal{M}_m(\{p\})\rangle = 0. \quad (2.47)$$

In the next Section we will be dealing with *colour correlated amplitudes*. These correspond to calculating the product of an amplitude for emitting a gluon from particle n with an amplitude for the emission of a gluon by particle o ,

$$\begin{aligned} |\mathcal{M}_m^{n,o}|^2 &= \langle \mathcal{M}_m(\{p\}) | \mathbf{T}_n \cdot \mathbf{T}_o | \mathcal{M}_m(\{p\}) \rangle \\ &= [\mathcal{M}_m^{c_1, \dots, c_n, \dots, c_o, \dots, c_m}(\{p\})]^* T_{c_n b_n}^{c_g} T_{c_o b_o}^{c_g} \mathcal{M}_m^{c_1, \dots, b_n, \dots, b_o, \dots, c_m}(\{p\}). \end{aligned} \quad (2.48)$$

The colour algebra is simply

$$\mathbf{T}_n \cdot \mathbf{T}_m = \begin{cases} \mathbf{T}_m \cdot \mathbf{T}_n & \text{if } m \neq n, \\ \mathbf{T}_n^2 = C_n & \text{if } m = n, \end{cases} \quad (2.49)$$

where C_n is the Casimir operator, i.e. $C_n = C_F$ if n is a (anti)quark or $C_n = C_A$ if n is a gluon (see Section 1.7).

2.4 Singular Behaviour of Loop Amplitudes

Let us begin by considering a general renormalised QCD amplitude $|\mathcal{M}\rangle$ in colour space with m external legs. We choose to work in the $\overline{\text{MS}}$ scheme and we use CDR. The general perturbative expansion of $|\mathcal{M}\rangle$ will have the following structure,

$$|\mathcal{M}\rangle = \left(\frac{\alpha_s}{2\pi}\right)^q \left[|\mathcal{M}^{(0)}\rangle + \left(\frac{\alpha_s}{2\pi}\right) |\mathcal{M}^{(1)}\rangle + \left(\frac{\alpha_s}{2\pi}\right)^2 |\mathcal{M}^{(2)}\rangle + \mathcal{O}(\alpha_s^3) \right], \quad (2.50)$$

where α_s denotes the strong coupling constant, and $|\mathcal{M}^{(i)}\rangle$ are the i -loop contributions to the renormalised amplitude. Notice that in contrast to the perturbative expansion we made for the $e^+e^- \rightarrow q\bar{q}$ matrix element (Eq. (2.2)) we have pulled all factors of α_s out of the matrix elements $|\mathcal{M}^{(i)}\rangle$. The overall coefficient in front of the expression, $(\alpha_s/2\pi)^q$ is general where q is half-integer, the specific value is process dependent. We know that the amplitudes $|\mathcal{M}^{(1)}\rangle, |\mathcal{M}^{(2)}\rangle, \dots$ will contain IR divergences. Catani and Seymour have shown [26] that we can explicitly isolate the singularities of the one-loop amplitude from the finite part with the following construction,

$$|\mathcal{M}^{(1)}\rangle = \mathbf{I}^{(1)}(\epsilon) |\mathcal{M}^{(0)}\rangle + |\mathcal{M}^{(1),\text{fin}}\rangle, \quad (2.51)$$

where $|\mathcal{M}^{(1),\text{fin}}\rangle$ represents the finite part of the one-loop amplitude in the $\epsilon \rightarrow 0$ limit.

The *insertion operator* $\mathbf{I}^{(1)}(\epsilon)$ acts in general on a colour vector $|\mathcal{M}^{(0)}\rangle$ generating the singular behaviour. It has a general structure

$$\mathbf{I}^{(1)}(\epsilon) = \frac{1}{2} \frac{e^{\epsilon\gamma_E}}{\Gamma(1-\epsilon)} \sum_i \nu_i^{\text{sing}}(\epsilon) \sum_{j \neq i} \mathbf{T}_i \cdot \mathbf{T}_j \left(\frac{\mu^2 e^{-i\lambda_{ij}\pi}}{2p_i \cdot p_j} \right)^\epsilon, \quad (2.52)$$

where $i, j = 1, 2, \dots, m$ and p_i is the momenta of the i -th external particle and

$$\lambda_{ij} = \begin{cases} 1 & \text{if partons } i \text{ and } j \text{ are both incoming or outgoing,} \\ 0 & \text{otherwise.} \end{cases} \quad (2.53)$$

The singular terms are embedded in the function $\mathcal{V}_i^{\text{sing}}(\epsilon)$:

$$\mathcal{V}_i^{\text{sing}}(\epsilon) = \frac{1}{\epsilon^2} + \frac{\gamma_i}{\epsilon}, \quad (2.54)$$

where

$$\gamma_i = \begin{cases} 3/2 & \text{if particle } i \text{ is a } \textit{quark} \text{ or } \textit{antiquark}, \\ \beta_0/C_A & \text{if particle } i \text{ is a } \textit{gluon}, \end{cases} \quad (2.55)$$

with β_0 the first beta function coefficient defined by Equation (1.39).

Catani has extended the formalism to work to two-loops [29]. At this level the situation is more complicated, the singularities now have a more complex structure. We can still factorise the poles from the finite part of the amplitude, and for the two-loop amplitude have the following construction

$$|\mathcal{M}^{(2)}\rangle = \mathbf{I}^{(1)}(\epsilon)|\mathcal{M}^{(1)}\rangle + \mathbf{I}^{(2)}(\epsilon)|\mathcal{M}^{(0)}\rangle + |\mathcal{M}^{(2),\text{fin}}\rangle, \quad (2.56)$$

where similarly, $|\mathcal{M}^{(2),\text{fin}}\rangle$ represents the finite part of the two-loop amplitude in the $\epsilon \rightarrow 0$ limit. The $\mathbf{I}^{(1)}(\epsilon)$ operator has the same definition as before given by equation (2.52). Acting on the one-loop amplitude $|\mathcal{M}^{(1)}\rangle$, the $\mathbf{I}^{(1)}(\epsilon)$ multiplies the singularities already present (both single and double poles) and produces poles $1/\epsilon$, $1/\epsilon^2$, $1/\epsilon^3$ and $1/\epsilon^4$. We have introduced a new operator, $\mathbf{I}^{(2)}(\epsilon)$, this term acts on the tree level amplitude $|\mathcal{M}^{(0)}\rangle$ and also produces poles up to order $1/\epsilon^4$. It has the

following structure

$$\begin{aligned} \mathbf{I}^{(2)}(\epsilon) = & -\frac{1}{2}\mathbf{I}^{(1)}(\epsilon) \left(\mathbf{I}^{(1)}(\epsilon) + \frac{2\beta_0}{\epsilon} \right) + \frac{e^{-\epsilon\gamma_E}\Gamma(1-2\epsilon)}{\Gamma(1-\epsilon)} \left(\frac{\beta_0}{\epsilon} + K \right) \mathbf{I}^{(1)}(2\epsilon) \\ & + \mathbf{H}^{(2)}(\epsilon), \end{aligned} \quad (2.57)$$

with,

$$K = \left(\frac{67}{18} - \frac{\pi^2}{6} \right) C_A - \frac{10}{9} T_R N_F. \quad (2.58)$$

The last term of equation (2.57) involves $\mathbf{H}^{(2)}(\epsilon)$ which produces only a single pole in ϵ and is given by,

$$\langle \mathcal{M}^{(0)} | \mathbf{H}^{(2)}(\epsilon) | \mathcal{M}^{(0)} \rangle = \frac{e^{\epsilon\gamma_E}}{4\epsilon\Gamma(1-\epsilon)} H^{(2)} \langle \mathcal{M}^{(0)} | \mathcal{M}^{(0)} \rangle, \quad (2.59)$$

where the constant $H^{(2)}$ is renormalisation-scheme-dependent. Using equation (2.56) we can therefore predict the pole structure for two-loop amplitudes exactly up to $\mathcal{O}(1/\epsilon^2)$, and also some of the $\mathcal{O}(1/\epsilon)$ structure but its complete form can at present only be found by explicit calculation of the amplitude with Feynman diagrams.

Using equations (2.51) and (2.56) we have factorised the IR singular contributions of the one- and two-loop amplitudes. The pole structure of the one-loop amplitude is completely determined and the pole structure of the two-loop amplitude completely determined to $\mathcal{O}(1/\epsilon^2)$. These predictions serve as a very strong test of a ME calculation. We use these later to check the pole structure of the our complete ME result.

2.4.1 Ultraviolet Renormalisation

Throughout we have been using *renormalised* amplitudes, however, in a calculation with Feynman diagrams we construct *unrenormalised* amplitudes, the two are of course related. If we consider the analogous perturbative series to (2.50) in terms

of unrenormalised amplitudes

$$|\mathcal{M}^{\text{un}}\rangle = \left(\frac{\alpha_0}{2\pi}\right)^q \left[|\mathcal{M}^{(0),\text{un}}\rangle + \left(\frac{\alpha_0}{2\pi}\right) |\mathcal{M}^{(1),\text{un}}\rangle + \left(\frac{\alpha_0}{2\pi}\right)^2 |\mathcal{M}^{(2),\text{un}}\rangle + \mathcal{O}(\alpha_u^3) \right], \quad (2.60)$$

then the renormalised amplitudes are found by replacing the bare coupling α_0 with the renormalised coupling α_s as determined by Equation (1.46). After substitution of α_0 and by comparison with the renormalised amplitude (2.50) order by order in α_s we find

$$\begin{aligned} |\mathcal{M}^{(0)}\rangle &= |\mathcal{M}^{(0),\text{un}}\rangle, \\ |\mathcal{M}^{(1)}\rangle &= S_\epsilon^{-1} |\mathcal{M}^{(1),\text{un}}\rangle - \frac{q\beta_0}{\epsilon} |\mathcal{M}^{(0),\text{un}}\rangle, \\ |\mathcal{M}^{(2)}\rangle &= S_\epsilon^{-2} |\mathcal{M}^{(2),\text{un}}\rangle - \frac{(1+q)\beta_0}{\epsilon} S_\epsilon^{-1} |\mathcal{M}^{(1),\text{un}}\rangle - \frac{q}{2} \left(\frac{\beta_1}{\epsilon} - \frac{\beta_0^2(1+q)}{\epsilon^2} \right) |\mathcal{M}^{(0),\text{un}}\rangle. \end{aligned} \quad (2.61)$$

where S_ϵ is defined by Equation (1.47).

2.4.2 $I^{(1)}(\epsilon)$ for $e^+e^- \rightarrow q\bar{q}$

To demonstrate the use of the $I^{(1)}(\epsilon)$ operator in predicting the pole structure of ME we construct a very simple example and verify the result for $e^+e^- \rightarrow q\bar{q}$ calculated in Section 2.2.2.

From the structure of $I^{(1)}(\epsilon)$ (Equation (2.52)) we see that we need to determine the products of all the colour-charge operators for the process, which in this example is simple since there is only one product, $\mathbf{T}_q \cdot \mathbf{T}_{\bar{q}}$. By colour conservation (Equation (2.47)) we have

$$\mathbf{T}_q = -\mathbf{T}_{\bar{q}}, \quad (2.62)$$

so that

$$\mathbf{T}_q \cdot \mathbf{T}_{\bar{q}} = -\mathbf{T}_q^2 = -\mathbf{T}_{\bar{q}}^2 = -C_F. \quad (2.63)$$

The equation for the insertion operator, which is a 1×1 matrix in colour space

becomes

$$\begin{aligned} I^{(1)}(\epsilon) &= -C_F \frac{e^{\epsilon\gamma_E}}{\Gamma(1-\epsilon)} \left[\frac{1}{\epsilon^2} + \frac{3}{2\epsilon} \right] \left(-\frac{\mu^2}{s} \right)^\epsilon \\ &= -\frac{C_F}{S_\epsilon} \frac{1}{\Gamma(1-\epsilon)} \left[\frac{1}{\epsilon^2} + \frac{3}{2\epsilon} \right] \left(-\frac{4\pi\mu^2}{s} \right)^\epsilon. \end{aligned} \quad (2.64)$$

Here we have used (1.47) to write $e^{\epsilon\gamma_E}$ in terms of S_ϵ to make the comparison with the virtual amplitude easier. This insertion operator acting on the tree level amplitude $|\mathcal{M}_{q\bar{q}}^{(0)}\rangle$ should produce the singular structure $|\mathcal{M}_{q\bar{q}}^{(1),\text{sing}}\rangle$ of the one-loop virtual amplitude $|\mathcal{M}_{q\bar{q}}^{(1)}\rangle$. That is

$$\langle \mathcal{M}_{q\bar{q}}^{(0)} | \mathcal{M}_{q\bar{q}}^{(1),\text{sing}} \rangle = \langle \mathcal{M}_{q\bar{q}}^{(0)} | \left(\frac{\alpha_s}{2\pi} \right) I^{(1)}(\epsilon) | \mathcal{M}_{q\bar{q}}^{(0)} \rangle, \quad (2.65)$$

where we have contracted with the tree-level amplitude. The factor of $\alpha_s/2\pi$ is present because it was factorised out of the definition of the perturbative expansion (Equation (2.50)). In principle the insertion operator should be acting on *renormalised* amplitudes. The relation between the renormalised and unrenormalised amplitudes is given by (2.61) where for this process we take $q = 0$. In this case the tree-level amplitudes remain unchanged. Making an ϵ -expansion of (2.65) gives the *predicted* singularity structure

$$\begin{aligned} \langle \mathcal{M}_{q\bar{q}}^{(0)} | \mathcal{M}_{q\bar{q}}^{(1),\text{sing}} \rangle_r &= \frac{C_F}{S_\epsilon} \frac{\alpha_s}{2\pi} \left(-\frac{4\pi\mu^2}{s} \right)^\epsilon \left[-\frac{1}{\epsilon^2} + \frac{(-3 + 2\gamma_E)}{2\epsilon} \right. \\ &\quad \left. + \left(-\frac{\gamma_E(\gamma_E - 3)}{2} + \frac{1}{2}\zeta_2 \right) + \mathcal{O}(\epsilon) \right] \langle \mathcal{M}_{q\bar{q}}^{(0)} | \mathcal{M}_{q\bar{q}}^{(0)} \rangle_r. \end{aligned} \quad (2.66)$$

The notation $\langle \dots | \dots \rangle_r$ indicates renormalised amplitudes. To compare with the *calculated* amplitude we require $\langle \mathcal{M}_{q\bar{q}}^{(0)} | \mathcal{M}_{q\bar{q}}^{(1)} \rangle_r$. This can be expressed in terms of

$\langle \mathcal{M}_{q\bar{q}}^{(0)} | \mathcal{M}_{q\bar{q}}^{(0)} \rangle_r$ (to match the previous result) by using the following trick,

$$\begin{aligned}
 \langle \mathcal{M}_{q\bar{q}}^{(0)} | \mathcal{M}_{q\bar{q}}^{(1)} \rangle_r &= \frac{1}{S_\epsilon} \langle \mathcal{M}_{q\bar{q}}^{(0)} | \mathcal{M}_{q\bar{q}}^{(1)} \rangle \quad (\text{renormalisation of } |\mathcal{M}_{q\bar{q}}^{(1)}\rangle \text{ by (2.61)}) \\
 &= \frac{1}{S_\epsilon} \frac{\sigma_{q\bar{q}}^1}{2\sigma_{q\bar{q}}^0} \langle \mathcal{M}_{q\bar{q}}^{(0)} | \mathcal{M}_{q\bar{q}}^{(0)} \rangle \\
 &= \frac{1}{S_\epsilon} \frac{\sigma_{q\bar{q}}^1}{2\sigma_{q\bar{q}}^0} \langle \mathcal{M}_{q\bar{q}}^{(0)} | \mathcal{M}_{q\bar{q}}^{(0)} \rangle_r. \tag{2.67}
 \end{aligned}$$

This relation just comes from Equations (2.7) and (2.8) and uses the fact that the integration over the two-body phase space factorises and cancels between the two cross sections $\sigma_{q\bar{q}}^0$ and $\sigma_{q\bar{q}}^1$. Combining (2.67) with the expression for $\sigma_{q\bar{q}}^1$ from Equation (2.27) gives,

$$\begin{aligned}
 \langle \mathcal{M}_{q\bar{q}}^{(0)} | \mathcal{M}_{q\bar{q}}^{(1)} \rangle_r &= \frac{C_F \alpha_s}{S_\epsilon 2\pi} \left(-\frac{4\pi\mu^2}{s} \right)^\epsilon \left[-\frac{1}{\epsilon^2} + \frac{(-3 + 2\gamma_E)}{2\epsilon} \right. \\
 &\quad \left. + \left(-4 - \frac{\gamma_E(\gamma_E - 3)}{2} + \frac{7}{2}\zeta_2 \right) + \mathcal{O}(\epsilon) \right] \langle \mathcal{M}_{q\bar{q}}^{(0)} | \mathcal{M}_{q\bar{q}}^{(0)} \rangle_r. \tag{2.68}
 \end{aligned}$$

Finally, from Equations (2.66) and (2.68) it can clearly be seen that the insertion operator correctly predicts the singularity structure and also the dependence on γ_E — thus providing a strong check of the calculation of $|\mathcal{M}_{q\bar{q}}^{(1)}\rangle$.

CHAPTER 3

Loop Integrals

3.1 Introduction

We saw in Chapter 2 that the calculation of ME, in particular, the virtual contributions, require the calculation of loop integrals. In the simple example of $e^+e^- \rightarrow q\bar{q}$ at NLO only a few simple one-loop integrals were required. In general, however, for a more complex ME at higher orders, a calculation may involve many *hundreds* of integrals with *multiple loops*. The integrals fall into two classes, *scalar* and *tensor*, depending on the structure present in the numerator of the integral. Tensor integrals are indicative of the spin structure of the theory. The number of loops are associated with the order to which we are working in perturbation theory.

In this thesis we calculate the NNLO $\mathcal{O}(\alpha_s^3)$ virtual contributions to the $e^+e^- \rightarrow q\bar{q}g$ ME. As we shall see in Chapter 4 at this order there are two components to the virtual contributions, the two-loop times tree amplitude as well one-loop times one-loop amplitude. Therefore, in this chapter we deal with the tools necessary to deal with both one- and two-loop integrals arising from this process.

It is only really in the past few years that significant technical developments in the field have made the calculation of large numbers of loop-integrals a tractable problem. Indeed, the techniques which we discuss have recently been put to great use

in the calculation of two-loop QED and QCD corrections to many $2 \rightarrow 2$ scattering processes with massless on-shell external particles [30, 31, 32, 33, 34, 35, 36].

We begin in Section 3.2 by introducing the general structure of loop integrals and the notation used to describe them. In Section 3.2.1 we find it convenient to introduce a practical tool called an *auxiliary diagram*. There are two types of auxiliary diagram corresponding to both planar and non-planar integrals. The idea of these diagrams is to encapsulate the structure of all the possible integrals enabling a more systematic approach to relating and reducing integrals of different kinds to simpler ones. With the idea of the auxiliary diagram we describe the symmetries of the integrals in Section 3.2.2.

The first approach to calculating loop-integrals considered in Section 3.3 is *parameterisation*. In particular we look at the Schwinger and Feynman parameterisations. In some cases, use of these techniques may enable direct evaluation of an integral, often by identification of the parameterised result as an integral representation of a hypergeometric function. However, in general, for all but the simplest integrals, more work is needed.

It is convenient at this point to talk about *tensor reduction*, that is, how we can relate integrals with tensorial structure in the numerator to simpler integrals. In Section 3.4 we discover that we can translate the task of calculating tensor integrals to that of calculating *simpler* scalar integrals in *higher dimensions*. Since this technique produces integrals in higher dimensions, Section 3.4.1 deals with the process of relating scalar integrals in different dimensions.

Having reduced the problem of calculating tensor integrals to that of calculating scalar integrals we introduce in Section 3.5 the technique of Integration-by-Parts (IBP) [17, 37, 38] a tool which is now commonly used in the calculation of loop integrals. The principle use of IBP is to construct linear relations between loop integrals of different complexity. By extracting more complicated integrals in favour of simpler ones the IBP relations can reduce the problem of calculating many

hundreds of integrals to a collection of a small set of so-called Master Integrals (MI).

More recently, a more automated approach to combining and solving the IBP relations has been suggested by Laporta [39]. In this approach both tensor and scalar integrals are treated on the *same* footing. By making this step we are able to use an algorithmic solution of the IBP equations relating all of the tensor and scalar integrals to a small set of MI in one fell swoop, circumventing the need for explicit tensor reduction and the calculation of scalar integrals in higher dimensions. The modified Laporta algorithm used in this thesis is presented in Section 3.6.

Finally, since the MI are not calculable by IBP — by definition, they must be determined by other techniques. Fortunately, there has been significant progress in this area too. In the past, techniques such as Mellin-Barnes (MB) and Negative Dimensions (NDIM) have been used for the calculation of MI [40, 41, 42, 43, 44]. These techniques are complicated when an integral is a function of many scales and the methods ultimately rely on one being able to identify the integral representation of hypergeometric functions. However, more recently Gehrmann and Remiddi have developed an approach to solving the MI by using *differential equations* [45, 46]. In fact, all the relevant MI, both planar and non-planar for *eeqqg* were calculated with differential equations [47, 48] paving the way for the calculation of the ME. In Section 3.7 we show how to construct and solve the differential equations for the MI.

3.2 Basic Notation / Generalities

In general, the loop integrals which we need to calculate are governed by the particular physical process which they are derived from. In this thesis we must calculate integrals which have the same generic structure characterised in Figure 3.1 by integrals with up to *four external legs* with *three on-shell* and *one off-shell*. The on-shell legs correspond to the q , \bar{q} and g whilst the off-shell leg corresponds to the γ^* . Since

we wish to calculate to NNLO in perturbation theory we require integrals with both *one-* and *two-loops*. Our emphasis will focus more on the calculation of the two-loop integrals, but the techniques are equally applicable to any number of loops via appropriate modifications. We begin our task by classifying the many integrals

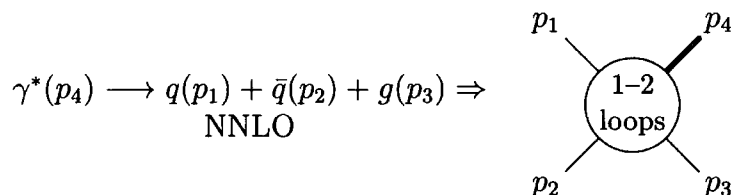


Figure 3.1: The generic integrals of interest have four external legs. Three legs are on-shell, $p_1^2 = p_2^2 = p_3^2 = 0$. One leg is off-shell, $p_4^2 = (-p_1 - p_2 - p_3)^2 \neq 0$. In general we must consider both one- and two-loop integrals.

which may be generated by the MEs. As we shall see in Chapter 4 there are a total (including tree, one-loop and two-loop) of 244 Feynman diagrams contributing to $e^+e^- \rightarrow q\bar{q}g$ at NNLO, of which, three example diagrams are shown in Figure 3.2. The first observation is that there are two types of diagram leading to two differ-

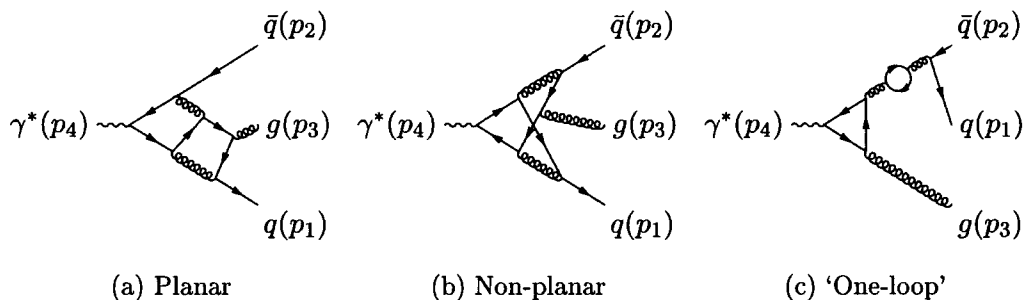


Figure 3.2: Example Feynman diagrams contributing to $e^+e^- \rightarrow q\bar{q}g$.

ent classes of integral, namely *planar* and *non-planar* integrals, two examples are shown in Figures 3.2(a) and 3.2(b). As we shall see, these are *distinct* and indeed are described by different sets of propagators — the non-planar propagators cannot be represented as a linear combination of planar propagators. A second observation is that the integrals carry a *tensor structure* in their numerator. This can be seen in the example of $e^+e^- \rightarrow q\bar{q}$ in Section 2.2.2. This is a direct consequence of the

spin structure of the particles in the interactions. A final remark is that some of the apparent two-loop graphs are in fact products of two one-loop graphs. This results in these integrals being far simpler than their true two-loop counterparts. An example of a diagram which is in fact a product of one-loop integrals is shown in Figure 3.2(c).

When referring to loop-integrals it is useful to speak about the *topology* of an integral. Integrals of the same topology have equivalent propagators. By this we mean they are either identical or can be made identical by a linear transformation of loop-momenta and a possible re-arrangement of the external momenta.

We write our general D -dimensional scalar integral with N_k loops and N_d propagators in the denominator as:

$$\mathcal{I}^D(\{\nu_{N_d}\})[1] = \int \frac{d^D k_1}{i\pi^{D/2}} \cdots \int \frac{d^D k_{N_k}}{i\pi^{D/2}} \frac{1}{A_1^{\nu_1} \cdots A_{N_d}^{\nu_{N_d}}}, \quad (3.1)$$

with propagators

$$\frac{1}{A_i} = \frac{1}{P_i^2 - m_i^2 + i0}. \quad (3.2)$$

The notation is straightforward. The set $\{\nu_{N_d}\}$ represents the powers of the propagators of the integral, effectively defining its topology. The '[1]' represents the structure of the numerator, in this case we have a scalar integral. Ultimately we would like to consider tensorial integrals, we can represent these generically by

$$\mathcal{I}^D(\{\nu_{N_d}\})[k_1^{\mu_1} \cdots k_1^{\mu_a} \cdots k_{N_k}^{\nu_1} \cdots k_{N_k}^{\nu_b}] = \int \frac{d^D k_1}{i\pi^{D/2}} \cdots \int \frac{d^D k_{N_k}}{i\pi^{D/2}} \frac{k_1^{\mu_1} \cdots k_1^{\mu_a} \cdots k_{N_k}^{\nu_1} \cdots k_{N_k}^{\nu_b}}{A_1^{\nu_1} \cdots A_{N_d}^{\nu_{N_d}}}. \quad (3.3)$$

All the integrals are also functions of the external momenta p_1, \dots, p_{N_p} or equivalently the external scales $s_{ij} = (p_i + p_j)^2$. We drop these presently for clarity but will introduce them when necessary.

For the i -th propagator defined in (3.2), the P_i term represents a linear combi-

nation of loop and external momenta

$$P_i = \sum_{j=1}^{N_k} a_j^i k_j + \sum_{j=1}^{N_p} b_j^i p_j, \quad (3.4)$$

with $a_j^i = -1, 0, 1$ and $b_j^i = -1, 0, 1$. The m_i represents the mass of the propagating particles. We will be working in the massless quark limit so for the rest of this thesis we take $m_i = 0$. The $i0$ term is the Feynman prescription which is used to specify the analytic properties of the integral when translating between different kinematic regions of phase space. This notation will be implied throughout but not written explicitly for clarity.

3.2.1 Auxiliary Diagrams

As we have already discussed, the physical process of interest imposes that we should calculate planar and non-planar two-loop graphs with four external legs. The corresponding integrals have a structure that can best be described in terms of so-called ‘*auxiliary diagrams*’. An auxiliary diagram is the most general diagram we can construct which contains all of the possible propagators. For a graph with N_k loops and N_p independent external momenta we can form $N_{sp} = N_p N_k + N_k(N_k + 1)/2$ independent scalar products. With three independent external momenta, $N_p = 3$ and two-loops, $N_k = 2$ there are nine possible scalar-products, $N_{sp} = 9$. The idea of the auxiliary diagram is to map these nine scalar-products as propagators. Later (in Section 3.5.1) we will represent scalar-products in the numerator of an integral (associated with tensor integrals) by propagators raised to negative powers. Figure 3.3 illustrates the auxiliary diagram for planar integrals. This diagram is non-physical but does satisfy momentum conservation. To obtain a real diagram one must shrink at least two of the propagators to zero. The process of shrinking a propagator to zero is called ‘*pinching*’. This also enables us to define a ‘*sub-topology*’ as a diagram created from a larger topology by a pinching.

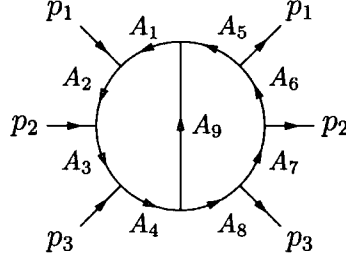


Figure 3.3: The two-loop planar auxiliary diagram. All nine possible scalar products are mapped to the propagators $A_1 \rightarrow A_9$ given by equations (3.5).

We also have the non-planar integrals. Due to the asymmetry caused by the off-shell leg we require two auxiliary diagrams. These are illustrated in Figures 3.4 and 3.5.

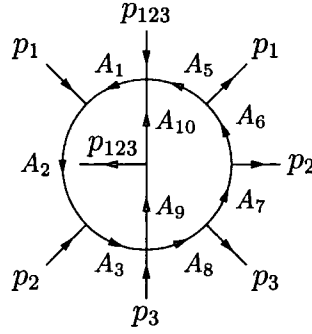


Figure 3.4: The two-loop non-planar auxiliary diagram with the off-shell leg inside.

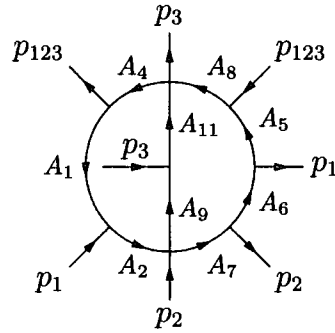


Figure 3.5: The two-loop non-planar auxiliary diagram with the off-shell leg outside.

Given these auxiliary diagrams we choose to define the propagators as follows:

$$\begin{aligned}
 A_1 &= k_1^2, & A_5 &= k_2^2, & A_9 &= (k_1 - k_2)^2, \\
 A_2 &= (k_1 + p_1)^2, & A_6 &= (k_2 + p_1)^2, & A_{10} &= (k_1 - k_2 - p_{123})^2, \\
 A_3 &= (k_1 + p_{12})^2, & A_7 &= (k_2 + p_{12})^2, & A_{11} &= (k_1 - k_2 + p_3)^2. \\
 A_4 &= (k_1 + p_{123})^2, & A_8 &= (k_2 + p_{123})^2, & &
 \end{aligned} \tag{3.5}$$

We have introduced a shorthand notation, $p_{i\dots j} \equiv p_i + \dots + p_j$. Since three external legs are on-shell and one off-shell we impose the following, ‘physically motivated’ conditions

$$p_1^2 = p_2^2 = p_3^2 = 0, \tag{3.6}$$

and

$$(p_1 + p_2 + p_3)^2 = p_{123}^2 = s_{123} \neq 0. \tag{3.7}$$

We will also use the following Mandelstam invariants

$$s_{12} = (p_1 + p_2)^2, \quad s_{13} = (p_1 + p_3)^2, \quad s_{23} = (p_2 + p_3)^2, \tag{3.8}$$

which fulfil

$$s_{12} + s_{13} + s_{23} = s_{123}. \tag{3.9}$$

3.2.2 Symmetries

If we look more closely at the auxiliary diagram for the planar diagrams, Figure 3.3, we can see that it exhibits a great deal of symmetry, this is one of the key advantages of the auxiliary diagrams. The symmetries arise from the exchange of both propagators and external momenta which leave the fundamental diagram (topology) unchanged. It is worth briefly mentioning the symmetries because they can greatly reduce the number of integrals that we need to calculate. The planar dia-

gram as it stands has three main symmetries. The first is trivial and arises due to the invariance of relabelling the loop momenta, $k_1 \leftrightarrow k_2$,

$$\mathcal{I}^D(\{\nu_1, \nu_2, \nu_3, \nu_4, \nu_5, \nu_6, \nu_7, \nu_8, \nu_9\}, \{s_{12}, s_{23}, s_{123}\}) [1] = \mathcal{I}^D(\{\nu_5, \nu_6, \nu_7, \nu_8, \nu_1, \nu_2, \nu_3, \nu_4, \nu_9\}, \{s_{12}, s_{23}, s_{123}\}) [1] . \quad (3.10)$$

Note that we have introduced the scales s_{ij} into the integral¹. The reason for this is that the symmetries are created by exchanging propagators as well as the external momentum, thus we need to keep track of both changes. The second symmetry is found by exchanging the external momenta, $p_1 \leftrightarrow p_3$,

$$\mathcal{I}^D(\{\nu_1, \nu_2, \nu_3, \nu_4, \nu_5, \nu_6, \nu_7, \nu_8, \nu_9\}, \{s_{12}, s_{23}, s_{123}\}) [1] = \mathcal{I}^D(\{\nu_4, \nu_3, \nu_2, \nu_1, \nu_8, \nu_7, \nu_6, \nu_5, \nu_9\}, \{s_{23}, s_{12}, s_{123}\}) [1] . \quad (3.11)$$

And finally we can apply both of the above symmetries at the same time, $k_1 \leftrightarrow k_2$ and $p_1 \leftrightarrow p_3$,

$$\mathcal{I}^D(\{\nu_1, \nu_2, \nu_3, \nu_4, \nu_5, \nu_6, \nu_7, \nu_8, \nu_9\}, \{s_{12}, s_{23}, s_{123}\}) [1] = \mathcal{I}^D(\{\nu_8, \nu_7, \nu_6, \nu_5, \nu_4, \nu_3, \nu_2, \nu_1, \nu_9\}, \{s_{23}, s_{12}, s_{123}\}) [1] . \quad (3.12)$$

As we take pinchings of the auxiliary diagram (we must pinch at least two propagators to produce a physical diagram) more symmetries may appear. For example, if we pinch propagators 4 and 8 then a $p_1 \leftrightarrow p_2$ symmetry emerges.

The non-planar diagrams do not exhibit any immediate symmetry, however, as we take pinchings and remove propagators symmetries may become apparent. Once we have pinched four of the nine propagators on either of the non-planar diagrams they become inherently planar. Once we reach this stage the symmetries already

¹We choose to label the integrals in terms of the scales s_{ij} rather than the momenta p_i since these are what actually appear in the final results of calculations.

identified for the planar diagrams can be applied.

By using the symmetries we can eliminate all similar diagrams and calculate a smaller set of integrals, i.e. we can remove all diagrams of the same topology which are related by a relabelling of propagators and/or momenta.

3.3 Parameterisation

In general it is very hard to take the loop integral defined in Equation (3.1) and directly perform the loop integration. Instead we begin by parameterising the integral in such a way that the integration over the loop momentum becomes trivial. What we are left with is a new integral representation which is usually more amenable to direct calculation. For many of the simple integrals these representations result in hypergeometric functions. As mentioned earlier, we will consider the two approaches of Schwinger and Feynman. The basic idea behind both of these approaches is to compress the product of propagators in the denominator into one quadratic term. By diagonalising the integral we are easily able to integrate away the loop momenta.

3.3.1 Schwinger Parameterisation

The idea of Schwinger is to use the property of the exponential function, $e^a e^b = e^{a+b}$ so that we can write the product of propagators a linear sum. To do this, we write the propagators by using the following relation

$$\frac{1}{A^\nu} = \frac{(-1)^\nu}{\Gamma(\nu)} \int_0^\infty dx x^{\nu-1} \exp(xA), \quad (3.13)$$

which applied to all propagators gives

$$\frac{1}{A_1^{\nu_1} \cdots A_{N_d}^{\nu_{N_d}}} = \left[\prod_{i=1}^{N_d} \frac{(-1)^{\nu_i}}{\Gamma(\nu_i)} \int_0^\infty dx_i x_i^{\nu_i-1} \right] \exp \left(\sum_{i=1}^{N_d} x_i A_i \right) \quad (3.14)$$

$$= \int \mathcal{D}x \exp \left(\sum_{i=1}^{N_d} x_i A_i \right), \quad (3.15)$$

where

$$\int \mathcal{D}x \equiv \left[\prod_{i=1}^{N_d} \frac{(-1)^{\nu_i}}{\Gamma(\nu_i)} \int_0^\infty dx_i x_i^{\nu_i-1} \right]. \quad (3.16)$$

Since we will use this notation later we have defined the shorthand $\int \mathcal{D}x$ to represent all integrations over the Schwinger parameters x_i .

The result of this parameterisation is to enable us to readily integrate away the dependence on the loop momenta k_i . To see how this is carried out it is useful to study the structure of propagator polynomial $\sum x_i A_i$. We can expand this term explicitly in the loop momenta, which for a two-loop integral gives rise to the following general quadratic structure

$$\sum_{i=1}^{N_d} x_i A_i = a k_1^2 + b k_2^2 + 2c k_1 \cdot k_2 + 2d \cdot k_1 + 2e \cdot k_2 + f, \quad (3.17)$$

where a, b, c, d^μ, e^μ and f are all linear in x_i . The structure of these coefficients is determined by the particular topology of an integral. They can be calculated generically for the auxiliary diagrams. To do this we simply substitute the propagators A_i given by (3.5) into the l.h.s. of Equation (3.17), expand and compare the coefficients

of k_i . For the *planar auxiliary diagram* of Figure 3.3 we get

$$\begin{aligned}
 a &= x_1 + x_2 + x_3 + x_4 + x_9 , \\
 b &= x_5 + x_6 + x_7 + x_8 + x_9 , \\
 c &= -x_9 , \\
 d^\mu &= (x_2 + x_3 + x_4)p_1^\mu + (x_3 + x_4)p_2^\mu + x_4p_3^\mu , \\
 e^\mu &= (x_6 + x_7 + x_8)p_1^\mu + (x_7 + x_8)p_2^\mu + x_8p_3^\mu , \\
 f &= (x_3 + x_7)s_{12} + (x_4 + x_8)s_{123} .
 \end{aligned} \tag{3.18}$$

This result can now be used for any topology by simply setting $x_i = 0$ for all pinched propagators A_i .

By diagonalising the polynomial of (3.17) with respect to k_1 and k_2 the corresponding integrals in these variables are easily calculable. Diagonalisation can be achieved with the following changes of variable

$$k_1^\mu \rightarrow K_1^\mu - \frac{c}{a}K_2^\mu + \mathcal{X}^\mu , \tag{3.19}$$

$$k_2^\mu \rightarrow K_2^\mu + \mathcal{Y}^\mu , \tag{3.20}$$

where

$$\mathcal{X}^\mu = \frac{ce^\mu - bd^\mu}{\mathcal{P}} , \tag{3.21}$$

$$\mathcal{Y}^\mu = \frac{cd^\mu - ae^\mu}{\mathcal{P}} , \tag{3.22}$$

and

$$\mathcal{P} = ab - c^2 . \tag{3.23}$$

Notice that \mathcal{X} , \mathcal{Y} and \mathcal{P} are all bilinear in x_i . We are able to make the diagonalisation

due to a specific property of scalar loop integrals. We make use of the fact that they are invariant under shifts of the loop momentum

$$\int \frac{d^D k_a}{i\pi^{D/2}} f(k_a) \equiv \int \frac{d^D k_b}{i\pi^{D/2}} f(k_b) \quad \text{where} \quad k_b = k_a + \delta. \quad (3.24)$$

Thus the process of diagonalisation by Equations (3.19) and (3.20) has no effect on the structure of the generic loop integral. The polynomial (3.17) becomes

$$\sum_{i=1}^{N_d} x_i A_i = a K_1^2 + \frac{\mathcal{P}}{a} K_2^2 + \frac{\mathcal{Q}}{\mathcal{P}}, \quad (3.25)$$

where

$$\mathcal{Q} = -ae^2 - bd^2 + 2c(e \cdot d) + f\mathcal{P}. \quad (3.26)$$

Evaluating \mathcal{P} and \mathcal{Q} for the planar auxiliary diagram gives

$$\mathcal{P} = (x_1 + x_2 + x_3 + x_4 + x_9)(x_5 + x_6 + x_7 + x_8 + x_9) - x_9^2 \quad (3.27)$$

and

$$\begin{aligned} \mathcal{Q} = & \left[((x_5 + x_6 + x_7 + x_8 + x_9)x_3 + x_7x_5 + x_7x_9)x_1 \right. \\ & \left. + ((x_2 + x_3 + x_4 + x_9)x_7 + x_3x_9)x_5 \right] s_{12} \\ & \left[((x_5 + x_6 + x_7 + x_8 + x_9)x_4 + x_8x_6 + x_9x_8)x_2 \right. \\ & \left. + ((x_1 + x_3 + x_4 + x_9)x_8 + x_4x_9)x_6 \right] s_{23} \\ & \left[((x_5 + x_6 + x_7 + x_8 + x_9)x_4 + x_8x_5 + x_9x_8)x_1 \right. \\ & \left. + ((x_2 + x_3 + x_4 + x_9)x_8 + x_4x_9)x_5 \right] s_{123}. \end{aligned} \quad (3.28)$$

We can now return our attention back to the loop integral itself to see what we have achieved. Consider the generic integral (3.1), in the two-loop limit (for which the polynomial (3.17) is valid). After Schwinger parameterisation (3.14) and diagonali-

sation we can write

$$\mathcal{I}^D(\{\nu_{N_d}\})[1] = \left[\prod_{i=1}^{N_d} \frac{(-1)^{\nu_i}}{\Gamma(\nu_i)} \int_0^\infty dx_i x_i^{\nu_i-1} \right] \times \int \frac{d^D K_1}{i\pi^{D/2}} \int \frac{d^D K_2}{i\pi^{D/2}} \exp \left(aK_1^2 + \frac{\mathcal{P}}{a} K_2^2 + \frac{\mathcal{Q}}{\mathcal{P}} \right), \quad (3.29)$$

or in shorthand notation

$$\mathcal{I}^D(\{\nu_{N_d}\})[1] = \int \mathcal{D}x \int \frac{d^D K_1}{i\pi^{D/2}} \int \frac{d^D K_2}{i\pi^{D/2}} \exp \left(aK_1^2 + \frac{\mathcal{P}}{a} K_2^2 + \frac{\mathcal{Q}}{\mathcal{P}} \right). \quad (3.30)$$

The loop integrations are now readily integrated in K_1 and K_2 (recall that \mathcal{P} and \mathcal{Q} are only functions of the Schwinger parameters x_i and the external momenta p_i). To carry out these integrations we make use of an important identity, the Minkowski space relation

$$\int \frac{d^D k}{i\pi^{D/2}} \exp(\Delta k^2) = \frac{1}{\Delta^{D/2}}. \quad (3.31)$$

Applying this to each integral in turn gives

$$\mathcal{I}^D(\{\nu_{N_d}\})[1] = \left[\prod_{i=1}^{N_d} \frac{(-1)^{\nu_i}}{\Gamma(\nu_i)} \int_0^\infty dx_i x_i^{\nu_i-1} \right] \frac{1}{\mathcal{P}^{D/2}} \exp \left(\frac{\mathcal{Q}}{\mathcal{P}} \right), \quad (3.32)$$

$$= \int \mathcal{D}x \frac{1}{\mathcal{P}^{D/2}} \exp \left(\frac{\mathcal{Q}}{\mathcal{P}} \right), \quad (3.33)$$

the Schwinger parameterised form of the loop-integral for the auxiliary diagram. All two-loop scalar integrals can be written in this form and the appropriate \mathcal{P} and \mathcal{Q} read directly from the diagram.

3.3.2 Feynman Parameterisation

We now look at the Feynman parameterisation. This works in a similar way to the Schwinger approach in that the method involves re-writing the product of propagators in a linear form which can easily be integrated. The technique of Feynman

parameterisation is particularly useful when one is calculating relatively simple integrals directly. We begin with the following relation

$$\frac{1}{A_1^{\nu_1} \cdots A_{N_d}^{\nu_{N_d}}} = \Gamma(N) \left[\prod_{i=1}^{N_d} \frac{1}{\Gamma(\nu_i)} \int_0^1 dx_i x_i^{\nu_i-1} \right] \delta \left(1 - \sum_{i=1}^{N_d} x_i \right) \left(\sum_{i=1}^{N_d} x_i A_i \right)^{-N}, \quad (3.34)$$

where

$$N = \sum_{i=1}^{N_d} \nu_i. \quad (3.35)$$

We observe that this relation produces exactly the same effect as the Schwinger parameterisation, namely, the product of propagators have been transformed into a linear polynomial. This polynomial is identical to that which we obtained by Schwinger parameterisation, i.e. Equation (3.17), meaning that we can use exactly the same changes of variables to diagonalise the loop integration. After applying the Feynman parameterisation (3.34) to the generic integral (3.1) and after diagonalisation, we get

$$\mathcal{I}^D(\{\nu_{N_d}\})[1] = \Gamma(N) \left[\prod_{i=1}^{N_d} \frac{1}{\Gamma(\nu_i)} \int_0^1 dx_i x_i^{\nu_i-1} \right] \delta \left(1 - \sum_{i=1}^{N_d} x_i \right) \times \int \frac{d^D K_1}{i\pi^{D/2}} \int \frac{d^D K_2}{i\pi^{D/2}} \left(aK_1^2 + \frac{\mathcal{P}}{a} K_2^2 + \frac{\mathcal{Q}}{\mathcal{P}} \right)^{-N}. \quad (3.36)$$

Note that K_1 , K_2 , \mathcal{P} and \mathcal{Q} have exactly the same definition in terms of the x_i as those for Schwinger parameterisation. To integrate away the loop momentum we make use of the following identity [1]

$$\int \frac{d^D k}{i\pi^{D/2}} \frac{1}{(k^2 - \Delta)^\alpha} = (-1)^\alpha \frac{\Gamma(\alpha - D/2)}{\Gamma(\alpha)} \Delta^{D/2-\alpha}. \quad (3.37)$$

Finally for the Feynman parameterisation after integration we obtain

$$\mathcal{I}^D(\{\nu_{N_d}\})[1] = (-1)^D \Gamma(N-D) \left[\prod_{i=1}^{N_d} \frac{1}{\Gamma(\nu_i)} \int_0^1 dx_i x_i^{\nu_i-1} \right] \delta\left(1 - \sum_{i=1}^{N_d} x_i\right) \times \mathcal{P}^{N-3D/2} \mathcal{Q}^{D-N}, \quad (3.38)$$

From this result we can now see an important feature of the Feynman method. This is that due to the delta function we effectively have one less integral over the Feynman parameters x_i to carry out than we did in the Schwinger parameterisation.

3.3.3 Direct Approaches to Integration

At this point it is not clear what we have achieved. So far we have transformed the integrations over the loop momenta to integrations over a new set of parameters. For Schwinger parameterisation the number of new parameters is equal to the number of propagators and for Feynman parameterisation is equal to the number of propagators minus one. This means that we have effectively increased the number of integrations! Despite the apparent increase in complexity these two parameterisations are particularly useful for evaluating simple loop integrals directly. Usually the integrations over the new parameters can be identified as the integral representations of hypergeometric functions, thus the apparent integrations need not be carried out explicitly at all.

3.4 Tensor Reduction

We can now turn our attention to tensor integrals. So far we have only considered scalar integrals. We have seen how the reparameterisation can enable us to directly evaluate simple integrals. We must now consider how we calculate tensor integrals.

The Schwinger parameterisation can be easily extended to describe tensor inte-

grals. Since the steps in the parameterisation only dealt with the propagators in the denominator of the loop integral, we can quite easily apply the same parameterisation to the tensor integral. We must however, be careful to remember that we diagonalised the result of the parameterisation and in doing so shifted the loop momenta. If we recall the diagonalised expression for the Schwinger integral before we integrated out the loop momenta, i.e. Equation (3.30),

$$\mathcal{I}^D(\{\nu_{N_d}\})[1] = \int \mathcal{D}x \int \frac{d^D K_1}{i\pi^{D/2}} \int \frac{d^D K_2}{i\pi^{D/2}} \exp\left(aK_1^2 + \frac{\mathcal{P}}{a}K_2^2 + \frac{\mathcal{Q}}{\mathcal{P}}\right). \quad (3.39)$$

Then we generalise this to include tensors by simply inserting them into the numerator

$$\begin{aligned} \mathcal{I}^D(\{\nu_{N_d}\})[k_1^{\mu_1} \dots k_1^{\mu_a} k_2^{\nu_1} \dots k_2^{\nu_b}] &= \int \mathcal{D}x \int \frac{d^D K_1}{i\pi^{D/2}} \int \frac{d^D K_2}{i\pi^{D/2}} \times \\ &\underbrace{\left(K_1^{\mu_1} - \frac{c}{a}K_2^{\mu_1} + \mathcal{X}^{\mu_1}\right)}_{k_1^{\mu_1}} \dots \underbrace{\left(K_1^{\mu_a} - \frac{c}{a}K_2^{\mu_a} + \mathcal{X}^{\mu_a}\right)}_{k_1^{\mu_a}} \underbrace{(K_2^{\nu_1} + \mathcal{Y}^{\nu_1})}_{k_2^{\nu_1}} \dots \underbrace{(K_2^{\nu_b} + \mathcal{Y}^{\nu_b})}_{k_2^{\nu_b}} \times \\ &\exp\left(aK_1^2 + \frac{\mathcal{P}}{a}K_2^2 + \frac{\mathcal{Q}}{\mathcal{P}}\right). \end{aligned} \quad (3.40)$$

Notice that we have replaced the tensors k_1^μ and k_2^ν on the right hand side of the generic tensor integral (3.3) with the corresponding shifted variables given by Equations (3.19) and (3.20). Again we can integrate out the loop momenta K_1 and K_2 easily using identities similar to the Minkowski space relation (3.31). For example,

$$\int \frac{d^D k}{i\pi^{D/2}} k^\mu \exp(\Delta k^2) = 0, \quad (3.41)$$

$$\int \frac{d^D k}{i\pi^{D/2}} k^\mu k^\nu \exp(\Delta k^2) = -\frac{1}{2\Delta} g^{\mu\nu} \frac{1}{\Delta^{D/2}}, \quad (3.42)$$

⋮

$$\int \frac{d^D k}{i\pi^{D/2}} k^\mu k^\nu k^\rho k^\sigma \exp(\Delta k^2) = \frac{1}{4\Delta^2} (g^{\mu\nu} g^{\rho\sigma} + g^{\mu\rho} g^{\nu\sigma} + g^{\mu\sigma} g^{\nu\rho}) \frac{1}{\Delta^{D/2}}. \quad (3.43)$$

So that, if we take a single tensor, for example $\mathcal{I}^D(\{\nu_{N_d}\})[k_1^\mu]$ we have,

$$\mathcal{I}^D(\{\nu_{N_d}\})[k_1^\mu] = \int \mathcal{D}x \int \frac{d^D K_1}{i\pi^{D/2}} \int \frac{d^D K_2}{i\pi^{D/2}} \left(K_1^\mu - \frac{c}{a} K_2^\mu + \mathcal{X}^\mu \right) \times \exp \left(a K_1^2 + \frac{\mathcal{P}}{a} K_2^2 + \frac{\mathcal{Q}}{\mathcal{P}} \right), \quad (3.44)$$

which can now be easily integrated in K_1 and K_2 to give,

$$\mathcal{I}^D(\{\nu_{N_d}\})[k_1^\mu] = \int \mathcal{D}x \mathcal{X}^\mu \frac{1}{\mathcal{P}^{D/2}} \exp \left(\frac{\mathcal{Q}}{\mathcal{P}} \right) \quad (3.45)$$

$$= \int \mathcal{D}x \frac{ce^\mu - bd^\mu}{\mathcal{P}} \frac{1}{\mathcal{P}^{D/2}} \exp \left(\frac{\mathcal{Q}}{\mathcal{P}} \right). \quad (3.46)$$

If we recall the definition of \mathcal{X}^μ from equation (3.21) and the appropriate a , b , c , d^μ , e^μ and f from equation (3.18), then we see that the numerator is a bilinear in x_i and the denominator is simply \mathcal{P} . We therefore absorb the x_i into $\mathcal{D}x$ by increasing the powers of the appropriate propagators, i.e.,

$$\frac{(-1)^{\nu_i}}{\Gamma(\nu_i)} x_i^{\nu_i-1} \times x_i \longrightarrow -\nu_i \frac{(-1)^{\nu_i+1}}{\Gamma(\nu_i+1)} x_i^{\nu_i} \sim -\nu_i \mathbf{i}^+, \quad (3.47)$$

such that,

$$\mathbf{i}^+ \mathcal{I}^D(\{\nu_{N_d}\})[1] = \mathcal{I}^D(\nu_1, \dots, \nu_i + 1, \dots, \nu_n)[1] \quad (3.48)$$

While we absorb the \mathcal{P} into the remaining factors,

$$\frac{1}{\mathcal{P}} \frac{1}{\mathcal{P}^{D/2}} \longrightarrow \frac{1}{\mathcal{P}^{(D+2)/2}} \sim \mathbf{d}^+, \quad (3.49)$$

such that,

$$\mathbf{d}^+ \mathcal{I}^D(\{\nu_{N_d}\})[1] = \mathcal{I}^{D+2}(\{\nu_n\})[1]. \quad (3.50)$$

If we put all this together we can see what has been achieved. We now have the ability to write tensor integrals as linear combination scalar integrals in higher di-

mensions with increased powers of propagators.

$$\mathcal{I}^D(\{\nu_{N_d}\})[k_1^\mu] = \sum_{i,j,k} \nu_i \nu_j p_k^\mu \mathbf{i}^+ \mathbf{j}^+ \mathbf{d}^+ \mathcal{I}^D(\{\nu_{N_d}\})[1] \quad (3.51)$$

$$= \sum_{i,j,k} \nu_i \nu_j p_k^\mu \mathcal{I}^{D+2}(\nu_1, \dots, \nu_i + 1, \dots, \nu_j + 1, \dots, \nu_{N_d})[1] \quad (3.52)$$

The sum over i, j and k will be determined by the particular topology of an integral, namely particular structure of the \mathcal{X}^μ . The process of writing the tensor integral as a combination of scalar integrals can be extended for more complicated tensors, we simply generate more terms in \mathcal{X} and \mathcal{Y} .

3.4.1 Dimensional Shift

We have seen how we can write tensor integrals as a sum of scalar integrals in higher dimensions. For every tensor index present we produce an increase in dimension by two, i.e., a fourth rank tensor will be described by a sum of scalar integrals in $D + 8$ dimensions and each having eight extra powers on the propagators. After re-expressing the tensor integrals we therefore expect to have integrals in $D, D + 2, D + 4, \dots$ dimensions. Rather than calculate all of these separately it would be convenient if they could all be related. Dimensional shift is just such a tool. The technique uses a trick similar to that which we used for the tensor reduction itself. If we go back to our integral after Schwinger parameterisation, equation (3.33),

$$\mathcal{I}^D(\{\nu_{N_d}\})[1] = \int \mathcal{D}x \frac{1}{\mathcal{P}^{D/2}} \exp\left(\frac{\mathcal{Q}}{\mathcal{P}}\right), \quad (3.53)$$

then we can add an extra factor of \mathcal{P} to both the numerator and denominator (leaving the integral unchanged). Recall that \mathcal{P} is only a function of the x_i , therefore, the factor in the numerator can be absorbed into the $\mathcal{D}x$ to increase powers of propagators and the \mathcal{P} in the denominator will increase the dimension, exactly as

we did before in equations (3.47) and (3.49). More explicitly,

$$\mathcal{I}^D(\{\nu_{N_d}\})[1] = \int \mathcal{D}x \frac{\mathcal{P}}{\mathcal{P}^{(D+2)/2}} \exp\left(\frac{\mathcal{Q}}{\mathcal{P}}\right), \quad (3.54)$$

$$= \sum_{i,j} \nu_i \nu_j \mathcal{I}^{D+2}(\nu_1, \dots, \nu_i + 1, \dots, \nu_j + 1, \dots, \nu_{N_d})[1]. \quad (3.55)$$

The sum over the indices i and j will be determined by the topology of an integral. The result is very similar to that which we produced for tensor integrals. Now however, we have a relation between scalar integrals in different dimensions. At present we are able to go no further, the integrals on the right-hand side of the expression all have higher powers of propagators. In Section 3.5 we will develop a technique called IBP which will enable us to reduce these powers of propagators to linear combinations of integrals with unit powers. Let us assume that we are able to do this for integrals on the right-hand side of our expression. We will get,

$$\mathcal{I}_i^D(\{\nu_{N_d}\})[1] = \sum_j C_{ij} \mathcal{I}_j^{D+2}(\{\nu_{N_d}\})[1]. \quad (3.56)$$

The integrals on both sides of the expression now have unit powers. The coefficients C_{ij} form an invertible matrix, these coefficients are produced by the action of the IBP reduction. We would like to work in the opposite sense however, that is, we would like to know integrals in $D+2$ dimensions in terms of integrals in D dimensions so, the final task is to invert the system.

We must now deal with a large number of scalar integrals with increased powers of propagators in higher dimensions. Note that for each index of a tensor integral we must raise the power of two propagators by one and increase the dimension by two. Then, for example, a fourth rank tensor (the highest required) will be a sum of integrals with eight extra powers of propagators and eight extra dimensions. An established method to deal with integrals with large numbers of powers of propagators is Integration-by-Parts.

3.5 Integration-by-Parts

The method of parameterisation discussed so far led to several techniques which are extremely useful for calculating many simple topology integrals. However, as we have seen, a matrix element calculation involves many scalar and tensor integrals. We may know how to deal with tensor integrals but what we have learnt is that a single tensor integral will reduce to a sum of many scalar integrals in higher dimensions with higher powers of propagators. We are left to calculate many hundreds of scalar integrals. Using the direct approach, is therefore, not a feasible one, it is too large a task — we need to look for a way of reducing the number of integrals that must be calculated by ‘brute force’. One such alternative approach is Integration-by-Parts (IBP). IBP is a powerful technique introduced by Tkachov and Chetyrkin in the 1980’s and is now widely used to calculate loop integrals [17, 37, 38]. The idea of the method is to circumvent calculating every individual integral but instead to relate integrals of different topology and with different powers of propagators to one and other. Using these relations we can then extract the more complicated integrals and write them in terms of the simpler ones. At the end of this reduction process we cannot eliminate all integrals since we are not solving the integrals directly, but what we are hopefully left with is a set of relations which will reduce many of the complicated integrals to a small set of easier integrals. This remaining set of integrals are known as Master Integrals (MI). It is the small number of MI which then have to then be calculated via a different method, usually by direct methods already discussed.

3.5.1 Construction of the IBP Identities

As mentioned, the idea behind IBP is to find relations between closed sets of integrals of varying complexity (i.e. different powers of propagators and different topology).

We use these relations to extract the complex integrals in terms of simpler ones.

To create these relations we make use of the translational invariance of dimensionally regulated loop integrals. This is expressed by following identity for the integral of a total derivative with vanishing surface terms

$$\int \frac{d^D k_1}{i\pi^{D/2}} \cdots \int \frac{d^D k_{N_k}}{i\pi^{D/2}} \frac{\partial}{\partial k_i^\mu} \left[\frac{V^\mu}{A_1^{\nu_1} \cdots A_{N_d}^{\nu_{N_d}}} \right] \equiv 0, \quad (3.57)$$

where $i = 1 \dots N_k$ and V^μ could be any linear combination of the loop momenta k_i^μ and external momenta p . We have chosen to use,

$$\begin{aligned} V^\mu &= k_i^\mu, \\ &k_i^\mu + p_1^\mu, \\ &k_i^\mu + p_1^\mu + p_2^\mu, & \text{for } i = 1, \dots, N_k \\ &\vdots \\ &k_i^\mu + p_1^\mu + \cdots + p_{N_p}^\mu. \end{aligned} \quad (3.58)$$

With all possible independent choices of momenta for V we can construct $N_{IBP} = N_k(N_k + N_p)$ IBP identities. With two-loops and three independent external momenta we get ten identities.

Let us consider the action of the derivative. We generate two types of term, the first term comes from the action of the derivative on the numerator, the second from the action on the denominator,

$$\frac{\partial}{\partial k_i^\mu} \left[\frac{V^\mu}{A_1^{\nu_1} \cdots A_{N_d}^{\nu_{N_d}}} \right] = \left(\frac{\partial V^\mu}{\partial k_i^\mu} \right) \frac{1}{A_1^{\nu_1} \cdots A_{N_d}^{\nu_{N_d}}} + V^\mu \left(\frac{\partial}{\partial k_i^\mu} \frac{1}{A_1^{\nu_1} \cdots A_{N_d}^{\nu_{N_d}}} \right) \quad (3.59)$$

For the first term, the derivative acting on V^μ will be zero unless it contains the momenta with which we are taking the derivative, in which case the result will simply be D . When the derivative acts on the second term we produce more interesting results. Firstly, it is convenient to recall our notation for the propagators A_i , defined

by equations (3.2) and (3.4),

$$\frac{1}{A_i} = \frac{1}{P_i^2} = \frac{1}{\left(\sum_j a_j^i k_j + \sum_j b_j^i p_j\right)^2}, \quad (3.60)$$

where we have taken the massless quark limit and dropped the '+i0' notation for brevity. We can now take the derivative,

$$V^\mu \left(\frac{\partial}{\partial k_i^\mu} \frac{1}{A_1^{\nu_1} \dots A_{N_d}^{\nu_{N_d}}} \right) = \sum_j \frac{-2\nu_j a_i^j}{A_1^{\nu_1} \dots A_j^{\nu_j+1} \dots A_{N_d}^{\nu_{N_d}}} \left(\sum_l a_l^j k_l \cdot V + \sum_l b_l^j p_l \cdot V \right). \quad (3.61)$$

The sum over j on the right-hand side is to indicate that we get a contribution from each propagator that contains the loop momentum k_i with which we are taking the derivative.

On the right-hand side of equation (3.61) we have created scalar products. Given our choice of V^μ (equation (3.58)) these products will either be products only involving external momenta or products with at least one loop momenta. The first kind can be trivially associated with the external scales, s_{12} , s_{23} and s_{123} . The latter, we write in terms of the basis set of propagators, given by equation (3.5). For example, with the planar propagators we can express all possible scalar products as,

$$\begin{aligned} k_1 \cdot k_1 &= A_1, & k_2 \cdot k_2 &= A_5, \\ k_1 \cdot p_1 &= \frac{1}{2}(A_2 - A_1), & k_2 \cdot p_1 &= \frac{1}{2}(A_6 - A_5), \\ k_1 \cdot p_2 &= \frac{1}{2}(A_3 - A_2 - s_{12}), & k_2 \cdot p_2 &= \frac{1}{2}(A_7 - A_6 - s_{12}), \\ k_1 \cdot p_3 &= \frac{1}{2}(A_4 - A_3 - s_{123} + s_{12}), & k_2 \cdot p_3 &= \frac{1}{2}(A_8 - A_7 - s_{123} + s_{12}), \\ k_1 \cdot k_2 &= \frac{1}{2}(A_1 + A_5 - A_9). \end{aligned} \quad (3.62)$$

In deriving these relations we have used the properties of the external legs given by equations (3.6) and (3.7). This allows us to set $p_1^2 = 0$ for example.

Now that the scalar products have been written in terms of the propagators we are able to cancel through with the propagators already present in the integral, i.e. those present in the denominator of equation (3.61). If a propagator is already present and we decrease its power then we have a *reducible numerator*. If the propagator is not present in the original integral then it will remain in the numerator and is called an *irreducible numerator*. We represent Irreducible Numerators (IN) by propagators which are raised to a negative power. Therefore, reducible numerators create simpler integrals with smaller powers of propagators, whereas the IN create more complex integrals with tensorial structure.

At present the introduction of IN is troublesome since we want to construct algorithms which can reduce purely scalar integrals which have propagators with increased powers in the denominator only. We see in the next section that we have to construct combinations of identities which are free of IN. When we come to consider a more automated approach to solving the IBP identities we see that we can actually use the IN to our advantage. The IN correspond to tensor integrals, precisely what we are trying to calculate! In the automated approach we therefore treat scalar and tensor integrals together and we use the IBP equations to do the tensor reduction for us. We eliminate the need for the technique which we have discussed in section 3.4 which produces scalar integrals with very high powers and requires a method to shift the dimensions of the scalar integrals.

3.5.2 IBP Identities for the Planar Auxiliary Diagram

We have seen how we can construct the IBP equations in a very general way. The method that we have outlined can be applied to both the planar and non-planar diagrams equally well. In this section we show the ten IBP equations for the planar auxiliary diagram to clarify our notation and to demonstrate the structure of the equations more explicitly. We use the i^+ and i^- notation that we have already

introduced, where, for example,

$$\frac{1}{A_1^{\nu_1} A_2^{\nu_2+1} A_3^{\nu_3-1} A_4^{\nu_4} \dots A_9^{\nu_9}} = \mathbf{2}^+ \mathbf{3}^- \frac{1}{A_1^{\nu_1} \dots A_9^{\nu_9}} \quad (3.63)$$

With this notation the ten planar IBP equations for the auxiliary diagram are,

$$\begin{aligned} s_{12}\nu_1 \mathbf{1}^+ \mathcal{I}^D(\{\nu_{N_d}\})[1] = \\ - (D - \nu_1 - \nu_2 - 2\nu_3 - \nu_4 - \nu_9) \mathcal{I}^D(\{\nu_{N_d}\})[1] \\ + \left((\nu_1 \mathbf{1}^+ + \nu_2 \mathbf{2}^+ + \nu_4 \mathbf{4}^+) \mathbf{3}^- + \nu_9 \mathbf{9}^+ (\mathbf{3}^- - \mathbf{7}^-) \right) \mathcal{I}^D(\{\nu_{N_d}\})[1], \end{aligned} \quad (3.64)$$

$$\begin{aligned} (s_{23}\nu_2 \mathbf{2}^+ + s_{123}\nu_1 \mathbf{1}^+) \mathcal{I}^D(\{\nu_{N_d}\})[1] = \\ - (D - \nu_1 - \nu_2 - \nu_3 - 2\nu_4 - \nu_9) \mathcal{I}^D(\{\nu_{N_d}\})[1] \\ + \left((\nu_1 \mathbf{1}^+ + \nu_2 \mathbf{2}^+ + \nu_3 \mathbf{3}^+) \mathbf{4}^- + \nu_9 \mathbf{9}^+ (\mathbf{4}^- - \mathbf{8}^-) \right) \mathcal{I}^D(\{\nu_{N_d}\})[1], \end{aligned} \quad (3.65)$$

$$\begin{aligned} (s_{12}\nu_3 \mathbf{3}^+ + s_{123}\nu_4 \mathbf{4}^+) \mathcal{I}^D(\{\nu_{N_d}\})[1] = \\ - (D - 2\nu_1 - \nu_2 - \nu_3 - \nu_4 - \nu_9) \mathcal{I}^D(\{\nu_{N_d}\})[1] \\ + \left((\nu_2 \mathbf{2}^+ + \nu_3 \mathbf{3}^+ + \nu_4 \mathbf{4}^+) \mathbf{1}^- + \nu_9 \mathbf{9}^+ (\mathbf{1}^- - \mathbf{5}^-) \right) \mathcal{I}^D(\{\nu_{N_d}\})[1], \end{aligned} \quad (3.66)$$

$$\begin{aligned} s_{23}\nu_4 \mathbf{4}^+ \mathcal{I}^D(\{\nu_{N_d}\})[1] = \\ - (D - \nu_1 - 2\nu_2 - \nu_3 - \nu_4 - \nu_9) \mathcal{I}^D(\{\nu_{N_d}\})[1] \\ + \left((\nu_1 \mathbf{1}^+ + \nu_3 \mathbf{3}^+ + \nu_4 \mathbf{4}^+) \mathbf{2}^- + \nu_9 \mathbf{9}^+ (\mathbf{2}^- - \mathbf{6}^-) \right) \mathcal{I}^D(\{\nu_{N_d}\})[1], \end{aligned} \quad (3.67)$$

$$\begin{aligned}
s_{12}\nu_5\mathbf{5}^+\mathcal{I}^D(\{\nu_{N_d}\})[1] = \\
- (D - \nu_5 - \nu_6 - 2\nu_7 - \nu_8 - \nu_9)\mathcal{I}^D(\{\nu_{N_d}\})[1] \\
+ \left((\nu_5\mathbf{5}^+ + \nu_6\mathbf{6}^+ + \nu_8\mathbf{8}^+) \mathbf{7}^- + \nu_9\mathbf{9}^+ (\mathbf{7}^- - \mathbf{3}^-) \right) \mathcal{I}^D(\{\nu_{N_d}\})[1], \quad (3.68)
\end{aligned}$$

$$\begin{aligned}
(s_{23}\nu_6\mathbf{6}^+ + s_{123}\nu_5\mathbf{5}^+)\mathcal{I}^D(\{\nu_{N_d}\})[1] = \\
- (D - \nu_5 - \nu_6 - \nu_7 - 2\nu_8 - \nu_9)\mathcal{I}^D(\{\nu_{N_d}\})[1] \\
+ \left((\nu_5\mathbf{5}^+ + \nu_6\mathbf{6}^+ + \nu_7\mathbf{7}^+) \mathbf{8}^- + \nu_9\mathbf{9}^+ (\mathbf{8}^- - \mathbf{4}^-) \right) \mathcal{I}^D(\{\nu_{N_d}\})[1], \quad (3.69)
\end{aligned}$$

$$\begin{aligned}
(s_{12}\nu_7\mathbf{7}^+ + s_{123}\nu_8\mathbf{8}^+)\mathcal{I}^D(\{\nu_{N_d}\})[1] = \\
- (D - 2\nu_5 - \nu_6 - \nu_7 - \nu_8 - \nu_9)\mathcal{I}^D(\{\nu_{N_d}\})[1] \\
+ \left((\nu_6\mathbf{6}^+ + \nu_7\mathbf{7}^+ + \nu_8\mathbf{8}^+) \mathbf{5}^- + \nu_9\mathbf{9}^+ (\mathbf{5}^- - \mathbf{1}^-) \right) \mathcal{I}^D(\{\nu_{N_d}\})[1], \quad (3.70)
\end{aligned}$$

$$\begin{aligned}
s_{23}\nu_8\mathbf{8}^+\mathcal{I}^D(\{\nu_{N_d}\})[1] = \\
- (D - \nu_5 - 2\nu_6 - \nu_7 - \nu_8 - \nu_9)\mathcal{I}^D(\{\nu_{N_d}\})[1] \\
+ \left((\nu_5\mathbf{5}^+ + \nu_7\mathbf{7}^+ + \nu_8\mathbf{8}^+) \mathbf{6}^- + \nu_9\mathbf{9}^+ (\mathbf{6}^- - \mathbf{2}^-) \right) \mathcal{I}^D(\{\nu_{N_d}\})[1], \quad (3.71)
\end{aligned}$$

$$\begin{aligned}
(D - \nu_5 - \nu_6 - \nu_7 - \nu_8 - 2\nu_9)\mathcal{I}^D(\{\nu_{N_d}\})[1] = \\
\left(\nu_5\mathbf{5}^+ (\mathbf{9}^- - \mathbf{1}^-) + \nu_6\mathbf{6}^+ (\mathbf{9}^- - \mathbf{2}^-) \right. \\
\left. + \nu_7\mathbf{7}^+ (\mathbf{9}^- - \mathbf{3}^-) + \nu_8\mathbf{8}^+ (\mathbf{9}^- - \mathbf{4}^-) \right) \mathcal{I}^D(\{\nu_{N_d}\})[1], \quad (3.72)
\end{aligned}$$

$$\begin{aligned}
(D - \nu_1 - \nu_2 - \nu_3 - \nu_4 - 2\nu_9) \mathcal{I}^D(\{\nu_{N_d}\})[1] = \\
\left(\nu_1 1^+ (9^- - 5^-) + \nu_2 2^+ (9^- - 6^-) \right. \\
\left. + \nu_3 3^+ (9^- - 7^-) + \nu_4 4^+ (9^- - 8^-) \right) \mathcal{I}^D(\{\nu_{N_d}\})[1]. \quad (3.73)
\end{aligned}$$

Note that each i^+ is accompanied by a corresponding ν_i , this means that it is impossible to increase powers of a propagator that is not already present.

It is these identities and their non-planar counterparts which are the key to realistically being able to reduce the many hundreds of scalar and tensor integrals to a manageable number.

We use these identities and combinations of them to reduce complicated integrals to simpler ones. When using the IBP relations we find that they divide the loop integrals into two different groups. In the first group are diagrams which can be completely reduced to integrals of smaller topology, i.e. sub-topologies, we refer to these as *reducible*. The second group are more complicated. These integrals cannot be completely reduced to smaller topologies. Even after application of the IBP identities, the fundamental topology we are trying to reduce remains. The best we can achieve with the IBP equations is to reduce the powers of these integrals to unity. These topologies are not reducible and produce so-called Master Integrals (MI).

In the following sections we give examples of using the IBP equations to reduce both types of integrals.

3.5.3 Example Application of IBP to a Reducible Integral

Let us consider an example of a completely reducible integral. We can take for instance a two-scale planar-triangle integral shown in figure 3.6. For this topology we must take the IBP identities (3.64)–(3.73) and substitute $\nu_2 = \nu_3 = \nu_6 = 0$. Studying the identities reveals that we have an identity which is free of IN automatically. That is, there are no i^- terms left which would act on propagators which are not present

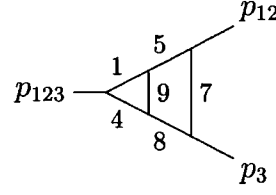


Figure 3.6: The two-scale planar triangle topology.

in the topology itself. More explicitly, there are no 2^- , 3^- or 6^- terms. One such identity is equation (3.73),

$$(D - \nu_1 - \nu_4 - 2\nu_9) \mathcal{I}^D(\{\nu_1, \nu_4, \nu_5, \nu_7, \nu_8, \nu_9\})[1] = \\ \left(\nu_1 1^+ (9^- - 5^-) + \nu_4 4^+ (9^- - 8^-) \right) \mathcal{I}^D(\{\nu_1, \nu_4, \nu_5, \nu_7, \nu_8, \nu_9\})[1]. \quad (3.74)$$

The action of this equation on the integral is represented diagrammatically in figure 3.7. We use a dot to denote a propagator with one extra power ($\nu_i \rightarrow \nu_i + 1$)

Figure 3.7: Pictorial representation of the action of the IBP equations on the two-scale triangle integral.

and a cross to denote a propagator with one less power ($\nu_i \rightarrow \nu_i - 1$).

We see that on the left-hand side we have the original integral. On the right-hand side we have integrals where we have decreased the power of one propagator at the expense of increasing another. The power of this identity comes when we apply it recursively. If we keep re-applying this identity to the integrals that we produce on

the right-hand side² we will gradually reduce the powers of propagators 5, 8 and 9 to zero at the expense of increasing the powers of propagators 1 and 4. When we reach a diagram in which a propagator power reaches zero we have a '*pinching*'. This means that a propagator shrinks to zero and we are left with a simpler topology. To see the action of a pinching figure 3.8 shows the effect of decreasing the power of propagator 9 to zero. By the repeated application of Equation (3.74) we can eventually reduce

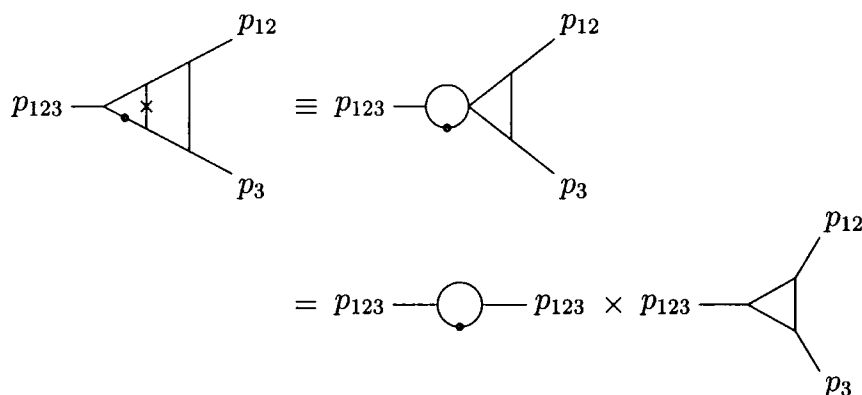


Figure 3.8: Pictorial representation of a pinching of the two-scale triangle integral.

the original integral to a sum of simpler integrals. In fact, when we pinch the 9-th propagator the two-loop integral reduces to a product of two one-loop integrals. These are far easier to calculate than the original integral and are known explicitly in terms of gamma functions. We will also produce simpler topologies when we pinch the other propagators 5 and 8. Remember however, that these simpler topologies will have higher powers of propagators caused by the reduction process.

We have just shown an example of a reducible integral. The action of the IBP equations enabled us to completely reduce the integral to simpler ones. If enough applications of the identity are made then the original topology can always be eliminated in terms of sub-topologies.

²Here we see the branching nature of the IBP equations. Every integral we create by the equations must also be reduced by IBP. These will in turn produce yet more integrals which must be reduced. This process keeps branching out until we finally arrive at simpler integrals which we can calculate by other means.

This method works extremely well for very simple integrals like the previous reducible case. For these integrals single identities or very simple linear combinations of identities can decrease powers of propagators in the integral. Repeated application of these identities will always eventually result in simpler topologies with higher powers of propagators. We hope the new integrals, i.e. the sub-topologies are simpler to calculate.

The situation is more complex when the identities contain terms which reduce the powers of propagators which are not present in the original integral. These terms lead to the presence of IN. To deal with IN we must eliminate them by constructing intricate combinations of identities. These identities often have to be applied in a very specific way to reduce an integral. Particular problems occur when we try to reduce an integral which is a MI. We consider the reduction of these integrals in the next section.

3.5.4 Example Application of IBP to an Irreducible Integral

In many cases the IBP equations cannot be applied directly to an integral. For certain topologies we have to deal with IN. Let us consider the Cbox₁ topology of figure 3.9 which has this feature, it turns out that this topology is a MI and cannot be completely reduced by IBP. We begin as we did in the reducible case, we set the

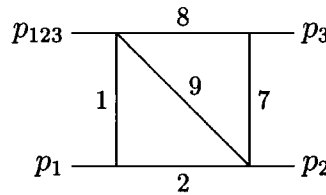


Figure 3.9: The Cbox₁ topology. This topology is a MI and so each propagator must be reduced to unit power individually.

propagators ν_3, ν_4, ν_5 and ν_6 to zero in all the IBP identities. Let us look at the first

of the IBP equations,

$$s_{12}\nu_1\mathbf{1}^+\mathcal{I}^D(\{\nu_1, \nu_2, \nu_7, \nu_8, \nu_9\})[1] = -(D - \nu_1 - \nu_2 - \nu_9)\mathcal{I}^D(\{\nu_1, \nu_2, \nu_7, \nu_8, \nu_9\})[1] \\ + \left((\nu_1\mathbf{1}^+ + \nu_2\mathbf{2}^+) \mathbf{3}^- + \nu_9\mathbf{9}^+ (\mathbf{3}^- - \mathbf{7}^-) \right) \mathcal{I}^D(\{\nu_1, \nu_2, \nu_7, \nu_8, \nu_9\})[1]. \quad (3.75)$$

We can now see the problem with the identity. The Cbox_1 topology does not contain the propagator A_3 in the denominator, however, there are three terms which contain $\mathbf{3}^-$. These terms produce IN, i.e., propagators with negative powers. The integrals which are produced by these terms are more complicated than the original, they have a tensorial structure. These terms do not help reduce the integral. To avoid these IN we must find combinations of the IBP equations which them. The IBP equations also produce IN corresponding to the lack of propagators 4, 5 and 6.

If we study IBP equation (3.68) we see that there is also a term with the structure $\nu_9\mathbf{9}^+\mathbf{3}^-$, all other terms free of IN. By taking a linear combination of this and the first equation (3.75), we can eliminate this particular term from our equation. By taking many more (complicated) combinations of equations which we do not demonstrate here, we can find a set of identities free of IN. An example identity would be,

$$\nu_1\mathbf{1}^+(D - 2 - 2\nu_1 - 2\nu_2)s_{12} = \\ + (D - 2 - 2\nu_9)\nu_9\mathbf{9}^+\mathbf{7}^- + 2(D - 1 - \nu_1 - \nu_2 - \nu_9)\nu_8\mathbf{8}^+\mathbf{7}^- \\ - (D - 1 - \nu_1 - \nu_2 - \nu_9)(3D - 2\nu_1 - 2\nu_2 - 4\nu_7 - 2\nu_8 - 2\nu_9). \quad (3.76)$$

This identity is assumed to be acting on the integral, $\mathcal{I}^D(\{\nu_1, \nu_2, \nu_7, \nu_8, \nu_9\})[1]$. We can see that this identity differs from that which we used for the reducible example. The structure is similar, there are the $\nu_i\mathbf{i}^+\mathbf{j}^-$ terms and the original integral with some polynomial coefficient in D . These terms are exactly what we had before. The difference is the appearance of the $\nu_1\mathbf{1}^+$ term on the left-hand side. This term although not an IN appears to be creating more complicated integrals by increasing

the power of the first propagator. However, the identity can be used to *decrease* the power of the first propagator. To see how this works, consider the action of the equation on following integral, $\text{Cbox}_1(1, 1, 1, 1, 1) \equiv \mathcal{I}^D(\{1, 1, 0, 0, 0, 0, 1, 1, 1\}) [1]$, we get the relation,

$$\begin{aligned} (D - 6)s_{12}\text{Cbox}_1(2, 1, 1, 1, 1) = \\ (D - 4)\text{Cbox}_1(1, 1, 0, 1, 2) + 2(D - 4)\text{Cbox}_1(1, 1, 0, 2, 1) \\ - 3(D - 4)^2\text{Cbox}_1(1, 1, 1, 1, 1). \end{aligned} \quad (3.77)$$

On the left-hand side we have the Cbox_1 with an increased power, on the right-hand side we have simpler integrals, i.e. pinchings and the Cbox_1 with unit powers – the Cbox_1 MI. If the propagator had higher powers then the identity could be applied recursively, each application reducing the power of the propagator by one.

More explicitly, we could just take equation (3.76) and substitute $\nu_1 \rightarrow \nu_1 - 1$ everywhere,

$$\begin{aligned} (\nu_1 - 1)(D - 2\nu_1 - 2\nu_2)s_{12} = \\ + (D - 2 - 2\nu_9)\nu_9\mathbf{9}^+\mathbf{7}^-\mathbf{1}^- + 2(D - \nu_1 - \nu_2 - \nu_9)\nu_8\mathbf{8}^+\mathbf{7}^-\mathbf{1}^- \\ - (D - \nu_1 - \nu_2 - \nu_9)(3D - 2\nu_1 - 2\nu_2 - 4\nu_7 - 2\nu_8 - 2\nu_9 + 2)\mathbf{1}^-. \end{aligned} \quad (3.78)$$

We can now see that the identity cannot be used to reduce the Cbox_1 with unit powers. The $\nu_1 - 1$ term on the left-hand side prevents us from doing so. The equation can only be applied recursively while $\nu_1 > 1$, however, this is sufficient to reduce any higher power to unity.

We can also construct other combinations of IBP equations to reduce each of the other propagators, we find similar identities hold. The complete set identities which

reduce all five propagators are,

$$\begin{aligned}
\nu_1 1^+ (D - 2 - 2\nu_1 - 2\nu_2) s_{12} = & \\
& + (D - 2 - 2\nu_9) \nu_9 9^+ 7^- + 2(D - 1 - \nu_1 - \nu_2 - \nu_9) \nu_8 8^+ 7^- \\
& - (D - 1 - \nu_1 - \nu_2 - \nu_9) (3D - 2\nu_1 - 2\nu_2 - 4\nu_7 - 2\nu_8 - 2\nu_9),
\end{aligned} \tag{3.79}$$

$$\begin{aligned}
\nu_2 2^+ (D - 2 - 2\nu_1 - 2\nu_2) s_{12} s_{23} = & \\
& + s_{12} (D - 2 - 2\nu_9) \nu_9 9^+ 8^- + 2s_{12} (D - 1 - \nu_1 - \nu_2 - \nu_9) \nu_7 7^+ 8^- \\
& - s_{123} (D - 2 - 2\nu_9) \nu_9 9^+ 7^- - 2s_{123} (D - 1 - \nu_1 - \nu_2 - \nu_9) \nu_8 8^+ 7^- \\
& - (D - 1 - \nu_1 - \nu_2 - \nu_9) (3D - 2\nu_1 - 2\nu_2 - 2\nu_7 - 4\nu_8 - 2\nu_9) s_{12} \\
& + (D - 1 - \nu_1 - \nu_2 - \nu_9) (3D - 2\nu_1 - 2\nu_2 - 4\nu_7 - 2\nu_8 - 2\nu_9) s_{123},
\end{aligned} \tag{3.80}$$

$$\begin{aligned}
\nu_7 7^+ (D - 2 - 2\nu_7 - 2\nu_8) s_{12} s_{23} = & \\
& + s_{23} (D - 2 - 2\nu_9) \nu_9 9^+ 1^- + 2s_{23} (D - 1 - \nu_7 - \nu_8 - \nu_9) \nu_2 2^+ 1^- \\
& - s_{123} (D - 2 - 2\nu_9) \nu_9 9^+ 2^- - 2s_{123} (D - 1 - \nu_7 - \nu_8 - \nu_9) \nu_1 1^+ 2^- \\
& - (D - 1 - \nu_7 - \nu_8 - \nu_9) (3D - 4\nu_1 - 2\nu_2 - 2\nu_7 - 2\nu_8 - 2\nu_9) s_{23} \\
& + (D - 1 - \nu_7 - \nu_8 - \nu_9) (3D - 2\nu_1 - 4\nu_2 - 2\nu_7 - 2\nu_8 - 2\nu_9) s_{123},
\end{aligned} \tag{3.81}$$

$$\begin{aligned}
\nu_8 8^+ (D - 2 - 2\nu_7 - 2\nu_8) s_{23} = & \\
& + (D - 2 - 2\nu_9) \nu_9 9^+ 2^- + 2(D - 1 - \nu_7 - \nu_8 - \nu_9) \nu_1 1^+ 2^- \\
& - (D - 1 - \nu_7 - \nu_8 - \nu_9) (3D - 2\nu_1 - 4\nu_2 - 2\nu_7 - 2\nu_8 - 2\nu_9),
\end{aligned} \tag{3.82}$$

$$\begin{aligned}
& \nu_9 \mathbf{9}^+ (D - 2 - 2\nu_9) s_{12} s_{23} = \\
& + s_{12} (D - 2 - 2\nu_9) \nu_9 \mathbf{9}^+ \mathbf{8}^- + 2s_{12} (D - 1 - \nu_1 - \nu_2 - \nu_9) \nu_7 \mathbf{7}^+ \mathbf{8}^- \\
& + s_{23} (D - 2 - 2\nu_9) \nu_9 \mathbf{9}^+ \mathbf{7}^- + 2s_{23} (D - 1 - \nu_1 - \nu_2 - \nu_9) \nu_8 \mathbf{8}^+ \mathbf{7}^- \\
& - s_{123} (D - 2 - 2\nu_9) \nu_9 \mathbf{9}^+ \mathbf{7}^- - 2s_{123} (D - 1 - \nu_1 - \nu_2 - \nu_9) \nu_8 \mathbf{8}^+ \mathbf{7}^- \\
& - (D - 1 - \nu_1 - \nu_2 - \nu_9) (3D - 2\nu_1 - 2\nu_2 - 2\nu_7 - 4\nu_8 - 2\nu_9) s_{12} \\
& - (D - 1 - \nu_1 - \nu_2 - \nu_9) (3D - 2\nu_1 - 2\nu_2 - 4\nu_7 - 2\nu_8 - 2\nu_9) s_{23} \\
& + (D - 1 - \nu_1 - \nu_2 - \nu_9) (3D - 2\nu_1 - 2\nu_2 - 4\nu_7 - 2\nu_8 - 2\nu_9) s_{123}.
\end{aligned} \tag{3.83}$$

All of the above IBP relations are understood to be acting on the generic integral, $\mathcal{I}^D(\{\nu_1, \nu_2, \nu_7, \nu_8, \nu_9\}) [1]$. Using each identity we can recursively reduce the power of each individual propagator to unity. The equations have a similar structure, in fact the symmetry between propagators $1 \leftrightarrow 8$ and $2 \leftrightarrow 7$ (with the exchange $p_1 \leftrightarrow p_3$ – the symmetry shown in equation (3.12)) can clearly be seen.

All of the identities (equations (3.79)– (3.83)) can be written in the form of equation (3.78) so that they can be directly applied to reduce the Cbox₁ topology. To construct an actual reduction algorithm from these equations is now simple. Each equation would be applied in turn to the Cbox₁ integral we are trying to reduce. Firstly, we might choose to recursively reduce the power of propagator 1 to unity using identity (3.79). We see that is done at the expense of increasing propagators 8 and 9. However, we also see that as well as decreasing propagator 1 we are also decreasing propagator 7. Although propagator 1 cannot be reduced to zero by this equation (because of the $\nu_1 - 1$ denominator), there is nothing to prevent propagator 7 from reducing to zero – this produces the pinchings, i.e. the simpler integrals. We would then move on to each propagator in turn and apply exactly the same procedure to the integrals, producing more pinchings until each power of the Cbox₁ had reached unity. We now see that the best we can do with the reduction for this topology is to reduce all propagators to unit power. The fact

that we cannot reduce the topology any further demonstrates that this topology is a MI. At this point though, the integral will have lower powers than it started with. We have to then use an alternative technique to calculate the C_{box_1} MI.

3.6 The Laporta Algorithm

So far we have developed a technique which allows us to write tensor integrals as linear combinations of scalar integrals with higher powers of propagators. We have seen that we can try to attack these integrals directly, but due to the large number of them this approach is impractical. We then saw that using the power of the IBP relations we could in fact group the different integrals together and relate scalar integrals with different powers of propagator (and even different topology) to one another. Using these relations we could extract the more complicated integrals in favour of simpler ones. The large set of scalar integrals can then be reduced to a smaller set of MI. At this point we can go no further, we have to rely on different techniques to solve the MI, perhaps direct integration. However, since there are fewer of them and they are in general simpler than the integrals we begin with we assume that we can solve them. In the last section we saw how the IBP could in some cases simply reduce an integral to simpler topologies or for more complicated topologies with a MI reduce the high propagator powers to unity. This approach works very well for simpler integrals, however, constructing the identities for more complicated topologies is laborious and non-trivial. Also, the recursive nature of the algorithms leads to very computer intensive calculations. Each time we apply an identity to an integral we produce a handful of integrals with lower powers of propagators, these in turn have to be reduced and also produce a number of simpler integrals. Since we require tensor integrals of rank four we know that we will produce scalar integrals with eight extra powers. The calculation of these integrals result in many hundreds of integrals by the IBP equations.

It was this motivation which led to the development of a more automated approach. Based on a paper of Laporta, we have implemented an algorithm which treats the tensor and scalar integrals on the same footing allowing for a more uniform approach to the reduction procedure and eliminates the need for the dimensional reduction.

3.6.1 The Algorithm Explained

In this approach we consider the solution of a finite system of IBP equations. The identities which we solve are generated from a set of chosen seed integrals. The set of identities form a linear system of equations with the integrals as unknowns. In general the system is under-determined and some integrals cannot be solved by the system. These are the MI. The system is solved with an algorithm which basically implements a Gauss elimination scheme. The final solution of the system will express all unknown integrals (both tensor and scalar) in terms of a finite set of MI. This approach is completely automatic and very simple and can be applied to integrals of any topology.

In words, the algorithm follows the following method. Let $\sum_k c_k W_k = 0$ be an IBP equation obtained from equation (3.57). The W_k are the integrals and the c_k are their coefficients. We take all identities which we have already solved in the system (where we have possibly expressed the integrals W_k in terms of other integrals) and substitute them into the new identity, which becomes, $\sum_k c'_k W'_k = 0$. An integral W'_l is chosen from the new identity according to some priority and expressed in terms of the other integrals, $W'_l = \sum_{k \neq l} (c'_k/c'_l) W'_k$. The new identity is added to the system and the integral W'_l is substituted into the rest of the system.

We consider reducing the generic integral (equation (3.1)). We allow the powers of the propagators (ν_i) to be either positive, representing the denominators of the integral or negative, representing the IN. We assume that there are N_d positive

powers meaning that there are $N_{sp} - N_d$ negative powers. Let us define the set t ,

$$t = \{i: \nu_i \geq 1\}. \quad (3.84)$$

This set contains the identifications of all propagators present in the denominator ($\nu_i \geq 0$) of an integral. Let us also define the set d ,

$$d = \{A_i: i \in t\}. \quad (3.85)$$

This is just the set of propagators in the denominator of an integral. For example, for the following integral,

$$\int \frac{d^D k_1}{i\pi^{D/2}} \int \frac{d^D k_2}{i\pi^{D/2}} \frac{1}{A_1^{\nu_1} A_3^{\nu_3} A_6^{\nu_6} A_9^{\nu_9}}, \quad (3.86)$$

with $\nu_1 \geq 1, \nu_3 \geq 1, \nu_6 \geq 1$ and $\nu_9 \geq 1$. We get, $t = \{1, 3, 6, 9\}$ and $d = \{A_1, A_3, A_6, A_9\}$.

We must also introduce some extra notation. We define the non-negative quantities M_d and M_p ,

$$M_p = \sum_{i=1}^{N_{sp}-N_d} -\nu_i \quad \text{for } \nu_i \leq 0, \quad (3.87)$$

$$M_d = \sum_{i=1}^{N_d} (\nu_i - 1) \quad \text{for } \nu_i \geq 1. \quad (3.88)$$

These correspond to the total sum of the powers of the irreducible numerators and the sum of the powers of the denominators above unity respectively.

3.6.2 The Algorithm

1. Let $n = N_k$.
2. Choose a combination of indices $i_1 < i_2 < \dots < i_n$ from the $\binom{N_d}{n}$ possible

combinations of the members of the set $t = \{i: \nu_i \geq 1\}$. Let $j_1 < j_2 < \dots < j_{N_{sp}-n}$ be the indices of the remaining propagators.

3. Consider the combinations of n different denominators chosen from the set $d = \{A_i: i \in t\}$; let A_{i_1}, \dots, A_{i_n} be one of these combinations.
4. Choose two integer non-negative constants a_i and b_i .
5. Let $M_d = 0$.
6. Let $M_p = 0$.
7. Consider a 'seed' integrand of the form,

$$W(n, i, j, \alpha, \beta) = \frac{1}{A_{i_1}^{\alpha_1} \dots A_{i_n}^{\alpha_n} A_{j_1}^{-\beta_1} \dots A_{j_{N_{sp}-n}}^{-\beta_{N_{sp}-n}}}, \quad (3.89)$$

and choose non-negative exponents α_k and β_k constrained such that,

$$\sum_{k=1}^n (\alpha_k - 1) = M_d \quad \text{and} \quad \sum_{k=1}^{N_{sp}-n} \beta_k = M_p, \quad (3.90)$$

that is, W belongs to the set $\left[n; \begin{smallmatrix} M_p \\ M_d \end{smallmatrix} \right]$.

8. Generate all the IBP identities.
9. Let,

$$\int \frac{d^D k_1}{i\pi^{D/2}} \dots \int \frac{d^D k_{N_k}}{i\pi^{D/2}} \sum_k c_k W_k = 0, \quad (3.91)$$

be one of the identities. W_k represents a generic integrand with either n or $n - 1$ denominators. Then:

- (a) Substitute all previously calculated integrals into the left-hand side of the IBP identity, i.e., equation (3.91). Let,

$$\int \frac{d^D k_1}{i\pi^{D/2}} \dots \int \frac{d^D k_{N_k}}{i\pi^{D/2}} \sum_k c'_k W'_k = 0, \quad (3.92)$$

be the result. If the identity is a linear combination of other identities in the system, *go to step 10*.

(b) If the new identity is linearly independent, choose an integrand W'_l ,

$$W'_l(n', i', j', \alpha', \beta') = \frac{1}{A_{i'_1}^{\alpha'_1} \cdots A_{i'_n}^{\alpha'_n} A_{j'_1}^{-\beta'_1} \cdots A_{j'_{N_{sp}-n'}}^{-\beta'_{N_{sp}-n'}}}, \quad (3.93)$$

from the new identity, equation (3.92), according to the following priorities. The integrand W'_l has:

- (i) the greatest number of denominators n' ,
- (ii) the greatest M_d' ,
- (iii) the greatest M_p' ,
- (iv) the greatest i'_1 , the greatest i'_2, \dots , the greatest i'_n ,
- (v) the greatest α'_1 , the greatest α'_2, \dots , the greatest α'_n ,
- (vi) the greatest β'_1 , the greatest β'_2, \dots , the greatest $\beta'_{N_{sp}-n'}$.

(c) Substitute and add the following identity to the system;

$$\int \frac{d^D k_1}{i\pi^{D/2}} \cdots \int \frac{d^D k_{N_k}}{i\pi^{D/2}} W'_l = - \int \frac{d^D k_1}{i\pi^{D/2}} \cdots \int \frac{d^D k_{N_k}}{i\pi^{D/2}} \sum_{k \neq l} \left(\frac{c'_k}{c'_l} \right) W'_k = 0. \quad (3.94)$$

10. Consider the next IBP identity from the $N_k(N_k + N_p)$ possible identities generated at *step 8* and *go to step 9, otherwise continue*.

11. Choose a new integrand W with different exponents α_k and β_k , belonging to the set $\left[n; \begin{smallmatrix} M_p \\ M_d \end{smallmatrix} \right]$ and *go to step 8*.

12. $M_p = M_p + 1$; if $M_p \leq a_i$ *go to step 7*.

13. $M_d = M_d + 1$; if $M_d \leq b_i$ *go to step 6*.

14. Choose a new combination of indices $i_1 < i_2 < \dots < i_n$ from the $\binom{N_d}{n}$ possible combinations of the members of the set $t = \{i: \nu_i \geq 1\}$. Let $j_1 < j_2 < \dots < j_{N_{sp}-n}$ be the indices of the remaining propagators and go to step 3, otherwise continue.
15. $n = n + 1$; if $n \leq N_d$ go to step 2, otherwise end.

The construction of a set of priorities for extraction of integrals is vital to the solution of the system. The priorities have been constructed so that we extract more complicated integrals and express them in terms of simpler integrals. The first priority $9(b)i$ arranges for integrals with the highest number of denominators to be extracted first. This means that ultimately, more complicated topologies will be expressed in terms of simpler ones. The second priority $9(b)ii$ deals with integrals where the denominators have powers higher than unity. We write integrals with higher powers in terms of those with lower powers. The third main priority $9(b)iii$ deals with the tensor integrals. Here we write integrals with higher tensor power in terms of those with lower power. Eventually, after enough applications, the process will express tensor integrals in terms of scalar integrals. The final priorities $9(b)iv$ – $9(b)vi$ make sure that we have an *absolute* set of priorities. This simply means that for any given n , M_d and M_p there are a set of integrals $\left[n; \begin{smallmatrix} M_p \\ M_d \end{smallmatrix}\right]$ and we need a way of ordering these. Note that integrals belonging to this set are of the same complexity and therefore these priorities do not effect the mechanism of the algorithm. They will, however, determine some of the MI we are left with at the end of the procedure. For some integrals we require more than one MI. The result is that we end up with both scalar and tensor MI (in the cases which we consider we deal with integrals with two MI, one scalar and one tensor). For the tensor MI the priorities will determine which propagator the tensor power will occur on. However, the system which we have solved will contain relations which enable us to write one tensor in terms of another, so we are able to change the basis set of MI, hence, these priorities do not

directly effect the end result of the calculation³.

The algorithm contains two adjustable parameters, a_i and b_i . These parameters control which identities are to be included in the system of equations which we solve. In the algorithm, a_i controls the cutoff for the sum of the powers of the tensors, b_i controls the cutoff for the sum of the powers of the denominators. We generate seed integrands with tensor and denominator powers up to these cutoffs. These parameters are chosen for each topology and cannot be predicted *a priori*.

Given a suitable choice of a_i and b_i the algorithm allows us to reduce all of the needed scalar and tensor integrals to linear combinations of MI. For the integrals which we require, namely scalar and tensor integrals up to rank four with unit powers of denominators, we have found that choosing $1 \leq a_i \leq 4$ and $b_i = 0$ was sufficient to reduce nearly all of the topologies. However, one topology with two MI did require setting $b_i = 1$.

3.7 Master Integrals

3.7.1 Calculating Master Integrals

The IBP identities already discussed in Section 3.5 allow us to express both tensor and scalar integrals of the form (3.3) as a linear combination of a few MI, that is, integrals that are no longer reducible by IBP but have to be calculated by other methods.

We have already discussed some of the alternative techniques in previous sections. These techniques proved invaluable for the calculation of MI for the on-shell case, in particular, MB was used to calculate several of the MI [40, 41, 42].

In this Section we discuss an alternative method to those already presented for the calculation of MI. This method for the calculation of the MI avoids the explicit

³We do not know if the modification of these priorities could lead to a more efficient solution of the system.

integration over the loop momenta has been successfully used by Gehrmann and Remiddi to calculate all of the planar and non-planar MI required for the calculation of the ME for $e^+e^- \rightarrow q\bar{q}g$ [47, 48]. In their calculation they derive differential equations in the external scales s_{12} , s_{23} , s_{123} for each MI, and solve these equations with appropriate boundary conditions.

3.7.2 Differential Equations for Master Integrals

There are different approaches to constructing the differential equations for the MI. One simple method is to use the Schwinger parameterised form of a generic scalar integral, that is Equation (3.33)

$$\mathcal{I}^D(\{\nu_{N_d}\})[1] = \int \mathcal{D}x \frac{1}{\mathcal{P}^{D/2}} \exp\left(\frac{\mathcal{Q}}{\mathcal{P}}\right). \quad (3.95)$$

where \mathcal{P} and \mathcal{Q} are given by Equations (3.23) and (3.26) respectively. All of the scale dependence of this equation is determined by the function \mathcal{Q} . If we denote a generic scale by S where $S = s_{12}, s_{23}, s_{123}$ then we can write the differential of a generic integral with respect to this scale as

$$\frac{\partial}{\partial S} \mathcal{I}^D(\{\nu_{N_d}\})[1] = \int \mathcal{D}x \left(\frac{\partial \mathcal{Q}}{\partial S}\right) \frac{1}{\mathcal{P}^{D/2}} \exp\left(\frac{\mathcal{Q}}{\mathcal{P}}\right). \quad (3.96)$$

The scale dependence of \mathcal{Q} is trivial, it is linear in s_{12} , s_{23} and s_{123} which are all multiplied by trilinear functions of the Schwinger parameters x_i , that is

$$\mathcal{Q} \sim S \sum x_i x_j x_k. \quad (3.97)$$

Thus, upon taking derivatives we produce three extra powers of Schwinger parameters in the numerator. As for the tensor reduction (Section 3.4), the extra x_i can be absorbed into $\mathcal{D}x$ and represent propagators with increased powers.

Things become clear if we construct the three differential equations for the planar auxiliary diagram, for which \mathcal{Q} is given explicitly by Equation (3.28). Using the same notation as Section 3.4, the differential equations for the scales s_{12} , s_{23} and s_{123} become:

$$\begin{aligned} \frac{\partial}{\partial s_{12}} \mathcal{I}^D(\{\nu_{N_d}\}) [1] = \\ - \left[((\nu_5 5^+ + \nu_6 6^+ + \nu_7 7^+ + \nu_8 8^+ + \nu_9 9^+) \nu_3 3^+ + \nu_7 7^+ \nu_5 5^+ + \nu_7 7^+ \nu_9 9^+) \nu_1 1^+ \right. \\ \left. + ((\nu_2 2^+ + \nu_3 3^+ + \nu_4 4^+ + \nu_9 9^+) \nu_7 7^+ + \nu_3 3^+ \nu_9 9^+) \nu_5 5^+ \right] \mathcal{I}^D(\{\nu_{N_d}\}) [1] \quad (3.98) \end{aligned}$$

$$\begin{aligned} \frac{\partial}{\partial s_{23}} \mathcal{I}^D(\{\nu_{N_d}\}) [1] = \\ - \left[((\nu_5 5^+ + \nu_6 6^+ + \nu_7 7^+ + \nu_8 8^+ + \nu_9 9^+) \nu_4 4^+ + \nu_8 8^+ \nu_6 6^+ + \nu_9 9^+ \nu_8 8^+) \nu_2 2^+ \right. \\ \left. + ((\nu_1 1^+ + \nu_3 3^+ + \nu_4 4^+ + \nu_9 9^+) \nu_8 8^+ + \nu_4 4^+ \nu_9 9^+) \nu_6 6^+ \right] \mathcal{I}^D(\{\nu_{N_d}\}) [1] \quad (3.99) \end{aligned}$$

$$\begin{aligned} \frac{\partial}{\partial s_{123}} \mathcal{I}^D(\{\nu_{N_d}\}) [1] = \\ - \left[((\nu_5 5^+ + \nu_6 6^+ + \nu_7 7^+ + \nu_8 8^+ + \nu_9 9^+) \nu_4 4^+ + \nu_8 8^+ \nu_5 5^+ + \nu_9 9^+ \nu_8 8^+) \nu_1 1^+ \right. \\ \left. + ((\nu_2 2^+ + \nu_3 3^+ + \nu_4 4^+ + \nu_9 9^+) \nu_8 8^+ + \nu_4 4^+ \nu_9 9^+) \nu_5 5^+ \right] \mathcal{I}^D(\{\nu_{N_d}\}) [1] \quad (3.100) \end{aligned}$$

The process for generating the differential equations for the MI is now simple. One takes the differential equations and sets all ν_i which do not appear in the MI which we are considering to zero. The extra powers which appear on the remaining propagators are then reduced by either the IBP identities or the Laporta algorithm. Since we are considering differential equations for MI then the IBP identities will not be able to completely reduce the r.h.s. to simpler integrals but the MI itself will remain with unit powers along with simpler integrals generated by the reduction. To make

things clearer we take the simple example of the Dart₂ integral

$$\text{Dart}_2(s_{12}, s_{123}) = \mathcal{I}^D(\{\nu_3, \nu_5, \nu_8, \nu_9\})[1] = \frac{p_{123}}{8} \begin{array}{c} \text{5} \\ \text{9} \\ \text{8} \end{array} \begin{array}{c} \text{3} \\ \text{p}_{12} \\ \text{p}_3 \end{array} . \quad (3.101)$$

This is actually a two-scale integral so there are only two independent differential equations. After reducing the differential equations with the IBP identities we obtain:

$$\begin{aligned} s_{123} \frac{\partial}{\partial s_{123}} \frac{p_{123}}{8} \begin{array}{c} \text{5} \\ \text{9} \\ \text{8} \end{array} \begin{array}{c} \text{3} \\ \text{p}_{12} \\ \text{p}_3 \end{array} &= \frac{D-4}{2} \frac{2s_{123} - s_{12}}{s_{123} - s_{12}} \frac{p_{123}}{8} \begin{array}{c} \text{5} \\ \text{9} \\ \text{8} \end{array} \begin{array}{c} \text{3} \\ \text{p}_{12} \\ \text{p}_3 \end{array} \\ &\quad - \frac{3D-8}{2} \frac{1}{s_{123} - s_{12}} \frac{p_{12}}{8} \begin{array}{c} \text{3} \\ \text{p}_{12} \\ \text{p}_3 \end{array} \end{aligned} \quad (3.102)$$

and

$$\begin{aligned} s_{12} \frac{\partial}{\partial s_{12}} \frac{p_{123}}{8} \begin{array}{c} \text{5} \\ \text{9} \\ \text{8} \end{array} \begin{array}{c} \text{3} \\ \text{p}_{12} \\ \text{p}_3 \end{array} &= -\frac{D-4}{2} \frac{s_{12}}{s_{123} - s_{12}} \frac{p_{123}}{8} \begin{array}{c} \text{5} \\ \text{9} \\ \text{8} \end{array} \begin{array}{c} \text{3} \\ \text{p}_{12} \\ \text{p}_3 \end{array} \\ &\quad + \frac{3D-8}{2} \frac{1}{s_{123} - s_{12}} \frac{p_{12}}{8} \begin{array}{c} \text{3} \\ \text{p}_{12} \\ \text{p}_3 \end{array} . \end{aligned} \quad (3.103)$$

Equations (3.102) and (3.103) are both *linear, inhomogeneous first order* differential equations of the form

$$\frac{\partial y(x)}{\partial x} + f(x)y(x) = g(x) , \quad (3.104)$$

which can be solved by the introduction of an integrating factor

$$I(x) = \exp \left(\int dx f(x) \right) , \quad (3.105)$$

such that $y(x) = 1/I(x)$ is a solution of the *homogeneous* differential equation. The general solution of the inhomogeneous equation is then

$$y(x) = \frac{1}{I(x)} \left(\int dx g(x) I(x) + C \right) , \quad (3.106)$$

where C is the constant of integration satisfying the boundary conditions. The boundary conditions can be directly read from the differential equations

$$\left. \begin{array}{c} \text{Diagram: A circle with a vertical line through its center. An incoming arrow from the left is labeled } p_{123}. \text{ An outgoing arrow at the top is labeled } p_{12}. \text{ An outgoing arrow at the bottom is labeled } p_3. \end{array} \right|_{s_{123}=0} = -\frac{3D-8}{D-4} \frac{1}{s_{12}} \text{Diagram: A circle with an incoming arrow from the left labeled } p_{12}. \quad (3.107)$$

The boundary condition for $s_{12} = 0$ cannot be determined from (3.103). For the s_{123} differential equation (3.102) we can calculate the integrating factor

$$I(s_{123}) = \frac{1}{((s_{12} - s_{123})s_{123})^{\frac{D}{2}-2}}. \quad (3.108)$$

The choice of integrating factor is not unique, we could choose

$$I(s_{123}) = \frac{1}{((s_{123} - s_{12})s_{123})^{\frac{D}{2}-2}}. \quad (3.109)$$

We select (3.108) by requiring a real integrating factor in the region $-s_{123} \geq -s_{12} \geq 0$. The resulting differential equation can be solved.

It turns out that the integral can be identified as an integral representation of the hypergeometric function ${}_2F_1$. After applying the boundary condition (3.107) we get

$$\begin{aligned} \text{Diagram: A circle with a vertical line through its center. An incoming arrow from the left is labeled } p_{123}. \text{ An outgoing arrow at the top is labeled } p_{12}. \text{ An outgoing arrow at the bottom is labeled } p_3. \end{aligned} &= A_1(s_{12} - s_{123})^{\frac{D}{2}-2}(-s_{123})^{\frac{D}{2}-2} \\ &- \frac{D-8}{2(D-3)} A_2 \frac{(-s_{12})^{D-3}}{-s_{123}} {}_2F_1\left(\frac{D}{2} - 1, 1; D-2; \frac{s_{12}}{s_{123}}\right). \quad (3.110) \end{aligned}$$

where the constants A_1 and A_2 are defined by

$$A_1(-s_{12})^{D-4} = \text{Diagram: A circle with a vertical line through its center. An incoming arrow from the left is labeled } p_{12}. \text{ An outgoing arrow at the top is labeled } p_1. \text{ An outgoing arrow at the bottom is labeled } p_2. \quad (3.111)$$

and

$$A_2(-s_{12})^{D-3} = \text{---} \xrightarrow{p_{12}} \bigcirc \text{---} . \quad (3.112)$$

Both of these integrals are one-scale and known in term of gamma functions. This shows the ‘bottom-up’ approach to calculating the MI, i.e. we have to know the simpler topologies in order to calculate the more complex ones.

3.7.3 The Master Integrals

The integrals appearing in the individual two-loop diagrams contain up to seven propagators in the denominator and up to four irreducible numerators. Using the reduction procedure described in section 3.6.2, all of the two-loop Feynman diagrams were reduced to a basis set of MI. Owing to the presence of the additional scale there are considerably more master topologies than in the on-shell case. Altogether there are 14 planar topologies and 5 non-planar topologies resulting in a total of 24 MI, as five topologies contain two MI.

The simpler MI are the single scale integrals, which can be written in terms of gamma functions,

$$\text{Sunrise}(s_{12}) = \text{---} \xrightarrow{p_{12}} \bigcirc \text{---} , \quad (3.113)$$

$$\text{Glass}(s_{12}) = \text{---} \xrightarrow{p_{12}} \bigcirc \bigcirc \text{---} , \quad (3.114)$$

$$\text{Dart}_1(s_{12}) = \text{---} \xrightarrow{p_{12}} \bigcirc \begin{matrix} \xrightarrow{p_1} \\ \xrightarrow{p_2} \end{matrix} , \quad (3.115)$$

as well as the more complicated,

$$\text{Xtri}_1(s_{12}) = \text{---} \xrightarrow{p_{12}} \begin{matrix} \nearrow \searrow \\ \nwarrow \nearrow \end{matrix} \begin{matrix} \xrightarrow{p_1} \\ \xrightarrow{p_2} \end{matrix} . \quad (3.116)$$

The two-scale master integrals can be written in terms of Γ functions,

$$\text{Tglass}(s_{12}, s_{123}) = \begin{array}{c} \xrightarrow{p_{12}} \text{---} \bigcirc \text{---} \bigcirc \text{---} \xrightarrow{p_{123}} \\ \uparrow p_3 \end{array}, \quad (3.117)$$

or as generalised polylogarithms or one-dimensional harmonic polylogarithms,

$$\text{Dart}_2(s_{12}, s_{123}) = \begin{array}{c} \xrightarrow{p_{123}} \text{---} \bigcirc \text{---} \xrightarrow{p_{12}} \\ \downarrow p_3 \end{array}, \quad (3.118)$$

$$\text{Dart}_2(s_{123}, s_{23}) = \begin{array}{c} \xrightarrow{p_{123}} \text{---} \bigcirc \text{---} \xrightarrow{p_1} \\ \downarrow p_{23} \end{array}, \quad (3.119)$$

$$\text{Plane}(s_{12}, s_{123}) = \begin{array}{c} \xrightarrow{p_{123}} \text{---} \triangle \text{---} \xrightarrow{p_{12}} \\ \downarrow p_3 \end{array}, \quad (3.120)$$

$$\text{Xtri}_2(s_{123}, s_{12}) = \begin{array}{c} \xrightarrow{p_{123}} \text{---} \triangle \text{---} \xrightarrow{p_{12}} \\ \downarrow p_3 \end{array}. \quad (3.121)$$

The three-scale MI can be written in terms of two-dimensional harmonic polylogarithms. There are the planar graphs,

$$\text{Abox}_1(s_{12}, s_{23}, s_{123}) = \begin{array}{c} \xrightarrow{p_{123}} \text{---} \text{---} \xrightarrow{p_3} \\ \uparrow p_1 \text{---} \bigcirc \text{---} p_2 \end{array}, \quad (3.122)$$

$$\text{Abox}_2(s_{12}, s_{23}, s_{123}) = \begin{array}{c} \xrightarrow{p_{123}} \text{---} \bigcirc \text{---} \xrightarrow{p_3} \\ \uparrow p_1 \text{---} \text{---} p_2 \end{array}, \quad (3.123)$$

$$\text{Cbox}_1(s_{12}, s_{23}, s_{123}) = \begin{array}{c} \xrightarrow{p_{123}} \text{---} \triangle \text{---} \xrightarrow{p_3} \\ \uparrow p_1 \text{---} \text{---} p_2 \end{array}, \quad (3.124)$$

$$\text{Cbox}_2(s_{12}, s_{23}, s_{123}) = \begin{array}{c} \xrightarrow{p_{123}} \text{---} \triangle \text{---} \xrightarrow{p_3} \\ \uparrow p_1 \text{---} \text{---} p_2 \end{array}, \quad (3.125)$$

$$\text{Tbox}_1(s_{12}, s_{23}, s_{123}) = \begin{array}{c} \xrightarrow{p_{123}} \text{---} \triangle \text{---} \xrightarrow{p_3} \\ \uparrow p_1 \text{---} \text{---} p_2 \end{array}, \quad (3.126)$$

$$\text{Pbox}_1(s_{12}, s_{23}, s_{123}) = \begin{array}{c} \xrightarrow{p_{123}} \text{---} \text{---} \xrightarrow{p_3} \\ \uparrow p_1 \text{---} \text{---} p_2 \end{array}, \quad (3.127)$$

$$\text{Bbox}(s_{12}, s_{23}, s_{123}) = \begin{array}{c} p_{123} \rightarrow \text{---} \text{---} \text{---} p_3 \\ \text{---} \text{---} \text{---} \\ p_1 \leftarrow \text{---} \text{---} \text{---} p_2 \end{array}, \quad (3.128)$$

and the non-planar graphs,

$$\text{Ebox}_1(s_{12}, s_{23}, s_{123}) = \begin{array}{c} p_{123} \rightarrow \text{---} \text{---} \text{---} p_3 \\ \text{---} \text{---} \text{---} \\ p_1 \leftarrow \text{---} \text{---} \text{---} p_2 \end{array}, \quad (3.129)$$

$$\text{Xbmo}_1(s_{12}, s_{23}, s_{123}) = \begin{array}{c} p_{123} \rightarrow \text{---} \text{---} \text{---} p_3 \\ \text{---} \text{---} \text{---} \\ p_1 \leftarrow \text{---} \text{---} \text{---} p_2 \end{array}, \quad (3.130)$$

$$\text{Xbmi}_1(s_{12}, s_{23}, s_{123}) = \begin{array}{c} p_{123} \rightarrow \text{---} \text{---} \text{---} p_3 \\ \text{---} \text{---} \text{---} \\ p_1 \leftarrow \text{---} \text{---} \text{---} p_2 \end{array}. \quad (3.131)$$

For the Cbox_2 , Pbox , Ebox , Xbmo and Xbmi topologies, a second MI is required.

$$\text{Cbox}_{2A}(s_{12}, s_{23}, s_{123}) = \begin{array}{c} p_{123} \rightarrow \text{---} \text{---} \text{---} p_3 \\ \text{---} \text{---} \text{---} \\ p_1 \leftarrow \text{---} \text{---} \text{---} p_2 \end{array}, \quad (3.132)$$

$$\text{Pbox}_2(s_{12}, s_{23}, s_{123}) = \begin{array}{c} p_{123} \rightarrow \text{---} \text{---} \text{---} p_3 \\ \text{---} \text{---} \text{---} \\ p_1 \leftarrow \text{---} \text{---} \text{---} p_2 \end{array}, \quad (3.133)$$

$$\text{Ebox}_2(s_{12}, s_{23}, s_{123}) = \begin{array}{c} p_{123} \rightarrow \text{---} \text{---} \text{---} p_3 \\ \text{---} \text{---} \text{---} \\ p_1 \leftarrow \text{---} \text{---} \text{---} p_2 \end{array}, \quad (3.134)$$

$$\text{Xbmo}_2(s_{12}, s_{23}, s_{123}) = \begin{array}{c} p_{123} \rightarrow \text{---} \text{---} \text{---} p_3 \\ \text{---} \text{---} \text{---} \\ p_1 \leftarrow \text{---} \text{---} \text{---} p_2 \end{array}, \quad (3.135)$$

$$\text{Xbmi}_2(s_{12}, s_{23}, s_{123}) = \begin{array}{c} p_{123} \rightarrow \text{---} \text{---} \text{---} p_3 \\ \text{---} \text{---} \text{---} \\ p_1 \leftarrow \text{---} \text{---} \text{---} p_2 \end{array}. \quad (3.136)$$

All of the MI above were calculated in terms of one- and two-dimensional harmonic polylogarithms (see Appendix F) by Gehrmann and Remiddi using differential equations in [47, 48].

CHAPTER 4

The NNLO Matrix Element for $e^+e^- \rightarrow q\bar{q}g$

In Chapters 2 and 3 we have built up the necessary tools to calculate ME and the corresponding loop integrals. By studying the formalism of Catani we have also seen how to analyse and predict the pole structure of the ME, enabling a positive check of these often complicated calculations.

As previously described in Chapter 1, the NNLO $\mathcal{O}(\alpha_s^3)$ calculation of the three-jet rate in e^+e^- annihilation has been considered an important project for a long time [28]. In terms of ME this calculation requires several components. Firstly, the tree level $\gamma^* \rightarrow 5$ partons¹ amplitude where two partons become soft or collinear, calculated in [49, 50, 51]. Secondly, the one-loop corrections to $\gamma^* \rightarrow 4$ partons amplitude with one parton becoming soft or collinear, calculated in [52, 53, 54, 55]. Finally, the two-loop (as well as the one-loop times one-loop) corrections to the $\gamma^* \rightarrow 3$ partons amplitude. While the former two contributions have been known for some time already, the two-loop amplitudes have presented an obstacle that prevented further progress on this calculation up to now.

In this Chapter we present the application of the techniques previously mentioned

¹As we have already done in Chapter 2, we ignore the initial e^+e^- interactions and consider $\gamma^* \rightarrow q\bar{q}g$.

to calculation of the ME for the process $e^+e^- \rightarrow q\bar{q}g$ at two-loops². We begin by introducing notation in Sections 4.1 and 4.2. In Section 4.3 we construct the insertion operator $\mathbf{I}^{(1)}(\epsilon)$ and the explicit pole structure prediction of Catani. All diagrams contributing to the calculation are displayed in Section 4.5. The general method for the calculation, that is, how all of the different pieces of the calculation fit together is described in Section 4.4. Finally, in Section 4.6 we present the finite one-loop times one-loop and two-loop contributions to the ME.

4.1 Notation

We consider the decay of a virtual photon into a quark–antiquark–gluon system:

$$\gamma^*(q) \longrightarrow q(p_1) + \bar{q}(p_2) + g(p_3). \quad (4.1)$$

The kinematics of this process can be fully described by the Mandelstam invariants

$$s_{12} = (p_1 + p_2)^2, \quad s_{13} = (p_1 + p_3)^2, \quad s_{23} = (p_2 + p_3)^2, \quad (4.2)$$

which fulfil

$$q^2 = s_{12} + s_{13} + s_{23} \equiv s_{123}. \quad (4.3)$$

At this point it is also convenient to define the dimensionless invariants

$$x = s_{12}/s_{123}, \quad y = s_{13}/s_{123}, \quad z = s_{23}/s_{123}, \quad (4.4)$$

which satisfy $x + y + z = 1$.

We begin, as usual, by defining the perturbative expansion of the amplitude. The conventions used are the same as those already defined in Section 2.4, we repeat them here for clarity. The calculation is performed in CDR, where $D = 4 - 2\epsilon$, and

²This Chapter is based on work carried out in [56].

all external particle states are taken to be D -dimensional. Renormalisation of UV divergences is performed in the $\overline{\text{MS}}$ scheme. The renormalised amplitude can be written as

$$|\mathcal{M}\rangle = \sqrt{4\pi\alpha}e_q\sqrt{4\pi\alpha_s} \left[|\mathcal{M}^{(0)}\rangle + \left(\frac{\alpha_s}{2\pi}\right) |\mathcal{M}^{(1)}\rangle + \left(\frac{\alpha_s}{2\pi}\right)^2 |\mathcal{M}^{(2)}\rangle + \mathcal{O}(\alpha_s^3) \right], \quad (4.5)$$

where α denotes the electromagnetic coupling constant, e_q the quark charge, α_s the QCD coupling constant at the renormalisation scale μ , and the $|\mathcal{M}^{(i)}\rangle$ are the i -loop contributions to the renormalised amplitude, they are vectors in colour space.

We write the squared amplitude, summed over spins, colours and quark flavours as

$$\langle \mathcal{M} | \mathcal{M} \rangle = \sum_{\text{spin, col}} |\mathcal{M}(\gamma^* \rightarrow q\bar{q}g)|^2 = \mathcal{T}(x, y, z). \quad (4.6)$$

If we use the definition of the amplitude from Equation (4.5) then the perturbative expansion of $\mathcal{T}(x, y, z)$ evaluated at renormalisation scale $\mu^2 = q^2 = s_{123}$ reads,

$$\begin{aligned} \mathcal{T}(x, y, z) = 16\pi^2\alpha \sum_q e_q^2 \alpha_s(q^2) & \left[\mathcal{T}^{(2)}(x, y, z) + \left(\frac{\alpha_s(q^2)}{2\pi}\right) \mathcal{T}^{(4)}(x, y, z) \right. \\ & \left. + \left(\frac{\alpha_s(q^2)}{2\pi}\right)^2 \mathcal{T}^{(6)}(x, y, z) + \mathcal{O}(\alpha_s^3(q^2)) \right], \quad (4.7) \end{aligned}$$

where

$$\mathcal{T}^{(2)}(x, y, z) = \langle \mathcal{M}^{(0)} | \mathcal{M}^{(0)} \rangle, \quad (4.8)$$

$$\mathcal{T}^{(4)}(x, y, z) = \langle \mathcal{M}^{(0)} | \mathcal{M}^{(1)} \rangle + \langle \mathcal{M}^{(1)} | \mathcal{M}^{(0)} \rangle, \quad (4.9)$$

$$\mathcal{T}^{(6)}(x, y, z) = \langle \mathcal{M}^{(1)} | \mathcal{M}^{(1)} \rangle + \langle \mathcal{M}^{(0)} | \mathcal{M}^{(2)} \rangle + \langle \mathcal{M}^{(2)} | \mathcal{M}^{(0)} \rangle. \quad (4.10)$$

$\mathcal{T}^{(2)}(x, y, z)$ represents the contribution from tree level interference and is easily



calculated from the simple Feynman diagrams,

$$\mathcal{T}^{(2)}(x, y, z) = 4V(1 - \epsilon) \left[(1 - \epsilon) \left(\frac{y}{z} + \frac{z}{y} \right) + \frac{2(1 - y - z) - 2\epsilon yz}{yz} \right], \quad (4.11)$$

where $V = N^2 - 1$, with N the number of colours. $\mathcal{T}^{(4)}(x, y, z)$ is more complicated, and represents the interference of tree level and one-loop diagrams. It was first derived in [23, 24]; we quote an explicit expression for it to all orders in ϵ in Section 4.3.5.

In this thesis we present the calculation of $\mathcal{T}^{(6)}(x, y, z)$. We break the calculation into two separate pieces,

$$\mathcal{T}^{(6)}(x, y, z) = \mathcal{T}^{(6,[1 \times 1])}(x, y, z) + T^{(6,[2 \times 0])}(x, y, z), \quad (4.12)$$

where we have a contribution arising from the one-loop self-interference,

$$\mathcal{T}^{(6,[1 \times 1])}(x, y, z) = \langle \mathcal{M}^{(1)} | \mathcal{M}^{(1)} \rangle, \quad (4.13)$$

and from the interference of tree and two-loop diagrams

$$T^{(6,[2 \times 0])}(x, y, z) = \langle \mathcal{M}^{(0)} | \mathcal{M}^{(2)} \rangle + \langle \mathcal{M}^{(2)} | \mathcal{M}^{(0)} \rangle. \quad (4.14)$$

At the same order in α_s , one finds also a contribution to three-jet final states from the self-interference of the $\gamma^* \rightarrow ggg$ amplitude. The matrix element for this process does not contain infrared or ultraviolet divergences; it was computed long ago and can be found in [57, 58].

For the remainder of this calculation we will set the renormalisation scale $\mu^2 =$

$q^2 = s_{123}$. The full scale dependence of the perturbative expansion is given by

$$\begin{aligned} \mathcal{T}(x, y, z) = & 16\pi^2 \alpha \sum_q e_q^2 \alpha_s(\mu^2) \left\{ \mathcal{T}^{(2)}(x, y, z) \right. \\ & + \left(\frac{\alpha_s(\mu^2)}{2\pi} \right) \left[\mathcal{T}^{(4)}(x, y, z) + b_0 \mathcal{T}^{(2)}(x, y, z) \ln \left(\frac{\mu^2}{q^2} \right) \right] \\ & + \left(\frac{\alpha_s(\mu^2)}{2\pi} \right)^2 \left[\mathcal{T}^{(6)}(x, y, z) + \left(2b_0 \mathcal{T}^{(4)}(x, y, z) + b_1 \mathcal{T}^{(2)}(x, y, z) \right) \ln \left(\frac{\mu^2}{q^2} \right) \right. \\ & \quad \left. \left. + b_0^2 \mathcal{T}^{(2)}(x, y, z) \ln^2 \left(\frac{\mu^2}{q^2} \right) \right] + \mathcal{O}(\alpha_s^3) \right\}. \quad (4.15) \end{aligned}$$

4.2 Ultraviolet Renormalisation

The renormalisation of the matrix element is carried out by replacing the bare coupling α_0 with the renormalised coupling $\alpha_s \equiv \alpha_s(\mu^2)$, evaluated at the renormalisation scale μ^2

$$\alpha_0 \mu_0^{2\epsilon} S_\epsilon = \alpha_s \mu^{2\epsilon} \left[1 - \frac{\beta_0}{\epsilon} \left(\frac{\alpha_s}{2\pi} \right) + \left(\frac{\beta_0^2}{\epsilon^2} - \frac{\beta_1}{2\epsilon} \right) \left(\frac{\alpha_s}{2\pi} \right)^2 + \mathcal{O}(\alpha_s^3) \right], \quad (4.16)$$

where

$$S_\epsilon = (4\pi)^\epsilon e^{-\epsilon\gamma_E} \quad \text{with Euler constant } \gamma_E = 0.5772\dots \quad (4.17)$$

and μ_0^2 is the mass parameter introduced in dimensional regularisation [17, 18, 19] to maintain a dimensionless coupling in the bare QCD Lagrangian density; β_0 and β_1 are the first two coefficients of the QCD β -function:

$$\beta_0 = \frac{11C_A - 4T_R N_F}{6}, \quad \beta_1 = \frac{17C_A^2 - 10C_A T_R N_F - 6C_F T_R N_F}{6}, \quad (4.18)$$

with the QCD colour factors

$$C_A = N, \quad C_F = \frac{N^2 - 1}{2N}, \quad T_R = \frac{1}{2}. \quad (4.19)$$

We denote the i -loop contribution to the unrenormalised amplitudes by $|\mathcal{M}^{(i),\text{un}}\rangle$, using the same normalisation as for the decomposition of the renormalised amplitude (4.5). The renormalised amplitudes are then obtained as

$$\begin{aligned} |\mathcal{M}^{(0)}\rangle &= |\mathcal{M}^{(0),\text{un}}\rangle, \\ |\mathcal{M}^{(1)}\rangle &= S_\epsilon^{-1} |\mathcal{M}^{(1),\text{un}}\rangle - \frac{\beta_0}{2\epsilon} |\mathcal{M}^{(0),\text{un}}\rangle, \\ |\mathcal{M}^{(2)}\rangle &= S_\epsilon^{-2} |\mathcal{M}^{(2),\text{un}}\rangle - \frac{3\beta_0}{2\epsilon} S_\epsilon^{-1} |\mathcal{M}^{(1),\text{un}}\rangle - \left(\frac{\beta_1}{4\epsilon} - \frac{3\beta_0^2}{8\epsilon^2} \right) |\mathcal{M}^{(0),\text{un}}\rangle. \end{aligned} \quad (4.20)$$

This can be trivially obtained from the general result in Chapter 2 by taking the general expression for the renormalised amplitudes, Equation (2.61), and substituting $q = 1/2$, corresponding to the overall factor of $\sqrt{\alpha_s}$ in front of the ME (4.5).

4.3 Infrared Factorisation

We know that we can further decompose the renormalised one- and two-loop contributions to $\mathcal{T}^{(6)}(x, y, z)$ given by Equations (4.13) and (4.14) into a combination of the *pole structure* and a *finite remainder*,

$$\mathcal{T}^{(6,[i \times j])}(x, y, z) = \mathcal{Poles}^{(i \times j)}(x, y, z) + \mathcal{Finite}^{(i \times j)}(x, y, z). \quad (4.21)$$

As we have seen in Section 2.4, Catani has shown how to organise the infrared pole structure of the one- and two-loop contributions renormalised in the $\overline{\text{MS}}$ scheme in terms of the tree and renormalised one-loop amplitudes, $|\mathcal{M}^{(0)}\rangle$ and $|\mathcal{M}^{(1)}\rangle$ respectively. In this Section we construct the explicit pole structure $\mathcal{Poles}^{(i \times j)}$ in terms of $\mathbf{I}^{(1)}(\epsilon)$ and $\mathbf{H}^{(2)}(\epsilon)$ and derive $\mathbf{I}^{(1)}(\epsilon)$ and $\mathbf{H}^{(2)}(\epsilon)$ corresponding to $\gamma^* \rightarrow q\bar{q}g$.

4.3.1 One-Loop Pole Structure

The expression for the one-loop interference $\mathcal{T}^{(6,[1\times 1])}$ (4.13) can be constructed from $\mathbf{I}^{(1)}(\epsilon)$ in the following way. Rearranging Equation (2.51) in terms of $|\mathcal{M}^{(1),\text{fin}}\rangle$

$$|\mathcal{M}^{(1),\text{fin}}\rangle = |\mathcal{M}^{(1)}\rangle - \mathbf{I}^{(1)}(\epsilon)|\mathcal{M}^{(0)}\rangle, \quad (4.22)$$

and taking the product with its conjugate gives

$$\begin{aligned} \langle \mathcal{M}^{(1),\text{fin}} | \mathcal{M}^{(1),\text{fin}} \rangle &= \langle \mathcal{M}^{(1)} | \mathcal{M}^{(1)} \rangle - \langle \mathcal{M}^{(1)} | \mathbf{I}^{(1)}(\epsilon) | \mathcal{M}^{(0)} \rangle \\ &\quad - \langle \mathcal{M}^{(0)} | \mathbf{I}^{(1)}(\epsilon)^\dagger | \mathcal{M}^{(1)} \rangle + \langle \mathcal{M}^{(0)} | \mathbf{I}^{(1)}(\epsilon)^\dagger \mathbf{I}^{(1)}(\epsilon) | \mathcal{M}^{(0)} \rangle \\ &= \langle \mathcal{M}^{(1)} | \mathcal{M}^{(1)} \rangle - 2\Re \left[\langle \mathcal{M}^{(1)} | \mathbf{I}^{(1)}(\epsilon) | \mathcal{M}^{(0)} \rangle \right] \\ &\quad + \langle \mathcal{M}^{(0)} | \mathbf{I}^{(1)}(\epsilon)^\dagger \mathbf{I}^{(1)}(\epsilon) | \mathcal{M}^{(0)} \rangle. \end{aligned} \quad (4.23)$$

The r.h.s. of this expression contains exactly $\mathcal{T}^{(6,[1\times 1])} = \langle \mathcal{M}^{(1)} | \mathcal{M}^{(1)} \rangle$, rearranging gives

$$\begin{aligned} \mathcal{T}^{(6,[1\times 1])}(x, y, z) &= \Re \left[2\langle \mathcal{M}^{(1)} | \mathbf{I}^{(1)}(\epsilon) | \mathcal{M}^{(0)} \rangle \right. \\ &\quad \left. - \langle \mathcal{M}^{(0)} | \mathbf{I}^{(1)}(\epsilon)^\dagger \mathbf{I}^{(1)}(\epsilon) | \mathcal{M}^{(0)} \rangle + \langle \mathcal{M}^{(1),\text{fin}} | \mathcal{M}^{(1),\text{fin}} \rangle \right]. \end{aligned} \quad (4.24)$$

We can now identify the *Finite* and *Poles* contributions to $\mathcal{T}^{(6,[1\times 1])}(x, y, z)$ given by Equation (4.21). This is simple to do, all terms containing a factor $\mathbf{I}^{(1)}(\epsilon)$ or $\mathbf{I}^{(1)}(\epsilon)^\dagger$ are singular and contribute to *Poles*, the remainder contribute to *Finite*, giving

$$\mathcal{F}^{(1\times 1)}(x, y, z) = \Re \left[\langle \mathcal{M}^{(1),\text{fin}} | \mathcal{M}^{(1),\text{fin}} \rangle \right] \quad (4.25)$$

and

$$\mathcal{Poles}^{(1 \times 1)}(x, y, z) = \Re \left[2\langle \mathcal{M}^{(1)} | \mathbf{I}^{(1)}(\epsilon) | \mathcal{M}^{(0)} \rangle - \langle \mathcal{M}^{(0)} | \mathbf{I}^{(1)}(\epsilon)^\dagger \mathbf{I}^{(1)}(\epsilon) | \mathcal{M}^{(0)} \rangle \right]. \quad (4.26)$$

4.3.2 Two-Loop Pole Structure

The expression for the contribution from the interference of tree and two-loop diagrams $T^{(6, [2 \times 0])}$ (4.14) can be constructed in terms of $\mathbf{I}^{(1)}(\epsilon)$ and $\mathbf{I}^{(2)}(\epsilon)$ in the following way. From Equation (4.14) we have

$$T^{(6, [2 \times 0])}(x, y, z) = \langle \mathcal{M}^{(0)} | \mathcal{M}^{(2)} \rangle + [\langle \mathcal{M}^{(0)} | \mathcal{M}^{(2)} \rangle]^\dagger = 2\Re [\langle \mathcal{M}^{(0)} | \mathcal{M}^{(2)} \rangle]. \quad (4.27)$$

The expression for $|\mathcal{M}^{(2)}\rangle$ in terms $|\mathcal{M}^{(0)}\rangle$, $|\mathcal{M}^{(1)}\rangle$, $\mathbf{I}^{(1)}(\epsilon)$ and $\mathbf{I}^{(2)}(\epsilon)$ is given by Equation (2.56). Upon substitution, (4.27) becomes

$$T^{(6, [2 \times 0])}(x, y, z) = 2\Re \left[\langle \mathcal{M}^{(0)} | \mathbf{I}^{(1)}(\epsilon) | \mathcal{M}^{(1)} \rangle + \langle \mathcal{M}^{(0)} | \mathbf{I}^{(2)}(\epsilon) | \mathcal{M}^{(0)} \rangle + \langle \mathcal{M}^{(0)} | \mathcal{M}^{(2), \text{fin}} \rangle \right]. \quad (4.28)$$

Re-writing $\mathbf{I}^{(2)}(\epsilon)$ in terms of $\mathbf{I}^{(1)}(\epsilon)$, $\mathbf{I}^{(1)}(2\epsilon)$ and $\mathbf{H}^{(2)}(\epsilon)$ via Equation (2.57) gives finally

$$\begin{aligned} T^{(6, [2 \times 0])}(x, y, z) = 2\Re \left[-\frac{1}{2} \langle \mathcal{M}^{(0)} | \mathbf{I}^{(1)}(\epsilon) \mathbf{I}^{(1)}(\epsilon) | \mathcal{M}^{(0)} \rangle - \frac{\beta_0}{\epsilon} \langle \mathcal{M}^{(0)} | \mathbf{I}^{(1)}(\epsilon) | \mathcal{M}^{(0)} \rangle \right. \\ + \langle \mathcal{M}^{(0)} | \mathbf{I}^{(1)}(\epsilon) | \mathcal{M}^{(1)} \rangle \\ + e^{-\epsilon\gamma_E} \frac{\Gamma(1-2\epsilon)}{\Gamma(1-\epsilon)} \left(\frac{\beta_0}{\epsilon} + K \right) \langle \mathcal{M}^{(0)} | \mathbf{I}^{(1)}(2\epsilon) | \mathcal{M}^{(0)} \rangle \\ + \langle \mathcal{M}^{(0)} | \mathbf{H}^{(2)}(\epsilon) | \mathcal{M}^{(0)} \rangle \\ \left. + \langle \mathcal{M}^{(0)} | \mathcal{M}^{(2), \text{fin}} \rangle \right]. \quad (4.29) \end{aligned}$$

As for the one-loop case, we can now identify the *Finite* and *Poles* contributions to $T^{(6,[2\times 0])}(x, y, z)$ given by equation (4.21). All terms containing a factor $\mathbf{I}^{(1)}(\epsilon)$, $\mathbf{I}^{(1)}(2\epsilon)$ or $\mathbf{H}^{(2)}(\epsilon)$ contribute to *Poles*, the remainder contribute to *Finite*, giving

$$\mathcal{F}inite^{(2\times 0)}(x, y, z) = 2\Re [\langle \mathcal{M}^{(0)} | \mathcal{M}^{(2),\text{fin}} \rangle] \quad (4.30)$$

and

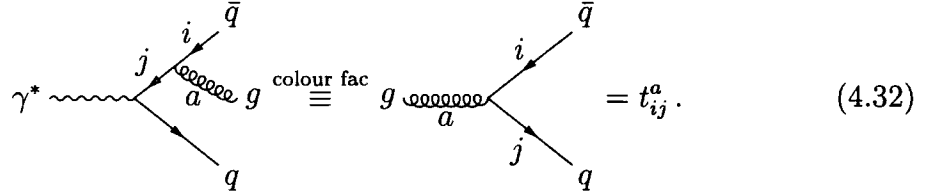
$$\begin{aligned} \mathcal{P}oles^{(2\times 0)}(x, y, z) = 2\Re \Bigg[& -\frac{1}{2} \langle \mathcal{M}^{(0)} | \mathbf{I}^{(1)}(\epsilon) \mathbf{I}^{(1)}(\epsilon) | \mathcal{M}^{(0)} \rangle - \frac{\beta_0}{\epsilon} \langle \mathcal{M}^{(0)} | \mathbf{I}^{(1)}(\epsilon) | \mathcal{M}^{(0)} \rangle \\ & + \langle \mathcal{M}^{(0)} | \mathbf{I}^{(1)}(\epsilon) | \mathcal{M}^{(1)} \rangle \\ & + e^{-\epsilon\gamma_E} \frac{\Gamma(1-2\epsilon)}{\Gamma(1-\epsilon)} \left(\frac{\beta_0}{\epsilon} + K \right) \langle \mathcal{M}^{(0)} | \mathbf{I}^{(1)}(2\epsilon) | \mathcal{M}^{(0)} \rangle \\ & + \langle \mathcal{M}^{(0)} | \mathbf{H}^{(2)}(\epsilon) | \mathcal{M}^{(0)} \rangle \Bigg]. \end{aligned} \quad (4.31)$$

It should be noted that, in this prescription, part of the finite terms in $\mathcal{T}^{(6,[i\times j])}$ are accounted for by the $\mathcal{O}(\epsilon^0)$ expansion of $\mathcal{P}oles^{(i\times j)}$. More importantly, these finite terms coming from the expansion of the predicted IR structure do not correspond to the *true* finite terms obtained from the ME calculation with Feynman diagrams, it is simply the ‘left-over’ piece from the Catani prediction — if it were the true finite remainder, we would not need to calculate the diagrams in the first place! The finite remainder $\mathcal{F}inite^{(i\times j)}$ which is obtained by subtracting the predicted IR structure (expanded through to $\mathcal{O}(\epsilon^0)$) from the renormalised ME, represents this difference.

In the following Sections we compute all the expressions needed to construct $\mathcal{P}oles^{(1\times 1)}$ and $\mathcal{P}oles^{(2\times 0)}$ so that we can compare them to the expressions obtained by explicit calculation of the Feynman Diagrams. In particular we need to calculate $\mathbf{I}^{(1)}(\epsilon)$ and $\mathbf{H}^{(2)}(\epsilon)$.

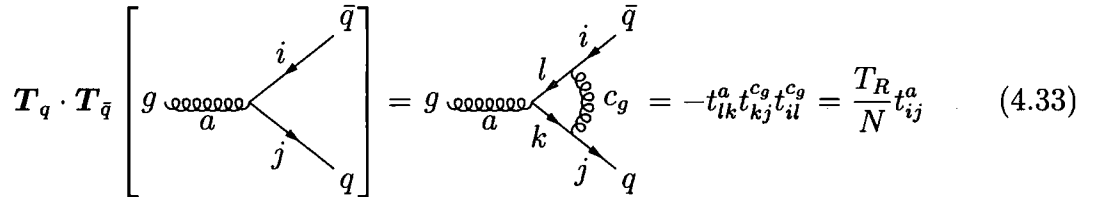
4.3.3 $I^{(1)}(\epsilon)$ for $e^+e^- \rightarrow q\bar{q}g$

We must now construct the $I^{(1)}(\epsilon)$ operator. For this particular process, there is only one colour structure present at tree level which, in terms of the gluon colour a and the quark and antiquark colours i and j , is simply t_{ij}^a . In colour space we have

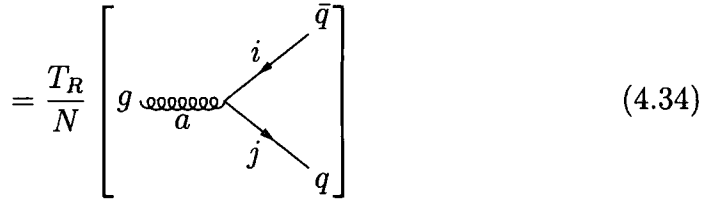


$$\gamma^* \rightarrow q \bar{q} g \text{ (gluon on quark)} \equiv g \text{ (gluon on antiquark)} = t_{ij}^a. \quad (4.32)$$

Adding higher loops does not introduce additional colour structures, and the amplitudes are therefore vectors in a one-dimensional space. Similarly, the infrared singularity operator $I^{(1)}(\epsilon)$ is a 1×1 matrix in the colour space. To evaluate $I^{(1)}(\epsilon)$ we need to consider the contributions from the radiation of a gluon between each pair of legs in the diagram, i.e. calculate the colour algebra $\mathbf{T}_i \cdot \mathbf{T}_j$. There are two distinct diagrams (we can use quark–antiquark symmetry to find the third diagram)



$$\mathbf{T}_q \cdot \mathbf{T}_{\bar{q}} \left[g \text{ (gluon on quark)} \right] = g \text{ (gluon on antiquark)} = -t_{lk}^a t_{kj}^{c_g} t_{il}^{c_g} = \frac{T_R}{N} t_{ij}^a \quad (4.33)$$



$$= \frac{T_R}{N} \left[g \text{ (gluon on quark)} \right] \quad (4.34)$$

and

$$T_{\bar{q}} \cdot T_g \left[g \text{---} \text{wavy line } a \text{---} \begin{array}{l} i \nearrow \bar{q} \\ j \searrow q \end{array} \right] = g \text{---} \text{wavy line } a \text{---} \begin{array}{l} \text{wavy line } c_g \text{---} i \nearrow \bar{q} \\ \text{wavy line } b \text{---} j \searrow q \end{array} \text{---} k = i f^{ac_g b} t_{ik}^{c_g} t_{kj}^b = -\frac{1}{2} N t_{ij}^a \quad (4.35)$$

$$= -\frac{1}{2} N \left[g \text{---} \text{wavy line } a \text{---} \begin{array}{l} i \nearrow \bar{q} \\ j \searrow q \end{array} \right], \quad (4.36)$$

where we have made use of two identities of the colour matrices. In the first expression we use the Fierz identity

$$t_{ij}^a t_{kl}^a = T_R \left(\delta_{il} \delta_{jk} - \frac{1}{N} \delta_{ij} \delta_{kl} \right), \quad (4.37)$$

in the second expression we use

$$f^{abc} t^b t^c = \frac{1}{2} i N t^a. \quad (4.38)$$

This provides the colour algebra

$$T_q \cdot T_{\bar{q}} = \frac{T_R}{N} \quad \text{and} \quad T_{\bar{q}} \cdot T_g = -\frac{1}{2} N. \quad (4.39)$$

Putting these terms together into Equation (2.52), the expression for $\mathbf{I}^{(1)}(\epsilon)$ becomes

$$\mathbf{I}^{(1)}(\epsilon) = -\frac{e^{\epsilon\gamma}}{2\Gamma(1-\epsilon)} \left[N \left(\frac{1}{\epsilon^2} + \frac{3}{4\epsilon} + \frac{\beta_0}{2N\epsilon} \right) (\mathbf{S}_{13} + \mathbf{S}_{23}) - \frac{1}{N} \left(\frac{1}{\epsilon^2} + \frac{3}{2\epsilon} \right) \mathbf{S}_{12} \right], \quad (4.40)$$

where (since we have set $\mu^2 = s_{123}$)

$$\mathbf{S}_{ij} = \left(-\frac{s_{123}}{s_{ij}} \right)^\epsilon. \quad (4.41)$$

Note that on expanding S_{ij} , imaginary parts are generated, the sign of which is fixed by the small imaginary part $+i0$ of s_{ij} . Other combinations such as $\langle \mathcal{M}^{(0)} | \mathbf{I}^{(1)}(\epsilon)^\dagger$ are obtained by using the hermitian conjugate operator $\mathbf{I}^{(1)}(\epsilon)^\dagger$, where the only practical change is that the sign of the imaginary part of \mathbf{S} is reversed.

The origin of the various terms in Eq. (4.40) is straightforward. Each parton pair ij in the event forms a radiating antenna of scale s_{ij} . Terms proportional to S_{ij} are cancelled by real radiation emitted from leg i and absorbed by leg j . The soft singularities $\mathcal{O}(1/\epsilon^2)$ are independent of the identity of the participating partons and are universal. However, the collinear singularities depend on the identities of the participating partons. For each quark we find a contribution of $3/(4\epsilon)$ and for each gluon we find a contribution of $\beta_0/(2\epsilon)$ coming from the integral over the collinear splitting function.

4.3.4 $H^{(2)}(\epsilon)$ for $e^+e^- \rightarrow q\bar{q}g$

The last term of Equation (4.31) involves $H^{(2)}(\epsilon)$ and only produces a single pole in ϵ and is given by equation (2.59). As with the single pole parts of $\mathbf{I}^{(1)}(\epsilon)$, the process-dependent $H^{(2)}$ can be constructed by counting the number of radiating partons present in the event. In this case, there is a quark–antiquark pair and a gluon present in the final state, so that

$$H^{(2)} = 2H_q^{(2)} + H_g^{(2)} \quad (4.42)$$

where in the $\overline{\text{MS}}$ scheme

$$H_g^{(2)} = \left(\frac{1}{2}\zeta_3 + \frac{5}{12} + \frac{11\pi^2}{144} \right) N^2 + \frac{5}{27} N_F^2 + \left(-\frac{\pi^2}{72} - \frac{89}{108} \right) N N_F - \frac{N_F}{4N}, \quad (4.43)$$

$$H_q^{(2)} = \left(\frac{7}{4}\zeta_3 + \frac{409}{864} - \frac{11\pi^2}{96} \right) N^2 + \left(-\frac{1}{4}\zeta_3 - \frac{41}{108} - \frac{\pi^2}{96} \right) \\ + \left(-\frac{3}{2}\zeta_3 - \frac{3}{32} + \frac{\pi^2}{8} \right) \frac{1}{N^2} + \left(\frac{\pi^2}{48} - \frac{25}{216} \right) \frac{(N^2 - 1)N_F}{N}, \quad (4.44)$$

so that

$$H^{(2)} = \left(4\zeta_3 + \frac{589}{432} - \frac{11\pi^2}{72} \right) N^2 + \left(-\frac{1}{2}\zeta_3 - \frac{41}{54} - \frac{\pi^2}{48} \right) \\ + \left(-3\zeta_3 - \frac{3}{16} + \frac{\pi^2}{4} \right) \frac{1}{N^2} + \left(-\frac{19}{18} + \frac{\pi^2}{36} \right) NN_F \\ + \left(-\frac{1}{54} - \frac{\pi^2}{24} \right) \frac{N_F}{N} + \frac{5}{27} N_F^2. \quad (4.45)$$

The factors $H_q^{(2)}$ and $H_g^{(2)}$ are directly related to those found in gluon–gluon scattering [34], quark–quark scattering [31, 32] and quark–gluon scattering [33] (which each involve four partons) as well as in the quark form factor [59, 60, 61, 62]. We also note that (on purely dimensional grounds) one might expect terms of the type S_{ij}^2 to be present in $H^{(2)}$. Of course such terms are $1 + \mathcal{O}(\epsilon)$ and therefore leave the pole part unchanged and only modify the finite remainder. At present it is not known how to systematically include these effects.

4.3.5 $\langle \mathcal{M}^{(0)} | \mathcal{M}^{(1)} \rangle$ for $e^+e^- \rightarrow q\bar{q}g$

Finally, since both $\mathbf{I}^{(1)}(\epsilon)$ and $\mathbf{H}^{(2)}(\epsilon)$ factorise completely, that is, they are just proportional to identity matrix in colour space then we have, for example, the following simplification

$$\langle \mathcal{M}^{(0)} | \mathbf{I}^{(1)}(\epsilon) | \mathcal{M}^{(1)} \rangle \rightarrow \mathbf{I}^{(1)}(\epsilon) \langle \mathcal{M}^{(0)} | \mathcal{M}^{(1)} \rangle. \quad (4.46)$$

Similar simplifications occur for the other combinations which involve $\mathbf{I}^{(1)}(\epsilon)$ and $\mathbf{H}^{(2)}(\epsilon)$.

Therefore, with this in mind, we see from Equations (4.26) and (4.31) that the only remaining pieces we have to calculate in order to construct $\mathcal{Poles}^{(i \times j)}$ are

the square of the Born amplitude, $\langle \mathcal{M}^{(0)} | \mathcal{M}^{(0)} \rangle$ which is already given by Equation (4.11), and also the renormalised interference of tree and one-loop amplitudes $\langle \mathcal{M}^{(0)} | \mathcal{M}^{(1)} \rangle$. This can be written to all orders in ϵ using the relation

$$\langle \mathcal{M}^{(0)} | \mathcal{M}^{(1)} \rangle = S_\epsilon^{-1} \langle \mathcal{M}^{(0),un} | \mathcal{M}^{(1),un} \rangle - \frac{\beta_0}{2\epsilon} \langle \mathcal{M}^{(0),un} | \mathcal{M}^{(0),un} \rangle, \quad (4.47)$$

where

$$\langle \mathcal{M}^{(0),un} | \mathcal{M}^{(1),un} \rangle = V \left(N f_1(y, z) + \frac{1}{N} f_2(y, z) + (y \leftrightarrow z) \right). \quad (4.48)$$

The functions $f_1(y, z)$ and $f_2(y, z)$ can be written in terms of the one-loop bubble integral and the one-loop box integral in $D = 6 - 2\epsilon$ dimensions, Box^6 :

$$\begin{aligned} f_1(y, z) = & \frac{1}{yz} \left[(-3 + \epsilon + 2\epsilon^2) \text{Bub}(s_{123}) + \left(-\frac{4}{\epsilon} + 12 - 8\epsilon \right) \text{Bub}(ys_{123}) \right] \\ & + \frac{y}{z} \left[\left(-\frac{2}{\epsilon} + 8 - 10\epsilon + 3\epsilon^2 + \epsilon^3 \right) \text{Bub}(zs_{123}) + (-3 + 4\epsilon + \epsilon^2 - 2\epsilon^3) \text{Bub}(s_{123}) \right. \\ & \quad \left. + \left(-\frac{2}{\epsilon} + 8 - 10\epsilon + 4\epsilon^2 \right) \text{Bub}(ys_{123}) \right] \\ & + \frac{1}{z} \left[\left(\frac{4}{\epsilon} - 12 + 9\epsilon - \epsilon^2 \right) \text{Bub}(zs_{123}) + (6 - 2\epsilon - 4\epsilon^2) \text{Bub}(s_{123}) \right. \\ & \quad \left. + \left(\frac{4}{\epsilon} - 12 + 8\epsilon \right) \text{Bub}(ys_{123}) \right] \\ & + \frac{y}{(1-z)^2} (1-\epsilon) \left[\text{Bub}(zs_{123}) - \text{Bub}(s_{123}) \right] \\ & + \frac{y}{(1-z)} \left[(3 - 5\epsilon + 2\epsilon^3) \text{Bub}(zs_{123}) + (-3 + 4\epsilon + \epsilon^2 - 2\epsilon^3) \text{Bub}(s_{123}) \right] \\ & + \frac{1}{(1-z)} (4 - 3\epsilon - 3\epsilon^2 - 2\epsilon^3) \left[\text{Bub}(s_{123}) - \text{Bub}(zs_{123}) \right] \\ & + (4 - 9\epsilon + 6\epsilon^2 - \epsilon^3) \text{Bub}(zs_{123}) \\ & + (1 - 2\epsilon) \left[\frac{1}{z} 8(-1 + \epsilon) + \frac{y^2}{z} (-2 + 4\epsilon - 2\epsilon^2) + \frac{y}{z} (6 - 8\epsilon + 2\epsilon^2) \right. \\ & \quad \left. + z(-2 + 2\epsilon - 8\epsilon^2) + (4 - 3\epsilon + 3\epsilon^2) \right. \\ & \quad \left. + \frac{1}{yz} 2(1 - \epsilon) \right] s_{123} \text{Box}^6(ys_{123}, zs_{123}, s_{123}), \end{aligned} \quad (4.49)$$

$$\begin{aligned}
f_2(y, z) = & \frac{1}{yz} \left[(3 - \epsilon - 2\epsilon^2) \text{Bub}(s_{123}) + \left(\frac{2}{\epsilon} - 6 + 4\epsilon \right) \text{Bub}((1 - y - z)s_{123}) \right] \\
& + \frac{y}{z} \left[-\epsilon^2(1 - \epsilon) \text{Bub}(zs_{123}) + (3 - 4\epsilon - \epsilon^2 + 2\epsilon^3) \text{Bub}(s_{123}) \right. \\
& \quad \left. + \left(\frac{2}{\epsilon} - 8 + 10\epsilon - 4\epsilon^2 \right) \text{Bub}((1 - y - z)s_{123}) \right] \\
& + \frac{1}{z} \left[\epsilon(1 - \epsilon) \text{Bub}(zs_{123}) + (-6 + 2\epsilon + 4\epsilon^2) \text{Bub}(s_{123}) \right. \\
& \quad \left. + \left(-\frac{4}{\epsilon} + 12 - 8\epsilon \right) \text{Bub}((1 - y - z)s_{123}) \right] \\
& + \frac{1}{(y + z)^2} 2 \left[\text{Bub}((1 - y - z)s_{123}) - \text{Bub}(s_{123}) \right] \\
& + \frac{1}{(y + z)} 2\epsilon \left[\text{Bub}(s_{123}) - 2\text{Bub}((1 - y - z)s_{123}) \right] \\
& + \frac{y}{(1 - z)^2} (1 - \epsilon) \left[\text{Bub}(s_{123}) - \text{Bub}(zs_{123}) \right] \\
& + \frac{y}{(1 - z)} \left[(3 - 4\epsilon - \epsilon^2 + 2\epsilon^3) \text{Bub}(s_{123}) + (-3 + 5\epsilon - 2\epsilon^3) \text{Bub}(zs_{123}) \right] \\
& + \frac{1}{(1 - z)} (2 + \epsilon - 5\epsilon^2 - 2\epsilon^3) \left[\text{Bub}(zs_{123}) - \text{Bub}(s_{123}) \right] \\
& + (2 - 7\epsilon + 2\epsilon^2 + 3\epsilon^3) \text{Bub}(zs_{123}) + (-4 + 10\epsilon - 4\epsilon^2) \text{Bub}((1 - y - z)s_{123}) \\
& + (1 - 2\epsilon) \left[(8 - 4\epsilon) - \frac{(1 - y)}{z} 4(1 - \epsilon) + (y + z)(-4 + 4\epsilon - 6\epsilon^2 - 2\epsilon^3) \right. \\
& \quad \left. + \frac{y^2}{z} (-2 + 4\epsilon - 2\epsilon^2) \right] s_{123} \text{Box}^6((1 - y - z)s_{123}, zs_{123}, s_{123}). \quad (4.50)
\end{aligned}$$

Explicit formulae for the bubble and box integrals are given in Appendix E.

4.4 Method

The calculation of the ME begins with the generation of the corresponding Feynman diagrams. To do this requires a program whereby we can input the physical model, namely the particle content and the vertices and output all physical topologies. This was implemented by use of the QGRAF [63] program. In particular, the Feynman diagrams contributing to the i -loop amplitude $|\mathcal{M}^{(i)}\rangle$ ($i = 0, 1, 2$) were all generated.

There are 2 diagrams at tree-level, 13 diagrams at one loop and 229 diagrams at two loops. The complete set is presented in Section 4.5.

The next step is to assign the propagators and vertices of the QGRAF output with the corresponding Feynman rules. After projecting $|\mathcal{M}^{(2)}\rangle$ by $\langle\mathcal{M}^{(0)}|$ and $|\mathcal{M}^{(1)}\rangle$ by $\langle\mathcal{M}^{(1)}|$ the summation over colours and spins is performed. When summing over the polarisations of the external gluon and off-shell photon, we use the Feynman gauge:

$$\sum_{\text{spins}} \epsilon_i^\mu \epsilon_i^{\nu*} = -g^{\mu\nu}. \quad (4.51)$$

This is valid because the gluon always couples to a conserved fermionic current, which selects only the physical degrees of polarisation. The use of an axial polarisation sum to project out the transverse polarisations (as applied in [34, 33]) is therefore not needed. This process is particularly suited to use of the computer algebra programs FORM2 [64] and FORM3 [65] which have built in routines to take traces of Dirac matrices. At this stage the loop integrals are identified along with irreducible numerators and translated into the standard $\mathcal{I}^D(\{\nu_1, \dots, \nu_{N_d}\})$ notation. The calculation at this point consists of all the ME expressed as sums of both scalar and tensor integrals.

The one-loop self-interference contribution $\mathcal{T}^{(6,[1 \times 1])}$ is computed by reducing all tensorial loop integrals according to the standard Passarino–Veltman procedure [66] to scalar one-loop two-point, three-point and four-point integrals. It has been known for a long time that those three-point integrals can be further reduced to linear combinations of two-point integrals using IBP identities. After this reduction, $\mathcal{T}^{(6,[1 \times 1])}$ is expressed as a bilinear combination of only two integrals: the one-loop bubble and the one-loop box, which are listed in Appendix E.

The computation of $T^{(6,[2 \times 0])}$ is by far less straightforward, however, we have presented all the necessary tools to make such a calculation possible in the previous Sections. The calculation proceeds as follows.

With the Laporta algorithm described in Section 3.6 the IBP relations are used to derive the reduction to MI of all possible scalar and tensor integrals which can possibly occur in the ME. For the process $\gamma^* \rightarrow q\bar{q}g$ this involves the computation of integrals with up to 7 propagators and 4 irreducible numerators. For this procedure the computer algebra program MAPLE [67] was chosen due to its ability to simplify and factor large equations. The reduction is implemented on a topology basis and for each topology a file of all integrals is constructed and output in a format suitable to be read by FORM. This procedure results in a collection of files expressing all scalar and tensor integrals in terms of MI.

The next step in calculation is obvious, the files created by MAPLE are read into the FORM program thus expressing the ME as a linear combination of all MI. At this point we are almost finished. The final step is to substitute the MI with their ϵ -expansions. For the purposes of this calculation, both the planar and non-planar MI were calculated by Gehrmann and Remiddi [47, 48] in terms of one- and two-dimensional harmonic polylogarithms. The ϵ -expansions for the MI were produced in a format suitable for input directly into the FORM program.

The final ME now expressed as ϵ -expansions can be compared to the Catani prediction for the pole structure. This is done by simple subtraction of the two expressions, the remainder, if it is indeed finite will be the $\mathcal{F}inite^{(i \times j)}$ term discussed in the previous sections. In Section 4.6 we present exactly these results.

The general strategy is summarised more clearly in Figure 4.1.

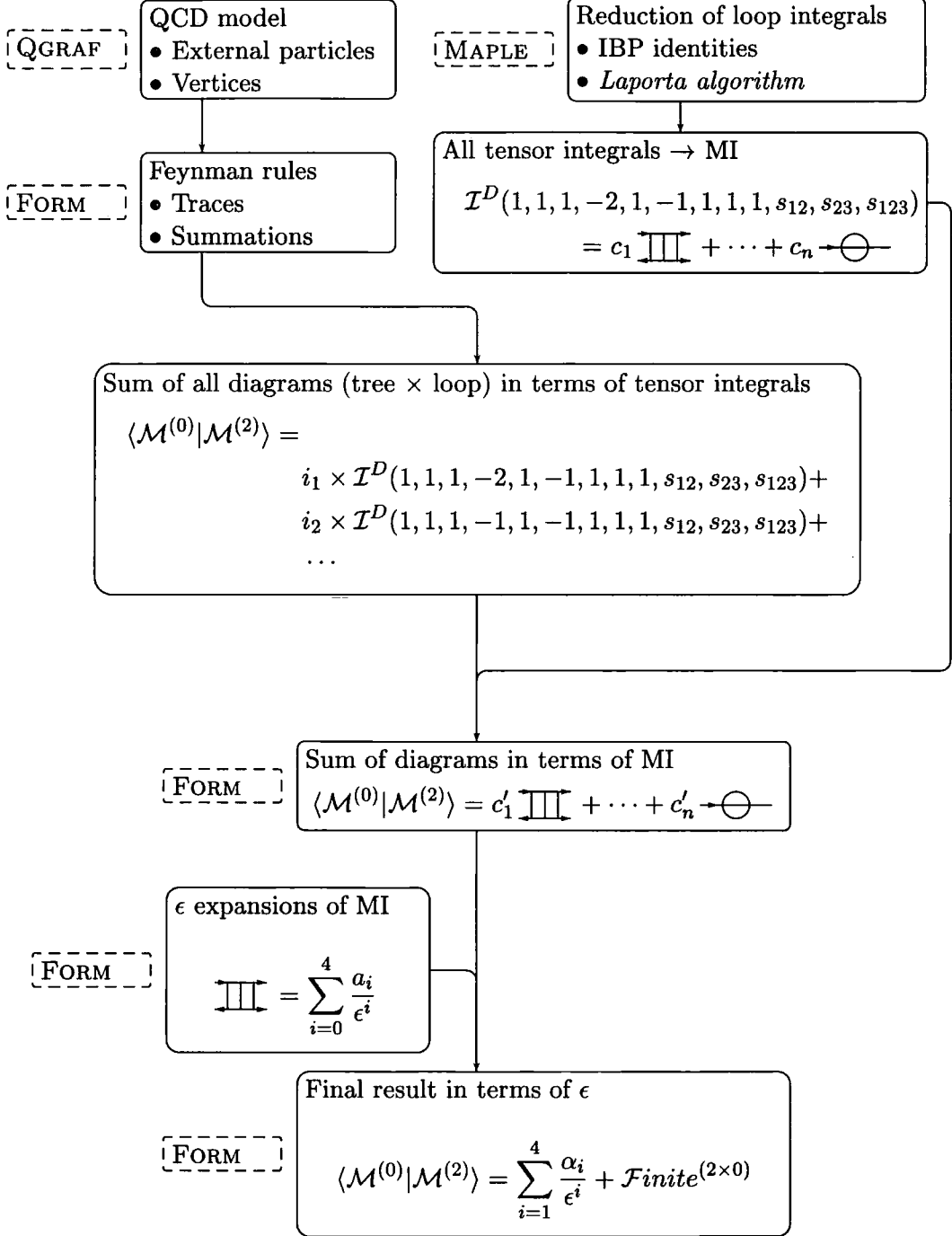
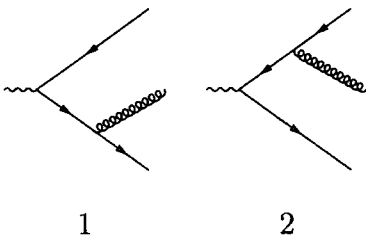


Figure 4.1: The general procedure for calculating matrix elements.

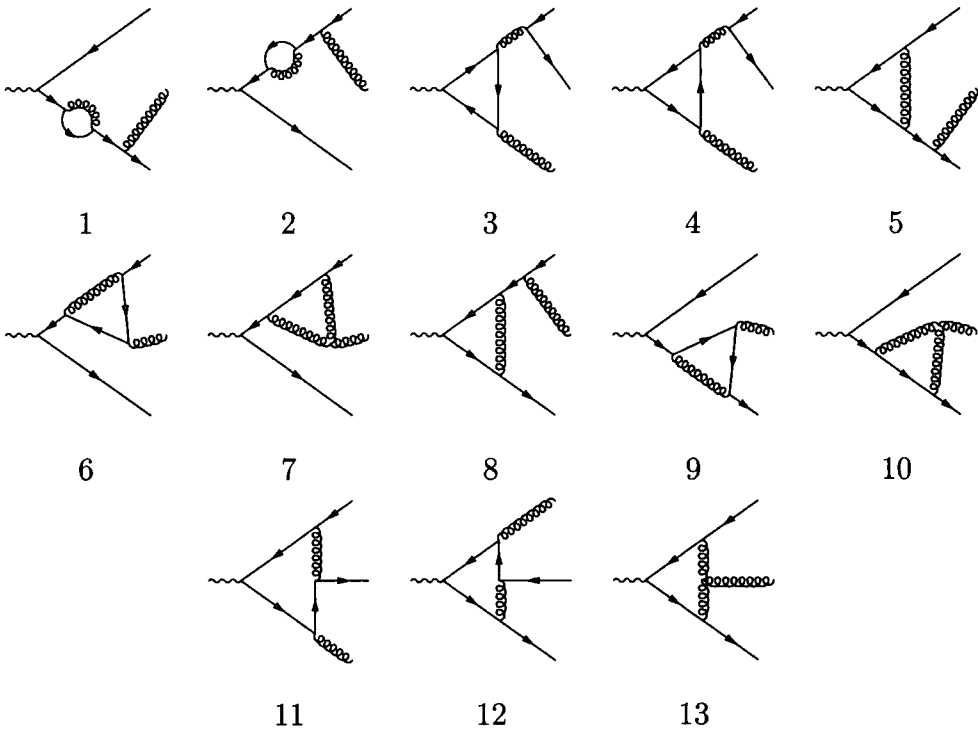
4.5 Diagrams

In this Section we present all of the Feynman diagrams which contribute to the process $\gamma^* \rightarrow q\bar{q}g$.

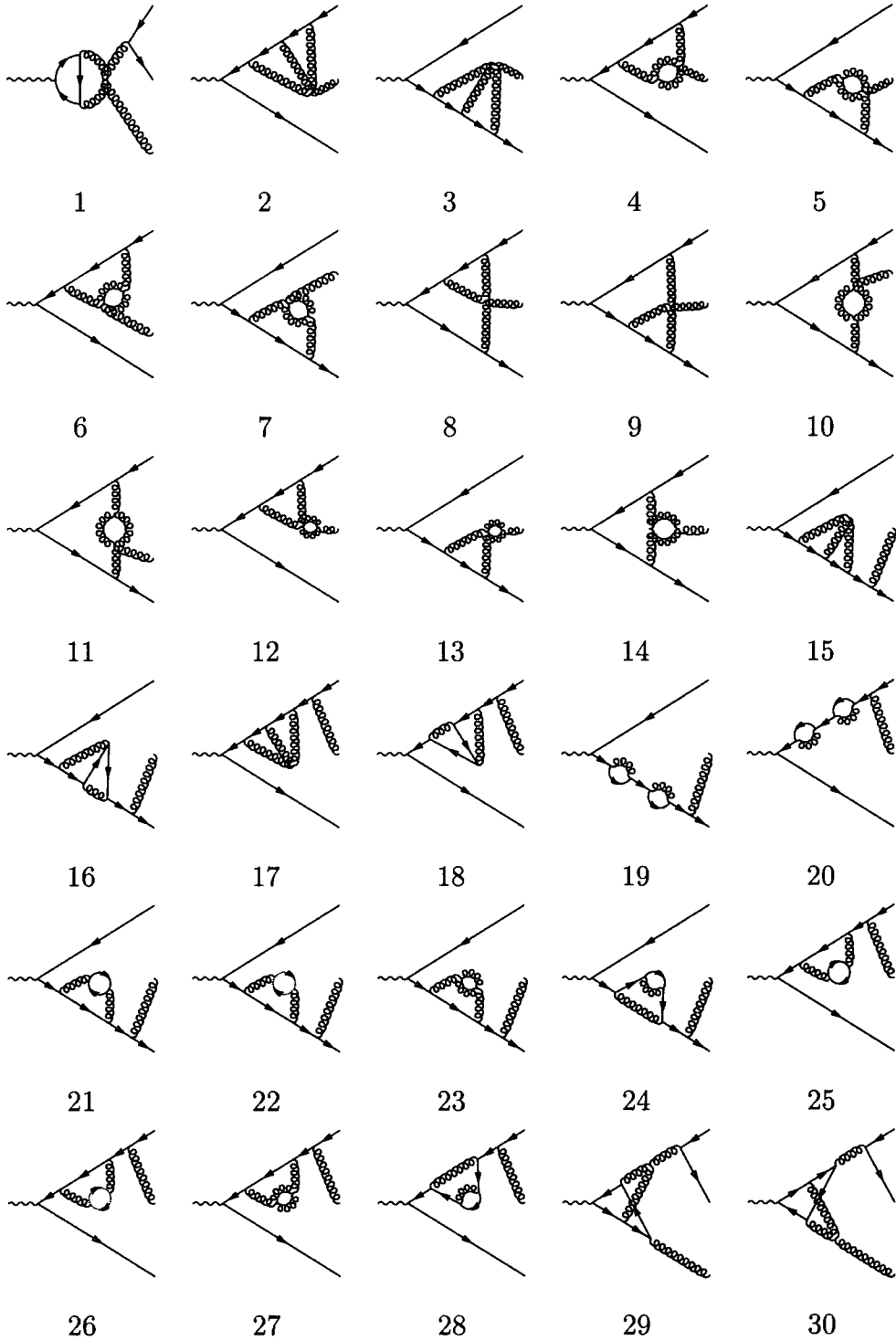
Tree Level Diagrams

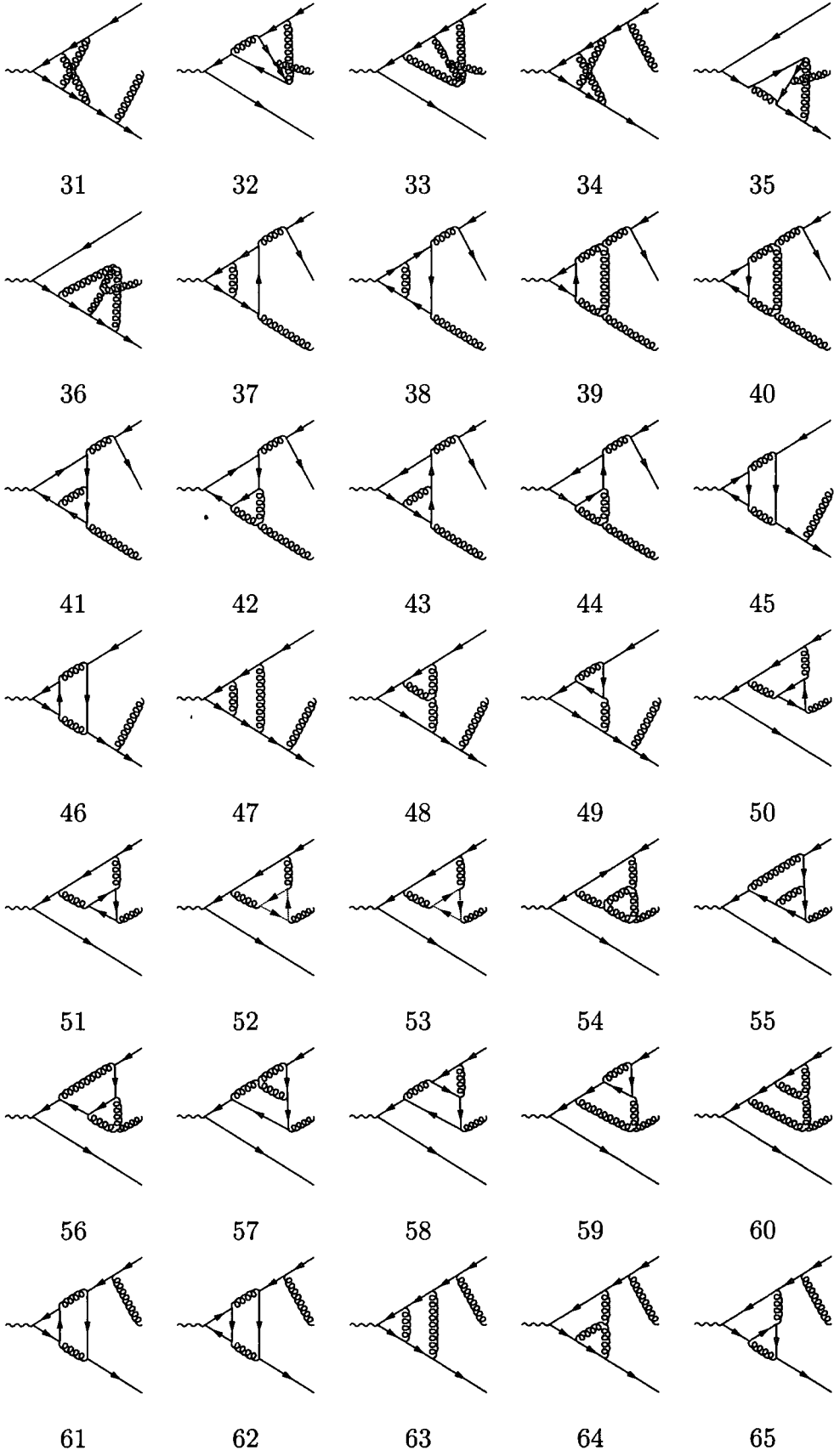


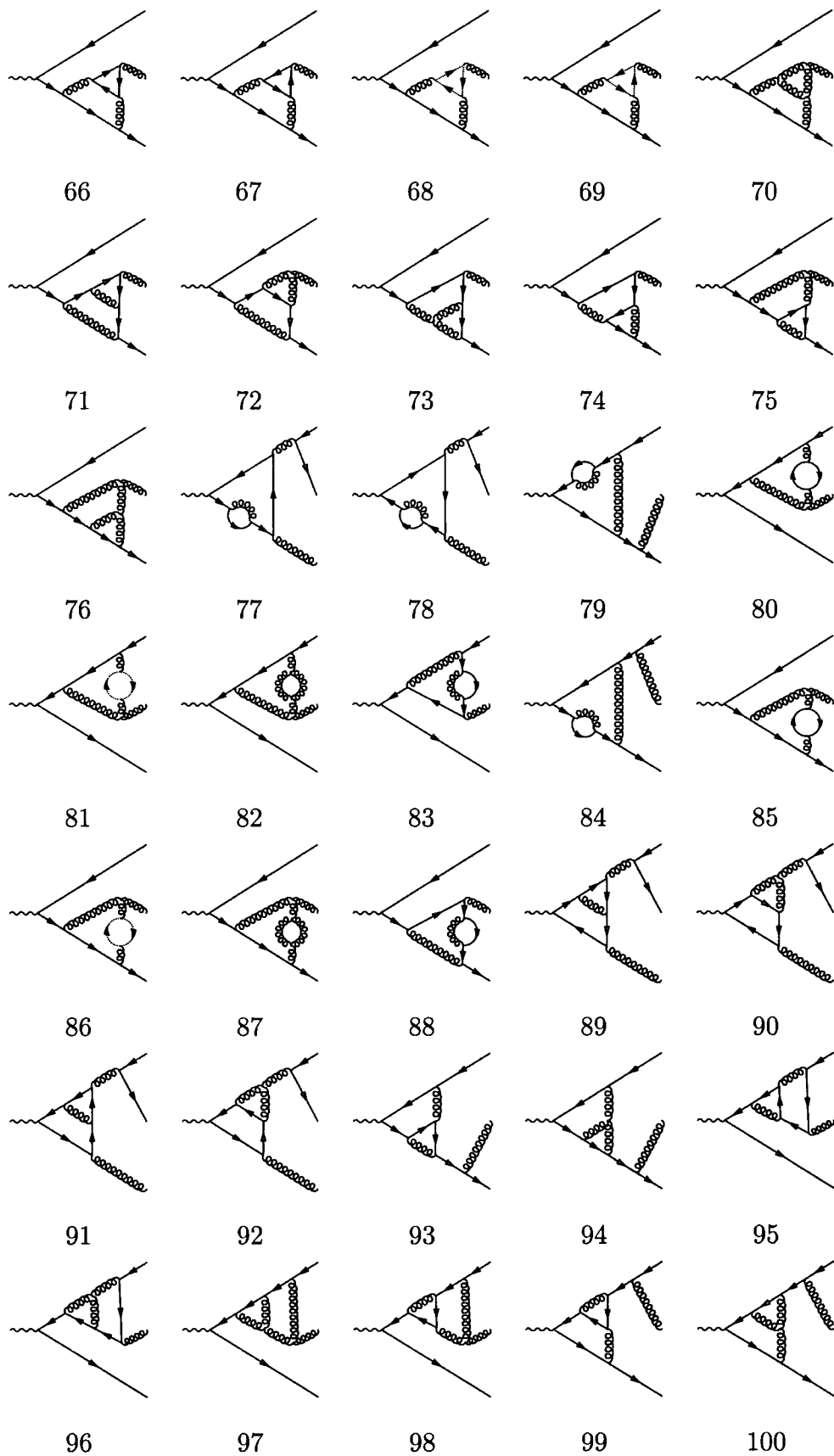
One-Loop Diagrams

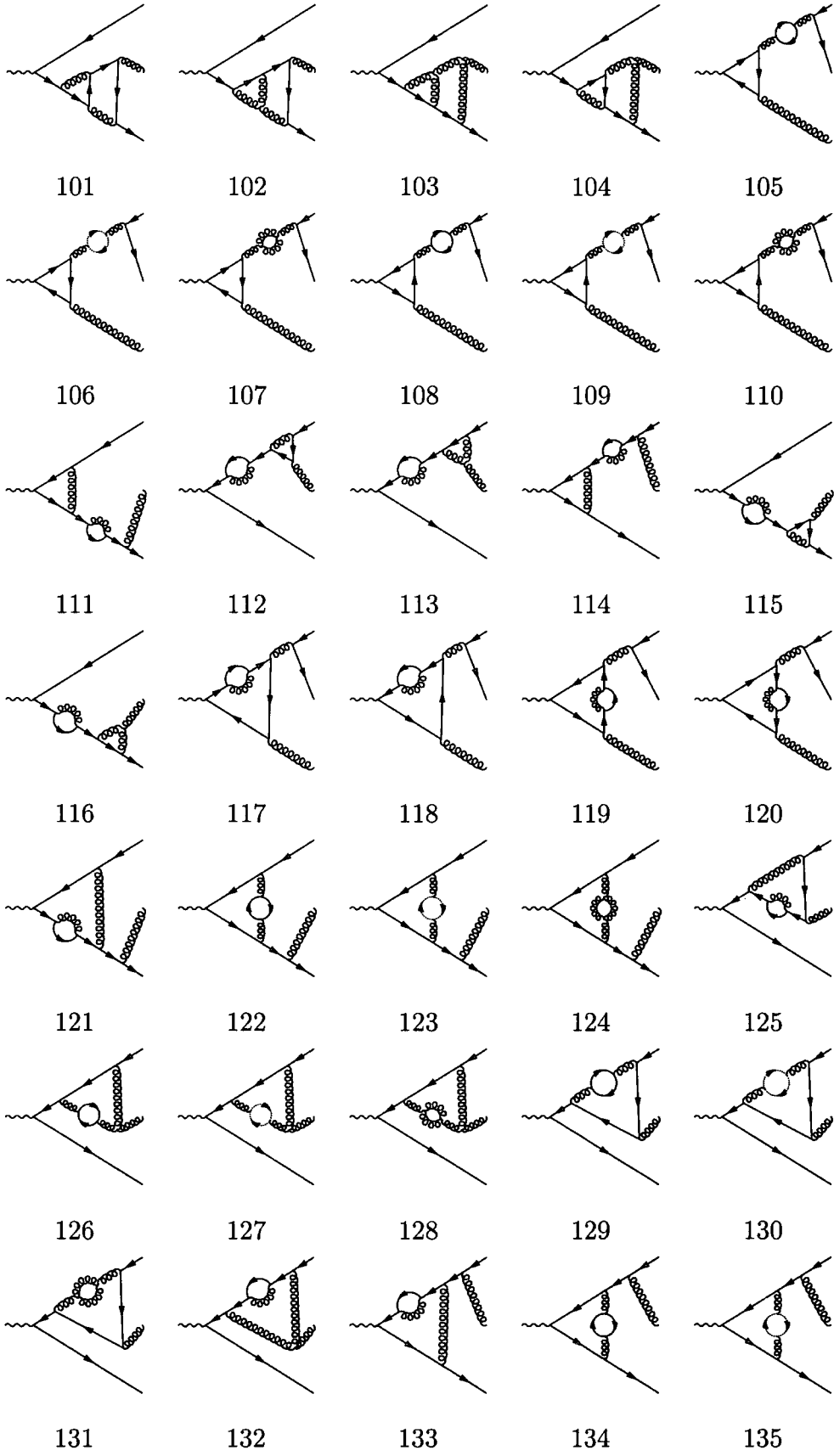


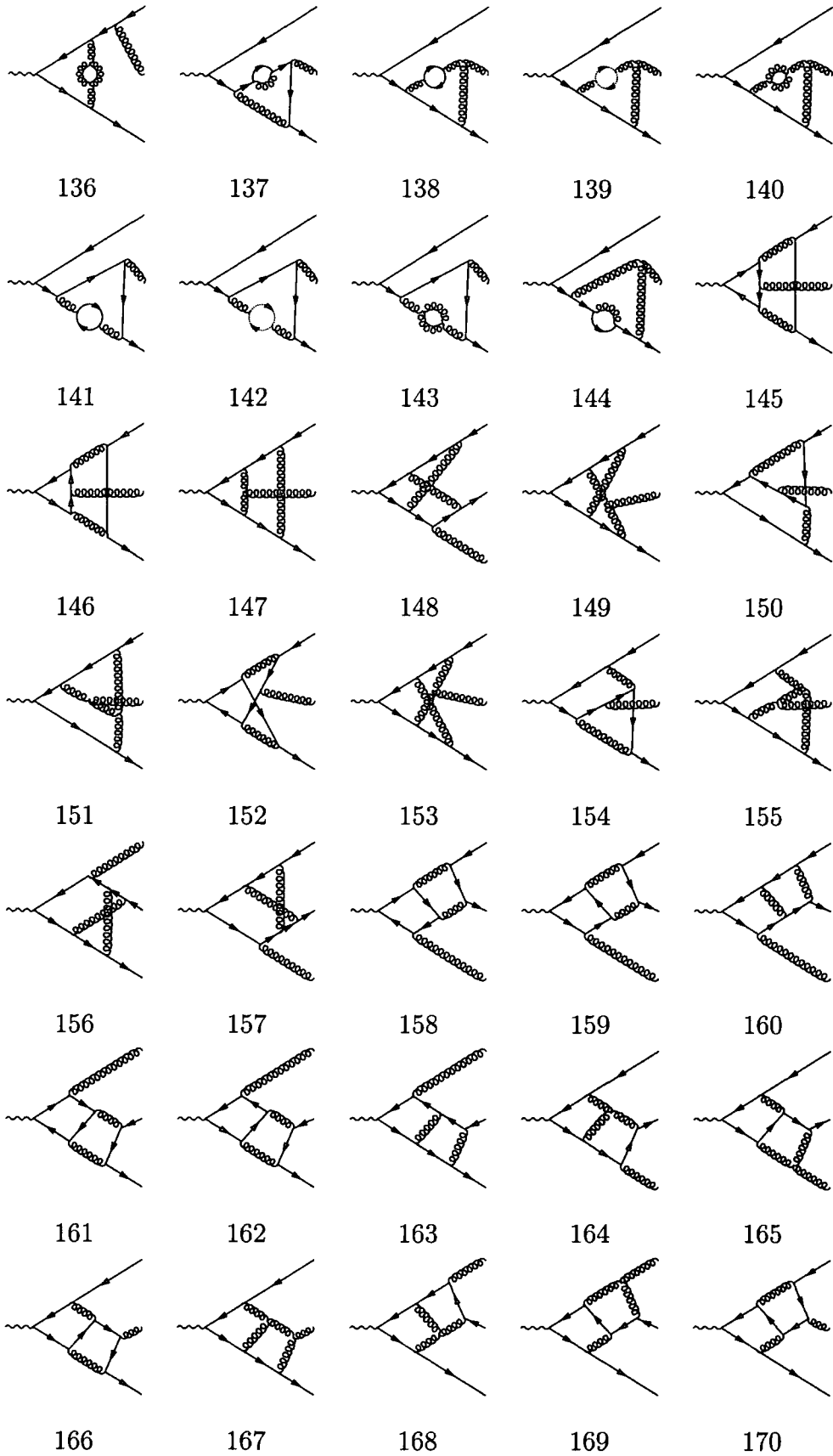
Two-Loop Diagrams

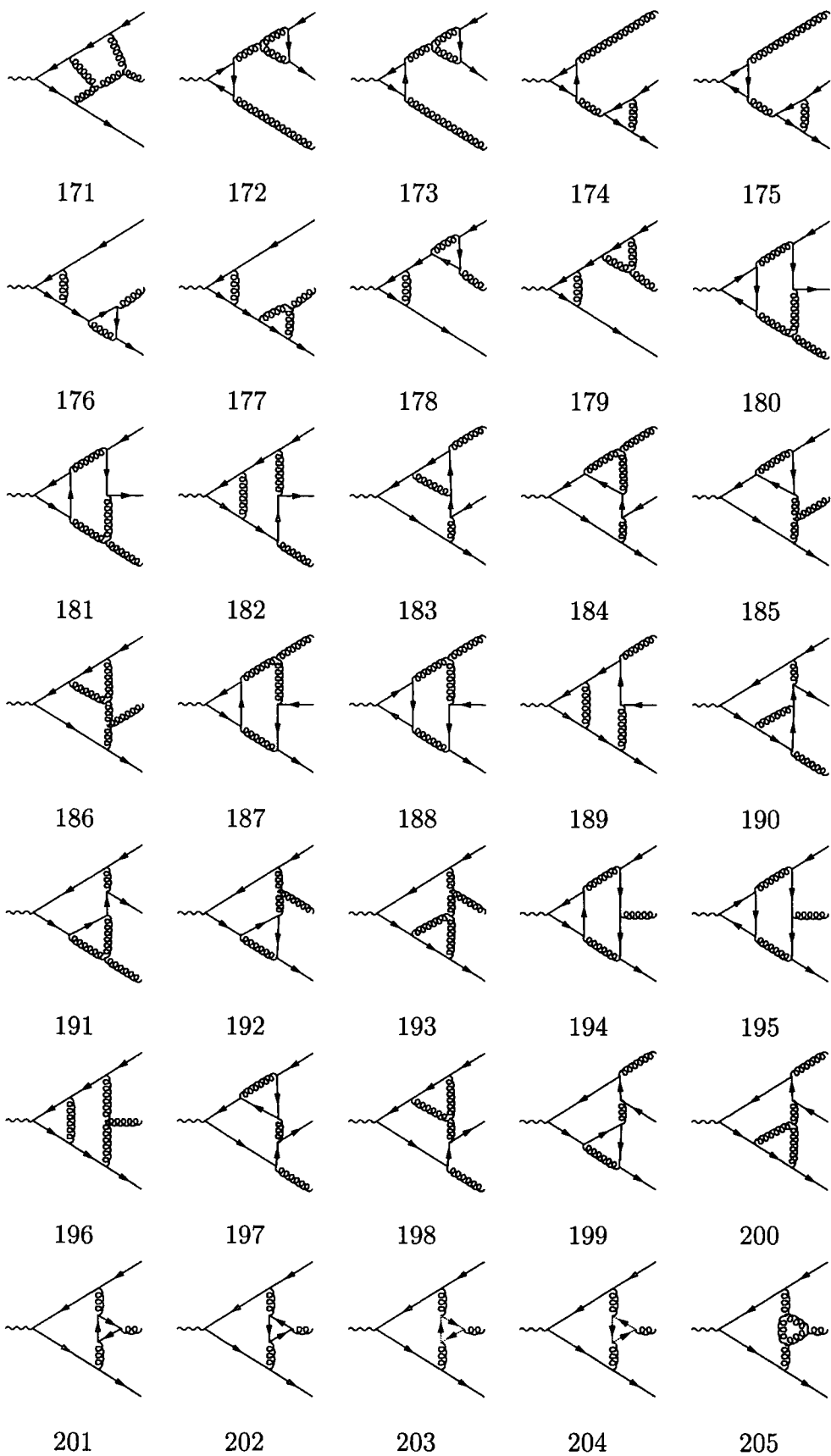


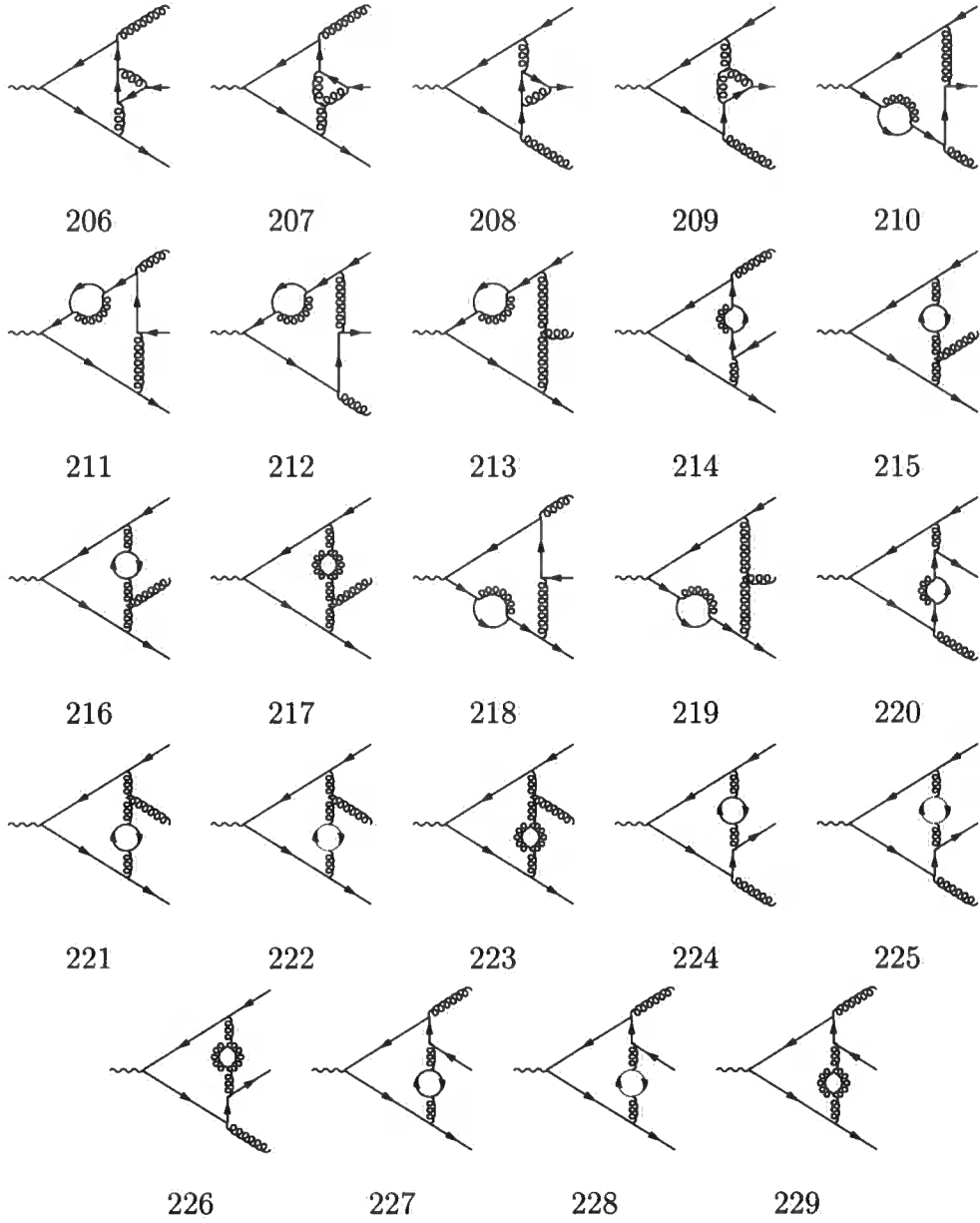












4.6 The Finite Contributions

The finite remainders of the one- and two-loop contributions to $\mathcal{T}^{(6)}$ can be decomposed according to their colour structure and the dependence on the number of quark flavours N_F . In the two-loop contribution, one finds moreover a term proportional to the charge-weighted sum of the quarks flavours $N_{F,\gamma}$ this equals, in the

case of purely electromagnetic interactions:

$$N_{F,\gamma} = \frac{\left(\sum_q e_q\right)^2}{\sum_q e_q^2}. \quad (4.52)$$

This term originates from diagrams containing a closed quark loop coupling to the virtual photon which first appear at the two-loop level.

The tree-level combination of invariants

$$T = \frac{y}{z} + \frac{z}{y} + \frac{2}{yz} - \frac{2}{y} - \frac{2}{z}, \quad (4.53)$$

frequently occurs in the finite part. We therefore extract this combination by expressing $1/(yz)$ by T according to the above equation.

4.6.1 One-Loop Contribution to $\mathcal{T}^{(6)}$

The finite remainder of the self-interference of the one-loop amplitude is decomposed as

$$\begin{aligned} \mathcal{F}^{(1 \times 1)}_{\text{finite}}(x, y, z) = V & \left[N^2 (A_{11}(y, z) + A_{11}(z, y)) + (B_{11}(y, z) + B_{11}(z, y)) \right. \\ & + \frac{1}{N^2} (C_{11}(y, z) + C_{11}(z, y)) + NN_F (D_{11}(y, z) + D_{11}(z, y)) \\ & \left. + \frac{N_F}{N} (E_{11}(y, z) + E_{11}(z, y)) + N_F^2 (F_{11}(y, z) + F_{11}(z, y)) \right], \end{aligned} \quad (4.54)$$

where the coefficients A_{11} , B_{11} , C_{11} , D_{11} , E_{11} and F_{11} are given in Appendix A.

4.6.2 Two-Loop Contribution to $\mathcal{T}^{(6)}$

The finite remainder of the interference of the two-loop amplitude with the tree-level amplitude is decomposed as

$$\begin{aligned}
 \mathcal{F}^{(2 \times 0)}_{\text{finite}}(x, y, z) = V & \left[N^2 (A_{20}(y, z) + A_{20}(z, y)) + (B_{20}(y, z) + B_{20}(z, y)) \right. \\
 & + \frac{1}{N^2} (C_{20}(y, z) + C_{20}(z, y)) + NN_F (D_{20}(y, z) + D_{20}(z, y)) \\
 & + \frac{N_F}{N} (E_{20}(y, z) + E_{20}(z, y)) + N_F^2 (F_{20}(y, z) + F_{20}(z, y)) \\
 & \left. + N_{F,\gamma} \left(\frac{4}{N} - N \right) (G_{20}(y, z) + G_{20}(z, y)) \right], \quad (4.55)
 \end{aligned}$$

where the coefficients A_{20} , B_{20} , C_{20} , D_{20} , E_{20} and F_{20} are given in Appendix B.

CHAPTER 5

The NNLO Helicity Amplitude for $e^+e^- \rightarrow q\bar{q}g$

In Chapter 4 we presented the calculation of the ME for $e^+e^- \rightarrow q\bar{q}g$ *averaged over all helicities*. The results were compared to the Catani prediction for the pole structure and the corresponding $\mathcal{F}inite^{(i \times j)}$ remainders presented. In this Chapter we extend the previous calculation to compute the two-loop *helicity amplitudes* for the same process¹.

As we have already discussed, the most precisely measured observables related to $e^+e^- \rightarrow 3$ jets are the jet production rate itself and a number of event-shape variables. The calculation of these phenomenologically most relevant applications, which also dominate the extraction of α_s , at NNLO accuracy requires only the *helicity averaged* squared matrix element at the two-loop level which we have just calculated. Nevertheless, the helicity amplitudes which we calculate here are interesting for a number of reasons:

- Oriented event-shape observables, which measure the spatial orientation of the final-state jets relative to the direction of the incoming beams require, even for unpolarised beams [69], the calculation of the polarisation tensor of the virtual

¹This Chapter is based on work carried out in [68].

photon mediating the interaction. This polarisation tensor can be recovered from the helicity amplitudes.

- Likewise, to determine the direction of the decay leptons in the crossed process, $V+1$ jet production at unpolarised hadron colliders, it is necessary to compute the polarisation tensor of the vector boson.
- Polarisation of the beams is an important option for the future linear e^+e^- collider TESLA [27], thus providing a direct measurement of event-shape observables in polarised e^+e^- annihilation.
- NNLO predictions for $(V+1)$ -jet production at the RHIC polarised proton–proton collider and for $(2+1)$ jet production at a currently discussed polarised upgrade of the HERA collider do require the calculation of the two-loop helicity amplitudes. These observables would then form part of a full NNLO determination of the polarised parton distribution functions in the proton.
- The study of formal aspects of two-loop matrix elements, such as their collinear limits or their high energy behaviour can be carried out more elegantly on the basis of the underlying helicity amplitudes.

Two-loop helicity amplitudes have up to now only been derived for $2 \rightarrow 2$ bosonic scattering processes with all external legs on-shell: for $gg \rightarrow \gamma\gamma$ [35], $\gamma\gamma \rightarrow \gamma\gamma$ [36, 70] and $gg \rightarrow gg$ [71, 72]. The latter calculation also confirmed earlier results for the squared two-loop $gg \rightarrow gg$ matrix element [34].

In the above calculations, which were all carried out within dimensional regularisation [17, 18, 19], two different methods were used to access the helicity structure of the matrix element: explicit contraction with the external polarisation vectors [35, 36, 71, 72] or projection onto the individual components of the Lorentz-invariant decomposition of the amplitude [70]. Once these are applied to expose the helicity structure, one is left with the task of computing a large num-

ber of two-loop integrals. Using exactly the same techniques as for the calculation of the ME in Chapter 4 these integrals can be reduced via the Laporta algorithm (Section 3.6) to MI, which were derived for massless on-shell two-loop four-point functions in [40, 41, 42, 46, 73, 74].

If an explicit contraction with the external polarisation vectors is performed, one also has to compute two-loop integrals over the $(D - 4)$ dimensional subspace of loop momenta, which reduce however to simple vacuum diagrams [72]. For $2 \rightarrow 2$ scattering processes with external fermions and all external legs on-shell ($e^+e^- \rightarrow e^+e^-$, $q\bar{q} \rightarrow q'\bar{q}'$, $q\bar{q} \rightarrow q\bar{q}$, $q\bar{q} \rightarrow gg$, $q\bar{q} \rightarrow g\gamma$ and $q\bar{q} \rightarrow \gamma\gamma$), only the squared, helicity-averaged two-loop matrix elements have been computed so far [30, 31, 32, 33, 75].

The method which we employ here to extract the two-loop helicity amplitudes for $e^+e^- \rightarrow q\bar{q}g$ is similar to the approach of [70]. That is, by applying projections on all components of the Lorentz-invariant decomposition of the amplitude. In this approach, the corresponding one-loop helicity amplitudes have already been derived in [25].

After carrying out UV renormalisation of the amplitudes in the $\overline{\text{MS}}$ scheme, one is left with poles which are purely of IR origin. The IR pole structure of the amplitudes can be predicted using Catani's IR factorisation formula [29] just as we did for the ME in the previous chapter. Again, we use this formalism to present the infrared poles and the finite parts of the helicity amplitudes in a compact form.

This Chapter is structured as follows: in Sections 5.1– 5.4, we outline the general method used to derive the helicity amplitudes. In Section 5.5 we discuss how the helicity amplitude calculation can be related to the previous calculation of the ME in Chapter 4. In Sections 5.6 and 5.7 we show the techniques used to extract the ultraviolet and infrared pole structure. In Section 5.8 the two-loop helicity amplitudes are computed in the Weyl–van der Waerden formalism, which is briefly described in Appendix G. Finally in Section 5.9 we present the finite contributions

to the helicity amplitudes.

5.1 Notation

We begin by defining our notation which closely follows that set out in Chapter 4². We consider the production of a quark–antiquark–gluon system in electron–positron annihilation

$$e^+(p_5) + e^-(p_6) \rightarrow \gamma^*(p_4) \longrightarrow q(p_1) + \bar{q}(p_2) + g(p_3). \quad (5.1)$$

Here too, we work with the Mandelstam invariants s_{12} , s_{13} and s_{23} defined by Equation (4.2) and the dimensionless invariants x , y and z defined by Equation (4.4).

The renormalised amplitude $|\mathcal{M}\rangle$ can be factorised as

$$|\mathcal{M}\rangle = V^\mu \mathcal{S}_\mu(q; g; \bar{q}), \quad (5.2)$$

where V^μ represents the lepton current and \mathcal{S}_μ denotes the hadron current. In the previous Chapter we considered the *unpolarised decay process*

$$\gamma^*(p_4) \longrightarrow q(p_1) + \bar{q}(p_2) + g(p_3), \quad (5.3)$$

for which the amplitude is related to Equation (5.2) by replacing the lepton current V^μ by the polarisation vector of the virtual photon ϵ_4^μ .

In a similar way to the ME, the hadron current may be perturbatively decom-

²There is a slight change of notation from the previous Chapter. Here we will denote the momentum of the virtual photon by p_4 as opposed to q .

posed as

$$\begin{aligned} \mathcal{S}_\mu(q; g; \bar{q}) = \sqrt{4\pi\alpha}e_q\sqrt{4\pi\alpha_s} T_{ij}^a \left[\mathcal{S}_\mu^{(0)}(q; g; \bar{q}) + \left(\frac{\alpha_s}{2\pi}\right) \mathcal{S}_\mu^{(1)}(q; g; \bar{q}) \right. \\ \left. + \left(\frac{\alpha_s}{2\pi}\right)^2 \mathcal{S}_\mu^{(2)}(q; g; \bar{q}) + \mathcal{O}(\alpha_s^3) \right], \end{aligned} \quad (5.4)$$

where e_q denotes the quark charge, a is the colour index for the gluon and i and j are the colour indices for quark and antiquark. α_s is the QCD coupling constant at the renormalisation scale μ , and the $\mathcal{S}_\mu^{(i)}$ are the i -loop contributions to the renormalised amplitude. As usual, renormalisation of ultraviolet divergences is performed in the $\overline{\text{MS}}$ scheme.

5.2 The General Tensor

We begin by writing the most general tensor structure for the hadron current $\mathcal{S}_\mu(q; g; \bar{q})$

$$\begin{aligned} \mathcal{S}_\mu(q; g; \bar{q}) = & \bar{u}(p_1)\not{p}_3u(p_2) (A_{11}\epsilon_3 \cdot p_1 p_{1\mu} + A_{12}\epsilon_3 \cdot p_1 p_{2\mu} + A_{13}\epsilon_3 \cdot p_1 p_{3\mu}) \\ & + \bar{u}(p_1)\not{p}_3u(p_2) (A_{21}\epsilon_3 \cdot p_2 p_{1\mu} + A_{22}\epsilon_3 \cdot p_2 p_{2\mu} + A_{23}\epsilon_3 \cdot p_2 p_{3\mu}) \\ & + \bar{u}(p_1)\gamma_\mu u(p_2) (B_1\epsilon_3 \cdot p_1 + B_2\epsilon_3 \cdot p_2) \\ & + \bar{u}(p_1)\not{p}_3u(p_2) (C_1p_{1\mu} + C_2p_{2\mu} + C_3p_{3\mu}) \\ & + D_1\bar{u}(p_1)\not{p}_3\not{p}_3\gamma_\mu u(p_2) \\ & + D_2\bar{u}(p_1)\gamma_\mu\not{p}_3\not{p}_3u(p_2), \end{aligned} \quad (5.5)$$

where the constraint $\epsilon_3 \cdot p_3 = 0$ has been applied. All coefficients are functions of the scales s_{13} , s_{23} and s_{123} . The above tensor structure is a priori D -dimensional, since the dimensionality of the external states has not yet been specified. The hadron

current is conserved and satisfies

$$\mathcal{S}_\mu(q; g; \bar{q}) p_4^\mu = 0; \quad (5.6)$$

it must also obey the QCD Ward identity when the gluon polarisation vector ϵ_3 is replaced with the gluon momentum,

$$\mathcal{S}_\mu(q; g; \bar{q})(\epsilon_3 \rightarrow p_3) = 0. \quad (5.7)$$

These constraints yield relations amongst the 13 distinct tensor structures and applying these identities gives the gauge-invariant form of the tensor,

$$\begin{aligned} \mathcal{S}_\mu(q; g; \bar{q}) = & A_{11}(s_{13}, s_{23}, s_{123})T_{11\mu} + A_{12}(s_{13}, s_{23}, s_{123})T_{12\mu} + A_{13}(s_{13}, s_{23}, s_{123})T_{13\mu} \\ & + A_{21}(s_{13}, s_{23}, s_{123})T_{21\mu} + A_{22}(s_{13}, s_{23}, s_{123})T_{22\mu} + A_{23}(s_{13}, s_{23}, s_{123})T_{23\mu} \\ & + B(s_{13}, s_{23}, s_{123})T_\mu, \end{aligned} \quad (5.8)$$

where A_{ij} and B are gauge-independent functions and the tensor structures $T_{IJ\mu}$ and T_μ are given by

$$T_{1J\mu} = \bar{u}(p_1)\not{p}_3u(p_2)\epsilon_3 \cdot p_1 p_{J\mu} - \frac{s_{13}}{2}\bar{u}(p_1)\not{\epsilon}_3u(p_2)p_{J\mu} + \frac{s_{J4}}{4}\bar{u}(p_1)\not{\epsilon}_3\not{p}_3\gamma_\mu u(p_2), \quad (5.9)$$

$$T_{2J\mu} = \bar{u}(p_1)\not{p}_3u(p_2)\epsilon_3 \cdot p_2 p_{J\mu} - \frac{s_{23}}{2}\bar{u}(p_1)\not{\epsilon}_3u(p_2)p_{J\mu} + \frac{s_{J4}}{4}\bar{u}(p_1)\gamma_\mu\not{p}_3\not{\epsilon}_3u(p_2), \quad (5.10)$$

$$\begin{aligned} T_\mu = & s_{23} \left(\bar{u}(p_1)\gamma_\mu u(p_2)\epsilon_3 \cdot p_1 + \frac{1}{2}\bar{u}(p_1)\not{\epsilon}_3\not{p}_3\gamma_\mu u(p_2) \right) \\ & - s_{13} \left(\bar{u}(p_1)\gamma_\mu u(p_2)\epsilon_3 \cdot p_2 + \frac{1}{2}\bar{u}(p_1)\gamma_\mu\not{p}_3\not{\epsilon}_3u(p_2) \right). \end{aligned} \quad (5.11)$$

Each of the tensor structures satisfies both current conservation and the QCD Ward identity. The coefficients are further related by symmetry under the interchange of

the quark and antiquark,

$$\begin{aligned}
A_{21}(s_{13}, s_{23}, s_{123}) &= -A_{12}(s_{23}, s_{13}, s_{123}) ; \\
A_{22}(s_{13}, s_{23}, s_{123}) &= -A_{11}(s_{23}, s_{13}, s_{123}) , \\
A_{23}(s_{13}, s_{23}, s_{123}) &= -A_{13}(s_{23}, s_{13}, s_{123}) , \\
B(s_{13}, s_{23}, s_{123}) &= B(s_{23}, s_{13}, s_{123}) .
\end{aligned} \tag{5.12}$$

5.3 Projectors for the Tensor Coefficients

The coefficients A_{IJ} and B may be easily extracted from a Feynman diagram calculation, by using projectors such that

$$\sum_{\text{spins}} \mathcal{P}(X) \epsilon_4^\mu \mathcal{S}_\mu(q; g; \bar{q}) = X(s_{13}, s_{23}, s_{123}) . \tag{5.13}$$

The explicit forms for the seven projectors in D space-time dimensions are,

$$\begin{aligned}
\mathcal{P}(A_{11}) = & \frac{(s_{23}s_{123}D + s_{13}s_{12}(D-2))}{2s_{13}^3s_{12}^2(D-3)s_{123}} T_{11}^\dagger \cdot \epsilon_4^* - \frac{(s_{13} + s_{23})(D-2)}{2s_{13}^2s_{12}^2(D-3)s_{123}} T_{12}^\dagger \cdot \epsilon_4^* \\
& - \frac{((s_{23} + s_{12})D + 2s_{13})}{2s_{12}s_{13}^3(D-3)s_{123}} T_{13}^\dagger \cdot \epsilon_4^* - \frac{(s_{23}s_{123}(D-2) + s_{13}s_{12}(D-4))}{2s_{23}s_{12}^2s_{13}^2s_{123}(D-3)} T_{21}^\dagger \cdot \epsilon_4^* \\
& + \frac{(s_{13} + s_{23})(D-4)}{2(D-3)s_{12}^2s_{123}s_{13}s_{23}} T_{22}^\dagger \cdot \epsilon_4^* + \frac{(s_{23} + s_{12})(D-4)}{2s_{23}s_{12}s_{13}^2s_{123}(D-3)} T_{23}^\dagger \cdot \epsilon_4^* \\
& - \frac{1}{2s_{13}^2s_{12}^2(D-3)} T^\dagger \cdot \epsilon_4^* ,
\end{aligned} \tag{5.14}$$

$$\begin{aligned}
\mathcal{P}(A_{12}) = & -\frac{(s_{13} + s_{23})(D-2)}{2s_{13}^2s_{12}^2(D-3)s_{123}} T_{11}^\dagger \cdot \epsilon_4^* + \frac{(D-2)(s_{23}s_{12}(D-4) + s_{13}s_{123}(D-2))}{2s_{13}^2s_{12}^2s_{23}(D-3)s_{123}(D-4)} T_{12}^\dagger \cdot \epsilon_4^* \\
& - \frac{(D-2)(s_{13} + s_{12})}{2s_{13}^2s_{12}s_{23}(D-3)s_{123}} T_{13}^\dagger \cdot \epsilon_4^* + \frac{((D-6)(D-2)(s_{13} + s_{23}) - 4s_{12})}{2(D-4)s_{12}^2s_{13}s_{23}s_{123}(D-3)} T_{21}^\dagger \cdot \epsilon_4^* \\
& - \frac{(s_{23}s_{12}(D-4) + s_{13}s_{123}(D-2))}{2s_{12}^2s_{13}s_{23}^2(D-3)s_{123}} T_{22}^\dagger \cdot \epsilon_4^* + \frac{(2s_{23} + (s_{13} + s_{12})(D-2))}{2s_{12}s_{13}s_{23}^2s_{123}(D-3)} T_{23}^\dagger \cdot \epsilon_4^* \\
& - \frac{(D-2)}{2(D-4)s_{12}^2s_{13}s_{23}(D-3)} T^\dagger \cdot \epsilon_4^* ,
\end{aligned} \tag{5.15}$$

$$\begin{aligned}
\mathcal{P}(A_{13}) = & -\frac{((s_{23} + s_{12})D + 2s_{13})}{2s_{12}s_{13}^3(D-3)s_{123}}T_{11}^\dagger \cdot \epsilon_4^* - \frac{(D-2)(s_{13} + s_{12})}{2s_{13}^2s_{12}s_{23}(D-3)s_{123}}T_{12}^\dagger \cdot \epsilon_4^* \\
& + \frac{(s_{13}s_{23}(D-2) + s_{12}s_{123}D)}{2s_{13}^3s_{12}s_{23}s_{123}(D-3)}T_{13}^\dagger \cdot \epsilon_4^* + \frac{((s_{12} + s_{23})(D-2) + 2s_{13})}{2s_{13}^2s_{12}s_{23}(D-3)s_{123}}T_{21}^\dagger \cdot \epsilon_4^* \\
& + \frac{(s_{13} + s_{12})(D-4)}{2s_{12}s_{13}s_{23}^2s_{123}(D-3)}T_{22}^\dagger \cdot \epsilon_4^* - \frac{(s_{13} + s_{12})(s_{23} + s_{12})(D-4)}{2s_{13}^2s_{12}s_{23}^2s_{123}(D-3)}T_{23}^\dagger \cdot \epsilon_4^* \\
& + \frac{1}{2s_{23}s_{13}^2s_{12}(D-3)}T^\dagger \cdot \epsilon_4^*, \tag{5.16}
\end{aligned}$$

$$\begin{aligned}
\mathcal{P}(A_{21}) = & -\frac{(s_{23}s_{123}(D-2) + s_{13}s_{12}(D-4))}{2s_{13}^2s_{12}^2s_{23}(D-3)s_{123}}T_{11}^\dagger \cdot \epsilon_4^* \\
& + \frac{(-4s_{12} + (s_{13} + s_{23})(D-6)(D-2))}{2(D-4)s_{12}^2s_{13}s_{23}s_{123}(D-3)}T_{12}^\dagger \cdot \epsilon_4^* \\
& + \frac{(s_{23} + s_{12})(D-2) + 2s_{13}}{2s_{13}^2s_{12}s_{23}(D-3)s_{123}}T_{13}^\dagger \cdot \epsilon_4^* \\
& + \frac{(D-2)(s_{23}s_{123}(D-2) + s_{13}s_{12}(D-4))}{2s_{12}^2s_{13}s_{23}^2s_{123}(D-3)(D-4)}T_{21}^\dagger \cdot \epsilon_4^* \\
& - \frac{(s_{13} + s_{23})(D-2)}{2s_{12}^2s_{23}^2s_{123}(D-3)}T_{22}^\dagger \cdot \epsilon_4^* - \frac{(s_{23} + s_{12})(D-2)}{2s_{13}s_{23}^2s_{12}(D-3)s_{123}}T_{23}^\dagger \cdot \epsilon_4^* \\
& + \frac{(D-2)}{2(D-4)s_{12}^2s_{13}s_{23}(D-3)}T^\dagger \cdot \epsilon_4^*, \tag{5.17}
\end{aligned}$$

$$\begin{aligned}
\mathcal{P}(A_{22}) = & \frac{(s_{13} + s_{23})(D-4)}{2s_{13}s_{12}^2s_{23}(D-3)s_{123}}T_{11}^\dagger \cdot \epsilon_4^* - \frac{(s_{23}s_{12}(D-4) + s_{13}s_{123}(D-2))}{2s_{12}^2s_{13}s_{23}^2(D-3)s_{123}}T_{12}^\dagger \cdot \epsilon_4^* \\
& + \frac{(s_{13} + s_{12})(D-4)}{2s_{13}s_{23}^2s_{12}(D-3)s_{123}}T_{13}^\dagger \cdot \epsilon_4^* - \frac{(s_{13} + s_{23})(D-2)}{2s_{12}^2s_{23}^2s_{123}(D-3)}T_{21}^\dagger \cdot \epsilon_4^* \\
& + \frac{(s_{23}s_{12}(D-2) + s_{13}s_{123}D)}{2s_{23}^3s_{12}^2(D-3)s_{123}}T_{22}^\dagger \cdot \epsilon_4^* - \frac{(s_{13}D + s_{12}D + 2s_{23})}{2s_{12}s_{23}^3s_{123}(D-3)}T_{23}^\dagger \cdot \epsilon_4^* \\
& + \frac{1}{2s_{23}^2s_{12}^2(D-3)}T^\dagger \cdot \epsilon_4^*, \tag{5.18}
\end{aligned}$$

$$\begin{aligned}
\mathcal{P}(A_{23}) = & \frac{(s_{23} + s_{12})(D-4)}{2s_{23}s_{12}s_{13}^2s_{123}(D-3)}T_{11}^\dagger \cdot \epsilon_4^* + \frac{(2s_{23} + (s_{13} + s_{12})(D-2))}{2s_{13}s_{23}^2s_{12}(D-3)s_{123}}T_{12}^\dagger \cdot \epsilon_4^* \\
& - \frac{(s_{13} + s_{12})(s_{23} + s_{12})(D-4)}{2s_{13}^2s_{12}s_{23}^2s_{123}(D-3)}T_{13}^\dagger \cdot \epsilon_4^* - \frac{(s_{23} + s_{12})(D-2)}{2s_{13}s_{23}^2s_{12}(D-3)s_{123}}T_{21}^\dagger \cdot \epsilon_4^* \\
& - \frac{((s_{13} + s_{12})D + 2s_{23})}{2s_{12}s_{23}^3s_{123}(D-3)}T_{22}^\dagger \cdot \epsilon_4^* + \frac{(s_{13}s_{23}(D-2) + s_{12}s_{123}D)}{2s_{13}s_{12}s_{23}^3s_{123}(D-3)}T_{23}^\dagger \cdot \epsilon_4^* \\
& - \frac{1}{2s_{23}^2s_{13}s_{12}(D-3)}T^\dagger \cdot \epsilon_4^*, \tag{5.19}
\end{aligned}$$

$$\begin{aligned}
\mathcal{P}(B) = & -\frac{1}{2(D-3)s_{12}^2s_{13}^2}T_{11}^\dagger \cdot \epsilon_4^* - \frac{(D-2)}{2(D-4)s_{12}^2s_{13}s_{23}(D-3)}T_{12}^\dagger \cdot \epsilon_4^* \\
& + \frac{1}{2s_{23}s_{12}(D-3)s_{13}^2}T_{13}^\dagger \cdot \epsilon_4^* + \frac{(D-2)}{2(D-4)s_{12}^2s_{13}s_{23}(D-3)}T_{21}^\dagger \cdot \epsilon_4^* \\
& + \frac{1}{2s_{23}^2s_{12}^2(D-3)}T_{22}^\dagger \cdot \epsilon_4^* - \frac{1}{2s_{13}s_{12}(D-3)s_{23}^2}T_{23}^\dagger \cdot \epsilon_4^* \\
& + \frac{1}{2(D-4)s_{12}^2s_{13}s_{23}}T^\dagger \cdot \epsilon_4^*. \tag{5.20}
\end{aligned}$$

5.4 The Expansion of the Tensor Coefficients

Each of the unrenormalised coefficients A_{IJ} and B has a perturbative expansion of the form

$$\begin{aligned}
A_{IJ}^{\text{un}} &= \sqrt{4\pi\alpha}e_q\sqrt{4\pi\alpha_s} \mathbf{T}_{ij}^a \left[A_{IJ}^{(0),\text{un}} + \left(\frac{\alpha_s}{2\pi}\right) A_{IJ}^{(1),\text{un}} + \left(\frac{\alpha_s}{2\pi}\right)^2 A_{IJ}^{(2),\text{un}} + \mathcal{O}(\alpha_s^3) \right], \\
B^{\text{un}} &= \sqrt{4\pi\alpha}e_q\sqrt{4\pi\alpha_s} \mathbf{T}_{ij}^a \left[B^{(0),\text{un}} + \left(\frac{\alpha_s}{2\pi}\right) B^{(1),\text{un}} + \left(\frac{\alpha_s}{2\pi}\right)^2 B^{(2),\text{un}} + \mathcal{O}(\alpha_s^3) \right], \tag{5.21}
\end{aligned}$$

where the dependence on $(s_{13}, s_{23}, s_{123})$ is implicit. At tree level,

$$A_{IJ}^{(0),\text{un}}(s_{13}, s_{23}, s_{123}) = 0, \tag{5.22}$$

$$B^{(0),\text{un}}(s_{13}, s_{23}, s_{123}) = \frac{2}{s_{13}s_{23}}. \tag{5.23}$$

The one-loop contributions can be written in terms of the one-loop box integral in $D = 6 - 2\epsilon$ dimensions, $\text{Box}^6(s_{ij}, s_{ik}, s_{ijk})$, and the one-loop bubble, $\text{Bub}(s_{ij})$, as

follows:

$$\begin{aligned}
A_{11}^{(1),\text{un}}(s_{13}, s_{23}, s_{123}) = & \\
& N \left[-\frac{(D-4)}{2(s_{13}+s_{12})s_{13}} \text{Bub}(s_{123}) - \frac{(D-4)}{2s_{12}s_{13}} [\text{Bub}(s_{13}) - \text{Bub}(s_{123})] \right. \\
& - \frac{((D-2)s_{23}s_{12} + (D-4)s_{23}s_{13} + 4s_{12}(s_{12}+s_{13}))}{2s_{12}s_{13}(s_{13}+s_{12})^2} [\text{Bub}(s_{23}) - \text{Bub}(s_{123})] \\
& \left. - \frac{(D-4)(4s_{12} + (D-2)s_{23})}{4s_{12}s_{13}} \text{Box}^6(s_{13}, s_{23}, s_{123}) \right] \\
& + \frac{1}{N} \left[\frac{(D-4)}{2(s_{13}+s_{12})s_{13}} \text{Bub}(s_{123}) + \frac{D}{2s_{13}^2} [\text{Bub}(s_{12}) - \text{Bub}(s_{123})] \right. \\
& + \frac{(s_{12}+s_{13})(Ds_{23} + 4s_{13}) + 2s_{23}s_{13}}{2(s_{13}+s_{12})^2s_{13}^2} [\text{Bub}(s_{23}) - \text{Bub}(s_{123})] \\
& + \frac{(D-4)(D-6)}{4s_{13}} \text{Box}^6(s_{12}, s_{13}, s_{123}) \\
& \left. + \frac{(D-2)(Ds_{23} + 4s_{13})}{4s_{13}^2} \text{Box}^6(s_{12}, s_{23}, s_{123}) \right], \tag{5.24}
\end{aligned}$$

$$\begin{aligned}
A_{12}^{(1),\text{un}}(s_{13}, s_{23}, s_{123}) = & \\
& N \left[-\frac{(D-10)}{2s_{12}(s_{23}+s_{12})} [\text{Bub}(s_{13}) - \text{Bub}(s_{123})] \right. \\
& - \frac{((D-10)s_{13} - 4s_{12})}{2s_{12}s_{13}(s_{13}+s_{12})} [\text{Bub}(s_{23}) - \text{Bub}(s_{123})] \\
& \left. + \frac{(4(D-4)s_{12} - (D-2)(D-10)s_{13})}{4s_{12}s_{13}} \text{Box}^6(s_{13}, s_{23}, s_{123}) \right] \\
& + \frac{1}{N} \left[\frac{(D-2)}{2s_{23}s_{13}} [\text{Bub}(s_{12}) - \text{Bub}(s_{123})] \right. \\
& + \frac{((D-2)s_{12} + 2(D-6)s_{23})}{2s_{23}s_{12}(s_{23}+s_{12})} [\text{Bub}(s_{13}) - \text{Bub}(s_{123})] \\
& + \frac{(D-6)(s_{12}+2s_{13})}{2s_{12}s_{13}(s_{13}+s_{12})} [\text{Bub}(s_{23}) - \text{Bub}(s_{123})] \\
& + \frac{((D-2)^2s_{12}s_{13} + 4(D-4)s_{12}s_{23})}{4s_{12}s_{13}s_{23}} \text{Box}^6(s_{12}, s_{13}, s_{123}) \\
& + \frac{2(D-4)(D-6)s_{13}s_{23}}{4s_{12}s_{13}s_{23}} \text{Box}^6(s_{12}, s_{13}, s_{123}) \\
& \left. + \frac{(D-6)((D-2)s_{12} + 2(D-4)s_{13})}{4s_{12}s_{13}} \text{Box}^6(s_{12}, s_{23}, s_{123}) \right], \tag{5.25}
\end{aligned}$$

$$\begin{aligned}
A_{13}^{(1),\text{un}}(s_{13}, s_{23}, s_{123}) = & \\
& N \left[\frac{(D-6)}{2(s_{13}+s_{12})s_{13}} [\text{Bub}(s_{23}) - \text{Bub}(s_{123})] \right. \\
& \quad \left. + \frac{(D-4)(D-6)}{4s_{13}} \text{Box}^6(s_{13}, s_{23}, s_{123}) \right] \\
& + \frac{1}{N} \left[-\frac{(D-4)}{s_{13}(s_{23}+s_{13})} \text{Bub}(s_{123}) - \frac{(D-4)}{2s_{23}s_{13}} [\text{Bub}(s_{13}) - \text{Bub}(s_{123})] \right. \\
& \quad + \frac{(4s_{12}s_{13}^2 - Ds_{12}(s_{13}+s_{23})^2)}{2(s_{23}+s_{13})^2s_{13}^2s_{23}} [\text{Bub}(s_{12}) - \text{Bub}(s_{123})] \\
& \quad - \frac{2(D-2)s_{13}s_{23}(s_{13}+s_{23})}{2(s_{23}+s_{13})^2s_{13}^2s_{23}} [\text{Bub}(s_{12}) - \text{Bub}(s_{123})] \\
& \quad - \frac{(2(D-3)s_{13}+Ds_{12})}{2s_{13}^2(s_{13}+s_{12})} [\text{Bub}(s_{23}) - \text{Bub}(s_{123})] \\
& \quad - \frac{(D-4)((D-2)s_{12}+4s_{23})}{4s_{23}s_{13}} \text{Box}^6(s_{12}, s_{13}, s_{123}) \\
& \quad \left. - \frac{(D-2)(Ds_{12}+2(D-4)s_{13})}{4s_{13}^2} \text{Box}^6(s_{12}, s_{23}, s_{123}) \right], \tag{5.26}
\end{aligned}$$

$$\begin{aligned}
B^{(1),\text{un}}(s_{13}, s_{23}, s_{123}) = & \\
& N \left[\frac{D^2-3D+4}{4(D-4)s_{13}s_{23}} \text{Bub}(s_{123}) \right. \\
& \quad + \frac{(4(D-3)s_{12}(s_{12}+s_{23})+(D-4)(D-7)s_{23}s_{13})}{2s_{12}s_{23}(s_{23}+s_{12})s_{13}(D-4)} [\text{Bub}(s_{13}) - \text{Bub}(s_{123})] \\
& \quad \left. + \frac{(4(D-3)s_{12}^2+(D-2)(D-7)s_{13}s_{23})}{8s_{12}s_{13}s_{23}} \text{Box}^6(s_{13}, s_{23}, s_{123}) \right] \\
& + \frac{1}{N} \left[\frac{(7D-16-D^2)}{4(D-4)s_{13}s_{23}} \text{Bub}(s_{123}) - \frac{(s_{12}+(D-6)s_{23})}{2(s_{23}+s_{12})s_{23}s_{12}} [\text{Bub}(s_{13}) - \text{Bub}(s_{123})] \right. \\
& \quad + \frac{(16-5D)}{4(D-4)s_{13}s_{23}} [\text{Bub}(s_{12}) - \text{Bub}(s_{123})] \\
& \quad - \frac{(4(D-3)s_{23}s_{12}+(D-4)(D-6)s_{13}s_{23})}{4s_{12}s_{13}s_{23}} \text{Box}^6(s_{12}, s_{13}, s_{123}) \\
& \quad + \frac{(D-2)s_{12}s_{13}}{4s_{12}s_{13}s_{23}} \text{Box}^6(s_{12}, s_{13}, s_{123}) \Big] \\
& + \left\{ s_{13} \leftrightarrow s_{23} \right\}. \tag{5.27}
\end{aligned}$$

Explicit expansions of the one-loop integrals around $\epsilon \sim 0$ in terms of HPLs and 2dHPLs are listed in Appendix E.

Similarly, the unrenormalised two-loop $A_{IJ}^{(2),\text{un}}$ and $B^{(2),\text{un}}$ coefficients were obtained analytically in terms of a basis set of two-loop MI by the reduction of all two

loop integrals using the Laporta algorithm (Section 3.6). This is exactly the same procedure carried out for the ME in Chapter 4. Since we have exactly two-loop integrals as the ME calculation the corresponding MIs are identical. As we have seen, the ϵ -expansions for each of the MIs have been derived in [47, 48] by solving differential equations. Therefore, the ϵ -expansions of $A_{IJ}^{(2),\text{un}}$ and $B^{(2),\text{un}}$ can be obtained by directly substituting the ϵ -expansions of the individual MIs.

5.5 Relation to the Matrix Element Calculation

We have already considered the case where the correlations with the lepton current are ignored in the previous Chapter 4. In this case, the squared amplitude for the process $\gamma^* \rightarrow q\bar{q}g$, summed over spins, colours and quark flavours, is denoted by

$$\langle \mathcal{M} | \mathcal{M} \rangle = \sum |\epsilon_4 \cdot \mathcal{S}(q; g; \bar{q})|^2 = \mathcal{T}(x, y, z). \quad (5.28)$$

The perturbative expansion of $\mathcal{T}(x, y, z)$ was calculated previously and is given by Equation (4.7). It was shown that the NNLO calculation of $\mathcal{T}(x, y, z)$ required two pieces, the one-loop self-interference (4.13)

$$\mathcal{T}^{(6,[1 \times 1])}(x, y, z) = \langle \mathcal{M}^{(1)} | \mathcal{M}^{(1)} \rangle, \quad (5.29)$$

and from the interference of tree and two-loop (4.14)

$$T^{(6,[2 \times 0])}(x, y, z) = \langle \mathcal{M}^{(0)} | \mathcal{M}^{(2)} \rangle + \langle \mathcal{M}^{(2)} | \mathcal{M}^{(0)} \rangle. \quad (5.30)$$

It is straightforward to obtain the interference of the tree and i -loop amplitudes in terms of the tensor coefficients, A_{IJ} and B . We find

$$\begin{aligned}
\langle \mathcal{M}^{(0)} | \mathcal{M}^{(i)} \rangle = & \frac{V}{2} \left\{ 2(1 - \epsilon) \left((s_{12}s_{123} + s_{12}s_{13} + s_{13}s_{23}) \right. \right. \\
& \left. \left. - \epsilon(s_{13} + s_{23})(s_{12} + s_{13}) \right) A_{11}^{(i)}(s_{13}, s_{23}, s_{123}) \right. \\
& + \left(2(s_{12} + s_{23})^2 - 2\epsilon(s_{123}s_{23} + (s_{12} + s_{23})^2) \right. \\
& \left. + 2\epsilon^2(s_{13} + s_{23})(s_{12} + s_{23}) \right) A_{12}^{(i)}(s_{13}, s_{23}, s_{123}) \\
& + 2(s_{23} - \epsilon(s_{13} + s_{23}))(s_{123} - \epsilon(s_{13} + s_{23})) A_{13}^{(i)}(s_{13}, s_{23}, s_{123}) \\
& + 2 \left(s_{13}^2 + s_{23}^2 + 2s_{12}s_{123} - 2\epsilon(s_{123}^2 - s_{12}s_{13} - s_{12}s_{23} - s_{13}s_{23}) \right. \\
& \left. \left. + \epsilon^2(s_{13} + s_{23})^2 \right) B^{(i)}(s_{13}, s_{23}, s_{123}) + \{p_1 \leftrightarrow p_2\} \right\}. \quad (5.31)
\end{aligned}$$

The above relation holds for the unrenormalised as well as for the renormalised matrix element, involving the appropriate unrenormalised or renormalised tensor coefficients respectively. Similar, but more lengthy, expressions can easily be obtained for the interference of i - and j -loop amplitudes. We have checked that inserting the expressions for $A_{IJ}^{(i)}$ and $B^{(i)}$ into Equation (5.31) reproduces our earlier results of Chapter 4 at the one- and two-loop level both at the master integral level and after making an expansion in ϵ .

5.6 Ultraviolet Renormalisation

The renormalisation of the matrix element is carried out by replacing the bare coupling α_0 with the renormalised coupling $\alpha_s \equiv \alpha_s(\mu^2)$, evaluated at the renormalisation scale μ^2 by exactly the same procedure as for the ME calculation and is shown in Section 4.2.

We denote the i -loop contribution to the unrenormalised coefficients by $A_{IJ}^{(i),\text{un}}$ and $B^{(i),\text{un}}$, using the same normalisation as for the decomposition of the renormalised amplitude (5.4); the dependence on $(s_{13}, s_{23}, s_{123})$ is always understood im-

plicitly. The renormalised coefficients are then obtained as

$$\begin{aligned} A_{IJ}^{(0)} &= 0, \\ A_{IJ}^{(1)} &= S_\epsilon^{-1} A_{IJ}^{(1),\text{un}}, \\ A_{IJ}^{(2)} &= S_\epsilon^{-2} A_{IJ}^{(2),\text{un}} - \frac{3\beta_0}{2\epsilon} S_\epsilon^{-1} A_{IJ}^{(1),\text{un}}, \end{aligned} \quad (5.32)$$

and

$$\begin{aligned} B^{(0)} &= B^{(0),\text{un}}, \\ B^{(1)} &= S_\epsilon^{-1} B^{(1),\text{un}} - \frac{\beta_0}{2\epsilon} B^{(0),\text{un}}, \\ B^{(2)} &= S_\epsilon^{-2} B^{(2),\text{un}} - \frac{3\beta_0}{2\epsilon} S_\epsilon^{-1} B^{(1),\text{un}} - \left(\frac{\beta_1}{4\epsilon} - \frac{3\beta_0^2}{8\epsilon^2} \right) B^{(0),\text{un}} \end{aligned} \quad (5.33)$$

For the remainder of this calculation we set the renormalisation scale $\mu^2 = q^2 = p_4^2$. The full scale dependence of the tensor coefficients is given by

$$\begin{aligned} A_{IJ} &= \sqrt{4\pi\alpha_e} \sqrt{4\pi\alpha_s} \mathbf{T}_{ij}^a \left\{ \left(\frac{\alpha_s(\mu^2)}{2\pi} \right) A_{IJ}^{(1)} \right. \\ &\quad \left. + \left(\frac{\alpha_s(\mu^2)}{2\pi} \right)^2 \left[A_{IJ}^{(2)} + \frac{3\beta_0}{2} A_{IJ}^{(1)} \ln \left(\frac{\mu^2}{q^2} \right) \right] + \mathcal{O}(\alpha_s^3) \right\}, \end{aligned} \quad (5.34)$$

$$\begin{aligned} B &= \sqrt{4\pi\alpha_e} \sqrt{4\pi\alpha_s} \mathbf{T}_{ij}^a \left\{ B^{(0)} + \left(\frac{\alpha_s(\mu^2)}{2\pi} \right) \left[B^{(1)} + \frac{\beta_0}{2} B^{(0)} \ln \left(\frac{\mu^2}{q^2} \right) \right] \right. \\ &\quad + \left(\frac{\alpha_s(\mu^2)}{2\pi} \right)^2 \left[B^{(2)} + \left(\frac{3\beta_0}{2} B^{(1)} + \frac{\beta_1}{2} B^{(0)} \right) \ln \left(\frac{\mu^2}{q^2} \right) \right. \\ &\quad \left. \left. + \frac{3\beta_0^2}{8} B^{(0)} \ln^2 \left(\frac{\mu^2}{q^2} \right) \right] + \mathcal{O}(\alpha_s^3) \right\}. \end{aligned} \quad (5.35)$$

5.7 Infrared Behavior of the Tensor Coefficients

After performing ultraviolet renormalisation, the amplitudes still contain singularities, which are of infrared origin and will be analytically cancelled by those occurring in radiative processes of the same order. As we saw in Chapter 2 Catani [29] has shown how to organise the infrared pole structure of the one- and two-loop contribu-

tions renormalised in the $\overline{\text{MS}}$ scheme in terms of the tree and renormalised one-loop amplitudes. The same procedure applies to the tensor coefficients. In particular, the infrared behaviour of the one-loop coefficients is given by

$$\begin{aligned} A_{IJ}^{(1)} &= A_{IJ}^{(1),\text{finite}}, \\ B^{(1)} &= \mathbf{I}^{(1)}(\epsilon)B^{(0)} + B^{(1),\text{finite}}, \end{aligned} \quad (5.36)$$

while the two-loop singularity structure is

$$\begin{aligned} A_{IJ}^{(2)} &= \mathbf{I}^{(1)}(\epsilon)A_{IJ}^{(1)} + A_{IJ}^{(2),\text{finite}}, \\ B^{(2)} &= \left(-\frac{1}{2}\mathbf{I}^{(1)}(\epsilon)\mathbf{I}^{(1)}(\epsilon) - \frac{\beta_0}{\epsilon}\mathbf{I}^{(1)}(\epsilon) \right. \\ &\quad \left. + e^{-\epsilon\gamma} \frac{\Gamma(1-2\epsilon)}{\Gamma(1-\epsilon)} \left(\frac{\beta_0}{\epsilon} + K \right) \mathbf{I}^{(1)}(2\epsilon) + \mathbf{H}^{(2)}(\epsilon) \right) B^{(0)} \\ &\quad + \mathbf{I}^{(1)}(\epsilon)B^{(1)} + B^{(2),\text{finite}}, \end{aligned} \quad (5.37)$$

where the constant K is

$$K = \left(\frac{67}{18} - \frac{\pi^2}{6} \right) C_A - \frac{10}{9} T_R N_F. \quad (5.38)$$

The finite remainders $A_{IJ}^{(i),\text{finite}}$ and $B^{(i),\text{finite}}$ remain to be calculated.

The insertion operator $\mathbf{I}^{(1)}(\epsilon)$ and $\mathbf{H}^{(2)}(\epsilon)$ have already been calculated in Chapter 4. $\mathbf{I}^{(1)}(\epsilon)$ for example, is given by Equation (4.40)

$$\mathbf{I}^{(1)}(\epsilon) = -\frac{e^{\epsilon\gamma}}{2\Gamma(1-\epsilon)} \left[N \left(\frac{1}{\epsilon^2} + \frac{3}{4\epsilon} + \frac{\beta_0}{2N\epsilon} \right) (\mathbf{S}_{13} + \mathbf{S}_{23}) - \frac{1}{N} \left(\frac{1}{\epsilon^2} + \frac{3}{2\epsilon} \right) \mathbf{S}_{12} \right], \quad (5.39)$$

where, since we have set $\mu^2 = s_{123}$,

$$\mathbf{S}_{ij} = \left(-\frac{s_{123}}{s_{ij}} \right)^\epsilon. \quad (5.40)$$

5.8 Helicity Amplitudes

We can extend the results of the previous section to include Z boson exchange,

$$e^+(p_5) + e^-(p_6) \rightarrow (Z^*, \gamma^*)(p_4) \longrightarrow q(p_1) + \bar{q}(p_2) + g(p_3), \quad (5.41)$$

where the off-shell vector boson now distinguishes between left- and right-handed fermions by keeping track of the helicity of the final state quarks³. A convenient method to evaluate the helicity amplitudes is in terms of Weyl–van der Waerden spinors, which is described briefly in Appendix G and in detail in [76, 77, 78].

It is also straightforward to include the spin-correlations with the initial state by contracting the hadronic current with the lepton current V_μ for fixed helicities of the initial state electron (and positron). Using the spinor calculus of Appendix G we can express the lepton current V_μ in terms of the helicities of the incident e^+ and e^- (with momenta p_5 and p_6 respectively). Explicitly,

$$V_\mu^\gamma(e^+, e^-) = e\sigma_\mu^{\dot{A}B} p_{6\dot{A}} p_{5B} \frac{L_{ee}^\gamma}{s}, \quad (5.42)$$

$$V_\mu^Z(e^+, e^-) = e\sigma_\mu^{\dot{A}B} p_{6\dot{A}} p_{5B} \frac{L_{ee}^Z}{s - M_Z^2 + i\Gamma_Z M_Z}, \quad (5.43)$$

$$V_\mu^\gamma(e^+, e^-) = e\sigma_\mu^{\dot{A}B} p_{5\dot{A}} p_{6B} \frac{R_{ee}^\gamma}{s}, \quad (5.44)$$

$$V_\mu^Z(e^+, e^-) = e\sigma_\mu^{\dot{A}B} p_{5\dot{A}} p_{6B} \frac{R_{ee}^Z}{s - M_Z^2 + i\Gamma_Z M_Z}. \quad (5.45)$$

The hadronic current \mathcal{S}_μ is related to the fixed helicity currents, \mathcal{S}_{AB} , by

$$\mathcal{S}_\mu(q+; g\lambda; \bar{q}-) = R_{f_1 f_2}^V \sqrt{2} \sigma_\mu^{\dot{A}B} \mathcal{S}_{AB}(q+; g\lambda; \bar{q}-), \quad (5.46)$$

³Note that the full matrix element for any process should be summed over both photon and Z -boson exchange.

and

$$\mathcal{S}_\mu(q-; g\lambda; \bar{q}+) = L_{f_1 f_2}^V \sqrt{2} \sigma_\mu^{\dot{A}B} \mathcal{S}_{\dot{A}B}(q-; g\lambda; \bar{q}+) . \quad (5.47)$$

As in Equation (5.4), the gauge boson coupling is extracted from $\mathcal{S}_{\dot{A}B}$. As mentioned earlier, the left- and right-handed currents couple with a different strength when the vector boson is a Z .

The currents with the quark helicities flipped follow from parity conservation:

$$\mathcal{S}_{\dot{A}B}(q-; g\lambda; \bar{q}+) = (\mathcal{S}_{\dot{B}A}(q+; g(-\lambda); \bar{q}-))^* . \quad (5.48)$$

Charge conjugation implies the following relations between currents with different helicities:

$$\mathcal{S}_{\dot{A}B}(q\lambda_q; g\lambda; \bar{q}\lambda_{\bar{q}}) = (-1) \mathcal{S}_{\dot{A}B}(\bar{q}\lambda_{\bar{q}}; g\lambda; q\lambda_q) . \quad (5.49)$$

All helicity amplitudes are therefore related to the amplitudes with $\lambda_q = +$ and $\lambda_{\bar{q}} = -$.

Explicitly, we find

$$\begin{aligned} \mathcal{S}_{\dot{A}B}(q+; g+; \bar{q}-) &= \alpha(y, z) \frac{p_{1\dot{A}D} p_2^D p_{2B}}{\langle p_1 p_3 \rangle \langle p_3 p_2 \rangle} + \beta(y, z) \frac{p_{3\dot{A}D} p_2^D p_{2B}}{\langle p_1 p_3 \rangle \langle p_3 p_2 \rangle} \\ &+ \gamma(y, z) \frac{p_{1\dot{C}B} p_3^{\dot{C}} p_{3\dot{A}}}{\langle p_1 p_3 \rangle \langle p_3 p_2 \rangle^*} + \delta(y, z) \frac{\langle p_1 p_3 \rangle^*}{\langle p_1 p_3 \rangle \langle p_1 p_2 \rangle^*} (p_{1\dot{A}B} + p_{2\dot{A}B} + p_{3\dot{A}B}) . \end{aligned} \quad (5.50)$$

The other helicity amplitudes are obtained from $\mathcal{S}_{\dot{A}B}(q+; g+; \bar{q}-)$ by the above parity and charge conjugation relations, while the coefficients α , β and γ are written in

terms of the tensor coefficients:

$$\begin{aligned}
\alpha(y, z) &= \frac{s_{23}s_{13}}{4} \left(2B(s_{13}, s_{23}, s_{123}) + A_{12}(s_{13}, s_{23}, s_{123}) \right. \\
&\quad \left. - A_{11}(s_{13}, s_{23}, s_{123}) \right), \\
\beta(y, z) &= \frac{s_{13}}{4} \left(2s_{23}B(s_{13}, s_{23}, s_{123}) + 2(s_{12} + s_{13})A_{11}(s_{13}, s_{23}, s_{123}) \right. \\
&\quad \left. + s_{23}(A_{12}(s_{13}, s_{23}, s_{123}) + A_{13}(s_{13}, s_{23}, s_{123})) \right), \\
\gamma(y, z) &= \frac{s_{13}s_{23}}{4} \left(A_{11}(s_{13}, s_{23}, s_{123}) - A_{13}(s_{13}, s_{23}, s_{123}) \right), \\
\delta(y, z) &= -\frac{s_{12}s_{13}}{4} A_{11}(s_{13}, s_{23}, s_{123}).
\end{aligned} \tag{5.51}$$

When the hadron tensor is contracted with ϵ_4^μ or the lepton current V^μ , the final term of Equation (5.50) vanishes⁴. Furthermore, current conservation implies the following relation between the four helicity coefficients,

$$\alpha(y, z) - \beta(y, z) - \gamma(y, z) - \frac{2s_{123}}{s_{12}} \delta(y, z) = 0. \tag{5.52}$$

This relation is fulfilled automatically once the tensor coefficients are inserted and does therefore not yield a further reduction of the tensor basis.

As with the tensor coefficients, the helicity amplitude coefficients α , β and γ are vectors in colour space and have perturbative expansions:

$$\Omega = \sqrt{4\pi\alpha}\sqrt{4\pi\alpha_s} \mathbf{T}_{ij}^a \left[\Omega^{(0)} + \left(\frac{\alpha_s}{2\pi}\right) \Omega^{(1)} + \left(\frac{\alpha_s}{2\pi}\right)^2 \Omega^{(2)} + \mathcal{O}(\alpha_s^3) \right],$$

for $\Omega = \alpha, \beta, \gamma$. The dependence on (y, z) is again implicit.

The ultraviolet and infrared properties of the helicity coefficients match those of

⁴And for this reason was omitted in [25].

the tensor coefficients,

$$\begin{aligned}\Omega^{(0)} &= \Omega^{(0),\text{un}}, \\ \Omega^{(1)} &= S_\epsilon^{-1} \Omega^{(1),\text{un}} - \frac{\beta_0}{2\epsilon} \Omega^{(0),\text{un}}, \\ \Omega^{(2)} &= S_\epsilon^{-2} \Omega^{(2),\text{un}} - \frac{3\beta_0}{2\epsilon} S_\epsilon^{-1} \Omega^{(1),\text{un}} - \left(\frac{\beta_1}{4\epsilon} - \frac{3\beta_0^2}{8\epsilon^2} \right) \Omega^{(0),\text{un}},\end{aligned}\tag{5.53}$$

and

$$\begin{aligned}\Omega^{(1)} &= \mathbf{I}^{(1)}(\epsilon) \Omega^{(0)} + \Omega^{(1),\text{finite}}, \\ \Omega^{(2)} &= \left(-\frac{1}{2} \mathbf{I}^{(1)}(\epsilon) \mathbf{I}^{(1)}(\epsilon) - \frac{\beta_0}{\epsilon} \mathbf{I}^{(1)}(\epsilon) \right. \\ &\quad \left. + e^{-\epsilon\gamma} \frac{\Gamma(1-2\epsilon)}{\Gamma(1-\epsilon)} \left(\frac{\beta_0}{\epsilon} + K \right) \mathbf{I}^{(1)}(2\epsilon) + \mathbf{H}^{(2)}(\epsilon) \right) \Omega^{(0)} \\ &\quad + \mathbf{I}^{(1)}(\epsilon) \Omega^{(1)} + \Omega^{(2),\text{finite}},\end{aligned}\tag{5.54}$$

where $\mathbf{I}^{(1)}(\epsilon)$ and $\mathbf{H}^{(2)}(\epsilon)$ are defined in Equations. (5.39) and (2.59) respectively.

5.9 The Finite Contributions

In this Section we present the finite contributions to the helicity amplitudes. At leading order we simply have

$$\alpha^{(0)}(y, z) = \beta^{(0)}(y, z) = 1 \quad \text{and} \quad \gamma^{(0)}(y, z) = 0.\tag{5.55}$$

5.9.1 One-Loop Contribution to Ω

The renormalised one-loop helicity amplitude coefficients can be straightforwardly obtained to all orders in ϵ from the tensor coefficients using Equations (5.24)–(5.27). For practical purposes, they are needed through to $\mathcal{O}(\epsilon^2)$ in evaluating the IR-divergent one-loop contribution to the two-loop amplitude, while only the finite piece is needed for the one-loop self-interference.

They can be decomposed according to their colour structure as follows:

$$\Omega^{(1),\text{finite}}(y, z) = N a_\Omega(y, z) + \frac{1}{N} b_\Omega(y, z) + \beta_0 c_\Omega(y, z). \quad (5.56)$$

The expansion of the coefficients through to ϵ^2 yields HPLs and 2dHPLs up to weight 4 for a_Ω , b_Ω and up to weight 3 for c_Ω . The explicit expressions are of considerable size, such that we only quote the ϵ^0 -terms (although these have been known already for a long time [25]). The expressions through to $\mathcal{O}(\epsilon^2)$ can be obtained in FORM format from the author. The one-loop coefficients can be found in Appendix C.

5.9.2 Two-Loop Contribution to Ω

The finite two-loop remainder is obtained by subtracting the predicted infrared structure (expanded through to $\mathcal{O}(\epsilon^0)$) from the renormalised helicity coefficient. We further decompose the finite remainder according to the colour structure, as follows:

$$\begin{aligned} \Omega^{(2),\text{finite}}(y, z) = & N^2 A_\Omega(y, z) + B_\Omega(y, z) + \frac{1}{N^2} C_\Omega(y, z) + N N_F D_\Omega(y, z) \\ & + \frac{N_F}{N} E_\Omega(y, z) + N_F^2 F_\Omega(y, z) + N_{F,V} \left(\frac{4}{N} - N \right) G_\Omega(y, z), \end{aligned} \quad (5.57)$$

where the last term is generated by graphs where the virtual gauge boson does not couple directly to the final-state quarks. This contribution is denoted by $N_{F,V}$ and is proportional to the charge weighted sum of the quark flavours. In the case of purely electromagnetic interactions we find,

$$N_{F,\gamma} = \frac{\sum_q e_q}{e_q}. \quad (5.58)$$

Including Z -interactions, the same class of diagrams yields not only a contribution from the vector component of the Z , which for the right-handed quark amplitude is

given by

$$N_{F,Z} = \frac{\sum_q (L_{qq}^Z + R_{qq}^Z)}{2R_{qq}^Z}, \quad (5.59)$$

but also a contribution involving the axial couplings of the Z [79]. This contribution vanishes if summed over isospin doublets. The large mass splitting of the third quark family induces a non-vanishing contribution from this class of diagrams, which can however not be computed within the framework of massless QCD employed here, but can only be obtained within an effective theory with large top-quark mass. In contrast to the vector contribution from these diagrams, which is finite, one could expect divergences in the axial vector contribution, which would be cancelled by the single unresolved limits of the corresponding axial contributions to four-parton final states [52, 53]. Results from the four-parton final states show that this axial contribution is numerically very small [80, 81].

The helicity coefficients contain HPLs and 2dHPLs up to weight 4 in the A , B , C and G -terms, up to weight 3 in the D - and E -terms (which do moreover contain only a limited subset of purely planar master integrals) and up to weight 2 in the F -term. The size of each helicity coefficient is comparable to the size of the helicity-averaged tree times two-loop matrix element presented in Appendix B. Therefore, we only quote the A - and D -terms of each coefficient, which form the leading colour contributions, and which turn out to be numerically dominant, approximating the full expressions to an accuracy of about 20%. The complete set of coefficients in FORM format can be obtained from the author. The leading colour terms can be found in Appendix D.

5.9.3 Summary

From the $\Omega^{(1),\text{finite}}$ and $\Omega^{(2),\text{finite}}$, it is possible to recover the finite pieces of the helicity-averaged tree times two-loop matrix elements (Appendix B) and one-loop

the size of $\mathcal{F}inite^{(1\times 1)}(x, y, z)$ in (4.54), it becomes clear that the squared one-loop amplitude can be evaluated much more elegantly by squaring the finite remainders of the helicity amplitudes than by computing the squared matrix element.

squared matrix elements (Appendix A) by squaring (5.50):

$$\begin{aligned}
\mathcal{F}inite^{(2\times 0)}(x, y, z) &= 8V \mathcal{R} \left[\frac{(1-y)(1-y-z)}{yz} \alpha^{(2),\text{finite}}(y, z) + \frac{1-y}{y} \beta^{(2),\text{finite}}(y, z) \right. \\
&\quad \left. - \gamma^{(2),\text{finite}}(y, z) + (y \leftrightarrow z) \right], \\
\mathcal{F}inite^{(1\times 1)}(x, y, z) &= 4V \mathcal{R} \left[(1-y-z) \left(\frac{(1-y-z)}{yz} + \frac{1}{2} \right) |\alpha^{(1),\text{finite}}(y, z)|^2 \right. \\
&\quad + \left(\frac{1-y-z}{2} + \frac{z}{y} \right) |\beta^{(1),\text{finite}}(y, z)|^2 \\
&\quad + \left(\frac{1-y-z}{2} + \frac{y}{z} \right) |\gamma^{(1),\text{finite}}(y, z)|^2 \\
&\quad + \left(-3 + y + z + \frac{2-2z}{y} \right) \alpha^{(1),\text{finite}}(y, z) \beta^{*(1),\text{finite}}(y, z) \\
&\quad - (1-y-z) \alpha^{(1),\text{finite}}(y, z) \gamma^{*(1),\text{finite}}(y, z) \\
&\quad \left. - (1+y+z) \beta^{(1),\text{finite}}(y, z) \gamma^{*(1),\text{finite}}(y, z) + (y \leftrightarrow z) \right].
\end{aligned} \tag{5.60}$$

It is important to notice that (5.60) corresponds, by the very nature of the Weyl–van der Waerden helicity formalism, to a scheme with external momenta and polarisation vectors in four dimensions (internal states are always taken to be D -dimensional), which is sometimes called the 't Hooft–Veltman scheme [17]. This scheme is different from the conventional dimensional regularisation used in Chapter 4, where all external momenta and polarisation vectors are D -dimensional. Nevertheless, one obtains from (5.60) the same $\mathcal{F}inite^{(1\times 1)}(x, y, z)$ as in Appendix A and $\mathcal{F}inite^{(2\times 0)}(x, y, z)$ as in Appendix B, since all scheme-dependent terms are correctly accounted for by the finite contributions arising from expanding the tree level and one-loop contributions in the renormalisation and infrared factorisation formulae.

It should also be noted that only the $\mathcal{O}(\epsilon^0)$ terms of $\Omega^{(1),\text{finite}}$ contribute to $\mathcal{F}inite^{(1\times 1)}(x, y, z)$, terms subleading in ϵ are not required, since no term is multiplied with a divergent factor. Comparing the size of these $\mathcal{O}(\epsilon^0)$ terms in (5.56) with

CHAPTER 6

Conclusions and Outlook

6.1 Summary

We have seen that higher order corrections in perturbative QCD are important for example in the calculation of event-shape variables and the precision determination of α_s . The motivation for higher orders is to increase accuracy and reduce unphysical scale dependence.

Due to its importance, we have focused on the NNLO calculation of the three-jet rate in e^+e^- annihilation. There are several components to the full calculation, many of which have already been calculated. Firstly, the tree level $\gamma^* \rightarrow 5$ partons amplitude where two partons become soft or collinear, calculated in [49, 50, 51]. Secondly, the one-loop corrections to $\gamma^* \rightarrow 4$ partons amplitude with one parton becoming soft or collinear, calculated in [52, 53, 54, 55]. Finally, the two-loop (as well as the one-loop times one-loop) corrections to the $\gamma^* \rightarrow 3$ partons amplitude. While the former two contributions have been known for some time already, the two-loop amplitudes for the three parton subprocess have presented an obstacle that prevented further progress on this calculation up to now.

In this thesis, we have presented the analytic formulae for the two-loop virtual corrections to the process $\gamma^* \rightarrow q\bar{q}g$, which arise from the interference of the two-loop

with the tree amplitude and from the self-interference of the one-loop amplitude. Together with the contribution from the self-interference of the one-loop amplitudes for $\gamma^* \rightarrow ggg$ [57, 58], these form the full $\mathcal{O}(\alpha_s^3)$ corrections to the three-parton subprocess, finally enabling the full calculation of $e^+e^- \rightarrow 3$ jets at NNLO.

In Chapter 2 we looked at the general calculation of matrix elements. We saw that there are two types of divergence arising from the singular behaviour of the loop integrals, UV and IR. The UV divergences are removed by renormalisation. The IR divergences are only eliminated when we calculate suitably inclusive quantities, for which the divergences cancel between the physically degenerate real and virtual contributions. This led to the discussion of the IR factorisation formula of Catani and Seymour which predicts the pole structure of the one- and two-loop virtual amplitudes.

The next stage in the calculation of the matrix element was to evaluate all the one- and two-loop integrals. In Chapter 3 we discussed different techniques for calculating loop-integrals in general. In particular we saw that by use of IBP identities we could relate all tensor and scalar integrals to a small set of MI. The process for solving the system of IBP identities was automated by use of an algorithm described by Laporta. We saw that the remaining MI could be solved by differential equations, in fact, all necessary MI for $\gamma^* \rightarrow q\bar{q}g$ were calculated by Gehrmann and Remiddi using this technique.

With the necessary tools in place we calculated the full matrix element in Chapter 4. Here we presented all the components for the calculation. In particular we showed all contributing Feynman diagrams and constructed the insertion operator required for the factorisation formula discussed in Chapter 2. By applying the factorisation formula we were subsequently able to make positive checks on our results by verifying that the pole structure indeed agrees with the prediction.

Knowledge of the helicity amplitudes allows additional information on the scattering process. In particular, observables that require knowledge of the polarisation

tensor of the virtual photon, such as oriented event shapes in unpolarised e^+e^- scattering or event shapes in polarised e^+e^- scattering, can be described at two-loop order. In Chapter 5 we have presented analytic formulae for the one- and two-loop virtual helicity amplitudes to the process $\gamma^* \rightarrow q\bar{q}g$. These amplitudes have been derived by defining projectors, which isolate the coefficients of the most general tensorial structure of the matrix element at any order in perturbation theory. Once the general tensor is known, the helicity amplitudes follow in a straightforward manner — they are linear combinations of the tensor coefficients. We applied the projectors directly to the Feynman diagrams and used the conventional approach of relating the ensuing tensor integrals to a basis set of master integrals. This latter step is identical to that employed to evaluate the interference of tree- and two-loop graphs in Chapter 4, apart from the fact that the projector is no longer the tree-level amplitude. As anticipated, the finite remainder from the interference of tree- and two-loop amplitudes can be reconstructed from the appropriate helicity amplitudes, with the difference between treating the external states in D -dimensions or four dimensions being isolated in the infrared-singular terms.

6.2 Outlook

As already mentioned, the virtual corrections form only part of a full NNLO calculation. All of the subprocesses must be combined in a way that allows all of the infrared singularities to cancel one another. This task is far from trivial, even though the factorisation properties of both the one-loop, one-unresolved-parton contribution [82, 83, 84, 85, 86, 87] and the tree-level, two-unresolved-parton contributions [88, 89, 90, 91, 92] have been studied. Although this is still an open and highly non-trivial issue, significant progress is anticipated in the future.

The remaining finite terms must then be combined into a numerical program implementing the experimental definition of jet observables and event-shape variables.

A first calculation involving the above features was presented for the case of photon-plus-one-jet final states in electron-positron annihilation in [93, 94], which involves both double radiation and single radiation from one-loop graphs, thus demonstrating the feasibility of this type of calculation. A prerequisite for such a numerical program is a stable and efficient next-to-leading order four-jet program, where the infrared singularities for the one-loop $\gamma^* \rightarrow 4$ partons are combined with the tree-level $\gamma^* \rightarrow 5$ parton with one parton unresolved. Four such programs currently exist [80, 81, 95, 96, 97], each of which could be used as a starting point for a full $\mathcal{O}(\alpha_s^3)$ NNLO three-jet program.

Similar results can in principle be obtained for $(2 + 1)$ -jet production in deep inelastic ep scattering or $(V + 1)$ -jet production in hadron-hadron collisions. However, the rather different domains of convergence of the HPLs and 2dHPLs makes this a non-trivial task, which is discussed in a separate paper [98]. Nevertheless, the helicity approach will provide information on the direction of the decay leptons in $(V + 1)$ -jet production (with or without polarised protons). Determination of the polarised parton distribution functions in polarised electron-proton scattering will also benefit from the knowledge of the two-loop helicity amplitudes in the appropriate kinematic region.

Note: Since the original calculations presented in this Thesis were performed, part of the results have been confirmed by an independent calculation using the methods described in [99, 100]. In [101], Moch, Uwer and Weinzierl obtain results for the full one-loop amplitude (5.56) and for the contributions to the two-loop amplitude (5.57) which are proportional to N_F (i.e. the terms D_Ω and E_Ω), all in agreement with the results presented here.

APPENDIX A

One-Loop Contribution to $\mathcal{T}^{(6)}$

The finite remainder of the self-interference of the one-loop amplitude is decomposed as

$$\begin{aligned}
 \mathcal{Finite}^{(1 \times 1)}(x, y, z) = V \Bigg[& N^2 (A_{11}(y, z) + A_{11}(z, y)) + (B_{11}(y, z) + B_{11}(z, y)) \\
 & + \frac{1}{N^2} (C_{11}(y, z) + C_{11}(z, y)) + NN_F (D_{11}(y, z) + D_{11}(z, y)) \\
 & + \frac{N_F}{N} (E_{11}(y, z) + E_{11}(z, y)) + N_F^2 (F_{11}(y, z) + F_{11}(z, y)) \Bigg],
 \end{aligned} \tag{A.1}$$

with

$$\begin{aligned}
 A_{11}(y, z) = & \frac{1}{2} + \frac{z}{4y} + \frac{1}{6y} \Big[-\pi^2 - 24 - 10H(0; z) - 6H(0; z)G(0; y) - 6H(1, 0; z) - 10G(0; y) \\
 & + 6G(1, 0; y) \Big] \\
 & + \frac{z}{6(1-y)^2} \Big[\pi^2 G(0; y) + 10H(0; z)G(0; y) + 12H(0; z)G(0, 0; y) \\
 & + 6H(1, 0; z)G(0; y) + 21G(0; y) + 23G(0, 0; y) - 6G(0, 1, 0; y) - 12G(1, 0, 0; y) \Big] \\
 & + \frac{z}{6(1-y)} \Big[\pi^2 + 3\pi^2 G(0; y) + 21 + 10H(0; z) + 36H(0; z)G(0; y) \\
 & + 36H(0; z)G(0, 0; y) + 6H(1, 0; z) + 18H(1, 0; z)G(0; y) + 73G(0; y) \\
 & + 33G(0, 0; y) - 18G(0, 1, 0; y) - 6G(1, 0; y) - 36G(1, 0, 0; y) \Big]
 \end{aligned}$$

$$\begin{aligned}
& + \frac{1}{3(1-y)} \left[-2\pi^2 G(0; y) - 20H(0; z)G(0; y) - 24H(0; z)G(0, 0; y) \right. \\
& - 12H(1, 0; z)G(0; y) - 42G(0; y) - 28G(0, 0; y) + 12G(0, 1, 0; y) \\
& \left. + 24G(1, 0, 0; y) \right] \\
& + \frac{T\pi^2}{72} \left[\pi^2 + 169 + 20H(0; z) + 12H(0; z)G(0; y) + 12H(1, 0; z) + 20G(0; y) \right. \\
& - 12G(1, 0; y) \left. \right] \\
& + \frac{T}{9} \left[+72 + 60H(0; z) + 61H(0; z)G(0; y) + 30H(0; z)G(0, 0; y) \right. \\
& - 9H(0; z)G(0, 1, 0; y) - 15H(0; z)G(1, 0; y) - 18H(0; z)G(1, 0, 0; y) \\
& + 25H(0, 0; z) + 30H(0, 0; z)G(0; y) + 18H(0, 0; z)G(0, 0; y) + 15H(0, 1, 0; z) \\
& + 9H(0, 1, 0; z)G(0; y) + 36H(1, 0; z) + 15H(1, 0; z)G(0; y) \\
& - 9H(1, 0; z)G(1, 0; y) + 30H(1, 0, 0; z) + 18H(1, 0, 0; z)G(0; y) \\
& + 9H(1, 0, 1, 0; z) + 18H(1, 1, 0, 0; z) + 60G(0; y) + 25G(0, 0; y) - 15G(0, 1, 0; y) \\
& \left. - 36G(1, 0; y) - 30G(1, 0, 0; y) + 9G(1, 0, 1, 0; y) + 18G(1, 1, 0, 0; y) \right], \\
B_{11}(y, z) = & \\
& + \frac{z}{6y} \left[-2\pi^2 H(0; z)G(1-z; y) - 2\pi^2 H(1; z)G(-z; y) + 2\pi^2 G(-z, 1-z; y) \right. \\
& + 3 - 42H(0; z)G(1-z; y) - 20H(0; z)G(1-z, 0; y) + 12H(0; z)G(1-z, 1, 0; y) \\
& + 2H(0; z)G(-z, 1-z; y) + 12H(0; z)G(-z, 1-z, 0; y) \\
& + 12H(0; z)G(-z, 0, 1-z; y) - 20H(0; z)G(0, 1-z; y) \\
& + 12H(0; z)G(0, -z, 1-z; y) + 12H(0; z)G(1, 1-z, 0; y) \\
& + 12H(0; z)G(1, 0, 1-z; y) - 4H(0, 0; z)G(1-z; y) - 24H(0, 0; z)G(1-z, 0; y) \\
& - 24H(0, 0; z)G(0, 1-z; y) - 2H(0, 1; z)G(-z; y) - 12H(0, 1; z)G(-z, 0; y) \\
& - 12H(0, 1; z)G(0, -z; y) - 12H(0, 1, 0; z)G(1-z; y) - 42H(1; z)G(-z; y) \\
& - 20H(1; z)G(-z, 0; y) + 12H(1; z)G(-z, 1, 0; y) - 20H(1; z)G(0, -z; y) \\
& + 12H(1; z)G(1, -z, 0; y) + 12H(1; z)G(1, 0, -z; y) + 12H(1, 0; z)G(-z, 1-z; y) \\
& - 2H(1, 0; z)G(-z; y) - 12H(1, 0; z)G(-z, 0; y) - 12H(1, 0; z)G(0, -z; y) \\
& - 24H(1, 0, 0; z)G(1-z; y) - 12H(1, 0, 1; z)G(-z; y) - 24H(1, 1, 0; z)G(-z; y) \\
& + 42G(-z, 1-z; y) + 20G(-z, 1-z, 0; y) - 12G(-z, 1-z, 1, 0; y) \\
& + 20G(-z, 0, 1-z; y) - 12G(-z, 1, 1-z, 0; y) - 12G(-z, 1, 0, 1-z; y) \\
& + 20G(0, -z, 1-z; y) - 12G(1, -z, 1-z, 0; y) - 12G(1, -z, 0, 1-z; y) \\
& \left. - 12G(1, 0, -z, 1-z; y) \right] \\
& + \frac{1}{6y} \left[-\pi^2 + 4\pi^2 H(0; z)G(1-z; y) + 4\pi^2 H(1; z)G(-z; y) - 4\pi^2 G(-z, 1-z; y) \right. \\
& - 10H(0; z) + 90H(0; z)G(1-z; y) + 40H(0; z)G(1-z, 0; y) \\
& - 24H(0; z)G(1-z, 1, 0; y) - 16H(0; z)G(-z, 1-z; y) \\
& - 24H(0; z)G(-z, 1-z, 0; y) - 24H(0; z)G(-z, 0, 1-z; y) \\
& + 40H(0; z)G(0, 1-z; y) - 24H(0; z)G(0, -z, 1-z; y) - 6H(0; z)G(0; y) \\
& \left. - 24H(0; z)G(1, 1-z, 0; y) - 24H(0; z)G(1, 0, 1-z; y) \right]
\end{aligned}$$

$$\begin{aligned}
& +32H(0,0;z)G(1-z;y) + 48H(0,0;z)G(1-z,0;y) \\
& +48H(0,0;z)G(0,1-z;y) + 6H(0,1;z) + 16H(0,1;z)G(-z;y) \\
& +24H(0,1;z)G(-z,0;y) + 24H(0,1;z)G(0,-z;y) + 24H(0,1,0;z)G(1-z;y) \\
& -9H(1;z) + 96H(1;z)G(-z;y) + 40H(1;z)G(-z,0;y) - 24H(1;z)G(-z,1,0;y) \\
& +40H(1;z)G(0,-z;y) - 6H(1;z)G(0;y) - 24H(1;z)G(1,-z,0;y) \\
& -24H(1;z)G(1,0,-z;y) - 6H(1,0;z) - 24H(1,0;z)G(-z,1-z;y) \\
& +16H(1,0;z)G(-z;y) + 24H(1,0;z)G(-z,0;y) + 24H(1,0;z)G(0,-z;y) \\
& +48H(1,0,0;z)G(1-z;y) + 24H(1,0,1;z)G(-z;y) + 48H(1,1,0;z)G(-z;y) \\
& +9G(1-z;y) + 6G(1-z,0;y) - 96G(-z,1-z;y) - 40G(-z,1-z,0;y) \\
& +24G(-z,1-z,1,0;y) - 40G(-z,0,1-z;y) + 24G(-z,1,1-z,0;y) \\
& +24G(-z,1,0,1-z;y) + 6G(0,1-z;y) - 40G(0,-z,1-z;y) - 10G(0;y) \\
& +24G(1,-z,1-z,0;y) + 24G(1,-z,0,1-z;y) + 24G(1,0,-z,1-z;y) \Big] \\
& + \frac{z}{6(1-y)^2} \Big[-\pi^2 G(0;y) - 6H(0;z)G(1-z,0;y) - 6H(0;z)G(0,1-z;y) \\
& -10H(0;z)G(0;y) - 12H(0;z)G(0,0;y) - 6H(0,1;z)G(0;y) \\
& -12H(1;z)G(-z,0;y) - 12H(1;z)G(0,-z;y) + 9H(1;z)G(0;y) \\
& +12H(1;z)G(0,0;y) - 6H(1,0;z)G(0;y) - 9G(1-z,0;y) - 12G(1-z,0,0;y) \\
& +12G(-z,1-z,0;y) + 12G(-z,0,1-z;y) - 9G(0,1-z;y) - 12G(0,1-z,0;y) \\
& +12G(0,-z,1-z;y) - 42G(0;y) - 12G(0,0,1-z;y) - 26G(0,0;y) \\
& +12G(0,1,0;y) + 24G(1,0,0;y) \Big] \\
& + \frac{z}{6(1-y)} \Big[-\pi^2 - 3\pi^2 G(0;y) - 42 - 10H(0;z) - 6H(0;z)G(1-z;y) \\
& -18H(0;z)G(1-z,0;y) - 18H(0;z)G(0,1-z;y) - 36H(0;z)G(0;y) \\
& -36H(0;z)G(0,0;y) - 6H(0,1;z) - 18H(0,1;z)G(0;y) + 9H(1;z) \\
& -12H(1;z)G(-z;y) - 36H(1;z)G(-z,0;y) - 36H(1;z)G(0,-z;y) \\
& +33H(1;z)G(0;y) + 36H(1;z)G(0,0;y) - 6H(1,0;z) - 18H(1,0;z)G(0;y) \\
& -9G(1-z;y) - 33G(1-z,0;y) - 36G(1-z,0,0;y) + 12G(-z,1-z;y) \\
& +36G(-z,1-z,0;y) + 36G(-z,0,1-z;y) - 33G(0,1-z;y) \\
& -36G(0,1-z,0;y) + 36G(0,-z,1-z;y) - 136G(0;y) - 36G(0,0,1-z;y) \\
& -6G(0,0;y) + 36G(0,1,0;y) + 12G(1,0;y) + 72G(1,0,0;y) \Big] \\
& + \frac{1}{(1-y)^2(y+z)^2} \Big[-H(1;z)G(0;y) + G(1-z,0;y) + G(0,1-z;y) \Big] \\
& + \frac{1}{(1-y)^2(y+z)} \Big[2H(1;z)G(0;y) - 2G(1-z,0;y) - 2G(0,1-z;y) + G(0;y) \Big] \\
& + \frac{1}{(1-y)^2} \Big[-H(1;z)G(0;y) + G(1-z,0;y) + G(0,1-z;y) - G(0;y) \Big] \\
& + \frac{1}{(1-y)(y+z)^2} \Big[-H(1;z) - 2H(1;z)G(0;y) + G(1-z;y) + 2G(1-z,0;y) \\
& + 2G(0,1-z;y) \Big] \\
& + \frac{1}{(1-y)(y+z)} \Big[1 + 2H(1;z) + 2H(1;z)G(0;y) - 2G(1-z;y) - 2G(1-z,0;y) \Big]
\end{aligned}$$

$$\begin{aligned}
& -2G(0, 1-z; y) + 2G(0; y) \Big] \\
& + \frac{1}{3(1-y)} \Big[\pi^2 G(0; y) - 3 + 12H(0; z)G(1-z, 0; y) + 12H(0; z)G(0, 1-z; y) \\
& + 10H(0; z)G(0; y) + 12H(0; z)G(0, 0; y) + 6H(0, 1; z)G(0; y) - 3H(1; z) \\
& + 18H(1; z)G(-z, 0; y) + 18H(1; z)G(0, -z; y) - 18H(1; z)G(0; y) \\
& - 12H(1; z)G(0, 0; y) + 6H(1, 0; z)G(0; y) + 3G(1-z; y) + 18G(1-z, 0; y) \\
& + 12G(1-z, 0, 0; y) - 18G(-z, 1-z, 0; y) - 18G(-z, 0, 1-z; y) \\
& + 18G(0, 1-z; y) + 12G(0, 1-z, 0; y) - 18G(0, -z, 1-z; y) + 66G(0; y) \\
& + 12G(0, 0, 1-z; y) + 14G(0, 0; y) - 12G(0, 1, 0; y) - 24G(1, 0, 0; y) \Big] \\
& + \frac{1}{6(y+z)^2} \Big[-2\pi^2 H(1; z) + 2\pi^2 G(1-z; y) + 11H(0; z)G(1-z; y) \\
& + 12H(0; z)G(1-z, 0; y) + 12H(0; z)G(0, 1-z; y) - 11H(0, 1; z) \\
& - 12H(0, 1; z)G(0; y) - 42H(1; z) - 11H(1; z)G(0; y) + 12H(1; z)G(1, 0; y) \\
& - 11H(1, 0; z) + 12H(1, 0; z)G(1-z; y) - 12H(1, 0; z)G(0; y) - 12H(1, 0, 1; z) \\
& - 24H(1, 1, 0; z) + 42G(1-z; y) + 11G(1-z, 0; y) - 12G(1-z, 1, 0; y) \\
& + 11G(0, 1-z; y) - 12G(1, 1-z, 0; y) - 12G(1, 0, 1-z; y) \Big] \\
& + \frac{1}{6(y+z)} \Big[2\pi^2 + 42 + 11H(0; z) + 12H(0; z)G(0; y) + 12H(1, 0; z) + 11G(0; y) \\
& - 12G(1, 0; y) \Big] \\
& + \frac{T\pi^2}{12} \Big[-8 - 2H(0; z)G(1-z; y) - 2H(0, 1; z) + 3H(1; z) - 4H(1; z)G(-z; y) \\
& + 2H(1; z)G(0; y) - 3G(1-z; y) - 2G(1-z, 0; y) + 4G(-z, 1-z; y) \\
& - 2G(0, 1-z; y) + 2G(1, 0; y) \Big] \\
& + \frac{T}{6} \Big[-96 - 40H(0; z) - 39H(0; z)G(1-z; y) - 29H(0; z)G(1-z, 0; y) \\
& - 12H(0; z)G(1-z, 0, 0; y) + 6H(0; z)G(1-z, 1, 0; y) \\
& + 20H(0; z)G(-z, 1-z; y) + 12H(0; z)G(-z, 1-z, 0; y) \\
& + 12H(0; z)G(-z, 0, 1-z; y) - 29H(0; z)G(0, 1-z; y) \\
& - 12H(0; z)G(0, 1-z, 0; y) + 12H(0; z)G(0, -z, 1-z; y) - 24H(0; z)G(0; y) \\
& - 12H(0; z)G(0, 0, 1-z; y) + 6H(0; z)G(0, 1, 0; y) + 6H(0; z)G(1, 1-z, 0; y) \\
& + 6H(0; z)G(1, 0, 1-z; y) + 10H(0; z)G(1, 0; y) + 12H(0; z)G(1, 0, 0; y) \\
& - 20H(0, 0; z)G(1-z; y) - 12H(0, 0; z)G(1-z, 0; y) \\
& - 12H(0, 0; z)G(0, 1-z; y) - 20H(0, 0, 1; z) - 12H(0, 0, 1; z)G(0; y) \\
& - 9H(0, 1; z) - 20H(0, 1; z)G(-z; y) - 12H(0, 1; z)G(-z, 0; y) \\
& - 12H(0, 1; z)G(0, -z; y) + 9H(0, 1; z)G(0; y) + 12H(0, 1; z)G(0, 0; y) \\
& + 6H(0, 1; z)G(1, 0; y) - 10H(0, 1, 0; z) - 6H(0, 1, 0; z)G(1-z; y) \\
& - 6H(0, 1, 0; z)G(0; y) - 6H(0, 1, 0, 1; z) - 12H(0, 1, 1, 0; z) + 36H(1; z) \\
& - 48H(1; z)G(-z; y) - 20H(1; z)G(-z, 0; y) + 12H(1; z)G(-z, 1, 0; y) \\
& - 20H(1; z)G(0, -z; y) + 39H(1; z)G(0; y) + 20H(1; z)G(0, 0; y) \\
& - 6H(1; z)G(0, 1, 0; y) + 12H(1; z)G(1, -z, 0; y) + 12H(1; z)G(1, 0, -z; y)
\end{aligned}$$

$$\begin{aligned}
& -9H(1; z)G(1, 0; y) - 12H(1; z)G(1, 0, 0; y) - 9H(1, 0; z) \\
& -9H(1, 0; z)G(1 - z; y) - 6H(1, 0; z)G(1 - z, 0; y) + 12H(1, 0; z)G(-z, 1 - z; y) \\
& -20H(1, 0; z)G(-z; y) - 12H(1, 0; z)G(-z, 0; y) - 6H(1, 0; z)G(0, 1 - z; y) \\
& -12H(1, 0; z)G(0, -z; y) + 19H(1, 0; z)G(0; y) + 12H(1, 0; z)G(0, 0; y) \\
& +6H(1, 0; z)G(1, 0; y) - 12H(1, 0, 0; z)G(1 - z; y) - 12H(1, 0, 0, 1; z) \\
& +9H(1, 0, 1; z) - 12H(1, 0, 1; z)G(-z; y) + 6H(1, 0, 1; z)G(0; y) \\
& -6H(1, 0, 1, 0; z) + 18H(1, 1, 0; z) - 24H(1, 1, 0; z)G(-z; y) \\
& +12H(1, 1, 0; z)G(0; y) - 36G(1 - z; y) - 39G(1 - z, 0; y) - 20G(1 - z, 0, 0; y) \\
& +6G(1 - z, 0, 1, 0; y) + 9G(1 - z, 1, 0; y) + 12G(1 - z, 1, 0, 0; y) \\
& +48G(-z, 1 - z; y) + 20G(-z, 1 - z, 0; y) - 12G(-z, 1 - z, 1, 0; y) \\
& +20G(-z, 0, 1 - z; y) - 12G(-z, 1, 1 - z, 0; y) - 12G(-z, 1, 0, 1 - z; y) \\
& -39G(0, 1 - z; y) - 20G(0, 1 - z, 0; y) + 6G(0, 1 - z, 1, 0; y) \\
& +20G(0, -z, 1 - z; y) - 40G(0; y) - 20G(0, 0, 1 - z; y) + 6G(0, 1, 1 - z, 0; y) \\
& +6G(0, 1, 0, 1 - z; y) + 10G(0, 1, 0; y) + 9G(1, 1 - z, 0; y) + 12G(1, 1 - z, 0, 0; y) \\
& -12G(1, -z, 1 - z, 0; y) - 12G(1, -z, 0, 1 - z; y) + 9G(1, 0, 1 - z; y) \\
& +12G(1, 0, 1 - z, 0; y) - 12G(1, 0, -z, 1 - z; y) + 48G(1, 0; y) \\
& +12G(1, 0, 0, 1 - z; y) + 20G(1, 0, 0; y) - 12G(1, 0, 1, 0; y) - 24G(1, 1, 0, 0; y) \Big] \\
& + \frac{\pi^2}{6} \Big[H(0; z) - 2H(0; z)G(1 - z; y) - 2H(0, 1; z) + 2H(1; z) - 4H(1; z)G(-z; y) \\
& + 2H(1; z)G(0; y) - 2G(1 - z; y) - 2G(1 - z, 0; y) + 4G(-z, 1 - z; y) \\
& - 2G(0, 1 - z; y) + G(0; y) + 2G(1, 0; y) \Big] \\
& + \frac{1}{6} \Big[21H(0; z) - 53H(0; z)G(1 - z; y) - 52H(0; z)G(1 - z, 0; y) \\
& - 24H(0; z)G(1 - z, 0, 0; y) + 12H(0; z)G(1 - z, 1, 0; y) \\
& + 22H(0; z)G(-z, 1 - z; y) + 24H(0; z)G(-z, 1 - z, 0; y) \\
& + 24H(0; z)G(-z, 0, 1 - z; y) - 52H(0; z)G(0, 1 - z; y) \\
& - 24H(0; z)G(0, 1 - z, 0; y) + 24H(0; z)G(0, -z, 1 - z; y) + 20H(0; z)G(0; y) \\
& - 24H(0; z)G(0, 0, 1 - z; y) + 12H(0; z)G(0, 0; y) + 12H(0; z)G(0, 1, 0; y) \\
& + 12H(0; z)G(1, 1 - z, 0; y) + 12H(0; z)G(1, 0, 1 - z; y) + 14H(0; z)G(1, 0; y) \\
& + 24H(0; z)G(1, 0, 0; y) + 2H(0, 0; z) - 4H(0, 0; z)G(1 - z; y) \\
& - 24H(0, 0; z)G(1 - z, 0; y) - 24H(0, 0; z)G(0, 1 - z; y) + 12H(0, 0; z)G(0; y) \\
& - 40H(0, 0, 1; z) - 24H(0, 0, 1; z)G(0; y) - 31H(0, 1; z) - 22H(0, 1; z)G(-z; y) \\
& - 24H(0, 1; z)G(-z, 0; y) - 24H(0, 1; z)G(0, -z; y) + 30H(0, 1; z)G(0; y) \\
& + 24H(0, 1; z)G(0, 0; y) + 12H(0, 1; z)G(1, 0; y) - 14H(0, 1, 0; z) \\
& - 12H(0, 1, 0; z)G(1 - z; y) - 12H(0, 1, 0; z)G(0; y) - 12H(0, 1, 0, 1; z) \\
& - 24H(0, 1, 1, 0; z) + 42H(1; z) - 84H(1; z)G(-z; y) - 22H(1; z)G(-z, 0; y) \\
& + 24H(1; z)G(-z, 1, 0; y) - 22H(1; z)G(0, -z; y) + 53H(1; z)G(0; y) \\
& + 4H(1; z)G(0, 0; y) - 12H(1; z)G(0, 1, 0; y) + 24H(1; z)G(1, -z, 0; y) \\
& + 24H(1; z)G(1, 0, -z; y) - 12H(1; z)G(1, 0; y) - 24H(1; z)G(1, 0, 0; y) \\
& + 11H(1, 0; z) - 12H(1, 0; z)G(1 - z; y) - 12H(1, 0; z)G(1 - z, 0; y)
\end{aligned}$$

$$\begin{aligned}
& +24H(1, 0; z)G(-z, 1 - z; y) - 22H(1, 0; z)G(-z; y) - 24H(1, 0; z)G(-z, 0; y) \\
& - 12H(1, 0; z)G(0, 1 - z; y) - 24H(1, 0; z)G(0, -z; y) + 38H(1, 0; z)G(0; y) \\
& + 24H(1, 0; z)G(0, 0; y) + 12H(1, 0; z)G(1, 0; y) + 12H(1, 0, 0; z) \\
& - 24H(1, 0, 0; z)G(1 - z; y) - 24H(1, 0, 0, 1; z) + 12H(1, 0, 1; z) \\
& - 24H(1, 0, 1; z)G(-z; y) + 12H(1, 0, 1; z)G(0; y) - 12H(1, 0, 1, 0; z) \\
& + 24H(1, 1, 0; z) - 48H(1, 1, 0; z)G(-z; y) + 24H(1, 1, 0; z)G(0; y) \\
& - 42G(1 - z; y) - 53G(1 - z, 0; y) - 4G(1 - z, 0, 0; y) + 12G(1 - z, 0, 1, 0; y) \\
& + 12G(1 - z, 1, 0; y) + 24G(1 - z, 1, 0, 0; y) + 84G(-z, 1 - z; y) \\
& + 22G(-z, 1 - z, 0; y) - 24G(-z, 1 - z, 1, 0; y) + 22G(-z, 0, 1 - z; y) \\
& - 24G(-z, 1, 1 - z, 0; y) - 24G(-z, 1, 0, 1 - z; y) - 53G(0, 1 - z; y) \\
& - 4G(0, 1 - z, 0; y) + 12G(0, 1 - z, 1, 0; y) + 22G(0, -z, 1 - z; y) + 21G(0; y) \\
& - 4G(0, 0, 1 - z; y) + 2G(0, 0; y) + 12G(0, 1, 1 - z, 0; y) + 12G(0, 1, 0, 1 - z; y) \\
& - 4G(0, 1, 0; y) + 12G(1, 1 - z, 0; y) + 24G(1, 1 - z, 0, 0; y) \\
& - 24G(1, -z, 1 - z, 0; y) - 24G(1, -z, 0, 1 - z; y) + 12G(1, 0, 1 - z; y) \\
& + 24G(1, 0, 1 - z, 0; y) - 24G(1, 0, -z, 1 - z; y) + 42G(1, 0; y) \\
& + 24G(1, 0, 0, 1 - z; y) - 8G(1, 0, 0; y) - 24G(1, 0, 1, 0; y) - 48G(1, 1, 0, 0; y) \Big],
\end{aligned}$$

$$C_{11}(y, z) =$$

$$\begin{aligned}
& \frac{z(1 - z)^2}{y^3} \Big[- 2H(0; z)G(1 - z, -z, 1 - z; y) - 4H(0; z)G(-z, 1 - z, 1 - z; y) \\
& + 4H(0, 0; z)G(1 - z, 1 - z; y) + 2H(0, 1; z)G(1 - z, -z; y) \\
& + 2H(0, 1; z)G(-z, 1 - z; y) - 2H(1; z)G(-z, 1 - z, -z; y) \\
& - 4H(1; z)G(-z, -z, 1 - z; y) + 2H(1, 0; z)G(1 - z, -z; y) \\
& + 2H(1, 0; z)G(-z, 1 - z; y) + 4H(1, 1; z)G(-z, -z; y) \\
& + 2G(-z, 1 - z, -z, 1 - z; y) + 4G(-z, -z, 1 - z, 1 - z; y) \Big] \\
& + \frac{z}{y^2} \Big[- 8H(0; z)G(1 - z, 1 - z; y) + 12H(0; z)G(1 - z, -z, 1 - z; y) \\
& + 24H(0; z)G(-z, 1 - z, 1 - z; y) - 2H(0; z)G(-z, 1 - z; y) \\
& - 24H(0, 0; z)G(1 - z, 1 - z; y) + 4H(0, 0; z)G(1 - z; y) \\
& - 12H(0, 1; z)G(1 - z, -z; y) + 4H(0, 1; z)G(1 - z; y) \\
& - 12H(0, 1; z)G(-z, 1 - z; y) + 2H(0, 1; z)G(-z; y) - 4H(1; z)G(1 - z, -z; y) \\
& + 12H(1; z)G(-z, 1 - z, -z; y) - 8H(1; z)G(-z, 1 - z; y) \\
& + 24H(1; z)G(-z, -z, 1 - z; y) - 12H(1, 0; z)G(1 - z, -z; y) \\
& + 4H(1, 0; z)G(1 - z; y) - 12H(1, 0; z)G(-z, 1 - z; y) + 2H(1, 0; z)G(-z; y) \\
& - 24H(1, 1; z)G(-z, -z; y) + 8H(1, 1; z)G(-z; y) + 4G(1 - z, -z, 1 - z; y) \\
& + 8G(-z, 1 - z, 1 - z; y) - 12G(-z, 1 - z, -z, 1 - z; y) \\
& - 24G(-z, -z, 1 - z, 1 - z; y) \Big] \\
& + \frac{z^2}{y^2} \Big[4H(0; z)G(1 - z, 1 - z; y) - 8H(0; z)G(1 - z, -z, 1 - z; y) \\
& - 16H(0; z)G(-z, 1 - z, 1 - z; y) + 2H(0; z)G(-z, 1 - z; y) \\
& + 16H(0, 0; z)G(1 - z, 1 - z; y) - 4H(0, 0; z)G(1 - z; y)
\end{aligned}$$

$$\begin{aligned}
& +8H(0, 1; z)G(1 - z, -z; y) - 2H(0, 1; z)G(1 - z; y) + 8H(0, 1; z)G(-z, 1 - z; y) \\
& - 2H(0, 1; z)G(-z; y) + 2H(1; z)G(1 - z, -z; y) - 8H(1; z)G(-z, 1 - z, -z; y) \\
& + 4H(1; z)G(-z, 1 - z; y) - 16H(1; z)G(-z, -z, 1 - z; y) \\
& + 8H(1, 0; z)G(1 - z, -z; y) - 2H(1, 0; z)G(1 - z; y) + 8H(1, 0; z)G(-z, 1 - z; y) \\
& - 2H(1, 0; z)G(-z; y) + 16H(1, 1; z)G(-z, -z; y) - 4H(1, 1; z)G(-z; y) \\
& - 2G(1 - z, -z, 1 - z; y) - 4G(-z, 1 - z, 1 - z; y) + 8G(-z, 1 - z, -z, 1 - z; y) \\
& + 16G(-z, -z, 1 - z, 1 - z; y) \Big] \\
& + \frac{1}{y^2} \Big[+ 4H(0; z)G(1 - z, 1 - z; y) - 4H(0; z)G(1 - z, -z, 1 - z; y) \\
& - 8H(0; z)G(-z, 1 - z, 1 - z; y) + 8H(0, 0; z)G(1 - z, 1 - z; y) \\
& + 4H(0, 1; z)G(1 - z, -z; y) - 2H(0, 1; z)G(1 - z; y) + 4H(0, 1; z)G(-z, 1 - z; y) \\
& + 2H(1; z)G(1 - z, -z; y) - 4H(1; z)G(-z, 1 - z, -z; y) + 4H(1; z)G(-z, 1 - z; y) \\
& - 8H(1; z)G(-z, -z, 1 - z; y) + 4H(1, 0; z)G(1 - z, -z; y) \\
& - 2H(1, 0; z)G(1 - z; y) + 4H(1, 0; z)G(-z, 1 - z; y) + 8H(1, 1; z)G(-z, -z; y) \\
& - 4H(1, 1; z)G(-z; y) - 2G(1 - z, -z, 1 - z; y) - 4G(-z, 1 - z, 1 - z; y) \\
& + 4G(-z, 1 - z, -z, 1 - z; y) + 8G(-z, -z, 1 - z, 1 - z; y) \Big] \\
& + \frac{z}{y} \Big[\frac{1}{4} + 14H(0; z)G(1 - z, 1 - z; y) + 4H(0; z)G(1 - z, 1 - z, 0; y) \\
& - 14H(0; z)G(1 - z, -z, 1 - z; y) + 5H(0; z)G(1 - z; y) \\
& + 4H(0; z)G(1 - z, 0, 1 - z; y) - 2H(0; z)G(1 - z, 1, 0; y) \\
& - 28H(0; z)G(-z, 1 - z, 1 - z; y) + 7H(0; z)G(-z, 1 - z; y) \\
& + 4H(0; z)G(0, 1 - z, 1 - z; y) - 2H(0; z)G(1, 1 - z, 0; y) \\
& - 2H(0; z)G(1, 0, 1 - z; y) + 2H(0, 0; z) + 24H(0, 0; z)G(1 - z, 1 - z; y) \\
& - 14H(0, 0; z)G(1 - z; y) + 4H(0, 0, 1; z)G(1 - z; y) + 2H(0, 1; z) \\
& + 14H(0, 1; z)G(1 - z, -z; y) - 7H(0, 1; z)G(1 - z; y) - 2H(0, 1; z)G(1 - z, 0; y) \\
& + 12H(0, 1; z)G(-z, 1 - z; y) - 7H(0, 1; z)G(-z; y) - 2H(0, 1; z)G(0, 1 - z; y) \\
& + 2H(0, 1, 0; z)G(1 - z; y) + 4H(0, 1, 1; z)G(-z; y) + 7H(1; z)G(1 - z, -z; y) \\
& + 2H(1; z)G(1 - z, -z, 0; y) - H(1; z)G(1 - z; y) + 2H(1; z)G(1 - z, 0, -z; y) \\
& - 16H(1; z)G(-z, 1 - z, -z; y) + 14H(1; z)G(-z, 1 - z; y) \\
& + 4H(1; z)G(-z, 1 - z, 0; y) - 32H(1; z)G(-z, -z, 1 - z; y) + 7H(1; z)G(-z; y) \\
& + 4H(1; z)G(-z, 0, 1 - z; y) - 2H(1; z)G(-z, 1, 0; y) + 2H(1; z)G(0, 1 - z, -z; y) \\
& + 4H(1; z)G(0, -z, 1 - z; y) - 2H(1; z)G(1, -z, 0; y) - 2H(1; z)G(1, 0, -z; y) \\
& + 2H(1, 0; z) + 14H(1, 0; z)G(1 - z, -z; y) - 7H(1, 0; z)G(1 - z; y) \\
& - 2H(1, 0; z)G(1 - z, 0; y) + 14H(1, 0; z)G(-z, 1 - z; y) - 7H(1, 0; z)G(-z; y) \\
& - 2H(1, 0; z)G(0, 1 - z; y) + 2H(1, 0, 1; z)G(-z; y) + H(1, 1; z) \\
& + 32H(1, 1; z)G(-z, -z; y) - 14H(1, 1; z)G(-z; y) - 4H(1, 1; z)G(-z, 0; y) \\
& - 4H(1, 1; z)G(0, -z; y) + G(1 - z, 1 - z; y) - 7G(1 - z, -z, 1 - z; y) \\
& - 2G(1 - z, -z, 1 - z, 0; y) - 2G(1 - z, -z, 0, 1 - z; y) - 2G(1 - z, 0, -z, 1 - z; y) \\
& - 14G(-z, 1 - z, 1 - z; y) - 4G(-z, 1 - z, 1 - z, 0; y) \\
& + 16G(-z, 1 - z, -z, 1 - z; y) - 7G(-z, 1 - z; y) - 4G(-z, 1 - z, 0, 1 - z; y)
\end{aligned}$$

$$\begin{aligned}
& +2G(-z, 1-z, 1, 0; y) + 32G(-z, -z, 1-z, 1-z; y) - 4G(-z, 0, 1-z, 1-z; y) \\
& +2G(-z, 1, 1-z, 0; y) + 2G(-z, 1, 0, 1-z; y) - 2G(0, 1-z, -z, 1-z; y) \\
& -4G(0, -z, 1-z, 1-z; y) + 2G(1, -z, 1-z, 0; y) + 2G(1, -z, 0, 1-z; y) \\
& +2G(1, 0, -z, 1-z; y) \Big] \\
& + \frac{1}{y} \Big[+4 - 20H(0; z)G(1-z, 1-z; y) - 8H(0; z)G(1-z, 1-z, 0; y) \\
& +16H(0; z)G(1-z, -z, 1-z; y) - 13H(0; z)G(1-z; y) \\
& -8H(0; z)G(1-z, 0, 1-z; y) + 4H(0; z)G(1-z, 1, 0; y) \\
& +32H(0; z)G(-z, 1-z, 1-z; y) - 4H(0; z)G(-z, 1-z; y) \\
& -8H(0; z)G(0, 1-z, 1-z; y) + 4H(0; z)G(1, 1-z, 0; y) \\
& +4H(0; z)G(1, 0, 1-z; y) - 24H(0, 0; z)G(1-z, 1-z; y) \\
& +8H(0, 0; z)G(1-z; y) - 8H(0, 0, 1; z)G(1-z; y) - H(0, 1; z) \\
& -16H(0, 1; z)G(1-z, -z; y) + 10H(0, 1; z)G(1-z; y) \\
& +4H(0, 1; z)G(1-z, 0; y) - 12H(0, 1; z)G(-z, 1-z; y) + 4H(0, 1; z)G(-z; y) \\
& +4H(0, 1; z)G(0, 1-z; y) - 4H(0, 1, 0; z)G(1-z; y) - 8H(0, 1, 1; z)G(-z; y) \\
& -\frac{3}{2}H(1; z) - 10H(1; z)G(1-z, -z; y) - 4H(1; z)G(1-z, -z, 0; y) \\
& +2H(1; z)G(1-z; y) - 4H(1; z)G(1-z, 0, -z; y) + 20H(1; z)G(-z, 1-z, -z; y) \\
& -20H(1; z)G(-z, 1-z; y) - 8H(1; z)G(-z, 1-z, 0; y) \\
& +40H(1; z)G(-z, -z, 1-z; y) - 14H(1; z)G(-z; y) - 8H(1; z)G(-z, 0, 1-z; y) \\
& +4H(1; z)G(-z, 1, 0; y) - 4H(1; z)G(0, 1-z, -z; y) - 8H(1; z)G(0, -z, 1-z; y) \\
& -H(1; z)G(0; y) + 4H(1; z)G(1, -z, 0; y) + 4H(1; z)G(1, 0, -z; y) - 2H(1, 0; z) \\
& -16H(1, 0; z)G(1-z, -z; y) + 10H(1, 0; z)G(1-z; y) \\
& +4H(1, 0; z)G(1-z, 0; y) - 16H(1, 0; z)G(-z, 1-z; y) + 4H(1, 0; z)G(-z; y) \\
& +4H(1, 0; z)G(0, 1-z; y) - 4H(1, 0, 1; z)G(-z; y) - 2H(1, 1; z) \\
& -40H(1, 1; z)G(-z, -z; y) + 20H(1, 1; z)G(-z; y) + 8H(1, 1; z)G(-z, 0; y) \\
& +8H(1, 1; z)G(0, -z; y) - 2G(1-z, 1-z; y) + 10G(1-z, -z, 1-z; y) \\
& +4G(1-z, -z, 1-z, 0; y) + 4G(1-z, -z, 0, 1-z; y) + \frac{3}{2}G(1-z; y) \\
& +4G(1-z, 0, -z, 1-z; y) + G(1-z, 0; y) + 20G(-z, 1-z, 1-z; y) \\
& +8G(-z, 1-z, 1-z, 0; y) - 20G(-z, 1-z, -z, 1-z; y) + 14G(-z, 1-z; y) \\
& +8G(-z, 1-z, 0, 1-z; y) - 4G(-z, 1-z, 1, 0; y) - 40G(-z, -z, 1-z, 1-z; y) \\
& +8G(-z, 0, 1-z, 1-z; y) - 4G(-z, 1, 1-z, 0; y) - 4G(-z, 1, 0, 1-z; y) \\
& +4G(0, 1-z, -z, 1-z; y) + G(0, 1-z; y) + 8G(0, -z, 1-z, 1-z; y) \\
& -4G(1, -z, 1-z, 0; y) - 4G(1, -z, 0, 1-z; y) - 4G(1, 0, -z, 1-z; y) \\
& -G(1, 0; y) \Big] \\
& + \frac{z}{2(1-y)^2} \Big[2H(0; z)G(1-z, 0; y) + 2H(0; z)G(0, 1-z; y) + 2H(0, 1; z)G(0; y) \\
& +4H(1; z)G(-z, 0; y) + 4H(1; z)G(0, -z; y) - 3H(1; z)G(0; y) \\
& -4H(1; z)G(0, 0; y) + 3G(1-z, 0; y) + 4G(1-z, 0, 0; y) - 4G(-z, 1-z, 0; y) \\
& -4G(-z, 0, 1-z; y) + 3G(0, 1-z; y) + 4G(0, 1-z, 0; y) - 4G(0, -z, 1-z; y)
\end{aligned}$$

$$\begin{aligned}
& +7G(0; y) + 4G(0, 0, 1 - z; y) + 1G(0, 0; y) - 2G(0, 1, 0; y) - 4G(1, 0, 0; y) \Big] \\
& + \frac{z}{2(1-y)} \Big[7 + 2H(0; z)G(1 - z; y) + 6H(0; z)G(1 - z, 0; y) \\
& + 6H(0; z)G(0, 1 - z; y) + 2H(0, 1; z) + 6H(0, 1; z)G(0; y) - 3H(1; z) \\
& + 4H(1; z)G(-z; y) + 12H(1; z)G(-z, 0; y) + 12H(1; z)G(0, -z; y) \\
& - 11H(1; z)G(0; y) - 12H(1; z)G(0, 0; y) + 3G(1 - z; y) + 11G(1 - z, 0; y) \\
& + 12G(1 - z, 0, 0; y) - 4G(-z, 1 - z; y) - 12G(-z, 1 - z, 0; y) \\
& - 12G(-z, 0, 1 - z; y) + 11G(0, 1 - z; y) + 12G(0, 1 - z, 0; y) \\
& - 12G(0, -z, 1 - z; y) + 21G(0; y) + 12G(0, 0, 1 - z; y) - 9G(0, 0; y) \\
& - 6G(0, 1, 0; y) - 2G(1, 0; y) - 12G(1, 0, 0; y) \Big] \\
& + \frac{1}{(1-y)^2(y+z)^2} \Big[H(1; z)G(0; y) - G(1 - z, 0; y) - G(0, 1 - z; y) \Big] \\
& + \frac{1}{(1-y)^2(y+z)} \Big[-2H(1; z)G(0; y) + 2G(1 - z, 0; y) + 2G(0, 1 - z; y) - G(0; y) \Big] \\
& + \frac{1}{(1-y)^2} \Big[+H(1; z)G(0; y) - G(1 - z, 0; y) - G(0, 1 - z; y) + G(0; y) \Big] \\
& + \frac{1}{(1-y)(y+z)^2} \Big[+H(1; z) - G(1 - z; y) \Big] \\
& + \frac{1}{(1-y)(y+z)} \Big[-1 - 2H(1; z) + 2G(1 - z; y) \Big] \\
& + \frac{1}{1-y} \Big[1 - 2H(0; z)G(1 - z, 0; y) - 2H(0; z)G(0, 1 - z; y) + H(1; z) \\
& - 2H(1; z)G(-z, 0; y) - 2H(1; z)G(0, -z; y) + 3H(1; z)G(0; y) - G(1 - z; y) \\
& - 3G(1 - z, 0; y) + 2G(-z, 1 - z, 0; y) + 2G(-z, 0, 1 - z; y) - 3G(0, 1 - z; y) \\
& + 2G(0, -z, 1 - z; y) - 8G(0; y) - 2G(0, 0; y) \Big] \\
& + \frac{1}{2(y+z)^2} \Big[-4H(0; z)G(1 - z, 1 - z; y) + H(0; z)G(1 - z; y) - H(0, 1; z) \\
& + 4H(0, 1, 1; z) + 14H(1; z) - 4H(1; z)G(1 - z, -z; y) + 8H(1; z)G(1 - z; y) \\
& + 4H(1; z)G(1 - z, 0; y) - 8H(1; z)G(-z, 1 - z; y) + 4H(1; z)G(0, 1 - z; y) \\
& - H(1; z)G(0; y) - 2H(1; z)G(1, 0; y) - H(1, 0; z) + 2H(1, 0; z)G(1 - z; y) \\
& + 2H(1, 0, 1; z) - 8H(1, 1; z) + 8H(1, 1; z)G(-z; y) - 4H(1, 1; z)G(0; y) \\
& - 8G(1 - z, 1 - z; y) - 4G(1 - z, 1 - z, 0; y) + 4G(1 - z, -z, 1 - z; y) \\
& - 14G(1 - z; y) - 4G(1 - z, 0, 1 - z; y) + G(1 - z, 0; y) + 2G(1 - z, 1, 0; y) \\
& + 8G(-z, 1 - z, 1 - z; y) - 4G(0, 1 - z, 1 - z; y) + G(0, 1 - z; y) \\
& + 2G(1, 1 - z, 0; y) + 2G(1, 0, 1 - z; y) \Big] \\
& + \frac{1}{2(y+z)} \Big[-14 + H(0; z) - 2H(0; z)G(1 - z; y) - 2H(0, 1; z) + 6H(1; z) \\
& - 4H(1; z)G(-z; y) + 2H(1; z)G(0; y) - 6G(1 - z; y) - 2G(1 - z, 0; y) \\
& + 4G(-z, 1 - z; y) - 2G(0, 1 - z; y) + G(0; y) + 2G(1, 0; y) \Big] \\
& + T \Big[8 + 3H(0; z)G(1 - z, 1 - z; y) + 2H(0; z)G(1 - z, 1 - z, 0; y)
\end{aligned}$$

$$\begin{aligned}
& -2H(0; z)G(1 - z, -z, 1 - z; y) + 4H(0; z)G(1 - z; y) \\
& + 2H(0; z)G(1 - z, 0, 1 - z; y) - H(0; z)G(1 - z, 1, 0; y) \\
& - 4H(0; z)G(-z, 1 - z, 1 - z; y) + 2H(0; z)G(0, 1 - z, 1 - z; y) \\
& - H(0; z)G(1, 1 - z, 0; y) - H(0; z)G(1, 0, 1 - z; y) \\
& + 2H(0, 0; z)G(1 - z, 1 - z; y) + 2H(0, 0, 1; z)G(1 - z; y) + 2H(0, 0, 1, 1; z) \\
& + 4H(0, 1; z) + 2H(0, 1; z)G(1 - z, -z; y) - H(0, 1; z)G(1, 0; y) \\
& + H(0, 1, 0; z)G(1 - z; y) + H(0, 1, 0, 1; z) - 3H(0, 1, 1; z) \\
& + 4H(0, 1, 1; z)G(-z; y) - 2H(0, 1, 1; z)G(0; y) - 6H(1; z) \\
& + 3H(1; z)G(1 - z, -z; y) + 2H(1; z)G(1 - z, -z, 0; y) \\
& + 2H(1; z)G(1 - z, 0, -z; y) - 3H(1; z)G(1 - z, 0; y) - 2H(1; z)G(1 - z, 0, 0; y) \\
& - 4H(1; z)G(-z, 1 - z, -z; y) + 6H(1; z)G(-z, 1 - z; y) \\
& + 4H(1; z)G(-z, 1 - z, 0; y) - 8H(1; z)G(-z, -z, 1 - z; y) + 8H(1; z)G(-z; y) \\
& + 4H(1; z)G(-z, 0, 1 - z; y) - 2H(1; z)G(-z, 1, 0; y) + 2H(1; z)G(0, 1 - z, -z; y) \\
& - 3H(1; z)G(0, 1 - z; y) - 2H(1; z)G(0, 1 - z, 0; y) + 4H(1; z)G(0, -z, 1 - z; y) \\
& - 4H(1; z)G(0; y) - 2H(1; z)G(0, 0, 1 - z; y) + H(1; z)G(0, 1, 0; y) \\
& - 2H(1; z)G(1, -z, 0; y) - 2H(1; z)G(1, 0, -z; y) + 2H(1; z)G(1, 0, 0; y) \\
& + 2H(1, 0; z)G(1 - z, -z; y) - H(1, 0; z)G(1 - z, 0; y) \\
& + 2H(1, 0; z)G(-z, 1 - z; y) - H(1, 0; z)G(0, 1 - z; y) + 2H(1, 0, 1; z)G(-z; y) \\
& - H(1, 0, 1; z)G(0; y) + 8H(1, 1; z)G(-z, -z; y) - 6H(1, 1; z)G(-z; y) \\
& - 4H(1, 1; z)G(-z, 0; y) - 4H(1, 1; z)G(0, -z; y) + 3H(1, 1; z)G(0; y) \\
& + 2H(1, 1; z)G(0, 0; y) + 3G(1 - z, 1 - z, 0; y) + 2G(1 - z, 1 - z, 0, 0; y) \\
& - 3G(1 - z, -z, 1 - z; y) - 2G(1 - z, -z, 1 - z, 0; y) - 2G(1 - z, -z, 0, 1 - z; y) \\
& + 6G(1 - z; y) + 3G(1 - z, 0, 1 - z; y) + 2G(1 - z, 0, 1 - z, 0; y) \\
& - 2G(1 - z, 0, -z, 1 - z; y) + 4G(1 - z, 0; y) + 2G(1 - z, 0, 0, 1 - z; y) \\
& - G(1 - z, 0, 1, 0; y) - 2G(1 - z, 1, 0, 0; y) - 6G(-z, 1 - z, 1 - z; y) \\
& - 4G(-z, 1 - z, 1 - z, 0; y) + 4G(-z, 1 - z, -z, 1 - z; y) - 8G(-z, 1 - z; y) \\
& - 4G(-z, 1 - z, 0, 1 - z; y) + 2G(-z, 1 - z, 1, 0; y) + 8G(-z, -z, 1 - z, 1 - z; y) \\
& - 4G(-z, 0, 1 - z, 1 - z; y) + 2G(-z, 1, 1 - z, 0; y) + 2G(-z, 1, 0, 1 - z; y) \\
& + 3G(0, 1 - z, 1 - z; y) + 2G(0, 1 - z, 1 - z, 0; y) - 2G(0, 1 - z, -z, 1 - z; y) \\
& + 4G(0, 1 - z; y) + 2G(0, 1 - z, 0, 1 - z; y) - G(0, 1 - z, 1, 0; y) \\
& - 4G(0, -z, 1 - z, 1 - z; y) + 2G(0, 0, 1 - z, 1 - z; y) - G(0, 1, 1 - z, 0; y) \\
& - G(0, 1, 0, 1 - z; y) - 2G(1, 1 - z, 0, 0; y) + 2G(1, -z, 1 - z, 0; y) \\
& + 2G(1, -z, 0, 1 - z; y) - 2G(1, 0, 1 - z, 0; y) + 2G(1, 0, -z, 1 - z; y) - 4G(1, 0; y) \\
& - 2G(1, 0, 0, 1 - z; y) + G(1, 0, 1, 0; y) + 2G(1, 1, 0, 0; y) + \frac{11}{4}H(1, 1; z) \\
& - \frac{11}{4}H(1; z)G(1 - z; y) + \frac{11}{4}G(1 - z, 1 - z; y) + \frac{3}{2}H(1; z)G(1, 0; y) \\
& - \frac{3}{2}H(1, 0; z)G(1 - z; y) - \frac{3}{2}H(1, 0, 1; z) - \frac{3}{2}G(1 - z, 1, 0; y) - \frac{3}{2}G(1, 1 - z, 0; y) \\
& - \frac{3}{2}G(1, 0, 1 - z; y) \Big]
\end{aligned}$$

$$\begin{aligned}
& -\frac{1}{2} - \frac{7}{2}H(0; z) + 10H(0; z)G(1 - z, 1 - z; y) + 8H(0; z)G(1 - z, 1 - z, 0; y) \\
& - 8H(0; z)G(1 - z, -z, 1 - z; y) + 4H(0; z)G(1 - z; y) \\
& + 8H(0; z)G(1 - z, 0, 1 - z; y) - 2H(0; z)G(1 - z, 0; y) \\
& - 4H(0; z)G(1 - z, 1, 0; y) - 16H(0; z)G(-z, 1 - z, 1 - z; y) \\
& + 5H(0; z)G(-z, 1 - z; y) + 8H(0; z)G(0, 1 - z, 1 - z; y) - 2H(0; z)G(0, 1 - z; y) \\
& - 4H(0; z)G(1, 1 - z, 0; y) - 4H(0; z)G(1, 0, 1 - z; y) + H(0; z)G(1, 0; y) \\
& + 3H(0, 0; z) + 8H(0, 0; z)G(1 - z, 1 - z; y) - 8H(0, 0; z)G(1 - z; y) \\
& - 2H(0, 0, 1; z) + 8H(0, 0, 1; z)G(1 - z; y) + 8H(0, 0, 1, 1; z) + 10H(0, 1; z) \\
& + 8H(0, 1; z)G(1 - z, -z; y) - 5H(0, 1; z)G(-z; y) - 3H(0, 1; z)G(0; y) \\
& - 4H(0, 1; z)G(1, 0; y) - H(0, 1, 0; z) + 4H(0, 1, 0; z)G(1 - z; y) \\
& + 4H(0, 1, 0, 1; z) - 10H(0, 1, 1; z) + 16H(0, 1, 1; z)G(-z; y) \\
& - 8H(0, 1, 1; z)G(0; y) - 7H(1; z) + 10H(1; z)G(1 - z, -z; y) \\
& + 8H(1; z)G(1 - z, -z, 0; y) - 6H(1; z)G(1 - z; y) + 8H(1; z)G(1 - z, 0, -z; y) \\
& - 10H(1; z)G(1 - z, 0; y) - 8H(1; z)G(1 - z, 0, 0; y) \\
& - 16H(1; z)G(-z, 1 - z, -z; y) + 20H(1; z)G(-z, 1 - z; y) \\
& + 16H(1; z)G(-z, 1 - z, 0; y) - 32H(1; z)G(-z, -z, 1 - z; y) + 14H(1; z)G(-z; y) \\
& + 16H(1; z)G(-z, 0, 1 - z; y) - 5H(1; z)G(-z, 0; y) - 8H(1; z)G(-z, 1, 0; y) \\
& + 8H(1; z)G(0, 1 - z, -z; y) - 10H(1; z)G(0, 1 - z; y) - 8H(1; z)G(0, 1 - z, 0; y) \\
& + 16H(1; z)G(0, -z, 1 - z; y) - 5H(1; z)G(0, -z; y) - 4H(1; z)G(0; y) \\
& - 8H(1; z)G(0, 0, 1 - z; y) + 8H(1; z)G(0, 0; y) + 4H(1; z)G(0, 1, 0; y) \\
& - 8H(1; z)G(1, -z, 0; y) - 8H(1; z)G(1, 0, -z; y) + 5H(1; z)G(1, 0; y) \\
& + 8H(1; z)G(1, 0, 0; y) + 3H(1, 0; z) + 8H(1, 0; z)G(1 - z, -z; y) \\
& - 5H(1, 0; z)G(1 - z; y) - 4H(1, 0; z)G(1 - z, 0; y) + 8H(1, 0; z)G(-z, 1 - z; y) \\
& - 5H(1, 0; z)G(-z; y) - 4H(1, 0; z)G(0, 1 - z; y) + H(1, 0; z)G(0; y) \\
& - 5H(1, 0, 1; z) + 8H(1, 0, 1; z)G(-z; y) - 4H(1, 0, 1; z)G(0; y) + 6H(1, 1; z) \\
& + 32H(1, 1; z)G(-z, -z; y) - 20H(1, 1; z)G(-z; y) - 16H(1, 1; z)G(-z, 0; y) \\
& - 16H(1, 1; z)G(0, -z; y) + 10H(1, 1; z)G(0; y) + 8H(1, 1; z)G(0, 0; y) \\
& + 6G(1 - z, 1 - z; y) + 10G(1 - z, 1 - z, 0; y) + 8G(1 - z, 1 - z, 0, 0; y) \\
& - 10G(1 - z, -z, 1 - z; y) - 8G(1 - z, -z, 1 - z, 0; y) - 8G(1 - z, -z, 0, 1 - z; y) \\
& + 7G(1 - z; y) + 10G(1 - z, 0, 1 - z; y) + 8G(1 - z, 0, 1 - z, 0; y) \\
& - 8G(1 - z, 0, -z, 1 - z; y) + 4G(1 - z, 0; y) + 8G(1 - z, 0, 0, 1 - z; y) \\
& - 8G(1 - z, 0, 0; y) - 4G(1 - z, 0, 1, 0; y) - 5G(1 - z, 1, 0; y) \\
& - 8G(1 - z, 1, 0, 0; y) - 20G(-z, 1 - z, 1 - z; y) - 16G(-z, 1 - z, 1 - z, 0; y) \\
& + 16G(-z, 1 - z, -z, 1 - z; y) - 14G(-z, 1 - z; y) - 16G(-z, 1 - z, 0, 1 - z; y) \\
& + 5G(-z, 1 - z, 0; y) + 8G(-z, 1 - z, 1, 0; y) + 32G(-z, -z, 1 - z, 1 - z; y) \\
& - 16G(-z, 0, 1 - z, 1 - z; y) + 5G(-z, 0, 1 - z; y) + 8G(-z, 1, 1 - z, 0; y) \\
& + 8G(-z, 1, 0, 1 - z; y) + 10G(0, 1 - z, 1 - z; y) + 8G(0, 1 - z, 1 - z, 0; y) \\
& - 8G(0, 1 - z, -z, 1 - z; y) + 4G(0, 1 - z; y) + 8G(0, 1 - z, 0, 1 - z; y) \\
& - 8G(0, 1 - z, 0; y) - 4G(0, 1 - z, 1, 0; y) - 16G(0, -z, 1 - z, 1 - z; y)
\end{aligned}$$

$$\begin{aligned}
& +5G(0, -z, 1-z; y) - \frac{7}{2}G(0; y) + 8G(0, 0, 1-z, 1-z; y) - 8G(0, 0, 1-z; y) \\
& +3G(0, 0; y) - 4G(0, 1, 1-z, 0; y) - 4G(0, 1, 0, 1-z; y) + 4G(0, 1, 0; y) \\
& -5G(1, 1-z, 0; y) - 8G(1, 1-z, 0, 0; y) + 8G(1, -z, 1-z, 0; y) \\
& +8G(1, -z, 0, 1-z; y) - 5G(1, 0, 1-z; y) - 8G(1, 0, 1-z, 0; y) \\
& +8G(1, 0, -z, 1-z; y) - 7G(1, 0; y) - 8G(1, 0, 0, 1-z; y) + 8G(1, 0, 0; y) \\
& +4G(1, 0, 1, 0; y) + 8G(1, 1, 0, 0; y), \\
D_{11}(y, z) = & \frac{1}{6y} [H(0; z) + G(0; y)] \\
& + \frac{z}{6(1-y)^2} [-H(0; z)G(0; y) - 2G(0, 0; y)] \\
& + \frac{z}{6(1-y)} [-H(0; z) - 3H(0; z)G(0; y) - G(0; y) - 6G(0, 0; y)] \\
& + \frac{1}{3(1-y)} [2H(0; z)G(0; y) + 4G(0, 0; y)] \\
& + \frac{T\pi^2}{36} [-22 - H(0; z) - G(0; y)] \\
& + \frac{T}{18} [-12H(0; z) - 10H(0; z)G(0; y) - 6H(0; z)G(0, 0; y) + 3H(0; z)G(1, 0; y) \\
& -10H(0, 0; z) - 6H(0, 0; z)G(0; y) - 3H(0, 1, 0; z) - 3H(1, 0; z)G(0; y) \\
& -6H(1, 0, 0; z) - 12G(0; y) - 10G(0, 0; y) + 3G(0, 1, 0; y) + 6G(1, 0, 0; y)], \\
E_{11}(y, z) = & \frac{z}{3y} [H(0; z)G(1-z, 0; y) - H(0; z)G(-z, 1-z; y) + H(0; z)G(0, 1-z; y) \\
& +2H(0, 0; z)G(1-z; y) + H(0, 1; z)G(-z; y) + H(1; z)G(-z, 0; y) \\
& +H(1; z)G(0, -z; y) + H(1, 0; z)G(-z; y) - G(-z, 1-z, 0; y) - G(-z, 0, 1-z; y) \\
& -G(0, -z, 1-z; y)] \\
& + \frac{1}{6y} [H(0; z) - 4H(0; z)G(1-z, 0; y) + 4H(0; z)G(-z, 1-z; y) \\
& -4H(0; z)G(0, 1-z; y) - 8H(0, 0; z)G(1-z; y) - 4H(0, 1; z)G(-z; y) \\
& -4H(1; z)G(-z, 0; y) - 4H(1; z)G(0, -z; y) - 4H(1, 0; z)G(-z; y) \\
& +4G(-z, 1-z, 0; y) + 4G(-z, 0, 1-z; y) + 4G(0, -z, 1-z; y) + G(0; y)] \\
& + \frac{z}{6(1-y)^2} [H(0; z)G(0; y) + 2G(0, 0; y)] \\
& + \frac{z}{6(1-y)} [H(0; z) + 3H(0; z)G(0; y) + G(0; y) + 6G(0, 0; y)] \\
& + \frac{1}{3(1-y)} [-H(0; z)G(0; y) - 2G(0, 0; y)] \\
& + \frac{1}{3(y+z)^2} [-H(0; z)G(1-z; y) + H(0, 1; z) + H(1; z)G(0; y) + H(1, 0; z) \\
& -G(1-z, 0; y) - G(0, 1-z; y)] \\
& + \frac{1}{3(y+z)} [-H(0; z) - G(0; y)]
\end{aligned}$$

$$\begin{aligned}
& + \frac{T}{12} \left[8H(0; z) + 3H(0; z)G(1 - z; y) + 4H(0; z)G(1 - z, 0; y) \right. \\
& - 4H(0; z)G(-z, 1 - z; y) + 4H(0; z)G(0, 1 - z; y) - 2H(0; z)G(1, 0; y) \\
& + 4H(0, 0; z)G(1 - z; y) + 4H(0, 0, 1; z) - 3H(0, 1; z) + 4H(0, 1; z)G(-z; y) \\
& + 2H(0, 1, 0; z) + 4H(1; z)G(-z, 0; y) + 4H(1; z)G(0, -z; y) - 3H(1; z)G(0; y) \\
& - 4H(1; z)G(0, 0; y) - 3H(1, 0; z) + 4H(1, 0; z)G(-z; y) - 2H(1, 0; z)G(0; y) \\
& + 3G(1 - z, 0; y) + 4G(1 - z, 0, 0; y) - 4G(-z, 1 - z, 0; y) - 4G(-z, 0, 1 - z; y) \\
& + 3G(0, 1 - z; y) + 4G(0, 1 - z, 0; y) - 4G(0, -z, 1 - z; y) + 8G(0; y) \\
& \left. + 4G(0, 0, 1 - z; y) - 2G(0, 1, 0; y) - 4G(1, 0, 0; y) \right] \\
& + \frac{1}{3} \left[H(0; z)G(1 - z; y) + 2H(0; z)G(1 - z, 0; y) - 2H(0; z)G(-z, 1 - z; y) \right. \\
& + 2H(0; z)G(0, 1 - z; y) - H(0; z)G(0; y) - H(0; z)G(1, 0; y) - H(0, 0; z) \\
& + 2H(0, 0; z)G(1 - z; y) + 2H(0, 0, 1; z) - H(0, 1; z) + 2H(0, 1; z)G(-z; y) \\
& + H(0, 1, 0; z) + 2H(1; z)G(-z, 0; y) + 2H(1; z)G(0, -z; y) - H(1; z)G(0; y) \\
& - 2H(1; z)G(0, 0; y) - H(1, 0; z) + 2H(1, 0; z)G(-z; y) - H(1, 0; z)G(0; y) \\
& + G(1 - z, 0; y) + 2G(1 - z, 0, 0; y) - 2G(-z, 1 - z, 0; y) - 2G(-z, 0, 1 - z; y) \\
& + G(0, 1 - z; y) + 2G(0, 1 - z, 0; y) - 2G(0, -z, 1 - z; y) + 2G(0, 0, 1 - z; y) \\
& \left. - G(0, 0; y) - G(0, 1, 0; y) - 2G(1, 0, 0; y) \right], \\
F_{11}(y, z) = & \\
& \frac{T}{36} \left[2\pi^2 + H(0; z)G(0; y) + H(0, 0; z) + G(0, 0; y) \right]. \tag{A.2}
\end{aligned}$$

APPENDIX B

Two-Loop Contribution to $\mathcal{T}^{(6)}$

The finite remainder of the interference of the two-loop amplitude with the tree-level amplitude is decomposed as

$$\begin{aligned}
 \mathcal{F}inite^{(2 \times 0)}(x, y, z) = V & \left[N^2 (A_{20}(y, z) + A_{20}(z, y)) + (B_{20}(y, z) + B_{20}(z, y)) \right. \\
 & + \frac{1}{N^2} (C_{20}(y, z) + C_{20}(z, y)) + NN_F (D_{20}(y, z) + D_{20}(z, y)) \\
 & + \frac{N_F}{N} (E_{20}(y, z) + E_{20}(z, y)) + N_F^2 (F_{20}(y, z) + F_{20}(z, y)) \\
 & \left. + N_{F,\gamma} \left(\frac{4}{N} - N \right) (G_{20}(y, z) + G_{20}(z, y)) \right], \quad (B.1)
 \end{aligned}$$

with

$$\begin{aligned}
 A_{20}(y, z) = & \frac{z}{12y} \left[2\pi^2 + 6\pi^2 H(0; z) - 12\pi^2 G(1; y) - 72\zeta_3 + 8H(0; z) - 36H(0; z)G(1, 0; y) \right. \\
 & \left. - 36H(0, 1, 0; z) + 39H(1, 0; z) + 39G(1, 0; y) + 72G(1, 1, 0; y) \right] \\
 & + \frac{1}{2y(y+z)} \left[17H(1, 0; z) + 17G(1, 0; y) \right] \\
 & + \frac{1}{36y} \left[-12\pi^2 - 24\pi^2 H(0; z) + 48\pi^2 G(1; y) + 288\zeta_3 + 457 - 84H(0; z) \right. \\
 & \left. - 36H(0; z)G(0; y) + 144H(0; z)G(1, 0; y) + 144H(0, 1, 0; z) - 306H(1, 0; z) \right. \\
 & \left. - 192G(0; y) - 234G(1, 0; y) - 288G(1, 1, 0; y) \right] \\
 & + \frac{z}{36(1-y)^2} \left[-\pi^2 + 6\pi^2 H(0; z) + 6\pi^2 H(1; z) - 6\pi^2 G(1-z; y) + 18\pi^2 G(0; y) \right]
 \end{aligned}$$

$$\begin{aligned}
 & -12\pi^2 G(1; y) + 36\zeta_3 - 36H(0; z)G(1 - z, 0; y) + 60H(0; z)G(0; y) \\
 & + 72H(0; z)G(0, 0; y) + 36H(0, 1, 0; z) - 36H(1, 0; z)G(1 - z; y) \\
 & + 36H(1, 0; z)G(0; y) + 36H(1, 1, 0; z) + 36G(1 - z, 1, 0; y) - 355G(0; y) \\
 & + 270G(0, 0; y) - 108G(0, 1, 0; y) + 6G(1, 0; y) - 72G(1, 0, 0; y) + 72G(1, 1, 0; y) \Big] \\
 & + \frac{z}{36(1 - y)} \Big[-33\pi^2 + 18\pi^2 H(0; z) + 18\pi^2 H(1; z) - 18\pi^2 G(1 - z; y) + 54\pi^2 G(0; y) \\
 & - 36\pi^2 G(1; y) + 108\zeta_3 - 277 + 60H(0; z) - 108H(0; z)G(1 - z, 0; y) \\
 & + 216H(0; z)G(0; y) + 216H(0; z)G(0, 0; y) + 108H(0, 1, 0; z) + 36H(1, 0; z) \\
 & - 108H(1, 0; z)G(1 - z; y) + 108H(1, 0; z)G(0; y) + 108H(1, 1, 0; z) \\
 & + 108G(1 - z, 1, 0; y) - 615G(0; y) + 594G(0, 0; y) - 324G(0, 1, 0; y) \\
 & + 198G(1, 0; y) - 216G(1, 0, 0; y) + 216G(1, 1, 0; y) \Big] \\
 & + \frac{z}{(y + z)^3} \Big[\frac{11\pi^2}{2} H(1; z) - \frac{11\pi^2}{2} G(1 - z; y) - 33H(0; z)G(1 - z, 0; y) \\
 & - 33H(0, 1, 0; z) - 33H(1, 0; z) - 33H(1, 0; z)G(1 - z; y) + 33H(1, 0; z)G(0; y) \\
 & + 33H(1, 1, 0; z) + 33G(1 - z, 1, 0; y) + 33G(0, 1, 0; y) - 33G(1, 0; y) \Big] \\
 & + \frac{z}{2(y + z)^2} \Big[-11\pi^2 - \frac{22\pi^2}{3} H(1; z) + \frac{22\pi^2}{3} G(1 - z; y) + 33H(0; z) \\
 & + 44H(0; z)G(1 - z, 0; y) - 66H(0; z)G(0; y) + 44H(0, 1, 0; z) - 22H(1, 0; z) \\
 & + 44H(1, 0; z)G(1 - z; y) - 44H(1, 0; z)G(0; y) - 44H(1, 1, 0; z) \\
 & - 44G(1 - z, 1, 0; y) - 33G(0; y) - 44G(0, 1, 0; y) + 110G(1, 0; y) \Big] \\
 & + \frac{z}{2(y + z)} \Big[\frac{11\pi^2}{6} - 11H(0; z) + 11H(0; z)G(0; y) + 11H(1, 0; z) \\
 & + 11G(0; y) - 11G(1, 0; y) \Big] \\
 & + \frac{z^2}{(y + z)^4} \Big[-\frac{11\pi^2}{2} H(1; z) + \frac{11\pi^2}{2} G(1 - z; y) + 33H(0; z)G(1 - z, 0; y) \\
 & + 33H(0, 1, 0; z) + 33H(1, 0; z)G(1 - z; y) - 33H(1, 0; z)G(0; y) - 33H(1, 1, 0; z) \\
 & - 33G(1 - z, 1, 0; y) - 33G(0, 1, 0; y) \Big] \\
 & + \frac{z^2}{(y + z)^3} \Big[\frac{11\pi^2}{2} + \frac{11\pi^2}{3} H(1; z) - \frac{11\pi^2}{3} G(1 - z; y) \\
 & - 22H(0; z)G(1 - z, 0; y) + 33H(0; z)G(0; y) - 22H(0, 1, 0; z) + 33H(1, 0; z) \\
 & - 22H(1, 0; z)G(1 - z; y) + 22H(1, 0; z)G(0; y) + 22H(1, 1, 0; z) \\
 & + 22G(1 - z, 1, 0; y) + 22G(0, 1, 0; y) - 33G(1, 0; y) \Big] \\
 & + \frac{z^2}{2(y + z)^2} \Big[-\frac{11\pi^2}{6} - 11H(0; z)G(0; y) - 11H(1, 0; z) + 11G(1, 0; y) \Big] \\
 & + \frac{1}{18(1 - y)} \Big[+23\pi^2 - 12\pi^2 H(0; z) - 12\pi^2 H(1; z) + 12\pi^2 G(1 - z; y) - 36\pi^2 G(0; y) \\
 & + 24\pi^2 G(1; y) - 72\zeta_3 + 72H(0; z)G(1 - z, 0; y) - 120H(0; z)G(0; y) \\
 & - 144H(0; z)G(0, 0; y) - 72H(0, 1, 0; z) - 18H(1, 0; z) + 72H(1, 0; z)G(1 - z; y) \\
 & - 72H(1, 0; z)G(0; y) - 72H(1, 1, 0; z) - 72G(1 - z, 1, 0; y) + 515G(0; y)
 \end{aligned}$$

$$\begin{aligned}
& -432G(0, 0; y) + 216G(0, 1, 0; y) - 138G(1, 0; y) + 144G(1, 0, 0; y) \\
& -144G(1, 1, 0; y) \Big] \\
& + \frac{1}{(y+z)^2} \Big[-\frac{7\pi^2}{3}H(1; z) + \frac{7\pi^2}{3}G(1-z; y) + 14H(0; z)G(1-z, 0; y) \\
& + 14H(0, 1, 0; z) + 14H(1, 0; z)G(1-z; y) - 14H(1, 0; z)G(0; y) - 14H(1, 1, 0; z) \\
& - 14G(1-z, 1, 0; y) - 14G(0, 1, 0; y) \Big] \\
& + \frac{1}{4(y+z)} \Big[\frac{28\pi^2}{3} + \frac{14\pi^2}{3}H(1; z) - \frac{14\pi^2}{3}G(1-z; y) - 22 + 11H(0; z) \\
& - 28H(0; z)G(1-z, 0; y) + 56H(0; z)G(0; y) - 28H(0, 1, 0; z) + 56H(1, 0; z) \\
& - 28H(1, 0; z)G(1-z; y) + 28H(1, 0; z)G(0; y) + 28H(1, 1, 0; z) \\
& + 28G(1-z, 1, 0; y) + 11G(0; y) + 28G(0, 1, 0; y) - 56G(1, 0; y) \Big] \\
& + \frac{T\pi^2}{216} \Big[-1045 + 147H(0; z) + 36H(0; z)G(1-z; y) + 108H(0; z)G(0; y) \\
& - 36H(0; z)G(1; y) + 72H(0, 1; z) + 54H(1; z) + 72H(1; z)G(1-z; y) \\
& - 72H(1; z)G(-z; y) - 36H(1; z)G(1; y) + 72H(1, 0; z) + 36H(1, 1; z) \\
& - 186G(1-z; y) + 36G(1-z, 0; y) - 72G(1-z, 1; y) + 72G(-z, 1-z; y) \\
& - 72G(0, 1-z; y) + 147G(0; y) - 72G(0, 1; y) + 36G(1, 1-z; y) + 132G(1; y) \\
& - 108G(1, 0; y) + 72G(1, 1; y) \Big] \\
& + \frac{T}{216} \Big[-\frac{99931}{12} + \frac{132\pi^4}{5} + 4776\zeta_3 - 216\zeta_3H(0; z) + 1080\zeta_3H(1; z) \\
& - 864\zeta_3G(1-z; y) - 216\zeta_3G(0; y) - 216\zeta_3G(1; y) + 304H(0; z) \\
& - 1116H(0; z)G(1-z, 0; y) - 216H(0; z)G(1-z, 1, 0; y) \\
& + 432H(0; z)G(-z, 1-z, 0; y) - 432H(0; z)G(0, 1-z, 0; y) - 144H(0; z)G(0; y) \\
& + 1512H(0; z)G(0, 0; y) - 216H(0; z)G(0, 1, 0; y) + 216H(0; z)G(1, 1-z, 0; y) \\
& - 36H(0; z)G(1, 0; y) - 432H(0; z)G(1, 0, 0; y) + 1920H(0, 0; z) \\
& + 1512H(0, 0; z)G(0; y) + 432H(0, 0; z)G(0, 0; y) + 864H(0, 0, 1, 0; z) \\
& + 1008H(0, 1, 0; z) - 216H(0, 1, 0; z)G(1-z; y) + 432H(0, 1, 0; z)G(-z; y) \\
& + 216H(0, 1, 0; z)G(0; y) - 216H(0, 1, 0; z)G(1; y) + 432H(0, 1, 1, 0; z) \\
& - 1095H(1, 0; z) - 1116H(1, 0; z)G(1-z; y) + 216H(1, 0; z)G(1-z, 0; y) \\
& + 432H(1, 0; z)G(-z, 1-z; y) - 432H(1, 0; z)G(-z, 0; y) \\
& - 432H(1, 0; z)G(0, 1-z; y) + 1152H(1, 0; z)G(0; y) \\
& + 216H(1, 0; z)G(1, 1-z; y) - 216H(1, 0; z)G(1, 0; y) + 1512H(1, 0, 0; z) \\
& + 432H(1, 0, 0; z)G(0; y) + 864H(1, 0, 1, 0; z) + 324H(1, 1, 0; z) \\
& + 432H(1, 1, 0; z)G(1-z; y) - 432H(1, 1, 0; z)G(-z; y) \\
& - 216H(1, 1, 0; z)G(1; y) + 432H(1, 1, 0, 0; z) + 216H(1, 1, 1, 0; z) \\
& + 216G(1-z, 0, 1, 0; y) + 1116G(1-z, 1, 0; y) + 432G(1-z, 1, 1, 0; y) \\
& - 432G(-z, 1-z, 1, 0; y) - 432G(-z, 0, 1, 0; y) + 432G(0, 1-z, 1, 0; y) \\
& + 304G(0; y) + 1920G(0, 0; y) - 432G(0, 0, 1, 0; y) - 1008G(0, 1, 0; y) \\
& + 432G(0, 1, 1, 0; y) - 216G(1, 1-z, 1, 0; y) + 1095G(1, 0; y) - 1512G(1, 0, 0; y)
\end{aligned}$$

$$\begin{aligned}
& +648G(1, 0, 1, 0; y) - 792G(1, 1, 0; y) + 432G(1, 1, 0, 0; y) - 432G(1, 1, 1, 0; y) \Big] \\
& + \frac{1}{2} \left[-\frac{7\pi^2}{3} + 1 - 14H(0; z)G(0; y) - 14H(1, 0; z) + 14G(1, 0; y) \right], \\
B_{20}(y, z) = & \frac{z}{y^2} \left[-3H(0; z)G(1 - z; y) - 3H(1; z)G(-z; y) + 3G(-z, 1 - z; y) \right] \\
& + \frac{z^2}{y^2} \left[H(0; z)G(1 - z; y) + H(1; z)G(-z; y) - G(-z, 1 - z; y) \right] \\
& + \frac{1}{y^2} \left[2H(0; z)G(1 - z; y) + 2H(1; z)G(-z; y) - 2G(-z, 1 - z; y) \right] \\
& + \frac{z\pi^2}{18y} \left[3H(0; z) - 24H(0; z)G(1 - z; y) + 21H(1; z) - 12H(1; z)G(1 - z; y) \right. \\
& + 12G(1 - z, 1 - z; y) + G(1 - z; y) + 12G(1 - z, 1; y) + 6G(0, 1 - z; y) \\
& \left. + 36G(1; y) \right] \\
& + \frac{z}{9y} \left[-27\zeta_3 - 90\zeta_3G(1 - z; y) - 36H(0; z) - 84H(0; z)G(1 - z, 1 - z; y) \right. \\
& + 18H(0; z)G(1 - z, 1 - z, 0; y) + 18H(0; z)G(1 - z, -z, 1 - z; y) \\
& + 152H(0; z)G(1 - z; y) - 57H(0; z)G(1 - z, 0; y) \\
& + 36H(0; z)G(-z, 1 - z, 1 - z; y) + 78H(0; z)G(-z, 1 - z; y) \\
& - 18H(0; z)G(-z, 0, 1 - z; y) - 18H(0; z)G(0, 1 - z, 1 - z; y) \\
& - 3H(0; z)G(0, 1 - z; y) + 36H(0; z)G(0, 1 - z, 0; y) \\
& + 18H(0; z)G(0, -z, 1 - z; y) + 54H(0; z)G(1, 0; y) \\
& - 18H(0, 0; z)G(1 - z, 1 - z; y) - 36H(0, 0; z)G(1 - z; y) \\
& - 18H(0, 0; z)G(1 - z, 0; y) - 18H(0, 0; z)G(0, 1 - z; y) - 9H(0, 0, 1; z) \\
& + 54H(0, 0, 1; z)G(1 - z; y) - 72H(0, 0, 1; z)G(-z; y) - 9H(0, 1; z) \\
& + 54H(0, 1; z)G(1 - z, -z; y) + 9H(0, 1; z)G(1 - z; y) \\
& - 18H(0, 1; z)G(1 - z, 0; y) - 108H(0, 1; z)G(-z, -z; y) + 6H(0, 1; z)G(-z; y) \\
& + 18H(0, 1; z)G(-z, 0; y) + 18H(0, 1; z)G(0, 1 - z; y) - 36H(0, 1; z)G(0, -z; y) \\
& + 9H(0, 1, 0; z) - 36H(0, 1, 0; z)G(1 - z; y) + 18H(0, 1, 0; z)G(-z; y) \\
& + 72H(1; z)G(1 - z, -z, -z; y) - 75H(1; z)G(1 - z, -z; y) \\
& - 18H(1; z)G(1 - z, -z, 0; y) - 18H(1; z)G(1 - z, 0, -z; y) \\
& + 36H(1; z)G(-z, 1 - z, -z; y) - 84H(1; z)G(-z, 1 - z; y) \\
& + 36H(1; z)G(-z, -z, 1 - z; y) - 108H(1; z)G(-z, -z, -z; y) \\
& + 84H(1; z)G(-z, -z; y) + 36H(1; z)G(-z, -z, 0; y) + 143H(1; z)G(-z; y) \\
& + 24H(1; z)G(-z, 0; y) - 18H(1; z)G(0, -z, 1 - z; y) - 18H(1; z)G(0, -z, -z; y) \\
& - 3H(1; z)G(0, -z; y) + 36H(1; z)G(0, -z, 0; y) + 9H(1; z)G(0; y) \\
& + 27H(1; z)G(1, 0; y) + 36H(1, 0; z)G(1 - z, 1 - z; y) \\
& - 18H(1, 0; z)G(1 - z, -z; y) + 57H(1, 0; z)G(1 - z; y) \\
& - 18H(1, 0; z)G(1 - z, 0; y) - 18H(1, 0; z)G(-z, 1 - z; y) - 78H(1, 0; z)G(-z; y) \\
& + 36H(1, 0; z)G(0, 1 - z; y) - 18H(1, 0; z)G(0, -z; y) \\
& - 18H(1, 0, 0; z)G(1 - z; y) - 36H(1, 0, 1; z) - 18H(1, 0, 1; z)G(1 - z; y)
\end{aligned}$$

$$\begin{aligned}
& -36H(1, 1; z)G(-z, -z; y) + 84H(1, 1; z)G(-z; y) + 18H(1, 1; z)G(0, -z; y) \\
& -18H(1, 1, 0; z) - 54H(1, 1, 0; z)G(1 - z; y) + 18H(1, 1, 0; z)G(-z; y) \\
& -18G(1 - z, 1 - z, 1, 0; y) + 75G(1 - z, -z, 1 - z; y) + 18G(1 - z, -z, 1 - z, 0; y) \\
& -72G(1 - z, -z, -z, 1 - z; y) + 18G(1 - z, -z, 0, 1 - z; y) \\
& +18G(1 - z, 0, -z, 1 - z; y) - 9G(1 - z, 0; y) + 18G(1 - z, 0, 1, 0; y) \\
& +54G(1 - z, 1, 0; y) - 36G(1 - z, 1, 1, 0; y) + 84G(-z, 1 - z, 1 - z; y) \\
& -36G(-z, 1 - z, -z, 1 - z; y) - 143G(-z, 1 - z; y) - 24G(-z, 1 - z, 0; y) \\
& +18G(-z, 1 - z, 1, 0; y) - 36G(-z, -z, 1 - z, 1 - z; y) - 84G(-z, -z, 1 - z; y) \\
& -36G(-z, -z, 1 - z, 0; y) + 108G(-z, -z, -z, 1 - z; y) - 36G(-z, -z, 0, 1 - z; y) \\
& -24G(-z, 0, 1 - z; y) + 18G(-z, 0, 1, 0; y) - 9G(0, 1 - z; y) \\
& +18G(0, -z, 1 - z, 1 - z; y) + 3G(0, -z, 1 - z; y) - 36G(0, -z, 1 - z, 0; y) \\
& +18G(0, -z, -z, 1 - z; y) - 36G(0, -z, 0, 1 - z; y) + 27G(0, 1, 0; y) \\
& -27G(1, 1 - z, 0; y) - 27G(1, 0, 1 - z; y) + 9G(1, 0; y) - 108G(1, 1, 0; y) \Big] \\
& + \frac{z^2}{y} \Big[2H(0; z)G(1 - z; y) + 2H(1; z)G(-z; y) - 2G(-z, 1 - z; y) \Big] \\
& + \frac{1}{y(y+z)} \Big[2H(0; z)G(1 - z; y) + 6H(0; z)G(-z, 1 - z; y) - 6H(0; z)G(0, 1 - z; y) \\
& -2H(0, 1; z) - 6H(0, 1; z)G(-z; y) + 6H(1; z)G(-z, 0; y) - 6H(1; z)G(0, -z; y) \\
& +2H(1; z)G(0; y) + 6H(1, 0; z)G(1 - z; y) - 6H(1, 0; z)G(-z; y) - 6H(1, 1, 0; z) \\
& -2G(1 - z, 0; y) + 6G(1 - z, 1, 0; y) - 6G(-z, 1 - z, 0; y) - 6G(-z, 0, 1 - z; y) \\
& -2G(0, 1 - z; y) + 6G(0, -z, 1 - z; y) + 6G(0, 1, 0; y) + 2G(1, 0; y) \Big] \\
& + \frac{\pi^2}{9y} \Big[-3 + 3H(0; z) + 24H(0; z)G(1 - z; y) - 15H(1; z) + 12H(1; z)G(1 - z; y) \\
& -12G(1 - z, 1 - z; y) - 7G(1 - z; y) - 12G(1 - z, 1; y) - 6G(0, 1 - z; y) \\
& -24G(1; y) \Big] \\
& + \frac{1}{9y} \Big[\frac{45}{2}H(1; z) - \frac{45}{2}G(1 - z; y) - 54\zeta_3 + 180\zeta_3G(1 - z; y) \\
& +139 + 57H(0; z) + 132H(0; z)G(1 - z, 1 - z; y) - 36H(0; z)G(1 - z, 1 - z, 0; y) \\
& -36H(0; z)G(1 - z, -z, 1 - z; y) - 250H(0; z)G(1 - z; y) \\
& +96H(0; z)G(1 - z, 0; y) - 72H(0; z)G(-z, 1 - z, 1 - z; y) \\
& -210H(0; z)G(-z, 1 - z; y) + 36H(0; z)G(-z, 0, 1 - z; y) \\
& +36H(0; z)G(0, 1 - z, 1 - z; y) + 96H(0; z)G(0, 1 - z; y) \\
& -72H(0; z)G(0, 1 - z, 0; y) - 36H(0; z)G(0, -z, 1 - z; y) - 9H(0; z)G(0; y) \\
& -72H(0; z)G(1, 0; y) + 36H(0, 0; z)G(1 - z, 1 - z; y) + 144H(0, 0; z)G(1 - z; y) \\
& +36H(0, 0; z)G(1 - z, 0; y) + 36H(0, 0; z)G(0, 1 - z; y) - 18H(0, 0, 1; z) \\
& -108H(0, 0, 1; z)G(1 - z; y) + 144H(0, 0, 1; z)G(-z; y) + 36H(0, 1; z) \\
& -108H(0, 1; z)G(1 - z, -z; y) + 36H(0, 1; z)G(1 - z, 0; y) \\
& +216H(0, 1; z)G(-z, -z; y) + 42H(0, 1; z)G(-z; y) - 36H(0, 1; z)G(-z, 0; y) \\
& -36H(0, 1; z)G(0, 1 - z; y) + 72H(0, 1; z)G(0, -z; y) + 18H(0, 1, 0; z) \\
& +72H(0, 1, 0; z)G(1 - z; y) - 36H(0, 1, 0; z)G(-z; y)
\end{aligned}$$

$$\begin{aligned}
& -144H(1; z)G(1 - z, -z, -z; y) + 132H(1; z)G(1 - z, -z; y) \\
& + 36H(1; z)G(1 - z, -z, 0; y) + 36H(1; z)G(1 - z, 0, -z; y) \\
& - 72H(1; z)G(-z, 1 - z, -z; y) + 132H(1; z)G(-z, 1 - z; y) \\
& - 72H(1; z)G(-z, -z, 1 - z; y) + 216H(1; z)G(-z, -z, -z; y) \\
& - 168H(1; z)G(-z, -z; y) - 72H(1; z)G(-z, -z, 0; y) - 214H(1; z)G(-z; y) \\
& - 30H(1; z)G(-z, 0; y) + 36H(1; z)G(0, -z, 1 - z; y) + 36H(1; z)G(0, -z, -z; y) \\
& + 96H(1; z)G(0, -z; y) - 72H(1; z)G(0, -z, 0; y) - 27H(1; z)G(0; y) \\
& - 18H(1; z)G(1, 0; y) - 18H(1, 0; z) - 72H(1, 0; z)G(1 - z, 1 - z; y) \\
& + 36H(1, 0; z)G(1 - z, -z; y) - 168H(1, 0; z)G(1 - z; y) \\
& + 36H(1, 0; z)G(1 - z, 0; y) + 36H(1, 0; z)G(-z, 1 - z; y) \\
& + 210H(1, 0; z)G(-z; y) - 72H(1, 0; z)G(0, 1 - z; y) + 36H(1, 0; z)G(0, -z; y) \\
& + 36H(1, 0, 0; z)G(1 - z; y) + 36H(1, 0, 1; z) + 36H(1, 0, 1; z)G(1 - z; y) \\
& + 72H(1, 1; z)G(-z, -z; y) - 132H(1, 1; z)G(-z; y) - 36H(1, 1; z)G(0, -z; y) \\
& + 72H(1, 1, 0; z) + 108H(1, 1, 0; z)G(1 - z; y) - 36H(1, 1, 0; z)G(-z; y) \\
& + 36G(1 - z, 1 - z, 1, 0; y) - 132G(1 - z, -z, 1 - z; y) \\
& - 36G(1 - z, -z, 1 - z, 0; y) + 144G(1 - z, -z, -z, 1 - z; y) \\
& - 36G(1 - z, -z, 0, 1 - z; y) - 36G(1 - z, 0, -z, 1 - z; y) + 27G(1 - z, 0; y) \\
& - 36G(1 - z, 0, 1, 0; y) - 108G(1 - z, 1, 0; y) + 72G(1 - z, 1, 1, 0; y) \\
& - 132G(-z, 1 - z, 1 - z; y) + 72G(-z, 1 - z, -z, 1 - z; y) + 214G(-z, 1 - z; y) \\
& + 30G(-z, 1 - z, 0; y) - 36G(-z, 1 - z, 1, 0; y) + 72G(-z, -z, 1 - z, 1 - z; y) \\
& + 168G(-z, -z, 1 - z; y) + 72G(-z, -z, 1 - z, 0; y) - 216G(-z, -z, -z, 1 - z; y) \\
& + 72G(-z, -z, 0, 1 - z; y) + 30G(-z, 0, 1 - z; y) - 36G(-z, 0, 1, 0; y) \\
& + 27G(0, 1 - z; y) - 36G(0, -z, 1 - z, 1 - z; y) - 96G(0, -z, 1 - z; y) \\
& + 72G(0, -z, 1 - z, 0; y) - 36G(0, -z, -z, 1 - z; y) + 72G(0, -z, 0, 1 - z; y) \\
& - 48G(0; y) - 54G(0, 1, 0; y) + 18G(1, 1 - z, 0; y) + 18G(1, 0, 1 - z; y) \\
& - 18G(1, 0; y) + 144G(1, 1, 0; y) \Big] \\
& + \frac{z}{9(1-y)^2} \Big[-11\pi^2 - \frac{27\pi^2}{2}H(0; z) - \frac{27\pi^2}{2}H(1; z) + \frac{27\pi^2}{2}G(1 - z; y) - 6\pi^2G(0; y) \\
& + 6\pi^2G(1; y) + 225\zeta_3 + \frac{81}{2}H(1; z)G(0; y) - \frac{81}{2}G(1 - z, 0; y) - \frac{81}{2}G(0, 1 - z; y) \\
& + 9H(0; z)G(1 - z, 0; y) - 72H(0; z)G(0, 1 - z; y) + 12H(0; z)G(0; y) \\
& - 9H(0; z)G(0, 0; y) + 81H(0, 0, 1; z) + 36H(0, 1; z) - 81H(0, 1; z)G(1 - z; y) \\
& - 9H(0, 1; z)G(0; y) - 81H(0, 1, 0; z) - 81H(1; z)G(1 - z, -z; y) \\
& + 36H(1; z)G(-z; y) - 81H(1; z)G(0, -z; y) + 27H(1; z)G(0, 0; y) - 36H(1, 0; z) \\
& + 81H(1, 0; z)G(1 - z; y) - 9H(1, 0; z)G(0; y) + 81H(1, 0, 1; z) - 81H(1, 1, 0; z) \\
& + 81G(1 - z, -z, 1 - z; y) - 27G(1 - z, 0, 0; y) - 36G(-z, 1 - z; y) \\
& - 27G(0, 1 - z, 0; y) + 81G(0, -z, 1 - z; y) + 37G(0; y) - 27G(0, 0, 1 - z; y) \\
& - 45G(0, 0; y) + 45G(0, 1, 0; y) + 30G(1, 0; y) + 36G(1, 0, 0; y) - 36G(1, 1, 0; y) \Big] \\
& + \frac{z}{18(1-y)} \Big[-9\pi^2H(0; z) - 9\pi^2H(1; z) + 9\pi^2G(1 - z; y) - 36\pi^2G(0; y)
\end{aligned}$$

$$\begin{aligned}
& +36\pi^2 G(1; y) + 54\zeta_3 + 62 + 60H(0; z) - 144H(0; z)G(1 - z; y) \\
& +54H(0; z)G(1 - z, 0; y) - 108H(0; z)G(0; y) - 54H(0; z)G(0, 0; y) \\
& +54H(0, 0, 1; z) - 18H(0, 1; z) - 54H(0, 1; z)G(1 - z; y) - 54H(0, 1; z)G(0; y) \\
& -54H(0, 1, 0; z) + 117H(1; z) - 54H(1; z)G(1 - z, -z; y) - 162H(1; z)G(-z; y) \\
& -54H(1; z)G(0, -z; y) + 99H(1; z)G(0; y) + 162H(1; z)G(0, 0; y) - 18H(1, 0; z) \\
& +54H(1, 0; z)G(1 - z; y) - 54H(1, 0; z)G(0; y) + 54H(1, 0, 1; z) - 54H(1, 1, 0; z) \\
& +54G(1 - z, -z, 1 - z; y) - 117G(1 - z; y) - 99G(1 - z, 0; y) \\
& -162G(1 - z, 0, 0; y) + 162G(-z, 1 - z; y) - 99G(0, 1 - z; y) \\
& -162G(0, 1 - z, 0; y) + 54G(0, -z, 1 - z; y) + 132G(0; y) - 162G(0, 0, 1 - z; y) \\
& -198G(0, 0; y) + 270G(0, 1, 0; y) + 18G(1, 0; y) + 216G(1, 0, 0; y) \\
& -216G(1, 1, 0; y) \Big] \\
& + \frac{z}{(y+z)^3} \Big[-2\pi^2 H(1; z) + 2\pi^2 G(1 - z; y) + 12H(0; z)G(1 - z, 0; y) \\
& +12H(0, 1, 0; z) + 12H(1, 0; z) + 12H(1, 0; z)G(1 - z; y) - 12H(1, 0; z)G(0; y) \\
& -12H(1, 1, 0; z) - 12G(1 - z, 1, 0; y) - 12G(0, 1, 0; y) + 12G(1, 0; y) \Big] \\
& + \frac{z}{(y+z)^2} \Big[2\pi^2 + \frac{4\pi^2}{3} H(1; z) - \frac{4\pi^2}{3} G(1 - z; y) - 6H(0; z) - 8H(0; z)G(1 - z, 0; y) \\
& +12H(0; z)G(0; y) - 8H(0, 1, 0; z) + 4H(1, 0; z) - 8H(1, 0; z)G(1 - z; y) \\
& +8H(1, 0; z)G(0; y) + 8H(1, 1, 0; z) + 8G(1 - z, 1, 0; y) + 6G(0; y) + 8G(0, 1, 0; y) \\
& -20G(1, 0; y) \Big] \\
& + \frac{z}{y+z} \Big[-\frac{\pi^2}{3} + 2H(0; z) - 2H(0; z)G(0; y) - 2H(1, 0; z) - 2G(0; y) + 2G(1, 0; y) \Big] \\
& + \frac{z^2}{(1-y)^3} \Big[+\frac{2\pi^2}{3} H(0; z) + \frac{2\pi^2}{3} H(1; z) - \frac{2\pi^2}{3} G(1 - z; y) \\
& -12\zeta_3 + 4H(0; z)G(0, 1 - z; y) - 4H(0, 0, 1; z) + 4H(0, 1; z)G(1 - z; y) \\
& +4H(0, 1, 0; z) + 4H(1; z)G(1 - z, -z; y) + 4H(1; z)G(0, -z; y) \\
& -4H(1, 0; z)G(1 - z; y) - 4H(1, 0, 1; z) + 4H(1, 1, 0; z) - 4G(1 - z, -z, 1 - z; y) \\
& -4G(0, -z, 1 - z; y) \Big] \\
& + \frac{z^2}{(1-y)^2} \Big[+4H(0; z)G(1 - z; y) + 4H(1; z)G(-z; y) - 4G(-z, 1 - z; y) \Big] \\
& + \frac{z^2}{1-y} \Big[+2H(0; z)G(1 - z; y) + 2H(1; z)G(-z; y) - 2G(-z, 1 - z; y) \Big] \\
& + \frac{z^2}{(y+z)^4} \Big[2\pi^2 H(1; z) - 2\pi^2 G(1 - z; y) - 12H(0; z)G(1 - z, 0; y) - 12H(0, 1, 0; z) \\
& -12H(1, 0; z)G(1 - z; y) + 12H(1, 0; z)G(0; y) + 12H(1, 1, 0; z) \\
& +12G(1 - z, 1, 0; y) + 12G(0, 1, 0; y) \Big] \\
& + \frac{z^2}{(y+z)^3} \Big[-2\pi^2 - \frac{4\pi^2}{3} H(1; z) + \frac{4\pi^2}{3} G(1 - z; y) + 8H(0; z)G(1 - z, 0; y) \\
& -12H(0; z)G(0; y) + 8H(0, 1, 0; z) - 12H(1, 0; z) + 8H(1, 0; z)G(1 - z; y) \\
& -8H(1, 0; z)G(0; y) - 8H(1, 1, 0; z) - 8G(1 - z, 1, 0; y) - 8G(0, 1, 0; y)
\end{aligned}$$

$$\begin{aligned}
 & +12G(1, 0; y) \Big] \\
 & + \frac{z^2}{(y+z)^2} \left[\frac{\pi^2}{3} + 2H(0; z)G(0; y) + 2H(1, 0; z) - 2G(1, 0; y) \right] \\
 & + \frac{1}{1-y-z} \left[\frac{\pi^2}{6} + H(0; z)G(0; y) + H(1, 0; z) - G(1, 0; y) \right] \\
 & + \frac{1}{9(1-y)} \left[10\pi^2 + 12\pi^2 H(0; z) + 9\pi^2 H(1; z) - 9\pi^2 G(1-z; y) + 12\pi^2 G(0; y) \right. \\
 & - 21\pi^2 G(1; y) - 234\zeta_3 + 54H(0; z)G(0, 1-z; y) + 21H(0; z)G(0; y) \\
 & + 18H(0; z)G(0, 0; y) - 18H(0; z)G(1, 0; y) - 90H(0, 0, 1; z) - 63H(0, 1; z) \\
 & + 90H(0, 1; z)G(1-z; y) + 36H(0, 1; z)G(0; y) + 54H(0, 1, 0; z) \\
 & + 90H(1; z)G(1-z, -z; y) - 63H(1; z)G(-z; y) + 90H(1; z)G(0, -z; y) \\
 & - 18H(1; z)G(0; y) - 72H(1; z)G(0, 0; y) + 63H(1, 0; z) - 54H(1, 0; z)G(1-z; y) \\
 & - 90H(1, 0, 1; z) + 54H(1, 1, 0; z) - 90G(1-z, -z, 1-z; y) + 18G(1-z, 0; y) \\
 & + 72G(1-z, 0, 0; y) - 36G(1-z, 1, 0; y) + 63G(-z, 1-z; y) + 18G(0, 1-z; y) \\
 & + 72G(0, 1-z, 0; y) - 90G(0, -z, 1-z; y) + 55G(0; y) + 72G(0, 0, 1-z; y) \\
 & + 108G(0, 0; y) - 108G(0, 1, 0; y) + 3G(1, 0; y) - 90G(1, 0, 0; y) \\
 & \left. + 126G(1, 1, 0; y) \right] \\
 & + \frac{1}{9(y+z)^2} \left[+ 18H(0; z)G(1-z, 1-z; y) + 27H(0; z)G(1-z; y) \right. \\
 & - 18H(0; z)G(-z, 1-z; y) - 72H(0, 0, 1; z) + 39H(0, 1; z) \\
 & + 36H(0, 1; z)G(1-z; y) - 90H(0, 1; z)G(-z; y) + 18H(0, 1; z)G(0; y) \\
 & + 18H(0, 1, 0; z) - 18H(0, 1, 1; z) + 230H(1; z) + 54H(1; z)G(1-z, -z; y) \\
 & - 102H(1; z)G(1-z; y) - 18H(1; z)G(1-z, 0; y) + 36H(1; z)G(-z, 1-z; y) \\
 & - 108H(1; z)G(-z, -z; y) + 66H(1; z)G(-z; y) + 18H(1; z)G(-z, 0; y) \\
 & - 18H(1; z)G(0, 1-z; y) + 18H(1; z)G(0, -z; y) - 27H(1; z)G(0; y) \\
 & - 27H(1, 0; z) - 18H(1, 0; z)G(1-z; y) + 18H(1, 0; z)G(-z; y) - 36H(1, 0, 1; z) \\
 & + 102H(1, 1; z) - 36H(1, 1; z)G(-z; y) + 18H(1, 1; z)G(0; y) + 18H(1, 1, 0; z) \\
 & + 102G(1-z, 1-z; y) + 18G(1-z, 1-z, 0; y) - 54G(1-z, -z, 1-z; y) \\
 & - 230G(1-z; y) + 18G(1-z, 0, 1-z; y) + 27G(1-z, 0; y) \\
 & - 36G(-z, 1-z, 1-z; y) - 66G(-z, 1-z; y) - 18G(-z, 1-z, 0; y) \\
 & + 108G(-z, -z, 1-z; y) - 18G(-z, 0, 1-z; y) + 18G(0, 1-z, 1-z; y) \\
 & \left. + 27G(0, 1-z; y) - 18G(0, -z, 1-z; y) \right] \\
 & + \frac{1}{9(y+z)} \left[- \frac{3\pi^2}{2} H(1; z) + \frac{3\pi^2}{2} G(1-z; y) - 170 - 18H(0; z)G(1-z; y) \right. \\
 & + 9H(0; z)G(1-z, 0; y) - 72H(0, 1; z) + 9H(0, 1, 0; z) - 123H(1; z) \\
 & - 90H(1; z)G(-z; y) + 18H(1; z)G(0; y) + 18H(1, 0; z) + 9H(1, 0; z)G(1-z; y) \\
 & - 9H(1, 0; z)G(0; y) - 9H(1, 1, 0; z) + 123G(1-z; y) - 18G(1-z, 0; y) \\
 & \left. - 9G(1-z, 1, 0; y) + 90G(-z, 1-z; y) - 18G(0, 1-z; y) - 9G(0, 1, 0; y) \right] \\
 & + \frac{T\pi^2}{72} \left[- 115 - 24H(0; z)G(1-z; y) - 12H(0; z)G(1; y) - 12H(0, 1; z) + 7H(1; z) \right]
 \end{aligned}$$

$$\begin{aligned}
& -48H(1; z)G(1 - z; y) + 36H(1; z)G(0; y) - 12H(1; z)G(1; y) - 12H(1, 0; z) \\
& + 12H(1, 1; z) + 48G(1 - z, 1 - z; y) + 19G(1 - z; y) - 24G(1 - z, 0; y) \\
& - 36G(0, 1 - z; y) + 48G(0, 1; y) + 12G(1, 1 - z; y) - 26G(1; y) + 36G(1, 0; y) \\
& - 48G(1, 1; y) \Big] \\
& + \frac{T}{54} \Big[-\frac{3\pi^4}{8} + \frac{15251}{12} - \frac{357}{2}\zeta_3 + 108\zeta_3H(1; z) - 270\zeta_3G(1 - z; y) + 162\zeta_3G(1; y) \\
& - 360H(0; z) - 198H(0; z)G(1 - z, 1 - z; y) + 108H(0; z)G(1 - z, 1 - z, 0; y) \\
& + 108H(0; z)G(1 - z, -z, 1 - z; y) + 78H(0; z)G(1 - z; y) \\
& + 54H(0; z)G(1 - z, 0, 1 - z; y) - 180H(0; z)G(1 - z, 0; y) \\
& - 108H(0; z)G(1 - z, 0, 0; y) + 54H(0; z)G(1 - z, 1, 0; y) \\
& + 108H(0; z)G(-z, 1 - z, 1 - z; y) + 297H(0; z)G(-z, 1 - z; y) \\
& - 108H(0; z)G(-z, -z, 1 - z; y) - 108H(0; z)G(0, 1 - z, 1 - z; y) \\
& - 180H(0; z)G(0, 1 - z; y) + 216H(0; z)G(0, -z, 1 - z; y) - 216H(0; z)G(0; y) \\
& + 54H(0; z)G(0, 1, 0; y) - 54H(0; z)G(1, 1 - z, 0; y) \\
& - 108H(0; z)G(1, 0, 1 - z; y) + 9H(0; z)G(1, 0; y) + 108H(0; z)G(1, 0, 0; y) \\
& - 378H(0, 0; z)G(1 - z; y) - 108H(0, 0; z)G(1 - z, 0; y) \\
& - 108H(0, 0; z)G(0, 1 - z; y) + 18H(0, 0, 1; z) + 216H(0, 0, 1; z)G(1 - z; y) \\
& - 432H(0, 0, 1; z)G(-z; y) - 108H(0, 0, 1; z)G(0; y) + 54H(0, 0, 1; z)G(1; y) \\
& + 216H(0, 0, 1, 0; z) + 348H(0, 1; z) + 324H(0, 1; z)G(1 - z, -z; y) \\
& - 279H(0, 1; z)G(1 - z; y) - 162H(0, 1; z)G(1 - z, 0; y) \\
& + 108H(0, 1; z)G(-z, 1 - z; y) - 540H(0, 1; z)G(-z, -z; y) \\
& - 63H(0, 1; z)G(-z; y) + 108H(0, 1; z)G(-z, 0; y) + 54H(0, 1; z)G(0, 1 - z; y) \\
& - 108H(0, 1; z)G(0, -z; y) - 117H(0, 1; z)G(0; y) + 108H(0, 1; z)G(0, 0; y) \\
& - 54H(0, 1; z)G(1, 1 - z; y) + 54H(0, 1; z)G(1, 0; y) - 252H(0, 1, 0; z) \\
& - 216H(0, 1, 0; z)G(1 - z; y) + 108H(0, 1, 0; z)G(-z; y) - 54H(0, 1, 0; z)G(0; y) \\
& - 54H(0, 1, 0; z)G(1; y) + 198H(0, 1, 1; z) - 108H(0, 1, 1; z)G(-z; y) \\
& + 108H(0, 1, 1, 0; z) + 17H(1; z) + 432H(1; z)G(1 - z, -z, -z; y) \\
& - 477H(1; z)G(1 - z, -z; y) - 108H(1; z)G(1 - z, -z, 0; y) \\
& + 297H(1; z)G(1 - z; y) - 108H(1; z)G(1 - z, 0, -z; y) \\
& + 198H(1; z)G(1 - z, 0; y) + 162H(1; z)G(1 - z, 1, 0; y) \\
& + 216H(1; z)G(-z, 1 - z, -z; y) - 396H(1; z)G(-z, 1 - z; y) \\
& - 108H(1; z)G(-z, 1 - z, 0; y) + 216H(1; z)G(-z, -z, 1 - z; y) \\
& - 648H(1; z)G(-z, -z, -z; y) + 234H(1; z)G(-z, -z; y) \\
& + 108H(1; z)G(-z, -z, 0; y) + 426H(1; z)G(-z; y) - 108H(1; z)G(-z, 0, 1 - z; y) \\
& + 108H(1; z)G(-z, 0, -z; y) - 297H(1; z)G(-z, 0; y) \\
& - 54H(1; z)G(0, 1 - z, -z; y) + 198H(1; z)G(0, 1 - z; y) \\
& - 108H(1; z)G(0, -z, 1 - z; y) + 108H(1; z)G(0, -z, -z; y) \\
& - 297H(1; z)G(0, -z; y) + 216H(1; z)G(0, -z, 0; y) - 78H(1; z)G(0; y) \\
& + 108H(1; z)G(0, 0, -z; y) + 378H(1; z)G(0, 0; y) - 54H(1; z)G(0, 1, 0; y) \\
& - 54H(1; z)G(1, 1 - z, -z; y) - 54H(1; z)G(1, 0, -z; y) - 81H(1; z)G(1, 0; y)
\end{aligned}$$

$$\begin{aligned}
& -108H(1; z)G(1, 0, 0; y) - 81H(1, 0; z) + 216H(1, 0; z)G(1 - z, 1 - z; y) \\
& -108H(1, 0; z)G(1 - z, -z; y) + 117H(1, 0; z)G(1 - z; y) \\
& -162H(1, 0; z)G(1 - z, 0; y) - 108H(1, 0; z)G(-z, 1 - z; y) \\
& +108H(1, 0; z)G(-z, -z; y) - 297H(1, 0; z)G(-z; y) - 216H(1, 0; z)G(0, -z; y) \\
& +171H(1, 0; z)G(0; y) + 108H(1, 0; z)G(0, 0; y) + 54H(1, 0; z)G(1, 1 - z; y) \\
& +54H(1, 0; z)G(1, 0; y) - 108H(1, 0, 0; z)G(1 - z; y) - 54H(1, 0, 0, 1; z) \\
& +360H(1, 0, 1; z) - 162H(1, 0, 1; z)G(1 - z; y) - 108H(1, 0, 1; z)G(-z; y) \\
& +54H(1, 0, 1; z)G(0; y) + 54H(1, 0, 1; z)G(1; y) + 108H(1, 0, 1, 0; z) \\
& -297H(1, 1; z) - 216H(1, 1; z)G(-z, -z; y) + 396H(1, 1; z)G(-z; y) \\
& +108H(1, 1; z)G(-z, 0; y) + 108H(1, 1; z)G(0, -z; y) - 198H(1, 1; z)G(0; y) \\
& +81H(1, 1, 0; z) - 378H(1, 1, 0; z)G(1 - z; y) + 108H(1, 1, 0; z)G(-z; y) \\
& +108H(1, 1, 0; z)G(0; y) - 54H(1, 1, 0; z)G(1; y) + 108H(1, 1, 0, 1; z) \\
& +162H(1, 1, 1, 0; z) - 297G(1 - z, 1 - z; y) - 198G(1 - z, 1 - z, 0; y) \\
& -216G(1 - z, 1 - z, 1, 0; y) + 477G(1 - z, -z, 1 - z; y) \\
& +108G(1 - z, -z, 1 - z, 0; y) - 432G(1 - z, -z, -z, 1 - z; y) \\
& +108G(1 - z, -z, 0, 1 - z; y) - 17G(1 - z; y) - 198G(1 - z, 0, 1 - z; y) \\
& +108G(1 - z, 0, -z, 1 - z; y) + 78G(1 - z, 0; y) - 378G(1 - z, 0, 0; y) \\
& +108G(1 - z, 0, 1, 0; y) - 162G(1 - z, 1, 1 - z, 0; y) - 162G(1 - z, 1, 0, 1 - z; y) \\
& +81G(1 - z, 1, 0; y) + 108G(1 - z, 1, 0, 0; y) + 396G(-z, 1 - z, 1 - z; y) \\
& +108G(-z, 1 - z, 1 - z, 0; y) - 216G(-z, 1 - z, -z, 1 - z; y) - 426G(-z, 1 - z; y) \\
& +108G(-z, 1 - z, 0, 1 - z; y) + 297G(-z, 1 - z, 0; y) \\
& -216G(-z, -z, 1 - z, 1 - z; y) - 234G(-z, -z, 1 - z; y) \\
& -108G(-z, -z, 1 - z, 0; y) + 648G(-z, -z, -z, 1 - z; y) \\
& -108G(-z, -z, 0, 1 - z; y) + 108G(-z, 0, 1 - z, 1 - z; y) + 297G(-z, 0, 1 - z; y) \\
& -108G(-z, 0, -z, 1 - z; y) - 198G(0, 1 - z, 1 - z; y) + 54G(0, 1 - z, -z, 1 - z; y) \\
& +78G(0, 1 - z; y) - 378G(0, 1 - z, 0; y) + 162G(0, 1 - z, 1, 0; y) \\
& +108G(0, -z, 1 - z, 1 - z; y) + 297G(0, -z, 1 - z; y) - 216G(0, -z, 1 - z, 0; y) \\
& -108G(0, -z, -z, 1 - z; y) - 216G(0, -z, 0, 1 - z; y) - 360G(0; y) \\
& -378G(0, 0, 1 - z; y) - 108G(0, 0, -z, 1 - z; y) + 108G(0, 0, 1, 0; y) \\
& +54G(0, 1, 1 - z, 0; y) + 54G(0, 1, 0, 1 - z; y) + 333G(0, 1, 0; y) \\
& -216G(0, 1, 1, 0; y) + 54G(1, 1 - z, -z, 1 - z; y) + 81G(1, 1 - z, 0; y) \\
& +108G(1, 1 - z, 0, 0; y) + 81G(1, 0, 1 - z; y) + 108G(1, 0, 1 - z, 0; y) \\
& +54G(1, 0, -z, 1 - z; y) + 3G(1, 0; y) + 108G(1, 0, 0, 1 - z; y) + 378G(1, 0, 0; y) \\
& -216G(1, 0, 1, 0; y) + 117G(1, 1, 0; y) - 216G(1, 1, 0, 0; y) + 216G(1, 1, 1, 0; y) \Big] \\
& + \frac{\pi^2}{18} \Big[11 + 9H(0; z) - 24H(0; z)G(1 - z; y) - 6H(0, 1; z) + 8H(1; z) \\
& -36H(1; z)G(1 - z; y) + 24H(1; z)G(0; y) + 6H(1; z)G(1; y) + 24H(1, 1; z) \\
& +24G(1 - z, 1 - z; y) + 2G(1 - z; y) - 24G(1 - z, 0; y) + 12G(1 - z, 1; y) \\
& -6G(0, 1 - z; y) + 9G(0; y) + 12G(0, 1; y) - 6G(1, 1 - z; y) - 10G(1; y) \\
& +24G(1, 0; y) - 6G(1, 1; y) \Big]
\end{aligned}$$

$$\begin{aligned}
& + \frac{1}{18} \left[288\zeta_3 + 180\zeta_3 H(1; z) - 360\zeta_3 G(1 - z; y) + 180\zeta_3 G(1; y) - 188H(0; z) \right. \\
& - 150H(0; z)G(1 - z, 1 - z; y) + 72H(0; z)G(1 - z, 1 - z, 0; y) \\
& + 72H(0; z)G(1 - z, -z, 1 - z; y) + 295H(0; z)G(1 - z; y) \\
& - 300H(0; z)G(1 - z, 0; y) - 36H(0; z)G(1 - z, 0, 0; y) \\
& + 72H(0; z)G(-z, 1 - z, 1 - z; y) + 216H(0; z)G(-z, 1 - z; y) \\
& - 72H(0; z)G(-z, -z, 1 - z; y) - 36H(0; z)G(0, 1 - z, 1 - z; y) \\
& - 156H(0; z)G(0, 1 - z; y) + 36H(0; z)G(0, 1 - z, 0; y) \\
& + 144H(0; z)G(0, -z, 1 - z; y) + 78H(0; z)G(0; y) - 72H(0; z)G(0, 0, 1 - z; y) \\
& + 18H(0; z)G(0, 0; y) + 36H(0; z)G(0, 1, 0; y) - 72H(0; z)G(1, 1 - z, 0; y) \\
& - 36H(0; z)G(1, 0, 1 - z; y) + 132H(0; z)G(1, 0; y) + 36H(0; z)G(1, 0, 0; y) \\
& + 36H(0; z)G(1, 1, 0; y) + 36H(0, 0; z) - 36H(0, 0; z)G(1 - z, 1 - z; y) \\
& - 108H(0, 0; z)G(1 - z; y) - 36H(0, 0; z)G(1 - z, 0; y) \\
& - 36H(0, 0; z)G(0, 1 - z; y) + 18H(0, 0; z)G(0; y) - 108H(0, 0, 0, 1; z) \\
& + 84H(0, 0, 1; z) + 180H(0, 0, 1; z)G(1 - z; y) - 288H(0, 0, 1; z)G(-z; y) \\
& + 36H(0, 0, 1; z)G(1; y) + 108H(0, 0, 1, 0; z) - 36H(0, 0, 1, 1; z) + 289H(0, 1; z) \\
& + 216H(0, 1; z)G(1 - z, -z; y) - 222H(0, 1; z)G(1 - z; y) \\
& - 72H(0, 1; z)G(1 - z, 0; y) + 72H(0, 1; z)G(-z, 1 - z; y) \\
& - 360H(0, 1; z)G(-z, -z; y) + 192H(0, 1; z)G(-z; y) + 72H(0, 1; z)G(-z, 0; y) \\
& - 72H(0, 1; z)G(0, -z; y) - 60H(0, 1; z)G(0; y) + 36H(0, 1; z)G(0, 0; y) \\
& - 36H(0, 1; z)G(1, 1 - z; y) - 114H(0, 1, 0; z) - 144H(0, 1, 0; z)G(1 - z; y) \\
& + 72H(0, 1, 0; z)G(-z; y) - 72H(0, 1, 0; z)G(0; y) + 36H(0, 1, 0; z)G(1; y) \\
& - 72H(0, 1, 0, 1; z) + 150H(0, 1, 1; z) - 72H(0, 1, 1; z)G(-z; y) \\
& + 36H(0, 1, 1; z)G(0; y) + 36H(0, 1, 1, 0; z) - 376H(1; z) \\
& + 288H(1; z)G(1 - z, -z, -z; y) - 372H(1; z)G(1 - z, -z; y) \\
& - 72H(1; z)G(1 - z, -z, 0; y) + 204H(1; z)G(1 - z; y) \\
& - 72H(1; z)G(1 - z, 0, -z; y) + 150H(1; z)G(1 - z, 0; y) \\
& + 36H(1; z)G(1 - z, 0, 0; y) + 36H(1; z)G(1 - z, 1, 0; y) \\
& + 144H(1; z)G(-z, 1 - z, -z; y) - 300H(1; z)G(-z, 1 - z; y) \\
& - 72H(1; z)G(-z, 1 - z, 0; y) + 144H(1; z)G(-z, -z, 1 - z; y) \\
& - 432H(1; z)G(-z, -z, -z; y) + 408H(1; z)G(-z, -z; y) \\
& + 72H(1; z)G(-z, -z, 0; y) + 584H(1; z)G(-z; y) - 72H(1; z)G(-z, 0, 1 - z; y) \\
& + 72H(1; z)G(-z, 0, -z; y) - 216H(1; z)G(-z, 0; y) - 36H(1; z)G(0, 1 - z, -z; y) \\
& + 150H(1; z)G(0, 1 - z; y) + 36H(1; z)G(0, 1 - z, 0; y) \\
& - 72H(1; z)G(0, -z, 1 - z; y) + 72H(1; z)G(0, -z, -z; y) - 216H(1; z)G(0, -z; y) \\
& + 144H(1; z)G(0, -z, 0; y) - 295H(1; z)G(0; y) + 36H(1; z)G(0, 0, 1 - z; y) \\
& - 36H(1; z)G(0, 0, -z; y) + 108H(1; z)G(0, 0; y) - 36H(1; z)G(1, 1 - z, -z; y) \\
& - 36H(1; z)G(1, 0, -z; y) - 72H(1; z)G(1, 0, 0; y) + 15H(1, 0; z) \\
& + 108H(1, 0; z)G(1 - z, 1 - z; y) - 72H(1, 0; z)G(1 - z, -z; y) \\
& + 6H(1, 0; z)G(1 - z; y) - 72H(1, 0; z)G(1 - z, 0; y)
\end{aligned}$$

$$\begin{aligned}
& -72H(1, 0; z)G(-z, 1 - z; y) + 72H(1, 0; z)G(-z, -z; y) - 216H(1, 0; z)G(-z; y) \\
& + 108H(1, 0; z)G(0, 1 - z; y) - 144H(1, 0; z)G(0, -z; y) + 168H(1, 0; z)G(0; y) \\
& + 36H(1, 0; z)G(0, 0; y) - 36H(1, 0; z)G(1, 1 - z; y) + 72H(1, 0; z)G(1, 0; y) \\
& + 18H(1, 0, 0; z) - 36H(1, 0, 0; z)G(1 - z; y) - 72H(1, 0, 0, 1; z) \\
& + 222H(1, 0, 1; z) - 36H(1, 0, 1; z)G(1 - z; y) - 72H(1, 0, 1; z)G(-z; y) \\
& + 36H(1, 0, 1; z)G(0; y) + 36H(1, 0, 1; z)G(1; y) + 72H(1, 0, 1, 0; z) \\
& - 204H(1, 1; z) - 144H(1, 1; z)G(-z, -z; y) + 300H(1, 1; z)G(-z; y) \\
& + 72H(1, 1; z)G(-z, 0; y) + 72H(1, 1; z)G(0, -z; y) - 150H(1, 1; z)G(0; y) \\
& - 36H(1, 1; z)G(0, 0; y) + 54H(1, 1, 0; z) - 216H(1, 1, 0; z)G(1 - z; y) \\
& + 72H(1, 1, 0; z)G(-z; y) + 36H(1, 1, 0; z)G(0; y) + 36H(1, 1, 0; z)G(1; y) \\
& + 108H(1, 1, 1, 0; z) - 204G(1 - z, 1 - z; y) - 150G(1 - z, 1 - z, 0; y) \\
& - 36G(1 - z, 1 - z, 0, 0; y) - 108G(1 - z, 1 - z, 1, 0; y) \\
& + 372G(1 - z, -z, 1 - z; y) + 72G(1 - z, -z, 1 - z, 0; y) \\
& - 288G(1 - z, -z, -z, 1 - z; y) + 72G(1 - z, -z, 0, 1 - z; y) + 376G(1 - z; y) \\
& - 150G(1 - z, 0, 1 - z; y) - 36G(1 - z, 0, 1 - z, 0; y) + 72G(1 - z, 0, -z, 1 - z; y) \\
& + 295G(1 - z, 0; y) - 36G(1 - z, 0, 0, 1 - z; y) - 108G(1 - z, 0, 0; y) \\
& + 108G(1 - z, 0, 1, 0; y) - 36G(1 - z, 1, 1 - z, 0; y) - 36G(1 - z, 1, 0, 1 - z; y) \\
& + 144G(1 - z, 1, 0; y) + 72G(1 - z, 1, 0, 0; y) - 72G(1 - z, 1, 1, 0; y) \\
& + 300G(-z, 1 - z, 1 - z; y) + 72G(-z, 1 - z, 1 - z, 0; y) \\
& - 144G(-z, 1 - z, -z, 1 - z; y) - 584G(-z, 1 - z; y) + 72G(-z, 1 - z, 0, 1 - z; y) \\
& + 216G(-z, 1 - z, 0; y) - 144G(-z, -z, 1 - z, 1 - z; y) - 408G(-z, -z, 1 - z; y) \\
& - 72G(-z, -z, 1 - z, 0; y) + 432G(-z, -z, -z, 1 - z; y) - 72G(-z, -z, 0, 1 - z; y) \\
& + 72G(-z, 0, 1 - z, 1 - z; y) + 216G(-z, 0, 1 - z; y) - 72G(-z, 0, -z, 1 - z; y) \\
& - 150G(0, 1 - z, 1 - z; y) - 36G(0, 1 - z, 1 - z, 0; y) + 36G(0, 1 - z, -z, 1 - z; y) \\
& + 295G(0, 1 - z; y) - 36G(0, 1 - z, 0, 1 - z; y) - 108G(0, 1 - z, 0; y) \\
& + 72G(0, 1 - z, 1, 0; y) + 72G(0, -z, 1 - z, 1 - z; y) + 216G(0, -z, 1 - z; y) \\
& - 144G(0, -z, 1 - z, 0; y) - 72G(0, -z, -z, 1 - z; y) - 144G(0, -z, 0, 1 - z; y) \\
& - 188G(0; y) - 36G(0, 0, 1 - z, 1 - z; y) - 108G(0, 0, 1 - z; y) \\
& + 36G(0, 0, -z, 1 - z; y) + 36G(0, 0; y) + 108G(0, 0, 1, 0; y) + 6G(0, 1, 0; y) \\
& - 72G(0, 1, 1, 0; y) + 36G(1, 1 - z, -z, 1 - z; y) + 72G(1, 1 - z, 0, 0; y) \\
& + 72G(1, 1 - z, 1, 0; y) + 72G(1, 0, 1 - z, 0; y) + 36G(1, 0, -z, 1 - z; y) \\
& - 310G(1, 0; y) + 72G(1, 0, 0, 1 - z; y) + 90G(1, 0, 0; y) - 144G(1, 0, 1, 0; y) \\
& + 60G(1, 1, 0; y) - 108G(1, 1, 0, 0; y) + 36G(1, 1, 1, 0; y) \Big], \\
C_{20}(y, z) = & \\
& + \frac{z}{y^2} \Big[6H(0; z)G(1 - z; y) + 6H(1; z)G(-z; y) - 6G(-z, 1 - z; y) \Big] \\
& + \frac{z^2}{y^2} \Big[-2H(0; z)G(1 - z; y) - 2H(1; z)G(-z; y) + 2G(-z, 1 - z; y) \Big] \\
& + \frac{1}{y^2} \Big[-4H(0; z)G(1 - z; y) - 4H(1; z)G(-z; y) + 4G(-z, 1 - z; y) \Big]
\end{aligned}$$

$$\begin{aligned}
& + \frac{z\pi^2}{6y} \left[-1 + 4H(0; z) + 10H(0; z)G(1 - z; y) + H(1; z) + 6H(1; z)G(1 - z; y) \right. \\
& + 10H(1; z)G(-z; y) - 16G(1 - z, 1 - z; y) + G(1 - z; y) + 2G(1 - z, 0; y) \\
& \left. + 4G(1 - z, 1; y) - 10G(-z, 1 - z; y) \right] \\
& + \frac{z}{4y} \left[-36\zeta_3 - 16\zeta_3 G(1 - z; y) - 4H(0; z) + 6H(0; z)G(1 - z, 1 - z; y) \right. \\
& - 40H(0; z)G(1 - z, 1 - z, 0; y) + 9H(0; z)G(1 - z; y) \\
& - 8H(0; z)G(1 - z, 0, 1 - z; y) - 24H(0; z)G(1 - z, 0; y) \\
& - 16H(0; z)G(-z, 1 - z, 1 - z; y) + 46H(0; z)G(-z, 1 - z; y) \\
& - 40H(0; z)G(-z, 1 - z, 0; y) - 10H(0; z)G(0, 1 - z; y) + 12H(0; z)G(1, 0; y) \\
& + 16H(0, 0; z)G(1 - z, 1 - z; y) + 40H(0, 0; z)G(1 - z, 0; y) - 4H(0, 0, 1; z) \\
& + 17H(0, 1; z) + 24H(0, 1; z)G(1 - z, 1 - z; y) - 14H(0, 1; z)G(1 - z; y) \\
& - 8H(0, 1; z)G(1 - z, 0; y) - 8H(0, 1; z)G(-z, 1 - z; y) \\
& - 24H(0, 1; z)G(-z, -z; y) + 14H(0, 1; z)G(-z; y) - 8H(0, 1, 0; z) \\
& + 32H(0, 1, 0; z)G(1 - z; y) - 40H(0, 1, 0; z)G(-z; y) - 6H(0, 1, 1; z) \\
& + 8H(0, 1, 1; z)G(-z; y) + 24H(1; z)G(1 - z, 1 - z, -z; y) \\
& - 8H(1; z)G(1 - z, -z; y) - 16H(1; z)G(1 - z, 0, -z; y) - 6H(1; z)G(1 - z, 0; y) \\
& - 24H(1; z)G(-z, 1 - z, -z; y) + 12H(1; z)G(-z, 1 - z; y) \\
& + 8H(1; z)G(-z, 1 - z, 0; y) - 24H(1; z)G(-z, -z, 1 - z; y) \\
& - 24H(1; z)G(-z, -z, -z; y) + 60H(1; z)G(-z, -z; y) + 24H(1; z)G(-z, -z, 0; y) \\
& + 26H(1; z)G(-z; y) + 8H(1; z)G(-z, 0, 1 - z; y) + 18H(1; z)G(-z, 0; y) \\
& - 6H(1; z)G(0, 1 - z; y) - 10H(1; z)G(0, -z; y) - 17H(1; z)G(0; y) \\
& + 24H(1; z)G(1, 0; y) - 13H(1, 0; z) - 40H(1, 0; z)G(1 - z, 1 - z; y) \\
& + 4H(1, 0; z)G(1 - z; y) - 24H(1, 0; z)G(-z, 1 - z; y) - 46H(1, 0; z)G(-z; y) \\
& + 40H(1, 0; z)G(-z, 0; y) + 40H(1, 0, 0; z)G(1 - z; y) - 10H(1, 0, 1; z) \\
& - 16H(1, 0, 1; z)G(1 - z; y) + 8H(1, 0, 1; z)G(-z; y) + 24H(1, 1; z)G(-z, -z; y) \\
& - 12H(1, 1; z)G(-z; y) - 8H(1, 1; z)G(-z, 0; y) + 6H(1, 1; z)G(0; y) \\
& - 20H(1, 1, 0; z) + 8H(1, 1, 0; z)G(1 - z; y) + 24H(1, 1, 0; z)G(-z; y) \\
& - 24G(1 - z, 1 - z, -z, 1 - z; y) + 6G(1 - z, 1 - z, 0; y) \\
& + 48G(1 - z, 1 - z, 1, 0; y) + 8G(1 - z, -z, 1 - z; y) + 6G(1 - z, 0, 1 - z; y) \\
& + 16G(1 - z, 0, -z, 1 - z; y) + 17G(1 - z, 0; y) - 48G(1 - z, 0, 1, 0; y) \\
& + 18G(1 - z, 1, 0; y) - 16G(1 - z, 1, 1, 0; y) - 12G(-z, 1 - z, 1 - z; y) \\
& - 8G(-z, 1 - z, 1 - z, 0; y) + 24G(-z, 1 - z, -z, 1 - z; y) - 26G(-z, 1 - z; y) \\
& - 8G(-z, 1 - z, 0, 1 - z; y) - 18G(-z, 1 - z, 0; y) + 64G(-z, 1 - z, 1, 0; y) \\
& + 24G(-z, -z, 1 - z, 1 - z; y) - 60G(-z, -z, 1 - z; y) - 24G(-z, -z, 1 - z, 0; y) \\
& + 24G(-z, -z, -z, 1 - z; y) - 24G(-z, -z, 0, 1 - z; y) - 8G(-z, 0, 1 - z, 1 - z; y) \\
& - 18G(-z, 0, 1 - z; y) + 64G(-z, 0, 1, 0; y) + 6G(0, 1 - z, 1 - z; y) \\
& + 17G(0, 1 - z; y) + 10G(0, -z, 1 - z; y) + 18G(0, 1, 0; y) - 24G(1, 1 - z, 0; y) \\
& \left. - 24G(1, 0, 1 - z; y) - 30G(1, 0; y) \right]
\end{aligned}$$

$$\begin{aligned}
& + \frac{z^2}{y} \left[-2H(0; z)G(1 - z; y) - 2H(1; z)G(-z; y) + 2G(-z, 1 - z; y) \right] \\
& + \frac{1}{2y(y + z)} \left[-6H(0; z)G(1 - z, 1 - z; y) - 17H(0; z)G(1 - z; y) \right. \\
& + 18H(0; z)G(-z, 1 - z; y) - 18H(0; z)G(0, 1 - z; y) + 17H(0, 1; z) \\
& + 6H(0, 1; z)G(1 - z; y) - 18H(0, 1; z)G(-z; y) - 6H(0, 1, 1; z) \\
& - 6H(1; z)G(1 - z, 0; y) + 18H(1; z)G(-z, 0; y) - 6H(1; z)G(0, 1 - z; y) \\
& - 18H(1; z)G(0, -z; y) - 17H(1; z)G(0; y) - 17H(1, 0; z) \\
& + 24H(1, 0; z)G(1 - z; y) - 18H(1, 0; z)G(-z; y) - 6H(1, 0, 1; z) \\
& + 6H(1, 1; z)G(0; y) - 24H(1, 1, 0; z) + 6G(1 - z, 1 - z, 0; y) \\
& + 6G(1 - z, 0, 1 - z; y) + 17G(1 - z, 0; y) + 18G(1 - z, 1, 0; y) \\
& - 18G(-z, 1 - z, 0; y) - 18G(-z, 0, 1 - z; y) + 6G(0, 1 - z, 1 - z; y) \\
& \left. + 17G(0, 1 - z; y) + 18G(0, -z, 1 - z; y) + 18G(0, 1, 0; y) - 34G(1, 0; y) \right] \\
& + \frac{\pi^2}{3y} \left[-4H(0; z)G(1 - z; y) + H(1; z) - 6H(1; z)G(1 - z; y) - 4H(1; z)G(-z; y) \right. \\
& + 10G(1 - z, 1 - z; y) - 6G(1 - z; y) - 2G(1 - z, 0; y) - 4G(1 - z, 1; y) \\
& \left. + 4G(-z, 1 - z; y) + G(1; y) \right] \\
& + \frac{1}{4y} \left[-8\zeta_3 + 80\zeta_3 G(1 - z; y) + 19 + 8H(0; z) - 12H(0; z)G(1 - z, 1 - z; y) \right. \\
& + 32H(0; z)G(1 - z, 1 - z, 0; y) + 26H(0; z)G(1 - z; y) \\
& + 16H(0; z)G(1 - z, 0, 1 - z; y) + 40H(0; z)G(1 - z, 0; y) \\
& + 32H(0; z)G(-z, 1 - z, 1 - z; y) - 108H(0; z)G(-z, 1 - z; y) \\
& + 32H(0; z)G(-z, 1 - z, 0; y) + 68H(0; z)G(0, 1 - z; y) - 16H(0; z)G(1, 0; y) \\
& - 32H(0, 0; z)G(1 - z, 1 - z; y) - 32H(0, 0; z)G(1 - z, 0; y) - 8H(0, 0, 1; z) \\
& - 26H(0, 1; z) - 48H(0, 1; z)G(1 - z, 1 - z; y) + 36H(0, 1; z)G(1 - z; y) \\
& + 16H(0, 1; z)G(1 - z, 0; y) + 16H(0, 1; z)G(-z, 1 - z; y) \\
& + 48H(0, 1; z)G(-z, -z; y) - 28H(0, 1; z)G(-z; y) + 16H(0, 1, 0; z) \\
& - 16H(0, 1, 0; z)G(1 - z; y) + 32H(0, 1, 0; z)G(-z; y) + 12H(0, 1, 1; z) \\
& - 16H(0, 1, 1; z)G(-z; y) - 2H(1; z) - 48H(1; z)G(1 - z, 1 - z, -z; y) \\
& + 24H(1; z)G(1 - z, -z; y) + 32H(1; z)G(1 - z, 0, -z; y) \\
& + 12H(1; z)G(1 - z, 0; y) + 48H(1; z)G(-z, 1 - z, -z; y) \\
& - 24H(1; z)G(-z, 1 - z; y) - 16H(1; z)G(-z, 1 - z, 0; y) \\
& + 48H(1; z)G(-z, -z, 1 - z; y) + 48H(1; z)G(-z, -z, -z; y) \\
& - 136H(1; z)G(-z, -z; y) - 48H(1; z)G(-z, -z, 0; y) \\
& - 16H(1; z)G(-z, 0, 1 - z; y) - 20H(1; z)G(-z, 0; y) + 12H(1; z)G(0, 1 - z; y) \\
& + 68H(1; z)G(0, -z; y) + 30H(1; z)G(0; y) - 24H(1; z)G(1, 0; y) + 26H(1, 0; z) \\
& + 32H(1, 0; z)G(1 - z, 1 - z; y) - 56H(1, 0; z)G(1 - z; y) \\
& + 108H(1, 0; z)G(-z; y) - 32H(1, 0; z)G(-z, 0; y) - 32H(1, 0, 0; z)G(1 - z; y) \\
& + 4H(1, 0, 1; z) + 32H(1, 0, 1; z)G(1 - z; y) - 16H(1, 0, 1; z)G(-z; y) \\
& \left. - 48H(1, 1; z)G(-z, -z; y) + 24H(1, 1; z)G(-z; y) + 16H(1, 1; z)G(-z, 0; y) \right]
\end{aligned}$$

$$\begin{aligned}
& -12H(1, 1; z)G(0; y) + 56H(1, 1, 0; z) - 16H(1, 1, 0; z)G(1 - z; y) \\
& + 48G(1 - z, 1 - z, -z, 1 - z; y) - 12G(1 - z, 1 - z, 0; y) \\
& - 48G(1 - z, 1 - z, 1, 0; y) - 24G(1 - z, -z, 1 - z; y) + 2G(1 - z; y) \\
& - 12G(1 - z, 0, 1 - z; y) - 32G(1 - z, 0, -z, 1 - z; y) - 30G(1 - z, 0; y) \\
& + 48G(1 - z, 0, 1, 0; y) - 36G(1 - z, 1, 0; y) + 32G(1 - z, 1, 1, 0; y) \\
& + 24G(-z, 1 - z, 1 - z; y) + 16G(-z, 1 - z, 1 - z, 0; y) \\
& - 48G(-z, 1 - z, -z, 1 - z; y) + 16G(-z, 1 - z, 0, 1 - z; y) + 20G(-z, 1 - z, 0; y) \\
& - 80G(-z, 1 - z, 1, 0; y) - 48G(-z, -z, 1 - z, 1 - z; y) + 136G(-z, -z, 1 - z; y) \\
& + 48G(-z, -z, 1 - z, 0; y) - 48G(-z, -z, -z, 1 - z; y) + 48G(-z, -z, 0, 1 - z; y) \\
& + 16G(-z, 0, 1 - z, 1 - z; y) + 20G(-z, 0, 1 - z; y) - 80G(-z, 0, 1, 0; y) \\
& - 12G(0, 1 - z, 1 - z; y) - 30G(0, 1 - z; y) - 68G(0, -z, 1 - z; y) - 36G(0, 1, 0; y) \\
& + 24G(1, 1 - z, 0; y) + 24G(1, 0, 1 - z; y) + 60G(1, 0; y) - 8G(1, 1, 0; y) \Big] \\
& + \frac{z}{4(1-y)^2} \Big[+ 5\pi^2 + \frac{14\pi^2}{3}H(0; z) + \frac{14\pi^2}{3}H(1; z) - \frac{14\pi^2}{3}G(1 - z; y) + \frac{2\pi^2}{3}G(0; y) \\
& - \frac{4\pi^2}{3}G(1; y) - 92\zeta_3 + 28H(0; z)G(0, 1 - z; y) + 12H(0; z)G(0; y) \\
& + 4H(0; z)G(0, 0; y) - 32H(0, 0, 1; z) - 16H(0, 1; z) + 32H(0, 1; z)G(1 - z; y) \\
& + 4H(0, 1; z)G(0; y) + 28H(0, 1, 0; z) + 32H(1; z)G(1 - z, -z; y) \\
& - 16H(1; z)G(-z; y) + 32H(1; z)G(0, -z; y) + 6H(1; z)G(0; y) \\
& - 4H(1; z)G(0, 0; y) + 16H(1, 0; z) - 28H(1, 0; z)G(1 - z; y) - 32H(1, 0, 1; z) \\
& + 28H(1, 1, 0; z) - 32G(1 - z, -z, 1 - z; y) - 6G(1 - z, 0; y) + 4G(1 - z, 0, 0; y) \\
& - 4G(1 - z, 1, 0; y) + 16G(-z, 1 - z; y) - 6G(0, 1 - z; y) + 4G(0, 1 - z, 0; y) \\
& - 32G(0, -z, 1 - z; y) + 23G(0; y) + 4G(0, 0, 1 - z; y) - 10G(0, 0; y) \\
& - 8G(0, 1, 0; y) - 14G(1, 0; y) - 8G(1, 0, 0; y) + 8G(1, 1, 0; y) \Big] \\
& + \frac{z}{4(1-y)} \Big[\frac{11\pi^2}{3} + 6\pi^2H(0; z) + 6\pi^2H(1; z) - 6\pi^2G(1 - z; y) \\
& + 2\pi^2G(0; y) - 4\pi^2G(1; y) - 132\zeta_3 + 17 + 4H(0; z) + 28H(0; z)G(1 - z; y) \\
& + 36H(0; z)G(0, 1 - z; y) + 12H(0; z)G(0, 0; y) - 48H(0, 0, 1; z) + 4H(0, 1; z) \\
& + 48H(0, 1; z)G(1 - z; y) + 12H(0, 1; z)G(0; y) + 36H(0, 1, 0; z) - 2H(1; z) \\
& + 48H(1; z)G(1 - z, -z; y) + 32H(1; z)G(-z; y) + 48H(1; z)G(0, -z; y) \\
& - 22H(1; z)G(0; y) - 12H(1; z)G(0, 0; y) - 36H(1, 0; z)G(1 - z; y) \\
& - 48H(1, 0, 1; z) + 36H(1, 1, 0; z) - 48G(1 - z, -z, 1 - z; y) + 2G(1 - z; y) \\
& + 22G(1 - z, 0; y) + 12G(1 - z, 0, 0; y) - 12G(1 - z, 1, 0; y) - 32G(-z, 1 - z; y) \\
& + 22G(0, 1 - z; y) + 12G(0, 1 - z, 0; y) - 48G(0, -z, 1 - z; y) + 39G(0; y) \\
& + 12G(0, 0, 1 - z; y) - 22G(0, 0; y) - 24G(0, 1, 0; y) - 26G(1, 0; y) \\
& - 24G(1, 0, 0; y) + 24G(1, 1, 0; y) \Big] \\
& + \frac{z}{(y+z)^3} \Big[- 6\pi^2H(1; z) + 6\pi^2G(1 - z; y) + 36H(0; z)G(1 - z, 0; y) \\
& + 36H(0, 1, 0; z) + 36H(1, 0; z) + 36H(1, 0; z)G(1 - z; y) - 36H(1, 0; z)G(0; y)
\end{aligned}$$

$$\begin{aligned}
& -36H(1, 1, 0; z) - 36G(1 - z, 1, 0; y) - 36G(0, 1, 0; y) + 36G(1, 0; y) \Big] \\
& + \frac{z}{(y+z)^2} \Big[+ 6\pi^2 + 4\pi^2 H(1; z) - 4\pi^2 G(1 - z; y) - 18H(0; z) \\
& - 24H(0; z)G(1 - z, 0; y) + 36H(0; z)G(0; y) - 24H(0, 1, 0; z) + 12H(1, 0; z) \\
& - 24H(1, 0; z)G(1 - z; y) + 24H(1, 0; z)G(0; y) + 24H(1, 1, 0; z) \\
& + 24G(1 - z, 1, 0; y) + 18G(0; y) + 24G(0, 1, 0; y) - 60G(1, 0; y) \Big] \\
& + \frac{z}{y+z} \Big[- \pi^2 + 6H(0; z) - 6H(0; z)G(0; y) - 6H(1, 0; z) - 6G(0; y) + 6G(1, 0; y) \Big] \\
& + \frac{z^2}{(1-y)^3} \Big[- \frac{2\pi^2}{3} H(0; z) - \frac{2\pi^2}{3} H(1; z) + \frac{2\pi^2}{3} G(1 - z; y) \\
& + 12\zeta_3 - 4H(0; z)G(0, 1 - z; y) + 4H(0, 0, 1; z) - 4H(0, 1; z)G(1 - z; y) \\
& - 4H(0, 1, 0; z) - 4H(1; z)G(1 - z, -z; y) - 4H(1; z)G(0, -z; y) \\
& + 4H(1, 0; z)G(1 - z; y) + 4H(1, 0, 1; z) - 4H(1, 1, 0; z) + 4G(1 - z, -z, 1 - z; y) \\
& + 4G(0, -z, 1 - z; y) \Big] \\
& + \frac{z^2}{(1-y)^2} \Big[- 4H(0; z)G(1 - z; y) - 4H(1; z)G(-z; y) + 4G(-z, 1 - z; y) \Big] \\
& + \frac{z^2}{1-y} \Big[- 2H(0; z)G(1 - z; y) - 2H(1; z)G(-z; y) + 2G(-z, 1 - z; y) \Big] \\
& + \frac{z^2}{(y+z)^4} \Big[+ 6\pi^2 H(1; z) - 6\pi^2 G(1 - z; y) - 36H(0; z)G(1 - z, 0; y) \\
& - 36H(0, 1, 0; z) - 36H(1, 0; z)G(1 - z; y) + 36H(1, 0; z)G(0; y) + 36H(1, 1, 0; z) \\
& + 36G(1 - z, 1, 0; y) + 36G(0, 1, 0; y) \Big] \\
& + \frac{z^2}{(y+z)^3} \Big[- 6\pi^2 - 4\pi^2 H(1; z) + 4\pi^2 G(1 - z; y) + 24H(0; z)G(1 - z, 0; y) \\
& - 36H(0; z)G(0; y) + 24H(0, 1, 0; z) - 36H(1, 0; z) + 24H(1, 0; z)G(1 - z; y) \\
& - 24H(1, 0; z)G(0; y) - 24H(1, 1, 0; z) - 24G(1 - z, 1, 0; y) - 24G(0, 1, 0; y) \\
& + 36G(1, 0; y) \Big] \\
& + \frac{z^2}{(y+z)^2} \Big[\pi^2 + 6H(0; z)G(0; y) + 6H(1, 0; z) - 6G(1, 0; y) \Big] \\
& + \frac{1}{1-y-z} \Big[- \frac{\pi^2}{3} - 2H(0; z)G(0; y) - 2H(1, 0; z) + 2G(1, 0; y) \Big] \\
& + \frac{1}{2(1-y)} \Big[- 2\pi^2 - \frac{8\pi^2}{3} H(0; z) - \frac{4\pi^2}{3} H(1; z) + \frac{4\pi^2}{3} G(1 - z; y) + \frac{2\pi^2}{3} G(0; y) \\
& + \frac{8\pi^2}{3} G(1; y) + 64\zeta_3 - 8H(0; z)G(1 - z, 0; y) - 16H(0; z)G(0, 1 - z; y) \\
& + 6H(0; z)G(0; y) + 4H(0; z)G(0, 0; y) + 8H(0; z)G(1, 0; y) + 20H(0, 0, 1; z) \\
& + 12H(0, 1; z) - 20H(0, 1; z)G(1 - z; y) - 4H(0, 1; z)G(0; y) - 8H(0, 1, 0; z) \\
& - 20H(1; z)G(1 - z, -z; y) + 12H(1; z)G(-z; y) - 20H(1; z)G(0, -z; y) \\
& - 2H(1; z)G(0; y) + 4H(1; z)G(0, 0; y) - 10H(1, 0; z) + 8H(1, 0; z)G(1 - z; y) \\
& + 8H(1, 0; z)G(0; y) + 20H(1, 0, 1; z) - 8H(1, 1, 0; z) + 20G(1 - z, -z, 1 - z; y) \\
& + 2G(1 - z, 0; y) - 4G(1 - z, 0, 0; y) + 12G(1 - z, 1, 0; y) - 12G(-z, 1 - z; y)
\end{aligned}$$

$$\begin{aligned}
& +2G(0, 1-z; y) - 4G(0, 1-z, 0; y) + 20G(0, -z, 1-z; y) - 5G(0; y) \\
& - 4G(0, 0, 1-z; y) - 4G(0, 0; y) - 16G(1, 1, 0; y) \Big] \\
& + \frac{1}{2(y+z)^2} \Big[\frac{22\pi^2}{3} H(1; z) - \frac{22\pi^2}{3} G(1-z; y) \\
& - 2H(0; z)G(1-z, 1-z; y) + 3H(0; z)G(1-z; y) - 44H(0; z)G(1-z, 0; y) \\
& - 2H(0; z)G(-z, 1-z; y) + 2H(0; z)G(0, 1-z; y) + 3H(0, 1; z) \\
& - 2H(0, 1; z)G(1-z; y) - 2H(0, 1; z)G(-z; y) - 44H(0, 1, 0; z) + 2H(0, 1, 1; z) \\
& + 27H(1; z) - 4H(1; z)G(1-z, -z; y) + 6H(1; z)G(1-z; y) \\
& + 2H(1; z)G(1-z, 0; y) - 4H(1; z)G(-z, 1-z; y) - 4H(1; z)G(-z, -z; y) \\
& + 6H(1; z)G(-z; y) + 2H(1; z)G(-z, 0; y) + 2H(1; z)G(0, 1-z; y) \\
& + 2H(1; z)G(0, -z; y) - 3H(1; z)G(0; y) - 3H(1, 0; z) - 44H(1, 0; z)G(1-z; y) \\
& + 2H(1, 0; z)G(-z; y) + 44H(1, 0; z)G(0; y) + 2H(1, 0, 1; z) - 6H(1, 1; z) \\
& + 4H(1, 1; z)G(-z; y) - 2H(1, 1; z)G(0; y) + 44H(1, 1, 0; z) - 6G(1-z, 1-z; y) \\
& - 2G(1-z, 1-z, 0; y) + 4G(1-z, -z, 1-z; y) - 27G(1-z; y) \\
& - 2G(1-z, 0, 1-z; y) + 3G(1-z, 0; y) + 46G(1-z, 1, 0; y) \\
& + 4G(-z, 1-z, 1-z; y) - 6G(-z, 1-z; y) - 2G(-z, 1-z, 0; y) \\
& + 4G(-z, -z, 1-z; y) - 2G(-z, 0, 1-z; y) - 2G(0, 1-z, 1-z; y) \\
& + 3G(0, 1-z; y) - 2G(0, -z, 1-z; y) + 46G(0, 1, 0; y) \Big] \\
& + \frac{1}{2(y+z)} \Big[-\frac{22\pi^2}{3} - 2\pi^2 H(1; z) + 2\pi^2 G(1-z; y) - 17 - 5H(0; z) \\
& - 4H(0; z)G(1-z; y) + 12H(0; z)G(1-z, 0; y) - 44H(0; z)G(0; y) - 4H(0, 1; z) \\
& + 12H(0, 1, 0; z) + 4H(1; z) - 4H(1; z)G(1-z; y) - 8H(1; z)G(-z; y) \\
& + 4H(1; z)G(0; y) - 42H(1, 0; z) + 12H(1, 0; z)G(1-z; y) - 12H(1, 0; z)G(0; y) \\
& + 4H(1, 1; z) - 12H(1, 1, 0; z) + 4G(1-z, 1-z; y) - 4G(1-z; y) - 4G(1-z, 0; y) \\
& - 12G(1-z, 1, 0; y) + 8G(-z, 1-z; y) - 4G(0, 1-z; y) - 5G(0; y) \\
& - 12G(0, 1, 0; y) + 46G(1, 0; y) \Big] \\
& + \frac{T\pi^2}{24} \Big[+29 + 6H(1; z) + 8H(1; z)G(1-z; y) - 16G(1-z, 1-z; y) + 12G(1-z; y) \\
& + 8G(1-z, 1; y) + 8G(0, 1-z; y) - 8G(0, 1; y) - 18G(1; y) + 8G(1, 1; y) \Big] \\
& + \frac{T}{8} \Big[-\frac{22\pi^4}{45} + \frac{255}{4} - 60\zeta_3 - 16\zeta_3 H(1; z) - 16\zeta_3 G(1-z; y) + 32\zeta_3 G(1; y) \\
& + 18H(0; z)G(1-z, 1-z; y) + 15H(0; z)G(1-z; y) \\
& - 8H(0; z)G(1-z, 0, 1-z; y) - 16H(0; z)G(-z, 1-z, 1-z; y) \\
& + 42H(0; z)G(-z, 1-z; y) - 16H(0; z)G(-z, -z, 1-z; y) \\
& + 16H(0; z)G(-z, 0, 1-z; y) - 42H(0; z)G(0, 1-z; y) \\
& + 16H(0; z)G(0, -z, 1-z; y) - 16H(0; z)G(0, 0, 1-z; y) \\
& + 16H(0, 0; z)G(1-z, 1-z; y) - 16H(0, 0, 1; z)G(1-z; y) \\
& + 8H(0, 0, 1; z)G(1; y) + 16H(0, 0, 1, 1; z) + 15H(0, 1; z) \\
& + 32H(0, 1; z)G(1-z, 1-z; y) + 6H(0, 1; z)G(1-z; y)
\end{aligned}$$

$$\begin{aligned}
& +8H(0, 1; z)G(1 - z, 0; y) - 16H(0, 1; z)G(-z, 1 - z; y) \\
& - 16H(0, 1; z)G(-z, -z; y) + 42H(0, 1; z)G(-z; y) + 8H(0, 1; z)G(0, 1 - z; y) \\
& - 8H(0, 1; z)G(1, 1 - z; y) - 8H(0, 1; z)G(1, 0; y) - 8H(0, 1, 0; z)G(1 - z; y) \\
& + 16H(0, 1, 0, 1; z) - 18H(0, 1, 1; z) + 16H(0, 1, 1; z)G(-z; y) \\
& - 16H(0, 1, 1; z)G(0; y) + 16H(0, 1, 1, 0; z) - 52H(1; z) \\
& + 32H(1; z)G(1 - z, 1 - z, -z; y) + 24H(1; z)G(1 - z, -z; y) \\
& - 18H(1; z)G(1 - z; y) - 18H(1; z)G(1 - z, 0; y) - 16H(1; z)G(1 - z, 0, 0; y) \\
& - 8H(1; z)G(1 - z, 1, 0; y) - 32H(1; z)G(-z, 1 - z, -z; y) \\
& + 36H(1; z)G(-z, 1 - z; y) + 16H(1; z)G(-z, 1 - z, 0; y) \\
& - 32H(1; z)G(-z, -z, 1 - z; y) - 32H(1; z)G(-z, -z, -z; y) \\
& + 84H(1; z)G(-z, -z; y) + 16H(1; z)G(-z, -z, 0; y) + 30H(1; z)G(-z; y) \\
& + 16H(1; z)G(-z, 0, 1 - z; y) + 16H(1; z)G(-z, 0, -z; y) - 42H(1; z)G(-z, 0; y) \\
& + 8H(1; z)G(0, 1 - z, -z; y) - 18H(1; z)G(0, 1 - z; y) \\
& - 16H(1; z)G(0, 1 - z, 0; y) + 16H(1; z)G(0, -z, 1 - z; y) \\
& + 16H(1; z)G(0, -z, -z; y) - 42H(1; z)G(0, -z; y) - 15H(1; z)G(0; y) \\
& - 16H(1; z)G(0, 0, 1 - z; y) - 16H(1; z)G(0, 0, -z; y) + 8H(1; z)G(0, 1, 0; y) \\
& - 8H(1; z)G(1, 1 - z, -z; y) - 8H(1; z)G(1, 0, -z; y) + 16H(1; z)G(1, 0, 0; y) \\
& + 13H(1, 0; z) + 24H(1, 0; z)G(1 - z; y) + 16H(1, 0; z)G(-z, -z; y) \\
& - 42H(1, 0; z)G(-z; y) + 16H(1, 0; z)G(0, 1 - z; y) - 16H(1, 0; z)G(0, -z; y) \\
& + 8H(1, 0, 0, 1; z) - 6H(1, 0, 1; z) - 24H(1, 0, 1; z)G(1 - z; y) \\
& + 16H(1, 0, 1; z)G(-z; y) - 8H(1, 0, 1; z)G(0; y) + 8H(1, 0, 1; z)G(1; y) \\
& + 18H(1, 1; z) + 32H(1, 1; z)G(-z, -z; y) - 36H(1, 1; z)G(-z; y) \\
& - 16H(1, 1; z)G(-z, 0; y) - 16H(1, 1; z)G(0, -z; y) + 18H(1, 1; z)G(0; y) \\
& + 16H(1, 1; z)G(0, 0; y) + 12H(1, 1, 0; z) - 8H(1, 1, 0; z)G(1 - z; y) \\
& + 16H(1, 1, 0, 1; z) + 16H(1, 1, 1, 0; z) - 32G(1 - z, 1 - z, -z, 1 - z; y) \\
& + 18G(1 - z, 1 - z; y) + 18G(1 - z, 1 - z, 0; y) + 16G(1 - z, 1 - z, 0, 0; y) \\
& - 24G(1 - z, -z, 1 - z; y) + 52G(1 - z; y) + 18G(1 - z, 0, 1 - z; y) \\
& + 16G(1 - z, 0, 1 - z, 0; y) + 15G(1 - z, 0; y) + 16G(1 - z, 0, 0, 1 - z; y) \\
& - 8G(1 - z, 0, 1, 0; y) + 8G(1 - z, 1, 1 - z, 0; y) + 8G(1 - z, 1, 0, 1 - z; y) \\
& - 42G(1 - z, 1, 0; y) - 16G(1 - z, 1, 0, 0; y) - 16G(1 - z, 1, 1, 0; y) \\
& - 36G(-z, 1 - z, 1 - z; y) - 16G(-z, 1 - z, 1 - z, 0; y) \\
& + 32G(-z, 1 - z, -z, 1 - z; y) - 30G(-z, 1 - z; y) - 16G(-z, 1 - z, 0, 1 - z; y) \\
& + 42G(-z, 1 - z, 0; y) + 16G(-z, 1 - z, 1, 0; y) + 32G(-z, -z, 1 - z, 1 - z; y) \\
& - 84G(-z, -z, 1 - z; y) - 16G(-z, -z, 1 - z, 0; y) + 32G(-z, -z, -z, 1 - z; y) \\
& - 16G(-z, -z, 0, 1 - z; y) - 16G(-z, 0, 1 - z, 1 - z; y) + 42G(-z, 0, 1 - z; y) \\
& - 16G(-z, 0, -z, 1 - z; y) + 16G(-z, 0, 1, 0; y) + 18G(0, 1 - z, 1 - z; y) \\
& + 16G(0, 1 - z, 1 - z, 0; y) - 8G(0, 1 - z, -z, 1 - z; y) + 15G(0, 1 - z; y) \\
& + 16G(0, 1 - z, 0, 1 - z; y) - 8G(0, 1 - z, 1, 0; y) - 16G(0, -z, 1 - z, 1 - z; y) \\
& + 42G(0, -z, 1 - z; y) - 16G(0, -z, -z, 1 - z; y) + 16G(0, 0, 1 - z, 1 - z; y) \\
& + 16G(0, 0, -z, 1 - z; y) - 8G(0, 1, 1 - z, 0; y) - 8G(0, 1, 0, 1 - z; y)
\end{aligned}$$

$$\begin{aligned}
& -42G(0, 1, 0; y) + 16G(0, 1, 1, 0; y) + 8G(1, 1 - z, -z, 1 - z; y) \\
& -16G(1, 1 - z, 0, 0; y) + 8G(1, 1 - z, 1, 0; y) - 16G(1, 0, 1 - z, 0; y) \\
& + 8G(1, 0, -z, 1 - z; y) - 28G(1, 0; y) - 16G(1, 0, 0, 1 - z; y) + 8G(1, 0, 1, 0; y) \\
& + 36G(1, 1, 0; y) + 16G(1, 1, 0, 0; y) - 16G(1, 1, 1, 0; y) \Big] \\
& + \frac{\pi^2}{6} \Big[9 - 7H(0; z) + 6H(0; z)G(1 - z; y) - 2H(0; z)G(1; y) + 4H(0, 1; z) - 24H(1; z) \\
& + 12H(1; z)G(1 - z; y) + 8H(1; z)G(-z; y) - 4H(1; z)G(0; y) - 6H(1; z)G(1; y) \\
& - 2H(1, 0; z) - 6H(1, 1; z) - 20G(1 - z, 1 - z; y) + 34G(1 - z; y) + 6G(1 - z, 0; y) \\
& + 8G(1 - z, 1; y) - 8G(-z, 1 - z; y) + 8G(0, 1 - z; y) - 7G(0; y) - 4G(0, 1; y) \\
& + 6G(1, 1 - z; y) - 10G(1; y) - 4G(1, 0; y) \Big] \\
& + \frac{1}{4} \Big[40\zeta_3 + 40\zeta_3 H(1; z) - 80\zeta_3 G(1 - z; y) + 40\zeta_3 G(1; y) - 2 - 29H(0; z) \\
& + 20H(0; z)G(1 - z, 1 - z; y) - 32H(0; z)G(1 - z, 1 - z, 0; y) \\
& - 4H(0; z)G(1 - z; y) + 32H(0; z)G(1 - z, 0; y) + 16H(0; z)G(1 - z, 0, 0; y) \\
& + 16H(0; z)G(1 - z, 1, 0; y) - 24H(0; z)G(-z, 1 - z, 1 - z; y) \\
& + 52H(0; z)G(-z, 1 - z; y) - 32H(0; z)G(-z, 1 - z, 0; y) \\
& - 24H(0; z)G(-z, -z, 1 - z; y) + 24H(0; z)G(-z, 0, 1 - z; y) \\
& + 8H(0; z)G(0, 1 - z, 1 - z; y) - 44H(0; z)G(0, 1 - z; y) \\
& + 16H(0; z)G(0, 1 - z, 0; y) + 24H(0; z)G(0, -z, 1 - z; y) + 40H(0; z)G(0; y) \\
& - 24H(0; z)G(0, 0, 1 - z; y) - 20H(0; z)G(0, 0; y) + 16H(0; z)G(1, 1 - z, 0; y) \\
& - 8H(0; z)G(1, 0, 1 - z; y) + 4H(0; z)G(1, 0; y) - 16H(0; z)G(1, 0, 0; y) \\
& - 16H(0; z)G(1, 1, 0; y) + 20H(0, 0; z) + 16H(0, 0; z)G(1 - z, 1 - z; y) \\
& - 4H(0, 0; z)G(1 - z; y) + 16H(0, 0; z)G(1 - z, 0; y) - 20H(0, 0; z)G(0; y) \\
& + 36H(0, 0, 1; z) - 16H(0, 0, 1; z)G(1 - z; y) + 16H(0, 0, 1; z)G(1; y) \\
& - 16H(0, 0, 1, 0; z) + 16H(0, 0, 1, 1; z) + 48H(0, 1; z)G(1 - z, 1 - z; y) \\
& - 52H(0, 1; z)G(1 - z; y) - 24H(0, 1; z)G(-z, 1 - z; y) \\
& - 24H(0, 1; z)G(-z, -z; y) + 84H(0, 1; z)G(-z; y) + 8H(0, 1; z)G(0, 1 - z; y) \\
& - 8H(0, 1; z)G(0; y) - 16H(0, 1; z)G(1, 1 - z; y) - 8H(0, 1; z)G(1, 0; y) \\
& - 28H(0, 1, 0; z) + 32H(0, 1, 0; z)G(1 - z; y) - 32H(0, 1, 0; z)G(-z; y) \\
& + 16H(0, 1, 0; z)G(0; y) - 24H(0, 1, 0; z)G(1; y) + 16H(0, 1, 0, 1; z) \\
& - 20H(0, 1, 1; z) + 24H(0, 1, 1; z)G(-z; y) - 16H(0, 1, 1; z)G(0; y) \\
& + 32H(0, 1, 1, 0; z) - 58H(1; z) + 48H(1; z)G(1 - z, 1 - z, -z; y) \\
& - 32H(1; z)G(1 - z, -z; y) - 4H(1; z)G(1 - z; y) - 20H(1; z)G(1 - z, 0; y) \\
& - 16H(1; z)G(1 - z, 0, 0; y) - 8H(1; z)G(1 - z, 1, 0; y) \\
& - 48H(1; z)G(-z, 1 - z, -z; y) + 40H(1; z)G(-z, 1 - z; y) \\
& + 24H(1; z)G(-z, 1 - z, 0; y) - 48H(1; z)G(-z, -z, 1 - z; y) \\
& - 48H(1; z)G(-z, -z, -z; y) + 136H(1; z)G(-z, -z; y) + 24H(1; z)G(-z, -z, 0; y) \\
& - 4H(1; z)G(-z; y) + 24H(1; z)G(-z, 0, 1 - z; y) + 24H(1; z)G(-z, 0, -z; y) \\
& - 52H(1; z)G(-z, 0; y) + 16H(1; z)G(0, 1 - z, -z; y) - 20H(1; z)G(0, 1 - z; y) \\
& - 16H(1; z)G(0, 1 - z, 0; y) + 24H(1; z)G(0, -z, 1 - z; y)
\end{aligned}$$

$$\begin{aligned}
& +24H(1; z)G(0, -z, -z; y) - 52H(1; z)G(0, -z; y) + 4H(1; z)G(0; y) \\
& -16H(1; z)G(0, 0, 1 - z; y) - 24H(1; z)G(0, 0, -z; y) + 4H(1; z)G(0, 0; y) \\
& +8H(1; z)G(0, 1, 0; y) - 16H(1; z)G(1, 1 - z, -z; y) - 16H(1; z)G(1, 0, -z; y) \\
& +24H(1; z)G(1, 0; y) + 16H(1; z)G(1, 0, 0; y) + 60H(1, 0; z) \\
& -40H(1, 0; z)G(1 - z, 1 - z; y) + 80H(1, 0; z)G(1 - z; y) \\
& +16H(1, 0; z)G(1 - z, 0; y) - 32H(1, 0; z)G(-z, 1 - z; y) \\
& +24H(1, 0; z)G(-z, -z; y) - 52H(1, 0; z)G(-z; y) + 32H(1, 0; z)G(-z, 0; y) \\
& +32H(1, 0; z)G(0, 1 - z; y) - 24H(1, 0; z)G(0, -z; y) - 36H(1, 0; z)G(0; y) \\
& -16H(1, 0; z)G(0, 0; y) + 24H(1, 0; z)G(1, 1 - z; y) - 16H(1, 0; z)G(1, 0; y) \\
& -20H(1, 0, 0; z) + 16H(1, 0, 0; z)G(1 - z; y) + 16H(1, 0, 0, 1; z) + 28H(1, 0, 1; z) \\
& -40H(1, 0, 1; z)G(1 - z; y) + 24H(1, 0, 1; z)G(-z; y) - 8H(1, 0, 1; z)G(0; y) \\
& +16H(1, 0, 1; z)G(1; y) - 24H(1, 0, 1, 0; z) + 4H(1, 1; z) \\
& +48H(1, 1; z)G(-z, -z; y) - 40H(1, 1; z)G(-z; y) - 24H(1, 1; z)G(-z, 0; y) \\
& -24H(1, 1; z)G(0, -z; y) + 20H(1, 1; z)G(0; y) + 16H(1, 1; z)G(0, 0; y) \\
& -64H(1, 1, 0; z) + 16H(1, 1, 0; z)G(1 - z; y) + 32H(1, 1, 0; z)G(-z; y) \\
& -16H(1, 1, 0; z)G(0; y) - 24H(1, 1, 0; z)G(1; y) + 24H(1, 1, 0, 1; z) \\
& -8H(1, 1, 1, 0; z) - 48G(1 - z, 1 - z, -z, 1 - z; y) + 4G(1 - z, 1 - z; y) \\
& +20G(1 - z, 1 - z, 0; y) + 16G(1 - z, 1 - z, 0, 0; y) + 40G(1 - z, 1 - z, 1, 0; y) \\
& +32G(1 - z, -z, 1 - z; y) + 58G(1 - z; y) + 20G(1 - z, 0, 1 - z; y) \\
& +16G(1 - z, 0, 1 - z, 0; y) - 4G(1 - z, 0; y) + 16G(1 - z, 0, 0, 1 - z; y) \\
& -4G(1 - z, 0, 0; y) - 48G(1 - z, 0, 1, 0; y) + 8G(1 - z, 1, 1 - z, 0; y) \\
& +8G(1 - z, 1, 0, 1 - z; y) - 100G(1 - z, 1, 0; y) - 32G(1 - z, 1, 0, 0; y) \\
& -32G(1 - z, 1, 1, 0; y) - 40G(-z, 1 - z, 1 - z; y) - 24G(-z, 1 - z, 1 - z, 0; y) \\
& +48G(-z, 1 - z, -z, 1 - z; y) + 4G(-z, 1 - z; y) - 24G(-z, 1 - z, 0, 1 - z; y) \\
& +52G(-z, 1 - z, 0; y) + 56G(-z, 1 - z, 1, 0; y) + 48G(-z, -z, 1 - z, 1 - z; y) \\
& -136G(-z, -z, 1 - z; y) - 24G(-z, -z, 1 - z, 0; y) + 48G(-z, -z, -z, 1 - z; y) \\
& -24G(-z, -z, 0, 1 - z; y) - 24G(-z, 0, 1 - z, 1 - z; y) + 52G(-z, 0, 1 - z; y) \\
& -24G(-z, 0, -z, 1 - z; y) + 56G(-z, 0, 1, 0; y) + 20G(0, 1 - z, 1 - z; y) \\
& +16G(0, 1 - z, 1 - z, 0; y) - 16G(0, 1 - z, -z, 1 - z; y) - 4G(0, 1 - z; y) \\
& +16G(0, 1 - z, 0, 1 - z; y) - 4G(0, 1 - z, 0; y) - 24G(0, 1 - z, 1, 0; y) \\
& -24G(0, -z, 1 - z, 1 - z; y) + 52G(0, -z, 1 - z; y) - 24G(0, -z, -z, 1 - z; y) \\
& -29G(0; y) + 16G(0, 0, 1 - z, 1 - z; y) - 4G(0, 0, 1 - z; y) \\
& +24G(0, 0, -z, 1 - z; y) + 20G(0, 0; y) - 16G(0, 0, 1, 0; y) - 8G(0, 1, 1 - z, 0; y) \\
& -8G(0, 1, 0, 1 - z; y) - 20G(0, 1, 0; y) + 16G(0, 1, 1, 0; y) \\
& +16G(1, 1 - z, -z, 1 - z; y) - 24G(1, 1 - z, 0; y) - 16G(1, 1 - z, 0, 0; y) \\
& -8G(1, 1 - z, 1, 0; y) - 24G(1, 0, 1 - z; y) - 16G(1, 0, 1 - z, 0; y) \\
& +16G(1, 0, -z, 1 - z; y) - 56G(1, 0; y) - 16G(1, 0, 0, 1 - z; y) + 24G(1, 0, 0; y) \\
& +24G(1, 0, 1, 0; y) + 40G(1, 1, 0; y) + 32G(1, 1, 0, 0; y) \Big],
\end{aligned}$$

$$\begin{aligned}
 D_{20}(y, z) = & \frac{z}{3y} \left[-2H(0; z) - 3H(1, 0; z) - 3G(1, 0; y) \right] \\
 & + \frac{1}{y(y+z)} \left[-2H(1, 0; z) - 2G(1, 0; y) \right] \\
 & + \frac{1}{18y} \left[-74 + 15H(0; z) + 36H(1, 0; z) + 15G(0; y) + 36G(1, 0; y) \right] \\
 & + \frac{z}{18(1-y)^2} \left[2\pi^2 - 3H(0; z)G(0; y) + 50G(0; y) - 18G(0, 0; y) - 12G(1, 0; y) \right] \\
 & + \frac{z}{18(1-y)} \left[6\pi^2 + 38 - 3H(0; z) - 9H(0; z)G(0; y) + 87G(0; y) - 54G(0, 0; y) \right. \\
 & \quad \left. - 36G(1, 0; y) \right] \\
 & + \frac{z}{(y+z)^3} \left[-2\pi^2 H(1; z) + 2\pi^2 G(1-z; y) + 12H(0; z)G(1-z, 0; y) \right. \\
 & \quad + 12H(0, 1, 0; z) + 12H(1, 0; z) + 12H(1, 0; z)G(1-z; y) - 12H(1, 0; z)G(0; y) \\
 & \quad \left. - 12H(1, 1, 0; z) - 12G(1-z, 1, 0; y) - 12G(0, 1, 0; y) + 12G(1, 0; y) \right] \\
 & + \frac{z}{(y+z)^2} \left[2\pi^2 + \frac{4\pi^2}{3}H(1; z) - \frac{4\pi^2}{3}G(1-z; y) - 6H(0; z) - 8H(0; z)G(1-z, 0; y) \right. \\
 & \quad + 12H(0; z)G(0; y) - 8H(0, 1, 0; z) + 4H(1, 0; z) - 8H(1, 0; z)G(1-z; y) \\
 & \quad + 8H(1, 0; z)G(0; y) + 8H(1, 1, 0; z) + 8G(1-z, 1, 0; y) + 6G(0; y) + 8G(0, 1, 0; y) \\
 & \quad \left. - 20G(1, 0; y) \right] \\
 & + \frac{z}{y+z} \left[-\frac{\pi^2}{3} + 2H(0; z) - 2H(0; z)G(0; y) - 2H(1, 0; z) - 2G(0; y) + 2G(1, 0; y) \right] \\
 & + \frac{z^2}{(y+z)^4} \left[2\pi^2 H(1; z) - 2\pi^2 G(1-z; y) - 12H(0; z)G(1-z, 0; y) - 12H(0, 1, 0; z) \right. \\
 & \quad - 12H(1, 0; z)G(1-z; y) + 12H(1, 0; z)G(0; y) + 12H(1, 1, 0; z) \\
 & \quad \left. + 12G(1-z, 1, 0; y) + 12G(0, 1, 0; y) \right] \\
 & + \frac{z^2}{(y+z)^3} \left[-2\pi^2 - \frac{4\pi^2}{3}H(1; z) + \frac{4\pi^2}{3}G(1-z; y) + 8H(0; z)G(1-z, 0; y) \right. \\
 & \quad - 12H(0; z)G(0; y) + 8H(0, 1, 0; z) - 12H(1, 0; z) + 8H(1, 0; z)G(1-z; y) \\
 & \quad - 8H(1, 0; z)G(0; y) - 8H(1, 1, 0; z) - 8G(1-z, 1, 0; y) - 8G(0, 1, 0; y) \\
 & \quad \left. + 12G(1, 0; y) \right] \\
 & + \frac{z^2}{3(y+z)^2} \left[\pi^2 + 6H(0; z)G(0; y) + 6H(1, 0; z) - 6G(1, 0; y) \right] \\
 & + \frac{1}{9(1-y)} \left[-4\pi^2 + 6H(0; z)G(0; y) - 70G(0; y) + 36G(0, 0; y) + 24G(1, 0; y) \right] \\
 & + \frac{1}{(y+z)^2} \left[\frac{2\pi^2}{3}H(1; z) - \frac{2\pi^2}{3}G(1-z; y) - 4H(0; z)G(1-z, 0; y) \right. \\
 & \quad - 4H(0, 1, 0; z) - 4H(1, 0; z)G(1-z; y) + 4H(1, 0; z)G(0; y) + 4H(1, 1, 0; z) \\
 & \quad \left. + 4G(1-z, 1, 0; y) + 4G(0, 1, 0; y) \right]
 \end{aligned}$$

$$\begin{aligned}
 & + \frac{1}{y+z} \left[-\frac{2\pi^2}{3} - \frac{\pi^2}{3} H(1; z) + \frac{\pi^2}{3} G(1-z; y) + 2 - H(0; z) + 2H(0; z)G(1-z, 0; y) \right. \\
 & - 4H(0; z)G(0; y) + 2H(0, 1, 0; z) - 4H(1, 0; z) + 2H(1, 0; z)G(1-z; y) \\
 & - 2H(1, 0; z)G(0; y) - 2H(1, 1, 0; z) - 2G(1-z, 1, 0; y) - G(0; y) - 2G(0, 1, 0; y) \\
 & \left. + 4G(1, 0; y) \right] \\
 & + \frac{T\pi^2}{216} \left[+431 - 12H(0; z) + 24G(1-z; y) - 12G(0; y) - 24G(1; y) \right] \\
 & + \frac{T}{18} \left[\frac{4345}{36} - 38\zeta_3 + 31H(0; z) + 12H(0; z)G(1-z, 0; y) \right. \\
 & + 10H(0; z)G(0; y) - 18H(0; z)G(0, 0; y) + 3H(0; z)G(1, 0; y) - 41H(0, 0; z) \\
 & - 18H(0, 0; z)G(0; y) - 3H(0, 1, 0; z) + 29H(1, 0; z) + 12H(1, 0; z)G(1-z; y) \\
 & - 15H(1, 0; z)G(0; y) - 18H(1, 0, 0; z) - 12G(1-z, 1, 0; y) + 31G(0; y) \\
 & - 41G(0, 0; y) + 3G(0, 1, 0; y) - 29G(1, 0; y) + 18G(1, 0, 0; y) + 12G(1, 1, 0; y) \left. \right] \\
 & + \frac{\pi^2}{3} + 2H(0; z)G(0; y) + 2H(1, 0; z) - 2G(1, 0; y), \\
 E_{20}(y, z) = & \frac{z}{9y} \left[-2\pi^2 G(1-z; y) + 12H(0; z)G(1-z, 1-z; y) - 47H(0; z)G(1-z; y) \right. \\
 & + 3H(0; z)G(1-z, 0; y) - 15H(0; z)G(-z, 1-z; y) + 3H(0; z)G(0, 1-z; y) \\
 & + 18H(0, 0; z)G(1-z; y) + 9H(0, 1; z) + 3H(0, 1; z)G(-z; y) \\
 & + 12H(1; z)G(1-z, -z; y) + 12H(1; z)G(-z, 1-z; y) - 12H(1; z)G(-z, -z; y) \\
 & - 38H(1; z)G(-z; y) + 3H(1; z)G(-z, 0; y) + 3H(1; z)G(0, -z; y) \\
 & - 9H(1; z)G(0; y) + 9H(1, 0; z) - 12H(1, 0; z)G(1-z; y) + 15H(1, 0; z)G(-z; y) \\
 & - 12H(1, 1; z)G(-z; y) - 12G(1-z, -z, 1-z; y) + 9G(1-z, 0; y) \\
 & - 12G(-z, 1-z, 1-z; y) + 38G(-z, 1-z; y) - 3G(-z, 1-z, 0; y) \\
 & + 12G(-z, -z, 1-z; y) - 3G(-z, 0, 1-z; y) + 9G(0, 1-z; y) \\
 & \left. - 3G(0, -z, 1-z; y) \right] \\
 & + \frac{1}{y(y+z)} \left[-2H(0; z)G(1-z; y) + 2H(0, 1; z) - 2H(1; z)G(0; y) + 2H(1, 0; z) \right. \\
 & \left. + 2G(1-z, 0; y) + 2G(0, 1-z; y) \right] \\
 & + \frac{1}{18y} \left[8\pi^2 G(1-z; y) - 38 + 3H(0; z) - 48H(0; z)G(1-z, 1-z; y) \right. \\
 & + 188H(0; z)G(1-z; y) - 12H(0; z)G(1-z, 0; y) + 60H(0; z)G(-z, 1-z; y) \\
 & - 12H(0; z)G(0, 1-z; y) - 72H(0, 0; z)G(1-z; y) - 36H(0, 1; z) \\
 & - 12H(0, 1; z)G(-z; y) - 48H(1; z)G(1-z, -z; y) - 48H(1; z)G(-z, 1-z; y) \\
 & + 48H(1; z)G(-z, -z; y) + 152H(1; z)G(-z; y) - 12H(1; z)G(-z, 0; y) \\
 & - 12H(1; z)G(0, -z; y) + 36H(1; z)G(0; y) - 36H(1, 0; z) \\
 & + 48H(1, 0; z)G(1-z; y) - 60H(1, 0; z)G(-z; y) + 48H(1, 1; z)G(-z; y) \\
 & + 48G(1-z, -z, 1-z; y) - 36G(1-z, 0; y) + 48G(-z, 1-z, 1-z; y) \\
 & - 152G(-z, 1-z; y) + 12G(-z, 1-z, 0; y) - 48G(-z, -z, 1-z; y) \\
 & \left. + 12G(-z, 0, 1-z; y) - 36G(0, 1-z; y) + 12G(0, -z, 1-z; y) + 15G(0; y) \right]
 \end{aligned}$$

$$\begin{aligned}
& + \frac{z}{18(1-y)^2} \left[-2\pi^2 + 3H(0; z)G(0; y) - 50G(0; y) + 18G(0, 0; y) + 12G(1, 0; y) \right] \\
& + \frac{z}{18(1-y)} \left[-6\pi^2 - 38 + 3H(0; z) + 9H(0; z)G(0; y) - 87G(0; y) + 54G(0, 0; y) \right. \\
& \quad \left. + 36G(1, 0; y) \right] \\
& + \frac{1}{9(1-y)} \left[2\pi^2 - 3H(0; z)G(0; y) + 38G(0; y) - 18G(0, 0; y) - 12G(1, 0; y) \right] \\
& + \frac{1}{9(y+z)^2} \left[-9H(0; z)G(1-z; y) - 3H(0, 1; z) - 26H(1; z) + 12H(1; z)G(1-z; y) \right. \\
& \quad - 12H(1; z)G(-z; y) + 9H(1; z)G(0; y) + 9H(1, 0; z) - 12H(1, 1; z) \\
& \quad - 12G(1-z, 1-z; y) + 26G(1-z; y) - 9G(1-z, 0; y) + 12G(-z, 1-z; y) \\
& \quad \left. - 9G(0, 1-z; y) \right] \\
& + \frac{1}{9(y+z)} \left[+38 - 9H(0; z) - 12H(1; z) + 12G(1-z; y) - 9G(0; y) \right] \\
& + \frac{T\pi^2}{36} \left[-7 + H(1; z) - 5G(1-z; y) + 4G(1; y) \right] \\
& + \frac{T}{108} \left[-\frac{4085}{6} + 6\zeta_3 + 72H(0; z) + 72H(0; z)G(1-z, 1-z; y) \right. \\
& \quad - 147H(0; z)G(1-z; y) + 36H(0; z)G(1-z, 0; y) - 108H(0; z)G(-z, 1-z; y) \\
& \quad + 36H(0; z)G(0, 1-z; y) - 18H(0; z)G(1, 0; y) + 108H(0, 0; z)G(1-z; y) \\
& \quad - 36H(0, 0, 1; z) - 201H(0, 1; z) + 72H(0, 1; z)G(1-z; y) - 36H(0, 1; z)G(-z; y) \\
& \quad + 72H(0, 1; z)G(0; y) + 18H(0, 1, 0; z) - 72H(0, 1, 1; z) + 68H(1; z) \\
& \quad + 144H(1; z)G(1-z, -z; y) - 108H(1; z)G(1-z; y) - 72H(1; z)G(1-z, 0; y) \\
& \quad + 144H(1; z)G(-z, 1-z; y) - 144H(1; z)G(-z, -z; y) - 348H(1; z)G(-z; y) \\
& \quad + 108H(1; z)G(-z, 0; y) - 72H(1; z)G(0, 1-z; y) + 108H(1; z)G(0, -z; y) \\
& \quad + 147H(1; z)G(0; y) - 108H(1; z)G(0, 0; y) - 81H(1, 0; z) \\
& \quad - 72H(1, 0; z)G(1-z; y) + 108H(1, 0; z)G(-z; y) - 18H(1, 0; z)G(0; y) \\
& \quad - 72H(1, 0, 1; z) + 108H(1, 1; z) - 144H(1, 1; z)G(-z; y) + 72H(1, 1; z)G(0; y) \\
& \quad + 108G(1-z, 1-z; y) + 72G(1-z, 1-z, 0; y) - 144G(1-z, -z, 1-z; y) \\
& \quad - 68G(1-z; y) + 72G(1-z, 0, 1-z; y) - 147G(1-z, 0; y) + 108G(1-z, 0, 0; y) \\
& \quad - 144G(-z, 1-z, 1-z; y) + 348G(-z, 1-z; y) - 108G(-z, 1-z, 0; y) \\
& \quad + 144G(-z, -z, 1-z; y) - 108G(-z, 0, 1-z; y) + 72G(0, 1-z, 1-z; y) \\
& \quad - 147G(0, 1-z; y) + 108G(0, 1-z, 0; y) - 108G(0, -z, 1-z; y) + 72G(0; y) \\
& \quad + 108G(0, 0, 1-z; y) - 18G(0, 1, 0; y) + 228G(1, 0; y) - 108G(1, 0, 0; y) \\
& \quad \left. - 72G(1, 1, 0; y) \right] \\
& + \frac{1}{9} \left[2\pi^2 + 2\pi^2 H(1; z) - 4\pi^2 G(1-z; y) + 2\pi^2 G(1; y) + 19H(0; z) \right. \\
& \quad + 12H(0; z)G(1-z, 1-z; y) - 29H(0; z)G(1-z; y) + 6H(0; z)G(1-z, 0; y) \\
& \quad - 18H(0; z)G(-z, 1-z; y) + 6H(0; z)G(0, 1-z; y) - 3H(0; z)G(0; y) \\
& \quad - 3H(0; z)G(1, 0; y) - 9H(0, 0; z) + 18H(0, 0; z)G(1-z; y) - 6H(0, 0, 1; z) \\
& \quad - 35H(0, 1; z) + 12H(0, 1; z)G(1-z; y) - 6H(0, 1; z)G(-z; y) \\
& \quad \left. + 12H(0, 1; z)G(0; y) + 3H(0, 1, 0; z) - 12H(0, 1, 1; z) + 38H(1; z) \right]
\end{aligned}$$

$$\begin{aligned}
& +24H(1; z)G(1 - z, -z; y) - 12H(1; z)G(1 - z; y) - 12H(1; z)G(1 - z, 0; y) \\
& +24H(1; z)G(-z, 1 - z; y) - 24H(1; z)G(-z, -z; y) - 64H(1; z)G(-z; y) \\
& +18H(1; z)G(-z, 0; y) - 12H(1; z)G(0, 1 - z; y) + 18H(1; z)G(0, -z; y) \\
& +29H(1; z)G(0; y) - 18H(1; z)G(0, 0; y) - 3H(1, 0; z) - 12H(1, 0; z)G(1 - z; y) \\
& +18H(1, 0; z)G(-z; y) - 3H(1, 0; z)G(0; y) - 12H(1, 0, 1; z) + 12H(1, 1; z) \\
& -24H(1, 1; z)G(-z; y) + 12H(1, 1; z)G(0; y) + 12G(1 - z, 1 - z; y) \\
& +12G(1 - z, 1 - z, 0; y) - 24G(1 - z, -z, 1 - z; y) - 38G(1 - z; y) \\
& +12G(1 - z, 0, 1 - z; y) - 29G(1 - z, 0; y) + 18G(1 - z, 0, 0; y) \\
& -24G(-z, 1 - z, 1 - z; y) + 64G(-z, 1 - z; y) - 18G(-z, 1 - z, 0; y) \\
& +24G(-z, -z, 1 - z; y) - 18G(-z, 0, 1 - z; y) + 12G(0, 1 - z, 1 - z; y) \\
& -29G(0, 1 - z; y) + 18G(0, 1 - z, 0; y) - 18G(0, -z, 1 - z; y) + 19G(0; y) \\
& +18G(0, 0, 1 - z; y) - 9G(0, 0; y) - 3G(0, 1, 0; y) + 32G(1, 0; y) - 18G(1, 0, 0; y) \\
& -12G(1, 1, 0; y) \Big],
\end{aligned}$$

$$F_{20}(y, z) =$$

$$\begin{aligned}
& \frac{T}{108} \Big[-17\pi^2 - 20H(0; z) + 3H(0; z)G(0; y) + 15H(0, 0; z) - 20G(0; y) \\
& +15G(0, 0; y) \Big],
\end{aligned}$$

$$G_{20}(y, z) =$$

$$\begin{aligned}
& \frac{z}{y^2} \Big[-9H(0; z)G(1 - z; y) - 9H(1; z)G(-z; y) + 9G(-z, 1 - z; y) \Big] \\
& + \frac{z^2}{y^2} \Big[3H(0; z)G(1 - z; y) + 3H(1; z)G(-z; y) - 3G(-z, 1 - z; y) \Big] \\
& + \frac{1}{y^2} \Big[6H(0; z)G(1 - z; y) + 6H(1; z)G(-z; y) - 6G(-z, 1 - z; y) \Big] \\
& + \frac{z\pi^2}{9y} \Big[12H(1; z)G(1 - z; y) - 12G(1 - z, 1 - z; y) - 2G(1 - z; y) \\
& +12G(1 - z, 0; y) - 2G(1; y) \Big] \\
& + \frac{z}{3y} \Big[-72\zeta_3 G(1 - z; y) - 9H(0; z) + 12H(0; z)G(1 - z, 1 - z; y) \\
& -18H(0; z)G(1 - z; y) - 4H(0; z)G(1 - z, 0; y) - 8H(0; z)G(-z, 1 - z; y) \\
& -4H(0; z)G(1, 0; y) + 24H(0, 0, 1; z)G(1 - z; y) + 24H(0, 1; z)G(1 - z, 1 - z; y) \\
& -8H(0, 1; z)G(1 - z; y) - 24H(0, 1; z)G(1 - z, 0; y) \\
& -24H(0, 1; z)G(-z, 1 - z; y) - 24H(0, 1; z)G(-z, -z; y) + 4H(0, 1, 1; z) \\
& +24H(0, 1, 1; z)G(-z; y) + 24H(1; z)G(1 - z, 1 - z, -z; y) \\
& +4H(1; z)G(1 - z, -z; y) - 24H(1; z)G(1 - z, 0, -z; y) + 4H(1; z)G(1 - z, 0; y) \\
& -24H(1; z)G(-z, 1 - z, -z; y) + 8H(1; z)G(-z, 1 - z; y) \\
& +24H(1; z)G(-z, 1 - z, 0; y) - 24H(1; z)G(-z, -z, 1 - z; y) \\
& -24H(1; z)G(-z, -z, -z; y) - 8H(1; z)G(-z, -z; y) + 24H(1; z)G(-z, -z, 0; y) \\
& -18H(1; z)G(-z; y) + 24H(1; z)G(-z, 0, 1 - z; y) - 8H(1; z)G(-z, 0; y) \\
& +4H(1; z)G(0, 1 - z; y) - 4H(1; z)G(1, 0; y) - 12H(1, 0; z)G(1 - z; y) \\
& +8H(1, 0; z)G(-z; y) + 4H(1, 0, 1; z) - 24H(1, 0, 1; z)G(1 - z; y)
\end{aligned}$$

$$\begin{aligned}
 & +24H(1, 0, 1; z)G(-z; y) + 24H(1, 1; z)G(-z, -z; y) - 8H(1, 1; z)G(-z; y) \\
 & - 24H(1, 1; z)G(-z, 0; y) - 4H(1, 1; z)G(0; y) + 4H(1, 1, 0; z) \\
 & - 24G(1 - z, 1 - z, -z, 1 - z; y) - 4G(1 - z, 1 - z, 0; y) \\
 & + 24G(1 - z, 1 - z, 1, 0; y) - 4G(1 - z, -z, 1 - z; y) - 4G(1 - z, 0, 1 - z; y) \\
 & + 24G(1 - z, 0, -z, 1 - z; y) - 24G(1 - z, 0, 1, 0; y) - 8G(-z, 1 - z, 1 - z; y) \\
 & - 24G(-z, 1 - z, 1 - z, 0; y) + 24G(-z, 1 - z, -z, 1 - z; y) + 18G(-z, 1 - z; y) \\
 & - 24G(-z, 1 - z, 0, 1 - z; y) + 8G(-z, 1 - z, 0; y) + 24G(-z, 1 - z, 1, 0; y) \\
 & + 24G(-z, -z, 1 - z, 1 - z; y) + 8G(-z, -z, 1 - z; y) - 24G(-z, -z, 1 - z, 0; y) \\
 & + 24G(-z, -z, -z, 1 - z; y) - 24G(-z, -z, 0, 1 - z; y) - 24G(-z, 0, 1 - z, 1 - z; y) \\
 & + 8G(-z, 0, 1 - z; y) + 24G(-z, 0, 1, 0; y) - 4G(0, 1 - z, 1 - z; y) \\
 & + 4G(1, 1 - z, 0; y) + 4G(1, 0, 1 - z; y) + 4G(1, 1, 0; y) \Big] \\
 & + \frac{z^2}{y} \Big[3H(0; z)G(1 - z; y) + 3H(1; z)G(-z; y) - 3G(-z, 1 - z; y) \Big] \\
 & + \frac{1}{3y(1 - y - z)} \Big[\frac{2\pi^2}{3}G(1; y) + 4H(0; z)G(-z, 1 - z; y) \\
 & + 4H(0; z)G(1, 0; y) + 4H(1; z)G(-z, -z; y) + 4H(1; z)G(-z, 0; y) \\
 & + 4H(1; z)G(1, 0; y) - 4H(1, 0; z)G(-z; y) - 4G(-z, 1 - z, 0; y) \\
 & - 4G(-z, -z, 1 - z; y) - 4G(-z, 0, 1 - z; y) - 4G(1, 1 - z, 0; y) - 4G(1, 0, 1 - z; y) \\
 & - 4G(1, 1, 0; y) \Big] \\
 & + \frac{1}{3y(1 - z)} \Big[\frac{2\pi^2}{3}G(1; y) + 4H(0; z)G(-z, 1 - z; y) \\
 & + 4H(0; z)G(1, 0; y) + 4H(1; z)G(-z, -z; y) + 4H(1; z)G(-z, 0; y) \\
 & + 4H(1; z)G(1, 0; y) - 4H(1, 0; z)G(-z; y) - 4G(-z, 1 - z, 0; y) \\
 & - 4G(-z, -z, 1 - z; y) - 4G(-z, 0, 1 - z; y) - 4G(1, 1 - z, 0; y) - 4G(1, 0, 1 - z; y) \\
 & - 4G(1, 1, 0; y) \Big] \\
 & + \frac{1}{3y(y + z)} \Big[8H(0; z)G(1 - z, 1 - z; y) - 8H(0, 1; z)G(1 - z; y) + 8H(0, 1, 1; z) \\
 & + 8H(1; z)G(1 - z, 0; y) + 8H(1; z)G(0, 1 - z; y) - 8H(1, 0; z)G(1 - z; y) \\
 & + 8H(1, 0, 1; z) - 8H(1, 1; z)G(0; y) + 8H(1, 1, 0; z) - 8G(1 - z, 1 - z, 0; y) \\
 & - 8G(1 - z, 0, 1 - z; y) - 8G(0, 1 - z, 1 - z; y) \Big] \\
 & + \frac{\pi^2}{9y} \Big[- 6H(1; z)G(1 - z; y) + 6G(1 - z, 1 - z; y) + G(1 - z; y) - 6G(1 - z, 0; y) \\
 & + G(1; y) \Big] \\
 & + \frac{1}{3y} \Big[36\zeta_3 G(1 - z; y) + 18H(0; z) - 12H(0; z)G(1 - z, 1 - z; y) \\
 & + 11H(0; z)G(1 - z; y) - 4H(0; z)G(1 - z, 0; y) - 2H(0; z)G(-z, 1 - z; y) \\
 & + 6H(0; z)G(0, 1 - z; y) + 2H(0; z)G(1, 0; y) - 12H(0, 0, 1; z)G(1 - z; y) \\
 & - 12H(0, 1; z)G(1 - z, 1 - z; y) + 4H(0, 1; z)G(1 - z; y) \\
 & + 12H(0, 1; z)G(1 - z, 0; y) + 12H(0, 1; z)G(-z, 1 - z; y) \Big]
 \end{aligned}$$

$$\begin{aligned}
& +12H(0, 1; z)G(-z, -z; y) + 6H(0, 1; z)G(-z; y) - 8H(0, 1, 1; z) \\
& -12H(0, 1, 1; z)G(-z; y) + 9H(1; z) - 12H(1; z)G(1 - z, 1 - z, -z; y) \\
& -8H(1; z)G(1 - z, -z; y) + 12H(1; z)G(1 - z, 0, -z; y) - 8H(1; z)G(1 - z, 0; y) \\
& +12H(1; z)G(-z, 1 - z, -z; y) - 4H(1; z)G(-z, 1 - z; y) \\
& -12H(1; z)G(-z, 1 - z, 0; y) + 12H(1; z)G(-z, -z, 1 - z; y) \\
& +12H(1; z)G(-z, -z, -z; y) + 4H(1; z)G(-z, -z; y) - 12H(1; z)G(-z, -z, 0; y) \\
& +11H(1; z)G(-z; y) - 12H(1; z)G(-z, 0, 1 - z; y) - 2H(1; z)G(-z, 0; y) \\
& -8H(1; z)G(0, 1 - z; y) + 6H(1; z)G(0, -z; y) + 2H(1; z)G(1, 0; y) \\
& +6H(1, 0; z)G(1 - z; y) + 2H(1, 0; z)G(-z; y) - 8H(1, 0, 1; z) \\
& +12H(1, 0, 1; z)G(1 - z; y) - 12H(1, 0, 1; z)G(-z; y) - 12H(1, 1; z)G(-z, -z; y) \\
& +4H(1, 1; z)G(-z; y) + 12H(1, 1; z)G(-z, 0; y) + 8H(1, 1; z)G(0; y) \\
& -8H(1, 1, 0; z) + 12G(1 - z, 1 - z, -z, 1 - z; y) + 8G(1 - z, 1 - z, 0; y) \\
& -12G(1 - z, 1 - z, 1, 0; y) + 8G(1 - z, -z, 1 - z; y) - 9G(1 - z; y) \\
& +8G(1 - z, 0, 1 - z; y) - 12G(1 - z, 0, -z, 1 - z; y) + 12G(1 - z, 0, 1, 0; y) \\
& +4G(-z, 1 - z, 1 - z; y) + 12G(-z, 1 - z, 1 - z, 0; y) \\
& -12G(-z, 1 - z, -z, 1 - z; y) - 11G(-z, 1 - z; y) + 12G(-z, 1 - z, 0, 1 - z; y) \\
& +2G(-z, 1 - z, 0; y) - 12G(-z, 1 - z, 1, 0; y) - 12G(-z, -z, 1 - z, 1 - z; y) \\
& -4G(-z, -z, 1 - z; y) + 12G(-z, -z, 1 - z, 0; y) - 12G(-z, -z, -z, 1 - z; y) \\
& +12G(-z, -z, 0, 1 - z; y) + 12G(-z, 0, 1 - z, 1 - z; y) + 2G(-z, 0, 1 - z; y) \\
& -12G(-z, 0, 1, 0; y) + 8G(0, 1 - z, 1 - z; y) - 6G(0, -z, 1 - z; y) \\
& -2G(1, 1 - z, 0; y) - 2G(1, 0, 1 - z; y) - 2G(1, 1, 0; y) \Big] \\
& + \frac{z}{3(1 - y - z)} \Big[-\frac{2\pi^2}{3}H(1; z) - \frac{2\pi^2}{3}G(1; y) - 8H(0; z)G(-z, 1 - z; y) \\
& +4H(0; z)G(0, 1 - z; y) - 4H(0; z)G(1, 0; y) + 8H(0, 0, 1; z) \\
& +8H(0, 1; z)G(-z; y) - 4H(0, 1; z)G(0; y) + 4H(0, 1, 0; z) - 8H(1; z)G(-z, 0; y) \\
& -4H(1; z)G(1, 0; y) + 8H(1, 0; z)G(-z; y) - 4H(1, 0; z)G(0; y) - 4H(1, 0, 1; z) \\
& -8H(1, 1, 0; z) + 8G(-z, 1 - z, 0; y) + 8G(-z, 0, 1 - z; y) - 4G(0, 1, 0; y) \\
& +4G(1, 1 - z, 0; y) + 4G(1, 0, 1 - z; y) + 4G(1, 1, 0; y) \Big] \\
& + \frac{z\pi^2}{3(1 - y)^2} \Big[-3 - H(0; z) - H(1; z) + G(1 - z; y) \Big] \\
& + \frac{z}{(1 - y)^2} \Big[6\zeta_3 - 2H(0; z)G(0, 1 - z; y) + 2H(0, 0, 1; z) + 6H(0, 1; z) \\
& -2H(0, 1; z)G(1 - z; y) - 2H(0, 1, 0; z) - 2H(1; z)G(1 - z, -z; y) \\
& +6H(1; z)G(-z; y) - 2H(1; z)G(0, -z; y) - 6H(1, 0; z) + 2H(1, 0; z)G(1 - z; y) \\
& +2H(1, 0, 1; z) - 2H(1, 1, 0; z) + 2G(1 - z, -z, 1 - z; y) - 6G(-z, 1 - z; y) \\
& +2G(0, -z, 1 - z; y) \Big] \\
& + \frac{z}{1 - y} \Big[3H(0; z) - 2H(0; z)G(1 - z; y) + 3H(1; z) - 2H(1; z)G(-z; y) - 3G(1 - z; y) \\
& +2G(-z, 1 - z; y) \Big]
\end{aligned}$$

$$\begin{aligned}
& + \frac{z}{3(y+z)^3} \left[-8H(0; z)G(1-z, 1-z; y) - 24H(0; z)G(1-z; y) + 24H(0, 1; z) \right. \\
& + 8H(0, 1; z)G(1-z; y) - 8H(0, 1, 1; z) - 8H(1; z)G(1-z, 0; y) \\
& - 8H(1; z)G(0, 1-z; y) - 24H(1; z)G(0; y) + 24H(1, 0; z) \\
& + 8H(1, 0; z)G(1-z; y) - 8H(1, 0, 1; z) + 8H(1, 1; z)G(0; y) - 8H(1, 1, 0; z) \\
& + 8G(1-z, 1-z, 0; y) + 8G(1-z, 0, 1-z; y) + 24G(1-z, 0; y) \\
& \left. + 8G(0, 1-z, 1-z; y) + 24G(0, 1-z; y) \right] \\
& + \frac{z}{3(y+z)^2} \left[-24H(0; z) + 4H(0; z)G(1-z, 1-z; y) + 16H(0; z)G(1-z; y) \right. \\
& - 16H(0, 1; z) - 4H(0, 1; z)G(1-z; y) + 4H(0, 1, 1; z) + 4H(1; z)G(1-z, 0; y) \\
& + 4H(1; z)G(0, 1-z; y) + 16H(1; z)G(0; y) - 16H(1, 0; z) \\
& - 4H(1, 0; z)G(1-z; y) + 4H(1, 0, 1; z) - 4H(1, 1; z)G(0; y) + 4H(1, 1, 0; z) \\
& - 4G(1-z, 1-z, 0; y) - 4G(1-z, 0, 1-z; y) - 16G(1-z, 0; y) \\
& \left. - 4G(0, 1-z, 1-z; y) - 16G(0, 1-z; y) + 24G(0; y) \right] \\
& + \frac{z}{3(y+z)} \left[8H(0; z) - 8H(0; z)G(1-z, 1-z; y) + 8H(0, 1; z)G(1-z; y) \right. \\
& - 8H(0, 1, 1; z) - 8H(1; z)G(1-z, 0; y) - 8H(1; z)G(0, 1-z; y) \\
& + 8H(1, 0; z)G(1-z; y) - 8H(1, 0, 1; z) + 8H(1, 1; z)G(0; y) - 8H(1, 1, 0; z) \\
& \left. + 8G(1-z, 1-z, 0; y) + 8G(1-z, 0, 1-z; y) + 8G(0, 1-z, 1-z; y) - 8G(0; y) \right] \\
& + \frac{z^2}{(1-y)^3} \left[\pi^2 H(0; z) + \pi^2 H(1; z) - \pi^2 G(1-z; y) - 18\zeta_3 + 6H(0; z)G(0, 1-z; y) \right. \\
& - 6H(0, 0, 1; z) + 6H(0, 1; z)G(1-z; y) + 6H(0, 1, 0; z) + 6H(1; z)G(1-z, -z; y) \\
& + 6H(1; z)G(0, -z; y) - 6H(1, 0; z)G(1-z; y) - 6H(1, 0, 1; z) + 6H(1, 1, 0; z) \\
& \left. - 6G(1-z, -z, 1-z; y) - 6G(0, -z, 1-z; y) \right] \\
& + \frac{z^2}{(1-y)^2} \left[6H(0; z)G(1-z; y) + 6H(1; z)G(-z; y) - 6G(-z, 1-z; y) \right] \\
& + \frac{z^2}{1-y} \left[3H(0; z)G(1-z; y) + 3H(1; z)G(-z; y) - 3G(-z, 1-z; y) \right] \\
& + \frac{1}{3(1-y-z)(1-y)} \left[-\frac{2\pi^2}{3}H(1; z) - 4H(0; z)G(-z, 1-z; y) \right. \\
& + 4H(0; z)G(0, 1-z; y) + 8H(0, 0, 1; z) + 8H(0, 1; z)G(-z; y) \\
& - 4H(0, 1; z)G(0; y) + 4H(0, 1, 0; z) + 4H(1; z)G(-z, -z; y) - 4H(1; z)G(-z, 0; y) \\
& + 4H(1, 0; z)G(-z; y) - 4H(1, 0; z)G(0; y) - 4H(1, 0, 1; z) - 8H(1, 1, 0; z) \\
& \left. + 4G(-z, 1-z, 0; y) - 4G(-z, -z, 1-z; y) + 4G(-z, 0, 1-z; y) - 4G(0, 1, 0; y) \right] \\
& + \frac{1}{3(1-y-z)} \left[\frac{2\pi^2}{3} + \frac{\pi^2}{2}H(1; z) - \frac{\pi^2}{2}G(1; y) - 3H(0; z)G(0, 1-z; y) \right. \\
& + 4H(0; z)G(0; y) - 3H(0; z)G(1, 0; y) - 6H(0, 0, 1; z) - 6H(0, 1; z)G(-z; y) \\
& + 3H(0, 1; z)G(0; y) - 3H(0, 1, 0; z) - 6H(1; z)G(-z, -z; y) - 3H(1; z)G(1, 0; y) \\
& + 4H(1, 0; z) + 3H(1, 0; z)G(0; y) + 3H(1, 0, 1; z) + 6H(1, 1, 0; z) \\
& \left. + 6G(-z, -z, 1-z; y) + 3G(0, 1, 0; y) + 3G(1, 1-z, 0; y) + 3G(1, 0, 1-z; y) \right]
\end{aligned}$$

$$\begin{aligned}
 & -4G(1, 0; y) + 3G(1, 1, 0; y) \Big] \\
 & + \frac{1}{1-y} \Big[-\frac{\pi^2}{2} + \frac{2\pi^2}{3}H(0; z) + \frac{2\pi^2}{3}H(1; z) - \frac{2\pi^2}{3}G(1-z; y) \\
 & -12\zeta_3 + 4H(0; z)G(0, 1-z; y) - H(0; z)G(0; y) - 4H(0, 0, 1; z) + H(0, 1; z) \\
 & + 4H(0, 1; z)G(1-z; y) + 4H(0, 1, 0; z) + 4H(1; z)G(1-z, -z; y) \\
 & + H(1; z)G(-z; y) + 4H(1; z)G(0, -z; y) - H(1; z)G(0; y) - H(1, 0; z) \\
 & - 4H(1, 0; z)G(1-z; y) - 4H(1, 0, 1; z) + 4H(1, 1, 0; z) - 4G(1-z, -z, 1-z; y) \\
 & + G(1-z, 0; y) - G(-z, 1-z; y) + G(0, 1-z; y) - 4G(0, -z, 1-z; y) + 3G(0; y) \\
 & + 2G(1, 0; y) \Big] \\
 & + \frac{1}{3(y+z)^2} \Big[-\pi^2H(1; z) + \pi^2G(1-z; y) - 6H(0; z)G(1-z, 1-z; y) \\
 & - 6H(0; z)G(1-z; y) + 6H(0; z)G(1-z, 0; y) - 6H(0; z)G(-z, 1-z; y) \\
 & + 6H(0; z)G(0, 1-z; y) - 6H(0, 1; z) - 6H(0, 1; z)G(1-z; y) \\
 & - 6H(0, 1; z)G(-z; y) + 6H(0, 1, 0; z) + 6H(0, 1, 1; z) + 24H(1; z) \\
 & - 12H(1; z)G(1-z, -z; y) - 8H(1; z)G(1-z; y) + 6H(1; z)G(1-z, 0; y) \\
 & - 12H(1; z)G(-z, 1-z; y) - 12H(1; z)G(-z, -z; y) - 12H(1; z)G(-z; y) \\
 & + 6H(1; z)G(-z, 0; y) + 6H(1; z)G(0, 1-z; y) + 6H(1; z)G(0, -z; y) \\
 & + 6H(1; z)G(0; y) + 6H(1, 0; z) + 6H(1, 0; z)G(1-z; y) + 6H(1, 0; z)G(-z; y) \\
 & - 6H(1, 0; z)G(0; y) + 6H(1, 0, 1; z) + 8H(1, 1; z) + 12H(1, 1; z)G(-z; y) \\
 & - 6H(1, 1; z)G(0; y) - 6H(1, 1, 0; z) + 8G(1-z, 1-z; y) - 6G(1-z, 1-z, 0; y) \\
 & + 12G(1-z, -z, 1-z; y) - 24G(1-z; y) - 6G(1-z, 0, 1-z; y) - 6G(1-z, 0; y) \\
 & + 12G(-z, 1-z, 1-z; y) + 12G(-z, 1-z; y) - 6G(-z, 1-z, 0; y) \\
 & + 12G(-z, -z, 1-z; y) - 6G(-z, 0, 1-z; y) - 6G(0, 1-z, 1-z; y) \\
 & - 6G(0, 1-z; y) - 6G(0, -z, 1-z; y) \Big] \\
 & + \frac{1}{3(y+z)} \Big[\pi^2 + \frac{\pi^2}{2}H(1; z) - \frac{\pi^2}{2}G(1-z; y) - 12H(0; z) - 12H(0; z)G(1-z; y) \\
 & - 3H(0; z)G(1-z, 0; y) + 6H(0; z)G(0; y) - 18H(0, 1; z) - 3H(0, 1, 0; z) \\
 & - 32H(1; z) - 8H(1; z)G(1-z; y) - 30H(1; z)G(-z; y) + 12H(1; z)G(0; y) \\
 & + 12H(1, 0; z) - 3H(1, 0; z)G(1-z; y) + 3H(1, 0; z)G(0; y) + 8H(1, 1; z) \\
 & + 3H(1, 1, 0; z) + 8G(1-z, 1-z; y) + 32G(1-z; y) - 12G(1-z, 0; y) \\
 & + 3G(1-z, 1, 0; y) + 30G(-z, 1-z; y) - 12G(0, 1-z; y) - 12G(0; y) \\
 & + 3G(0, 1, 0; y) \Big] \\
 & + \frac{T}{6} \Big[-\frac{2\pi^2}{3}G(1-z; y) + \frac{2\pi^2}{3}G(1; y) + 4H(0; z)G(1-z, 1-z; y) \\
 & - 4H(0; z)G(1-z, 0; y) + 4H(0; z)G(1, 0; y) - 4H(0, 1, 1; z) - 9H(1; z) \\
 & + 4H(1; z)G(1-z, -z; y) - 4H(1; z)G(1-z, 0; y) + 8H(1; z)G(-z, 1-z; y) \\
 & - 4H(1; z)G(0, 1-z; y) + 4H(1; z)G(1, 0; y) - 4H(1, 0; z)G(1-z; y) \\
 & - 4H(1, 0, 1; z) - 8H(1, 1; z)G(-z; y) + 4H(1, 1; z)G(0; y) - 4H(1, 1, 0; z) \\
 & + 4G(1-z, 1-z, 0; y) - 4G(1-z, -z, 1-z; y) + 9G(1-z; y) \\
 & + 4G(1-z, 0, 1-z; y) - 8G(-z, 1-z, 1-z; y) + 4G(0, 1-z, 1-z; y) \Big]
 \end{aligned}$$

$$\begin{aligned}
& -4G(1, 1-z, 0; y) - 4G(1, 0, 1-z; y) - 4G(1, 1, 0; y) \Big] \\
& + \frac{\pi^2}{18} \Big[25 - 12H(0; z) + 6H(0; z)G(1-z; y) - 6H(0; z)G(1; y) - 23H(1; z) \\
& + 12H(1; z)G(1-z; y) - 6H(1; z)G(1; y) - 6H(1, 0; z) - 6H(1, 1; z) \\
& - 12G(1-z, 1-z; y) + 22G(1-z; y) + 6G(1-z, 0; y) - 12G(0; y) \\
& + 6G(1, 1-z; y) + G(1; y) \Big] \\
& + \frac{1}{3} \Big[72\zeta_3 + 18\zeta_3 H(1; z) - 36\zeta_3 G(1-z; y) + 18\zeta_3 G(1; y) - 5H(0; z) \\
& + 11H(0; z)G(1-z, 1-z; y) + 5H(0; z)G(1-z; y) \\
& + 6H(0; z)G(1-z, 0, 1-z; y) + 4H(0; z)G(1-z, 0; y) \\
& - 6H(0; z)G(-z, 1-z, 1-z; y) + 9H(0; z)G(-z, 1-z; y) \\
& - 6H(0; z)G(-z, -z, 1-z; y) + 6H(0; z)G(-z, 0, 1-z; y) \\
& + 6H(0; z)G(0, 1-z, 1-z; y) - 22H(0; z)G(0, 1-z; y) \\
& + 6H(0; z)G(0, -z, 1-z; y) + H(0; z)G(0; y) - 6H(0; z)G(0, 0, 1-z; y) \\
& - 6H(0; z)G(1, 0, 1-z; y) - 2H(0; z)G(1, 0; y) - 2H(0, 0, 1; z) \\
& + 6H(0, 0, 1; z)G(1; y) - 11H(0, 1; z) + 12H(0, 1; z)G(1-z, 1-z; y) \\
& - 9H(0, 1; z)G(1-z; y) - 6H(0, 1; z)G(1-z, 0; y) - 6H(0, 1; z)G(-z, 1-z; y) \\
& - 6H(0, 1; z)G(-z, -z; y) + 7H(0, 1; z)G(-z; y) + 13H(0, 1; z)G(0; y) \\
& - 6H(0, 1; z)G(1, 1-z; y) - 10H(0, 1, 0; z) + 6H(0, 1, 0; z)G(1-z; y) \\
& - 6H(0, 1, 0; z)G(1; y) - 11H(0, 1, 1; z) + 6H(0, 1, 1; z)G(-z; y) - 10H(1; z) \\
& + 12H(1; z)G(1-z, 1-z, -z; y) + 2H(1; z)G(1-z, -z; y) \\
& + 16H(1; z)G(1-z; y) - 11H(1; z)G(1-z, 0; y) - 12H(1; z)G(-z, 1-z, -z; y) \\
& + 22H(1; z)G(-z, 1-z; y) + 6H(1; z)G(-z, 1-z, 0; y) \\
& - 12H(1; z)G(-z, -z, 1-z; y) - 12H(1; z)G(-z, -z, -z; y) \\
& + 16H(1; z)G(-z, -z; y) + 6H(1; z)G(-z, -z, 0; y) - 6H(1; z)G(-z; y) \\
& + 6H(1; z)G(-z, 0, 1-z; y) + 6H(1; z)G(-z, 0, -z; y) - 9H(1; z)G(-z, 0; y) \\
& + 6H(1; z)G(0, 1-z, -z; y) - 11H(1; z)G(0, 1-z; y) \\
& + 6H(1; z)G(0, -z, 1-z; y) + 6H(1; z)G(0, -z, -z; y) - 9H(1; z)G(0, -z; y) \\
& - 5H(1; z)G(0; y) - 6H(1; z)G(0, 0, -z; y) - 6H(1; z)G(1, 1-z, -z; y) \\
& - 6H(1; z)G(1, 0, -z; y) - 2H(1; z)G(1, 0; y) + H(1, 0; z) \\
& - 6H(1, 0; z)G(1-z, 1-z; y) + 13H(1, 0; z)G(1-z; y) \\
& + 6H(1, 0; z)G(-z, -z; y) - 9H(1, 0; z)G(-z; y) - 6H(1, 0; z)G(0, -z; y) \\
& - 2H(1, 0; z)G(0; y) + 6H(1, 0; z)G(1, 1-z; y) + 6H(1, 0, 0, 1; z) \\
& + 11H(1, 0, 1; z) - 12H(1, 0, 1; z)G(1-z; y) + 6H(1, 0, 1; z)G(-z; y) \\
& + 6H(1, 0, 1; z)G(1; y) - 6H(1, 0, 1, 0; z) - 16H(1, 1; z) \\
& + 12H(1, 1; z)G(-z, -z; y) - 22H(1, 1; z)G(-z; y) - 6H(1, 1; z)G(-z, 0; y) \\
& - 6H(1, 1; z)G(0, -z; y) + 11H(1, 1; z)G(0; y) - 12H(1, 1, 0; z) \\
& + 6H(1, 1, 0; z)G(1-z; y) - 6H(1, 1, 0; z)G(1; y) + 6H(1, 1, 0, 1; z) \\
& - 6H(1, 1, 1, 0; z) - 12G(1-z, 1-z, -z, 1-z; y) - 16G(1-z, 1-z; y) \\
& + 11G(1-z, 1-z, 0; y) + 6G(1-z, 1-z, 1, 0; y) - 2G(1-z, -z, 1-z; y)
\end{aligned}$$

$$\begin{aligned}
& +10G(1-z; y) + 11G(1-z, 0, 1-z; y) + 5G(1-z, 0; y) - 6G(1-z, 0, 1, 0; y) \\
& -24G(1-z, 1, 0; y) - 22G(-z, 1-z, 1-z; y) - 6G(-z, 1-z, 1-z, 0; y) \\
& +12G(-z, 1-z, -z, 1-z; y) + 6G(-z, 1-z; y) - 6G(-z, 1-z, 0, 1-z; y) \\
& +9G(-z, 1-z, 0; y) + 6G(-z, 1-z, 1, 0; y) + 12G(-z, -z, 1-z, 1-z; y) \\
& -16G(-z, -z, 1-z; y) - 6G(-z, -z, 1-z, 0; y) + 12G(-z, -z, -z, 1-z; y) \\
& -6G(-z, -z, 0, 1-z; y) - 6G(-z, 0, 1-z, 1-z; y) + 9G(-z, 0, 1-z; y) \\
& -6G(-z, 0, -z, 1-z; y) + 6G(-z, 0, 1, 0; y) + 11G(0, 1-z, 1-z; y) \\
& -6G(0, 1-z, -z, 1-z; y) + 5G(0, 1-z; y) - 6G(0, -z, 1-z, 1-z; y) \\
& +9G(0, -z, 1-z; y) - 6G(0, -z, -z, 1-z; y) - 5G(0; y) + 6G(0, 0, -z, 1-z; y) \\
& +G(0, 1, 0; y) + 6G(1, 1-z, -z, 1-z; y) + 2G(1, 1-z, 0; y) + 2G(1, 0, 1-z; y) \\
& +6G(1, 0, -z, 1-z; y) - 6G(1, 0; y) - G(1, 1, 0; y) \Big]. \tag{B.2}
\end{aligned}$$

APPENDIX C

One-Loop Contribution to Ω

The finite remainder of the self-interference of the one-loop amplitude is decomposed as

$$\Omega^{(1),\text{finite}}(y, z) = N a_{\Omega}(y, z) + \frac{1}{N} b_{\Omega}(y, z) + \beta_0 c_{\Omega}(y, z). \quad (\text{C.1})$$

with

$$\begin{aligned} a_{\alpha}(y, z) &= \\ & -\frac{7}{4} - \frac{\pi^2}{12} + \frac{3}{8}H(0; z) - \frac{1}{2}H(0, z)G(0; y) - \frac{1}{2}H(1, 0; z) - \frac{3}{8}G(0; y) + \frac{1}{2}G(1, 0; y) \\ & - \frac{1}{4(1-z)^2}H(0; z) - \frac{1}{4(1-z)}(1 + 2H(0; z)) + \mathcal{O}(\epsilon), \\ b_{\alpha}(y, z) &= \\ & \frac{z^2}{2y^2}(H(0; z)G(1-z; y) + H(1; z)G(-z; y) - G(-z, 1-z; y)) + \frac{z}{2y}(-H(0; z) \\ & + 2H(0; z)G(1-z; y) - H(1; z) + 2H(1; z)G(-z; y) + G(1-z; y) \\ & - 2G(-z, 1-z; y)) + \frac{1}{2y(1-z)}H(0; z) - \frac{1}{2y}H(0; z) + \frac{1}{4(1-z)^2}H(0; z) \\ & + \frac{1}{4(1-z)}(1 + 2H(0; z)) + \frac{7}{4} - \frac{3}{4}H(0; z) + \frac{1}{2}H(0; z)G(1-z; y) + \frac{1}{2}H(0, 1; z) \\ & - \frac{3}{4}H(1; z) + H(1; z)G(-z; y) - \frac{1}{2}H(1; z)G(0; y) + \frac{3}{4}G(1-z; y) + \frac{1}{2}G(1-z, 0; y) \\ & - G(-z, 1-z; y) + \frac{1}{2}G(0, 1-z; y) - \frac{1}{2}G(1, 0; y) + \mathcal{O}(\epsilon), \\ c_{\alpha}(y, z) &= \\ & -\frac{1}{4}H(0; z) - \frac{1}{4}G(0; y) + \frac{i\pi}{2} + \mathcal{O}(\epsilon), \\ a_{\beta}(y, z) &= \end{aligned}$$

$$\begin{aligned}
& -\frac{3}{2} - \frac{\pi^2}{12} + \frac{3}{8}H(0; z) - \frac{1}{2}H(0; z)G(0; y) - \frac{1}{2}H(1, 0; z) - \frac{3}{8}G(0; y) + \frac{1}{2}G(1, 0; y) \\
& + \frac{1}{4(1-z)}H(0; z) + \mathcal{O}(\epsilon), \\
b_\beta(y, z) = & \frac{z(1-z)}{2y^2}(-H(0; z)G(1-z; y) - H(1; z)G(-z; y) + G(-z, 1-z; y)) + \frac{z}{2y}(-H(0; z) \\
& + 2H(0; z)G(1-z; y) - H(1; z) + 2H(1; z)G(-z; y) + G(1-z; y) \\
& - 2G(-z, 1-z; y)) + \frac{1}{2y}(-2H(0; z)G(1-z; y) + H(1; z) - 2H(1; z)G(-z; y) \\
& - G(1-z; y) + 2G(-z, 1-z; y)) + \frac{z}{2(y+z)^2}(-H(1; z) + G(1-z; y)) + \frac{z}{2(y+z)} \\
& - \frac{1}{4(1-z)}H(0; z) + \frac{1}{2(y+z)}(H(1; z) - G(1-z; y)) + \frac{3}{2} - \frac{3}{4}H(0; z) \\
& + \frac{1}{2}H(0; z)G(1-z; y) + \frac{1}{2}H(0, 1; z) - \frac{3}{4}H(1; z) + H(1; z)G(-z; y) - \frac{1}{2}H(1; z)G(0; y) \\
& + \frac{3}{4}G(1-z; y) + \frac{1}{2}G(1-z, 0; y) - G(-z, 1-z; y) + \frac{1}{2}G(0, 1-z; y) - \frac{1}{2}G(1, 0; y)) \\
& + \mathcal{O}(\epsilon), \\
c_\beta(y, z) = & -\frac{1}{4}H(0; z) - \frac{1}{4}G(0; y) + \frac{i\pi}{2} + \mathcal{O}(\epsilon), \\
a_\gamma(y, z) = & -\frac{1}{4} + \frac{1}{4(1-z)^2}H(0; z) + \frac{1}{4(1-z)}(1 - H(0; z)) + \mathcal{O}(\epsilon), \\
b_\gamma(y, z) = & \frac{1}{4} + \frac{z}{2y^2}(-H(0; z)G(1-z; y) - H(1; z)G(-z; y) + G(-z, 1-z; y)) \\
& - \frac{1}{2y(1-z)}H(0; z) + \frac{1}{2y}(H(0; z) + H(1; z) - G(1-z; y)) + \frac{z}{2(y+z)^2}(H(1; z) \\
& - G(1-z; y)) - \frac{z}{2(y+z)} + \frac{1}{2(y+z)}(-H(1; z) + G(1-z; y)) - \frac{1}{4(1-z)^2}H(0; z) \\
& + \frac{1}{4(1-z)}(-1 + H(0; z)) + \mathcal{O}(\epsilon), \\
c_\gamma(y, z) = & 0.
\end{aligned}$$

It should be noted that these finite pieces of the one-loop coefficients can equally well be written in terms of ordinary logarithms and dilogarithms (See for example [23, 25]). The reason to express them in terms of HPLs and 2dHPLs here is their usage in the infrared counter-term of the two-loop coefficients, which cannot be fully expressed in terms of logarithmic and polylogarithmic functions.

APPENDIX D

Two-Loop Contribution to Ω

The finite remainder of the interference of the two-loop amplitude with the tree-level amplitude is decomposed as

$$\begin{aligned} \Omega^{(2),\text{finite}}(y, z) = & N^2 A_\Omega(y, z) + B_\Omega(y, z) + \frac{1}{N^2} C_\Omega(y, z) + N N_F D_\Omega(y, z) \\ & + \frac{N_F}{N} E_\Omega(y, z) + N_F^2 F_\Omega(y, z) + N_{F,V} \left(\frac{4}{N} - N \right) G_\Omega(y, z), \quad (\text{D.1}) \end{aligned}$$

with

$$\begin{aligned} A_\alpha(y, z) = & \frac{1}{48y(1-z)} \left[\pi^2 - 13\text{H}(0; z) + 6\text{H}(1, 0; z) + 6\text{G}(1, 0; y) \right] \\ & - \frac{1}{48y(1-y-z)} \left[\pi^2 - 13\text{H}(0; z) + 6\text{H}(1, 0; z) + 6\text{G}(1, 0; y) \right] \\ & - \frac{z}{16(1-y)^2} \text{G}(0; y) - \frac{z}{16(1-y)} + \frac{z}{12(1-y-z)^2} \left[-\frac{5\pi^2}{6} - 5\text{H}(0; z)\text{G}(0; y) \right. \\ & \left. - 5\text{H}(1, 0; z) + 5\text{G}(1, 0; y) \right] \\ & + \frac{z}{16(1-y-z)} \left[\frac{14\pi^2}{3} - 11\text{H}(0; z) + 28\text{H}(0; z)\text{G}(0; y) + 28\text{H}(1, 0; z) \right. \\ & \left. + 11\text{G}(0; y) - 28\text{G}(1, 0; y) \right] \\ & + \frac{z^2}{16(1-y-z)^2} \left[\frac{11\pi^2}{6} + 11\text{H}(0; z)\text{G}(0; y) + 11\text{H}(1, 0; z) - 11\text{G}(1, 0; y) \right] \\ & + \frac{1}{3(1-y)} \text{G}(0; y) + \frac{1}{48(1-z)^2} \left[-\frac{\pi^2}{6} + \pi^2(3\text{H}(0; z) + 3\text{H}(1; z) - \text{G}(1-z; y)) \right] \end{aligned}$$

$$\begin{aligned}
& +G(0; y)) + 6\zeta_3 - \frac{355}{6}H(0; z) - 6H(0; z)G(1 - z, 0; y) + 10H(0; z)G(0; y) \\
& + 45H(0, 0; z) + 12H(0, 0; z)G(0; y) + 18H(0, 1, 0; z) - H(1, 0; z) \\
& - 6H(1, 0; z)G(1 - z; y) + 6H(1, 0; z)G(0; y) + 12H(1, 0, 0; z) + 18H(1, 1, 0; z) \\
& + 6G(1 - z, 1, 0; y) - 6G(0, 1, 0; y) \Big] \\
& + \frac{1}{72(1 - z)} \Big[\pi^2 (-8 + 9H(0; z) + 9H(1; z) - 3G(1 - z; y) + 3G(0; y)) + 18\zeta_3 \\
& - \frac{277}{4} - 65H(0; z) - 18H(0; z)G(1 - z, 0; y) + 39H(0; z)G(0; y) + 81H(0, 0; z) \\
& + 36H(0, 0; z)G(0; y) + 54H(0, 1, 0; z) - 48H(1, 0; z) - 18H(1, 0; z)G(1 - z; y) \\
& + 18H(1, 0; z)G(0; y) + 36H(1, 0, 0; z) + 54H(1, 1, 0; z) + 18G(1 - z, 1, 0; y) \\
& + 15G(0; y) - 18G(0, 1, 0; y) - 9G(1, 0; y) \Big] \\
& + \frac{1}{48(1 - y - z)^2} \Big[-2\pi^2 H(1; z) - \pi^2 G(0; y) + 12\zeta_3 - 6H(1, 0; z)G(0; y) \\
& - 12H(1, 1, 0; z) - 6G(0, 1, 0; y) \Big] \\
& + \frac{1}{48(1 - y - z)} \Big[-4\pi^2 H(1; z) - 2\pi^2 G(0; y) + 24\zeta_3 - 13H(0; z) - 12H(1, 0; z)G(0; y) \\
& - 24H(1, 1, 0; z) - 20G(0; y) - 12G(0, 1, 0; y) \Big] \\
& + \frac{\pi^2}{288} \Big[-\frac{928}{3} - 5H(0; z) + 12H(0; z)G(1 - z; y) + 36H(0; z)G(0; y) \\
& - 12H(0; z)G(1; y) + 24H(0, 1; z) + 24H(1; z)G(1 - z; y) - 24H(1; z)G(-z; y) \\
& - 12H(1; z)G(1; y) + 24H(1, 0; z) + 12H(1, 1; z) - 44G(1 - z; y) + 12G(1 - z, 0; y) \\
& - 24G(1 - z, 1; y) + 24G(-z, 1 - z; y) - 24G(0, 1 - z; y) + 49G(0; y) - 24G(0, 1; y) \\
& + 12G(1, 1 - z; y) + 44G(1; y) - 36G(1, 0; y) + 24G(1, 1; y) \Big] \\
& + \frac{\zeta_3}{72} \Big[317 - 18H(0; z) + 90H(1; z) - 72G(1 - z; y) - 18G(0; y) - 18G(1; y) \Big] \\
& + \frac{11\pi^4}{360} + \frac{1}{72} \Big[-\frac{89959}{144} + \frac{2149}{12}H(0; z) - 66H(0; z)G(1 - z, 0; y) \\
& - 18H(0; z)G(1 - z, 1, 0; y) + 36H(0; z)G(-z, 1 - z, 0; y) \\
& - 36H(0; z)G(0, 1 - z, 0; y) - 66H(0; z)G(0; y) + 126H(0; z)G(0, 0; y) \\
& - 18H(0; z)G(0, 1, 0; y) + 18H(0; z)G(1, 1 - z, 0; y) - 3H(0; z)G(1, 0; y) \\
& - 36H(0; z)G(1, 0, 0; y) + \frac{23}{2}H(0, 0; z) + 72H(0, 0; z)G(0; y) \\
& + 36H(0, 0; z)G(0, 0; y) + 72H(0, 0, 1, 0; z) + 3H(0, 1, 0; z) \\
& - 18H(0, 1, 0; z)G(1 - z; y) + 36H(0, 1, 0; z)G(-z; y) + 18H(0, 1, 0; z)G(0; y) \\
& - 18H(0, 1, 0; z)G(1; y) + 36H(0, 1, 1, 0; z) - 71H(1, 0; z) \\
& - 66H(1, 0; z)G(1 - z; y) + 18H(1, 0; z)G(1 - z, 0; y) \\
& + 36H(1, 0; z)G(-z, 1 - z; y) - 36H(1, 0; z)G(-z, 0; y) \\
& - 36H(1, 0; z)G(0, 1 - z; y) + 96H(1, 0; z)G(0; y) + 18H(1, 0; z)G(1, 1 - z; y) \\
& - 18H(1, 0; z)G(1, 0; y) + 72H(1, 0, 0; z) + 36H(1, 0, 0; z)G(0; y) \\
& + 72H(1, 0, 1, 0; z) + 36H(1, 1, 0; z)G(1 - z; y) - 36H(1, 1, 0; z)G(-z; y)
\end{aligned}$$

$$\begin{aligned}
& -18H(1, 1, 0; z)G(1; y) + 36H(1, 1, 0, 0; z) + 18H(1, 1, 1, 0; z) \\
& + 18G(1 - z, 0, 1, 0; y) + 66G(1 - z, 1, 0; y) + 36G(1 - z, 1, 1, 0; y) \\
& - 36G(-z, 1 - z, 1, 0; y) - 36G(-z, 0, 1, 0; y) + 36G(0, 1 - z, 1, 0; y) + \frac{49}{3}G(0; y) \\
& + 160G(0, 0; y) - 36G(0, 0, 1, 0; y) - 30G(0, 1, 0; y) + 36G(0, 1, 1, 0; y) \\
& - 18G(1, 1 - z, 1, 0; y) + 71G(1, 0; y) - 126G(1, 0, 0; y) + 54G(1, 0, 1, 0; y) \\
& - 66G(1, 1, 0; y) + 36G(1, 1, 0, 0; y) - 36G(1, 1, 1, 0; y) \Big] \\
& + i\pi \left\{ -\frac{11}{16(1-z)^2}H(0; z) + \frac{1}{16(1-z)} \left[-11 - 22H(0; z) \right] \right. \\
& + 2\zeta_3 + \frac{1}{48} \left[-\frac{44\pi^2}{3} - \frac{2345}{18} - 11H(0; z) - 66H(0; z)G(0; y) \right. \\
& \left. \left. - 66H(1, 0; z) - 110G(0; y) + 66G(1, 0; y) \right] \right\}, \\
D_\alpha(y, z) = & \frac{1}{12y(1-z)}H(0; z) - \frac{1}{12y(1-y-z)}H(0; z) \\
& + \frac{z}{6(1-y-z)^2} \left[\frac{\pi^2}{6} + H(0; z)G(0; y) + H(1, 0; z) - G(1, 0; y) \right] \\
& + \frac{z}{4(1-y-z)} \left[-\frac{\pi^2}{3} + H(0; z) - 2H(0; z)G(0; y) - 2H(1, 0; z) - G(0; y) \right. \\
& \left. + 2G(1, 0; y) \right] \\
& + \frac{z^2}{4(1-y-z)^2} \left[-\frac{\pi^2}{6} - H(0; z)G(0; y) - H(1, 0; z) + G(1, 0; y) \right] \\
& - \frac{1}{12(1-y)}G(0; y) + \frac{1}{72(1-z)^2} \left[\pi^2 + 25H(0; z) - \frac{3}{2}H(0; z)G(0; y) - 9H(0, 0; z) \right. \\
& \left. + 6H(1, 0; z) \right] \\
& + \frac{1}{144(1-z)} \left[4\pi^2 + 38 + 37H(0; z) - 6H(0; z)G(0; y) - 36H(0, 0; z) + 24H(1, 0; z) \right. \\
& \left. - 3G(0; y) \right] \\
& + \frac{1}{12(1-y-z)} \left[H(0; z) + 2G(0; y) \right] \\
& + \frac{\pi^2}{72} \left[\frac{395}{12} - H(0; z) + 2G(1-z; y) - G(0; y) - 2G(1; y) \right] \\
& - \frac{19}{36}\zeta_3 + \frac{1}{144} \left[\frac{3661}{18} - 25H(0; z) + 24H(0; z)G(1-z, 0; y) \right. \\
& + 29H(0; z)G(0; y) - 36H(0; z)G(0, 0; y) + 6H(0; z)G(1, 0; y) - 28H(0, 0; z) \\
& - 36H(0, 0; z)G(0; y) - 6H(0, 1, 0; z) + 40H(1, 0; z) + 24H(1, 0; z)G(1-z; y) \\
& - 30H(1, 0; z)G(0; y) - 36H(1, 0, 0; z) - 24G(1-z, 1, 0; y) + 53G(0; y) \\
& - 82G(0, 0; y) + 6G(0, 1, 0; y) - 40G(1, 0; y) + 36G(1, 0, 0; y) + 24G(1, 1, 0; y) \Big] \\
& + i\pi \left\{ \frac{1}{8(1-z)^2}H(0; z) + \frac{1}{8(1-z)} \left[1 + 2H(0; z) \right] \right\}
\end{aligned}$$

$$\begin{aligned}
 & + \frac{1}{48} \left[\frac{8\pi^2}{3} - \frac{28}{3} + 13H(0; z) + 12H(0; z)G(0; y) + 12H(1, 0; z) + 31G(0; y) \right. \\
 & \left. - 12G(1, 0; y) \right] \Big\}, \\
 A_\beta(y, z) = & - \frac{z}{16(1-y)^2} G(0; y) - \frac{z}{16(1-y)} + \frac{z}{16(y+z)^2} \left[\frac{47\pi^2}{3} H(1; z) \right. \\
 & - \frac{47\pi^2}{3} G(1-z; y) - 94H(0; z)G(1-z, 0; y) - 94H(0, 1, 0; z) - 99H(1, 0; z) \\
 & - 94H(1, 0; z)G(1-z; y) + 94H(1, 0; z)G(0; y) + 94H(1, 1, 0; z) \\
 & + 94G(1-z, 1, 0; y) + 94G(0, 1, 0; y) - 99G(1, 0; y) \Big] \\
 & + \frac{z}{16(y+z)} \left[- \frac{47\pi^2}{3} + 11 + 44H(0; z) - 94H(0; z)G(0; y) - 94H(1, 0; z) - 55G(0; y) \right. \\
 & \left. + 94G(1, 0; y) \right] \\
 & + \frac{z}{12(1-y-z)^2} \left[\frac{5\pi^2}{6} - \frac{\pi^2}{2} H(1; z) - \frac{\pi^2}{4} G(0; y) + 3\zeta_3 + 5H(0; z)G(0; y) \right. \\
 & + 5H(1, 0; z) - \frac{3}{2} H(1, 0; z)G(0; y) - 3H(1, 1, 0; z) - \frac{3}{2} G(0, 1, 0; y) - 5G(1, 0; y) \Big] \\
 & + \frac{z}{12(1-y-z)} \left[- \frac{19\pi^2}{3} + 5H(0; z) - 38H(0; z)G(0; y) - 38H(1, 0; z) - \frac{53}{4} G(0; y) \right. \\
 & \left. + 38G(1, 0; y) \right] \\
 & + \frac{z^2}{8(y+z)^3} \left[- 11\pi^2 H(1; z) + 11\pi^2 G(1-z; y) + 66H(0; z)G(1-z, 0; y) \right. \\
 & + 66H(0, 1, 0; z) + 33H(1, 0; z) + 66H(1, 0; z)G(1-z; y) - 66H(1, 0; z)G(0; y) \\
 & - 66H(1, 1, 0; z) - 66G(1-z, 1, 0; y) - 66G(0, 1, 0; y) + 33G(1, 0; y) \Big] \\
 & + \frac{z^2}{16(y+z)^2} \left[+ 22\pi^2 - 33H(0; z) + 132H(0; z)G(0; y) + 132H(1, 0; z) + 33G(0; y) \right. \\
 & \left. - 132G(1, 0; y) \right] \\
 & + \frac{z^2}{16(y+z)} \left[11\pi^2 - 11H(0; z) + 66H(0; z)G(0; y) + 66H(1, 0; z) + 11G(0; y) \right. \\
 & \left. - 66G(1, 0; y) \right] \\
 & + \frac{z^2}{48(1-y-z)^2} \left[- \frac{53\pi^2}{6} - 53H(0; z)G(0; y) - 53H(1, 0; z) + 53G(1, 0; y) \right] \\
 & + \frac{z^2}{16(1-y-z)} \left[11\pi^2 - 11H(0; z) + 66H(0; z)G(0; y) + 66H(1, 0; z) + 11G(0; y) \right. \\
 & \left. - 66G(1, 0; y) \right] \\
 & + \frac{z^3}{8(y+z)^4} \left[\frac{11\pi^2}{2} H(1; z) - \frac{11\pi^2}{2} G(1-z; y) - 33H(0; z)G(1-z, 0; y) \right. \\
 & - 33H(0, 1, 0; z) - 33H(1, 0; z)G(1-z; y) + 33H(1, 0; z)G(0; y) + 33H(1, 1, 0; z) \\
 & \left. + 33G(1-z, 1, 0; y) + 33G(0, 1, 0; y) \right]
 \end{aligned}$$

$$\begin{aligned}
& + \frac{z^3}{8(y+z)^3} \left[-\frac{11\pi^2}{2} - 33H(0; z)G(0; y) - 33H(1, 0; z) + 33G(1, 0; y) \right] \\
& + \frac{z^3}{16(y+z)^2} \left[-\frac{11\pi^2}{2} - 33H(0; z)G(0; y) - 33H(1, 0; z) + 33G(1, 0; y) \right] \\
& + \frac{z^3}{8(y+z)} \left[-\frac{11\pi^2}{6} - 11H(0; z)G(0; y) - 11H(1, 0; z) + 11G(1, 0; y) \right] \\
& + \frac{z^3}{16(1-y-z)^2} \left[\frac{11\pi^2}{6} + 11H(0; z)G(0; y) + 11H(1, 0; z) - 11G(1, 0; y) \right] \\
& + \frac{z^3}{8(1-y-z)} \left[-\frac{11\pi^2}{6} - 11H(0; z)G(0; y) - 11H(1, 0; z) + 11G(1, 0; y) \right] \\
& + \frac{5}{24(1-y)}G(0; y) + \frac{1}{48(1-z)} \left[\pi^2 \left(\frac{1}{6} - 3H(0; z) - 3H(1; z) + G(1-z; y) \right. \right. \\
& \quad \left. \left. - G(0; y) \right) - 6\zeta_3 + \frac{355}{6}H(0; z) + 6H(0; z)G(1-z, 0; y) - 10H(0; z)G(0; y) \right. \\
& \quad \left. - 45H(0, 0; z) - 12H(0, 0; z)G(0; y) - 18H(0, 1, 0; z) + H(1, 0; z) \right. \\
& \quad \left. + 6H(1, 0; z)G(1-z; y) - 6H(1, 0; z)G(0; y) - 12H(1, 0, 0; z) - 18H(1, 1, 0; z) \right. \\
& \quad \left. - 6G(1-z, 1, 0; y) + 6G(0, 1, 0; y) \right] \\
& + \frac{1}{8(y+z)} \left[-\frac{7\pi^2}{3}H(1; z) + \frac{7\pi^2}{3}G(1-z; y) + 14H(0; z)G(1-z, 0; y) \right. \\
& \quad \left. + 14H(0, 1, 0; z) + 25H(1, 0; z) + 14H(1, 0; z)G(1-z; y) - 14H(1, 0; z)G(0; y) \right. \\
& \quad \left. - 14H(1, 1, 0; z) - 14G(1-z, 1, 0; y) - 14G(0, 1, 0; y) + 25G(1, 0; y) \right] \\
& + \frac{1}{8(1-y-z)^2} \left[\frac{\pi^2}{3}H(1; z) + \frac{\pi^2}{6}G(0; y) - 2\zeta_3 + H(1, 0; z)G(0; y) \right. \\
& \quad \left. + 2H(1, 1, 0; z) + G(0, 1, 0; y) \right] \\
& + \frac{1}{24(1-y-z)} \left[\frac{13\pi^2}{6} + 10H(0; z)G(0; y) + 13H(1, 0; z) + 10G(0; y) \right. \\
& \quad \left. - 7G(1, 0; y) \right] \\
& + \frac{\pi^2}{288} \left[-\frac{946}{3} - 5H(0; z) + 12H(0; z)G(1-z; y) + 36H(0; z)G(0; y) \right. \\
& \quad \left. - 12H(0; z)G(1; y) + 24H(0, 1; z) + 24H(1; z)G(1-z; y) - 24H(1; z)G(-z; y) \right. \\
& \quad \left. - 12H(1; z)G(1; y) + 24H(1, 0; z) + 12H(1, 1; z) - 44G(1-z; y) + 12G(1-z, 0; y) \right. \\
& \quad \left. - 24G(1-z, 1; y) + 24G(-z, 1-z; y) - 24G(0, 1-z; y) + 49G(0; y) - 24G(0, 1; y) \right. \\
& \quad \left. + 12G(1, 1-z; y) + 44G(1; y) - 36G(1, 0; y) + 24G(1, 1; y) \right] \\
& + \frac{11\pi^4}{360} + \frac{\zeta_3}{72} \left[317 - 18H(0; z) + 90H(1; z) - 72G(1-z; y) - 18G(0; y) - 18G(1; y) \right] \\
& + \frac{1}{144} \left[-\frac{79987}{72} + \frac{1735}{6}H(0; z) - 132H(0; z)G(1-z, 0; y) \right. \\
& \quad \left. - 36H(0; z)G(1-z, 1, 0; y) + 72H(0; z)G(-z, 1-z, 0; y) \right. \\
& \quad \left. - 72H(0; z)G(0, 1-z, 0; y) - 150H(0; z)G(0; y) + 252H(0; z)G(0, 0; y) \right. \\
& \quad \left. - 36H(0; z)G(0, 1, 0; y) + 36H(0; z)G(1, 1-z, 0; y) - 6H(0; z)G(1, 0; y) \right. \\
& \quad \left. - 72H(0; z)G(1, 0, 0; y) + 23H(0, 0; z) + 144H(0, 0; z)G(0; y) \right]
\end{aligned}$$

$$\begin{aligned}
& +72H(0,0;z)G(0,0;y) + 144H(0,0,1,0;z) + 6H(0,1,0;z) \\
& -36H(0,1,0;z)G(1-z;y) + 72H(0,1,0;z)G(-z;y) + 36H(0,1,0;z)G(0;y) \\
& -36H(0,1,0;z)G(1;y) + 72H(0,1,1,0;z) - 160H(1,0;z) \\
& -132H(1,0;z)G(1-z;y) + 36H(1,0;z)G(1-z,0;y) \\
& +72H(1,0;z)G(-z,1-z;y) - 72H(1,0;z)G(-z,0;y) \\
& -72H(1,0;z)G(0,1-z;y) + 192H(1,0;z)G(0;y) + 36H(1,0;z)G(1,1-z;y) \\
& -36H(1,0;z)G(1,0;y) + 144H(1,0,0;z) + 72H(1,0,0;z)G(0;y) \\
& +144H(1,0,1,0;z) + 72H(1,1,0;z)G(1-z;y) - 72H(1,1,0;z)G(-z;y) \\
& -36H(1,1,0;z)G(1;y) + 72H(1,1,0,0;z) + 36H(1,1,1,0;z) \\
& +36G(1-z,0,1,0;y) + 132G(1-z,1,0;y) + 72G(1-z,1,1,0;y) \\
& -72G(-z,1-z,1,0;y) - 72G(-z,0,1,0;y) + 72G(0,1-z,1,0;y) + \frac{8}{3}G(0;y) \\
& +320G(0,0;y) - 72G(0,0,1,0;y) - 60G(0,1,0;y) + 72G(0,1,1,0;y) \\
& -36G(1,1-z,1,0;y) + 160G(1,0;y) - 252G(1,0,0;y) + 108G(1,0,1,0;y) \\
& -132G(1,1,0;y) + 72G(1,1,0,0;y) - 72G(1,1,1,0;y) \Big] \\
& +i\pi \left\{ \frac{11}{16(1-z)}H(0;z) + 2\zeta_3 + \frac{1}{48} \left[-\frac{44\pi^2}{3} - \frac{1751}{18} - 11H(0;z) - 66H(0;z)G(0;y) \right. \right. \\
& \left. \left. - 66H(1,0;z) - 110G(0;y) + 66G(1,0;y) \right] \right\},
\end{aligned}$$

$$D_\beta(y,z) =$$

$$\begin{aligned}
& \frac{z}{4(y+z)^2} \left[-\frac{4\pi^2}{3}H(1;z) + \frac{4\pi^2}{3}G(1-z;y) + 8H(0;z)G(1-z,0;y) + 8H(0,1,0;z) \right. \\
& +9H(1,0;z) + 8H(1,0;z)G(1-z;y) - 8H(1,0;z)G(0;y) - 8H(1,1,0;z) \\
& \left. -8G(1-z,1,0;y) - 8G(0,1,0;y) + 9G(1,0;y) \right] \\
& + \frac{z}{4(y+z)} \left[\frac{4\pi^2}{3} - 1 - 4H(0;z) + 8H(0;z)G(0;y) + 8H(1,0;z) + 5G(0;y) \right. \\
& \left. -8G(1,0;y) \right] \\
& + \frac{z}{6(1-y-z)^2} \left[-\frac{\pi^2}{6} - H(0;z)G(0;y) - H(1,0;z) + G(1,0;y) \right] \\
& + \frac{z}{12(1-y-z)} \left[\frac{7\pi^2}{3} - 2H(0;z) + 14H(0;z)G(0;y) + 14H(1,0;z) \right. \\
& \left. +5G(0;y) - 14G(1,0;y) \right] \\
& + \frac{z^2}{2(y+z)^3} \left[\pi^2H(1;z) - \pi^2G(1-z;y) - 6H(0;z)G(1-z,0;y) - 6H(0,1,0;z) \right. \\
& -3H(1,0;z) - 6H(1,0;z)G(1-z;y) + 6H(1,0;z)G(0;y) + 6H(1,1,0;z) \\
& \left. +6G(1-z,1,0;y) + 6G(0,1,0;y) - 3G(1,0;y) \right] \\
& + \frac{z^2}{4(y+z)^2} \left[-2\pi^2 + 3H(0;z) - 12H(0;z)G(0;y) - 12H(1,0;z) - 3G(0;y) \right. \\
& \left. +12G(1,0;y) \right]
\end{aligned}$$

$$\begin{aligned}
& + \frac{z^2}{4(y+z)} \left[-\pi^2 + H(0; z) - 6H(0; z)G(0; y) - 6H(1, 0; z) - G(0; y) + 6G(1, 0; y) \right] \\
& + \frac{z^2}{12(1-y-z)^2} \left[\frac{5\pi^2}{6} + 5H(0; z)G(0; y) + 5H(1, 0; z) - 5G(1, 0; y) \right] \\
& + \frac{z^2}{4(1-y-z)} \left[-\pi^2 + H(0; z) - 6H(0; z)G(0; y) - 6H(1, 0; z) - G(0; y) + 6G(1, 0; y) \right] \\
& + \frac{z^3}{2(y+z)^4} \left[-\frac{\pi^2}{2}H(1; z) + \frac{\pi^2}{2}G(1-z; y) + 3H(0; z)G(1-z, 0; y) + 3H(0, 1, 0; z) \right. \\
& + 3H(1, 0; z)G(1-z; y) - 3H(1, 0; z)G(0; y) - 3H(1, 1, 0; z) - 3G(1-z, 1, 0; y) \\
& \left. - 3G(0, 1, 0; y) \right] \\
& + \frac{z^3}{2(y+z)^3} \left[\frac{\pi^2}{2} + 3H(0; z)G(0; y) + 3H(1, 0; z) - 3G(1, 0; y) \right] \\
& + \frac{z^3}{4(y+z)^2} \left[\frac{\pi^2}{2} + 3H(0; z)G(0; y) + 3H(1, 0; z) - 3G(1, 0; y) \right] \\
& + \frac{z^3}{2(y+z)} \left[\frac{\pi^2}{6} + H(0; z)G(0; y) + H(1, 0; z) - G(1, 0; y) \right] \\
& + \frac{z^3}{4(1-y-z)^2} \left[-\frac{\pi^2}{6} - H(0; z)G(0; y) - H(1, 0; z) + G(1, 0; y) \right] \\
& + \frac{z^3}{2(1-y-z)} \left[\frac{\pi^2}{6} + H(0; z)G(0; y) + H(1, 0; z) - G(1, 0; y) \right] \\
& - \frac{1}{12(1-y)}G(0; y) + \frac{1}{72(1-z)} \left[-\pi^2 - 25H(0; z) + \frac{3}{2}H(0; z)G(0; y) + 9H(0, 0; z) \right. \\
& \left. - 6H(1, 0; z) \right] \\
& + \frac{1}{2(y+z)} \left[\frac{\pi^2}{6}H(1; z) - \frac{\pi^2}{6}G(1-z; y) - H(0; z)G(1-z, 0; y) \right. \\
& - H(0, 1, 0; z) - 2H(1, 0; z) - H(1, 0; z)G(1-z; y) + H(1, 0; z)G(0; y) \\
& + H(1, 1, 0; z) + G(1-z, 1, 0; y) + G(0, 1, 0; y) - 2G(1, 0; y) \left. \right] \\
& + \frac{1}{6(1-y-z)} \left[-\frac{\pi^2}{6} - H(0; z)G(0; y) - H(1, 0; z) - G(0; y) + G(1, 0; y) \right] \\
& + \frac{\pi^2}{72} \left[\frac{395}{12} - H(0; z) + 2G(1-z; y) - G(0; y) - 2G(1; y) \right] \\
& - \frac{19}{36}\zeta_3 + \frac{1}{144} \left[\frac{2977}{18} - 10H(0; z) + 24H(0; z)G(1-z, 0; y) \right. \\
& + 29H(0; z)G(0; y) - 36H(0; z)G(0, 0; y) + 6H(0; z)G(1, 0; y) - 28H(0, 0; z) \\
& - 36H(0, 0; z)G(0; y) - 6H(0, 1, 0; z) + 40H(1, 0; z) + 24H(1, 0; z)G(1-z; y) \\
& - 30H(1, 0; z)G(0; y) - 36H(1, 0, 0; z) - 24G(1-z, 1, 0; y) + 56G(0; y) \\
& - 82G(0, 0; y) + 6G(0, 1, 0; y) - 40G(1, 0; y) + 36G(1, 0, 0; y) + 24G(1, 1, 0; y) \left. \right] \\
& + i\pi \left\{ -\frac{1}{8(1-z)}H(0; z) + \frac{1}{48} \left[\frac{8\pi^2}{3} - \frac{46}{3} + 13H(0; z) + 12H(0; z)G(0; y) \right. \right. \\
& \left. \left. + 12H(1, 0; z) + 31G(0; y) - 12G(1, 0; y) \right] \right\},
\end{aligned}$$

$$\begin{aligned}
A_\gamma(y, z) = & + \frac{1}{48y(1-z)} \left[-\pi^2 + 13H(0; z) - 6H(1, 0; z) - 6G(1, 0; y) \right] \\
& + \frac{1}{48y(1-y-z)} \left[\pi^2 - 13H(0; z) + 6H(1, 0; z) + 6G(1, 0; y) \right] \\
& + \frac{z}{16(y+z)^2} \left[-\frac{11\pi^2}{3}H(1; z) + \frac{11\pi^2}{3}G(1-z; y) + 22H(0; z)G(1-z, 0; y) \right. \\
& + 22H(0, 1, 0; z) + 55H(1, 0; z) + 22H(1, 0; z)G(1-z; y) - 22H(1, 0; z)G(0; y) \\
& - 22H(1, 1, 0; z) - 22G(1-z, 1, 0; y) - 22G(0, 1, 0; y) + 55G(1, 0; y) \left. \right] \\
& + \frac{z}{16(y+z)} \left[\frac{11\pi^2}{3} - 11 - 22H(0; z) + 22H(0; z)G(0; y) + 22H(1, 0; z) \right. \\
& + 33G(0; y) - 22G(1, 0; y) \left. \right] \\
& + \frac{z}{8(1-y-z)^2} \left[\frac{\pi^2}{3}H(1; z) + \frac{\pi^2}{6}G(0; y) - 2\zeta_3 + H(1, 0; z)G(0; y) \right. \\
& + 2H(1, 1, 0; z) + G(0, 1, 0; y) \left. \right] \\
& + \frac{z}{48(1-y-z)} \left[\frac{10\pi^2}{3} + 13H(0; z) + 20H(0; z)G(0; y) + 20H(1, 0; z) \right. \\
& + 20G(0; y) - 20G(1, 0; y) \left. \right] \\
& + \frac{z^2}{8(y+z)^3} \left[\frac{22\pi^2}{3}H(1; z) - \frac{22\pi^2}{3}G(1-z; y) - 44H(0; z)G(1-z, 0; y) \right. \\
& - 44H(0, 1, 0; z) - 33H(1, 0; z) - 44H(1, 0; z)G(1-z; y) + 44H(1, 0; z)G(0; y) \\
& + 44H(1, 1, 0; z) + 44G(1-z, 1, 0; y) + 44G(0, 1, 0; y) - 33G(1, 0; y) \left. \right] \\
& + \frac{z^2}{16(y+z)^2} \left[-\frac{44\pi^2}{3} + 33H(0; z) - 88H(0; z)G(0; y) - 88H(1, 0; z) - 33G(0; y) \right. \\
& + 88G(1, 0; y) \left. \right] \\
& + \frac{z^2}{16(y+z)} \left[-\frac{22\pi^2}{3} + 11H(0; z) - 44H(0; z)G(0; y) - 44H(1, 0; z) - 11G(0; y) \right. \\
& + 44G(1, 0; y) \left. \right] \\
& + \frac{z^2}{12(1-y-z)^2} \left[\frac{5\pi^2}{6} + 5H(0; z)G(0; y) + 5H(1, 0; z) - 5G(1, 0; y) \right] \\
& + \frac{z^2}{16(1-y-z)} \left[-\frac{22\pi^2}{3} + 11H(0; z) - 44H(0; z)G(0; y) - 44H(1, 0; z) - 11G(0; y) \right. \\
& + 44G(1, 0; y) \left. \right] \\
& + \frac{z^3}{8(y+z)^4} \left[-\frac{11\pi^2}{2}H(1; z) + \frac{11\pi^2}{2}G(1-z; y) + 33H(0; z)G(1-z, 0; y) \right. \\
& + 33H(0, 1, 0; z) + 33H(1, 0; z)G(1-z; y) - 33H(1, 0; z)G(0; y) - 33H(1, 1, 0; z) \\
& - 33G(1-z, 1, 0; y) - 33G(0, 1, 0; y) \left. \right] \\
& + \frac{z^3}{8(y+z)^3} \left[\frac{11\pi^2}{2} + 33H(0; z)G(0; y) + 33H(1, 0; z) - 33G(1, 0; y) \right]
\end{aligned}$$

$$\begin{aligned}
 & + \frac{z^3}{16(y+z)^2} \left[\frac{11\pi^2}{2} + 33H(0; z)G(0; y) + 33H(1, 0; z) - 33G(1, 0; y) \right] \\
 & + \frac{z^3}{8(y+z)} \left[\frac{11\pi^2}{6} + 11H(0; z)G(0; y) + 11H(1, 0; z) - 11G(1, 0; y) \right] \\
 & + \frac{z^3}{16(1-y-z)^2} \left[-\frac{11\pi^2}{6} - 11H(0; z)G(0; y) - 11H(1, 0; z) + 11G(1, 0; y) \right] \\
 & + \frac{z^3}{8(1-y-z)} \left[\frac{11\pi^2}{6} + 11H(0; z)G(0; y) + 11H(1, 0; z) - 11G(1, 0; y) \right] \\
 & + \frac{1}{48(1-z)^2} \left[\pi^2 \left(\frac{1}{6} - 3H(0; z) - 3H(1; z) + G(1-z; y) - G(0; y) \right) - 6\zeta_3 \right. \\
 & + \frac{355}{6}H(0; z) + 6H(0; z)G(1-z, 0; y) - 10H(0; z)G(0; y) - 45H(0, 0; z) \\
 & - 12H(0, 0; z)G(0; y) - 18H(0, 1, 0; z) + H(1, 0; z) + 6H(1, 0; z)G(1-z; y) \\
 & - 6H(1, 0; z)G(0; y) - 12H(1, 0, 0; z) - 18H(1, 1, 0; z) - 6G(1-z, 1, 0; y) \\
 & \left. + 6G(0, 1, 0; y) \right] \\
 & + \frac{1}{48(1-z)} \left[\pi^2 \left(-\frac{7}{6} + 3H(0; z) + 3H(1; z) - G(1-z; y) + G(0; y) \right) + 6\zeta_3 + \frac{277}{6} \right. \\
 & - \frac{493}{6}H(0; z) - 6H(0; z)G(1-z, 0; y) + 4H(0; z)G(0; y) + 45H(0, 0; z) \\
 & + 12H(0, 0; z)G(0; y) + 18H(0, 1, 0; z) - 7H(1, 0; z) - 6H(1, 0; z)G(1-z; y) \\
 & + 6H(1, 0; z)G(0; y) + 12H(1, 0, 0; z) + 18H(1, 1, 0; z) + 6G(1-z, 1, 0; y) \\
 & \left. - 10G(0; y) - 6G(0, 1, 0; y) + 6G(1, 0; y) \right] \\
 & + \frac{1}{48(1-y-z)} \left[-\pi^2 + 13H(0; z) - 6H(1, 0; z) - 6G(1, 0; y) \right] \\
 & + \frac{1}{48} \left[\pi^2 - \frac{277}{6} + 23H(0; z) + 6H(0; z)G(0; y) + 6H(1, 0; z) + 10G(0; y) - 6G(1, 0; y) \right] \\
 & + i\pi \left\{ \frac{11}{16(1-z)^2} H(0; z) + \frac{11}{16(1-z)} \left[1 - H(0; z) \right] - \frac{11}{16} \right\}, \\
 D_\gamma(y; z) = & \\
 & - \frac{1}{12y(1-z)} H(0; z) + \frac{1}{12y(1-y-z)} H(0; z) + \frac{z}{4(y+z)^2} \left[\frac{\pi^2}{3} H(1; z) \right. \\
 & - \frac{\pi^2}{3} G(1-z; y) - 2H(0; z)G(1-z, 0; y) - 2H(0, 1, 0; z) - 5H(1, 0; z) \\
 & - 2H(1, 0; z)G(1-z; y) + 2H(1, 0; z)G(0; y) + 2H(1, 1, 0; z) + 2G(1-z, 1, 0; y) \\
 & \left. + 2G(0, 1, 0; y) - 5G(1, 0; y) \right] \\
 & + \frac{z}{4(y+z)} \left[-\frac{\pi^2}{3} + 1 + 2H(0; z) - 2H(0; z)G(0; y) - 2H(1, 0; z) - 3G(0; y) \right. \\
 & \left. + 2G(1, 0; y) \right] \\
 & + \frac{z}{12(1-y-z)} \left[-\frac{\pi^2}{3} - H(0; z) - 2H(0; z)G(0; y) - 2H(1, 0; z) - 2G(0; y) \right. \\
 & \left. + 2G(1, 0; y) \right]
 \end{aligned}$$

$$\begin{aligned}
& + \frac{z^2}{2(y+z)^3} \left[-\frac{2\pi^2}{3} H(1; z) + \frac{2\pi^2}{3} G(1-z; y) + 4H(0; z)G(1-z, 0; y) + 4H(0, 1, 0; z) \right. \\
& + 3H(1, 0; z) + 4H(1, 0; z)G(1-z; y) - 4H(1, 0; z)G(0; y) - 4H(1, 1, 0; z) \\
& \left. - 4G(1-z, 1, 0; y) - 4G(0, 1, 0; y) + 3G(1, 0; y) \right] \\
& + \frac{z^2}{4(y+z)^2} \left[\frac{4\pi^2}{3} - 3H(0; z) + 8H(0; z)G(0; y) + 8H(1, 0; z) + 3G(0; y) \right. \\
& \left. - 8G(1, 0; y) \right] \\
& + \frac{z^2}{4(y+z)} \left[\frac{2\pi^2}{3} - H(0; z) + 4H(0; z)G(0; y) + 4H(1, 0; z) + G(0; y) \right. \\
& \left. - 4G(1, 0; y) \right] \\
& + \frac{z^2}{6(1-y-z)^2} \left[-\frac{\pi^2}{6} - H(0; z)G(0; y) - H(1, 0; z) + G(1, 0; y) \right] \\
& + \frac{z^2}{4(1-y-z)} \left[\frac{2\pi^2}{3} - H(0; z) + 4H(0; z)G(0; y) + 4H(1, 0; z) + G(0; y) \right. \\
& \left. - 4G(1, 0; y) \right] \\
& + \frac{z^3}{2(y+z)^4} \left[\frac{\pi^2}{2} H(1; z) - \frac{\pi^2}{2} G(1-z; y) - 3H(0; z)G(1-z, 0; y) \right. \\
& - 3H(0, 1, 0; z) - 3H(1, 0; z)G(1-z; y) + 3H(1, 0; z)G(0; y) + 3H(1, 1, 0; z) \\
& \left. + 3G(1-z, 1, 0; y) + 3G(0, 1, 0; y) \right] \\
& + \frac{z^3}{2(y+z)^3} \left[-\frac{\pi^2}{2} - 3H(0; z)G(0; y) - 3H(1, 0; z) + 3G(1, 0; y) \right] \\
& + \frac{z^3}{4(y+z)^2} \left[-\frac{\pi^2}{2} - 3H(0; z)G(0; y) - 3H(1, 0; z) + 3G(1, 0; y) \right] \\
& + \frac{z^3}{2(y+z)} \left[-\frac{\pi^2}{6} - H(0; z)G(0; y) - H(1, 0; z) + G(1, 0; y) \right] \\
& + \frac{z^3}{4(1-y-z)^2} \left[\frac{\pi^2}{6} + H(0; z)G(0; y) + H(1, 0; z) - G(1, 0; y) \right] \\
& + \frac{z^3}{2(1-y-z)} \left[-\frac{\pi^2}{6} - H(0; z)G(0; y) - H(1, 0; z) + G(1, 0; y) \right] \\
& + \frac{1}{72(1-z)^2} \left[-\pi^2 - 25H(0; z) + \frac{3}{2}H(0; z)G(0; y) + 9H(0, 0; z) - 6H(1, 0; z) \right] \\
& + \frac{1}{144(1-z)} \left[2\pi^2 - 38 + 65H(0; z) - 3H(0; z)G(0; y) - 18H(0, 0; z) + 12H(1, 0; z) \right. \\
& \left. + 3G(0; y) \right] \\
& - \frac{1}{12(1-y-z)} H(0; z) + \frac{19}{72} - \frac{5}{48} H(0; z) - \frac{1}{48} G(0; y) + i\pi \left\{ -\frac{1}{8(1-z)^2} H(0; z) \right. \\
& \left. + \frac{1}{8(1-z)} \left[-1 + H(0; z) \right] + \frac{1}{8} \right\}. \tag{D.2}
\end{aligned}$$

APPENDIX E

One-Loop Master Integrals

In this appendix, we list the expansions for the one-loop master integrals appearing in $\langle \mathcal{M}^{(0)} | \mathcal{M}^{(1)} \rangle$ and $\langle \mathcal{M}^{(1)} | \mathcal{M}^{(1)} \rangle$. These squared amplitudes can be expressed in terms of only two master integrals evaluated at $D = 4 - 2\epsilon$,

$$\begin{aligned} \text{Bub}(s_{12}) &= \text{Diagram: a circle with an incoming line from the left labeled } p_{12} \text{ and an outgoing line to the right,} \\ &= \int \frac{d^D k_1}{(2\pi)^D} \frac{1}{k_1^2 (k_1 + p_{12})^2}, \end{aligned} \quad (\text{E.1})$$

$$\begin{aligned} \text{Box}(s_{23}, s_{13}, s_{123}) &= \text{Diagram: a square with vertices labeled } p_1 \text{ (bottom-left), } p_2 \text{ (bottom-right), } p_3 \text{ (top-right), and } p_{123} \text{ (top-left).} \\ &= \int \frac{d^D k_1}{(2\pi)^D} \frac{1}{k_1^2 (k_1 - p_2)^2 (k_1 - p_2 - p_3)^2 (k_1 - p_1 - p_2 - p_3)^2}. \end{aligned} \quad (\text{E.2})$$

Note that in Chapter 4 we have written the one-loop functions f_1 and f_2 in terms of the one-loop box integral in $D = 6 - 2\epsilon$. This is straightforwardly related to the box integral in $D = 4 - 2\epsilon$ dimensions by

$$\begin{aligned} \text{Box}^6(s_{23}, s_{13}, s_{123}) &= -\frac{s_{13}s_{23}}{2(D-3)s_{12}} \text{Box}(s_{23}, s_{13}, s_{123}) \\ &\quad - \frac{2}{s_{12}(D-4)} (\text{Bub}(s_{13}) + \text{Bub}(s_{23}) - \text{Bub}(s_{123})). \end{aligned} \quad (\text{E.3})$$

Closed expressions for these integrals for symbolic D in terms of Γ -functions and the ${}_2F_1$ hypergeometric function have been known for a long time (see e.g. [25, 45]). The bubble integral reads

$$\text{Bub}(s_{12}) = i \frac{(4\pi)^\epsilon \Gamma(1+\epsilon) \Gamma^2(1-\epsilon)}{16\pi^2 \Gamma(1-2\epsilon)} (-s_{12})^{-\epsilon} \frac{1}{\epsilon(1-2\epsilon)}. \quad (\text{E.4})$$

In the present context, an expansion of the box integral to the second order in ϵ is required.

$$\begin{aligned} \text{Box}(s_{23}, s_{13}, s_{123}) = i \frac{(4\pi)^\epsilon \Gamma(1+\epsilon) \Gamma^2(1-\epsilon)}{16\pi^2 \Gamma(1-2\epsilon)} (-s_{123})^{-2-\epsilon} \times \\ \frac{1}{yz} \sum_{i=-2}^2 \frac{l_{4.1,i} \left(\frac{s_{13}}{s_{123}}, \frac{s_{23}}{s_{123}} \right)}{\epsilon^i} + \mathcal{O}(\epsilon^3), \quad (\text{E.5}) \end{aligned}$$

with

$$l_{4.1,2}(y, z) = 2, \quad (\text{E.6})$$

$$l_{4.1,1}(y, z) = -2H(0; z) - 2G(0; y), \quad (\text{E.7})$$

$$\begin{aligned} l_{4.1,0}(y, z) = 2H(0; z)G(0; y) + 2H(0, 0; z) + 2H(1, 0; z) + 2G(0, 0; y) - 2G(1, 0; y) \\ + \frac{\pi^2}{3}, \quad (\text{E.8}) \end{aligned}$$

$$\begin{aligned} l_{4.1,-1}(y, z) = 2H(0; z)G(1-z, 0; y) + 2H(1, 0; z)G(1-z; y) - 2H(1, 0; z)G(0; y) \\ - 2H(0; z)G(0, 0; y) - 2H(0, 1, 0; z) - 2H(1, 0, 0; z) - 2H(1, 1, 0; z) \\ - 2H(0, 0; z)G(0; y) - 2H(0, 0, 0; z) - 2G(1-z, 1, 0; y) - 2G(0, 0, 0; y) \\ + 2G(0, 1, 0; y) + 2G(1, 0, 0; y) \\ + \frac{\pi^2}{3} [-H(0; z) - H(1; z) + G(1-z; y) - G(0; y)], \quad (\text{E.9}) \end{aligned}$$

$$\begin{aligned} l_{4.1,-2}(y, z) = 2H(0; z)G(1-z, 1-z, 0; y) + 2H(0, 0, 0; z)G(0; y) + 2H(0, 0, 0, 0; z) \\ - 2H(0; z)G(1-z, 0, 0; y) - 2H(0, 0; z)G(1-z, 0; y) + 2H(0, 0, 1, 0; z) \\ + 2H(1, 0; z)G(1-z, 1-z; y) + 2H(0; z)G(0, 0, 0; y) + 2H(0, 1, 0, 0; z) \\ - 2H(1, 0; z)G(0, 1-z; y) + 2H(0, 0; z)G(0, 0; y) + 2H(0, 1, 1, 0; z) \\ - 2H(0; z)G(0, 1-z, 0; y) - 2H(1, 1, 0; z)G(1-z; y) + 2H(1, 0, 0, 0; z) \\ + 2H(1, 1, 0; z)G(0; y) - 2H(0, 1, 0; z)G(1-z; y) + 2H(0, 1, 0; z)G(0; y) \\ - 2H(1, 0; z)G(1-z, 0; y) + 2G(1-z, 0, 1, 0; y) + 2G(1-z, 1, 0, 0; y) \\ + 2G(0, 0, 0, 0; y) - 2G(1-z, 1-z, 1, 0; y) - 2H(1, 0, 0; z)G(1-z; y) \\ + 2H(1, 0; z)G(0, 0; y) + 2H(1, 0, 0; z)G(0; y) + 2G(0, 1-z, 1, 0; y) \end{aligned}$$

$$\begin{aligned}
& +2H(1, 0, 1, 0; z) + 2H(1, 1, 0, 0; z) + 2H(1, 1, 1, 0; z) - 2G(0, 0, 1, 0; y) \\
& - 2G(0, 1, 0, 0; y) - 2G(1, 0, 0, 0; y) + \frac{7\pi^4}{180} \\
& + \frac{\pi^2}{3} \left[-H(0; z)G(1 - z; y) + H(0; z)G(0; y) + H(0, 0; z) + H(0, 1; z) \right. \\
& - G(1 - z, 0; y) + H(1; z)G(0; y) + H(1, 0; z) + H(1, 1; z) + G(0, 0; y) \\
& \left. - H(1; z)G(1 - z; y) + G(1 - z, 1 - z; y) - G(0, 1 - z; y) \right]. \quad (E.10)
\end{aligned}$$

APPENDIX F

Harmonic Polylogarithms

The generalised polylogarithms $S_{n,p}(x)$ of Nielsen [102] turn out to be insufficient for the computation of multi-scale integrals beyond one loop. To overcome this limitation, one has to extend generalised polylogarithms to *harmonic polylogarithms* [47, 48, 103].

Harmonic polylogarithms are obtained by the repeated integration of rational factors. If these rational factors contain, besides the integration variable, only constants, the resulting functions are one-dimensional harmonic polylogarithms (or simply harmonic polylogarithms, HPLs) [103, 104]. If the rational factors depend on a further variable, one obtains two-dimensional harmonic polylogarithms (2dHPLs) [47, 48, 105]. In the following, we define both classes of functions, and summarise their properties.

F.1 One-Dimensional Harmonic Polylogarithms

The HPLs, introduced in [103], are one-variable functions $H(\vec{a}; x)$ depending, besides the argument x , on a set of indices, grouped for convenience into the vector \vec{a} , whose components can take one of the three values $(1, 0, -1)$ and whose number is the

weight w of the HPL. More explicitly, the three HPLs with $w = 1$ are defined as

$$\begin{aligned} H(1; x) &= \int_0^x \frac{dx'}{1-x'} = -\ln(1-x), \\ H(0; x) &= \ln x, \\ H(-1; x) &= \int_0^x \frac{dx'}{1+x'} = \ln(1+x); \end{aligned} \tag{F.1}$$

their derivatives can be written as

$$\frac{d}{dx} H(a; x) = f(a; x), \quad a = 1, 0, -1, \tag{F.2}$$

where the 3 rational fractions $f(a; x)$ are given by

$$\begin{aligned} f(1; x) &= \frac{1}{1-x}, \\ f(0; x) &= \frac{1}{x}, \\ f(-1; x) &= \frac{1}{1+x}. \end{aligned} \tag{F.3}$$

For weight w larger than 1, write $\vec{a} = (a, \vec{b})$, where a is the leftmost component of \vec{a} and \vec{b} stands for the vector of the remaining $(w-1)$ components. The harmonic polylogarithms of weight w are then defined as follows: if all the w components of \vec{a} take the value 0, \vec{a} is said to take the value $\vec{0}_w$ and

$$H(\vec{0}_w; x) = \frac{1}{w!} \ln^w x, \tag{F.4}$$

while, if $\vec{a} \neq \vec{0}_w$,

$$H(\vec{a}; x) = \int_0^x dx' f(a; x') H(\vec{b}; x'). \tag{F.5}$$

In any case the derivatives can be written in the compact form

$$\frac{d}{dx} H(\vec{a}; x) = f(a; x) H(\vec{b}; x), \tag{F.6}$$

where, again, a is the leftmost component of \vec{a} and \vec{b} stands for the remaining $(w-1)$ components.

It is immediate to see, from the very definition Equation (F.5), that there are 3^w HPLs of weight w , and that they are linearly independent. The HPLs are generalisations of Nielsen's polylogarithms [102]. The function $S_{n,p}(x)$, in Nielsen's notation, is equal to the HPL whose first n indices are all equal to 0 and the remaining p indices all equal to 1:

$$S_{n,p}(x) = H(\vec{0}_n, \vec{1}_p; x); \quad (\text{F.7})$$

in particular the Euler polylogarithms $\text{Li}_n(x) = S_{n-1,1}(x)$ correspond to

$$\text{Li}_n(x) = H(\vec{0}_{n-1}, 1; x). \quad (\text{F.8})$$

As shown in [103], the product of two HPLs of a same argument x and weights p, q can be expressed as a combination of HPLs of that argument and weight $r = p + q$, according to the product identity

$$H(\vec{p}; x)H(\vec{q}; x) = \sum_{\vec{r}=\vec{p} \uplus \vec{q}} H(\vec{r}; x), \quad (\text{F.9})$$

where \vec{p} and \vec{q} stand for the p and q components of the indices of the two HPLs, while $\vec{p} \uplus \vec{q}$ represents all mergers of \vec{p} and \vec{q} into the vector \vec{r} with r components, in which the relative orders of the elements of \vec{p} and \vec{q} are preserved.

The explicit formulae relevant up to weight 4 are

$$H(a; x)H(b; x) = H(a, b; x) + H(b, a; x), \quad (\text{F.10})$$

$$H(a; x)H(b, c; x) = H(a, b, c; x) + H(b, a, c; x) + H(b, c, a; x), \quad (\text{F.11})$$

$$\begin{aligned} H(a; x)H(b, c, d; x) &= H(a, b, c, d; x) + H(b, a, c, d; x) + H(b, c, a, d; x) \\ &\quad + H(b, c, d, a; x), \end{aligned} \quad (\text{F.12})$$

$$\begin{aligned} H(a, b; x)H(c, d; x) &= H(a, b, c, d; x) + H(a, c, b, d; x) + H(a, c, d, b; x) \\ &\quad + H(c, a, b, d; x) + H(c, a, d, b; x) + H(c, d, a, b; x), \end{aligned} \quad (\text{F.13})$$

where a, b, c, d are indices taking any of the values $(1, 0, -1)$. The formulae can be easily verified, one at a time, by observing that they are true at some specific point (such as $x = 0$, where all the HPLs vanish except in the otherwise trivial case in which all the indices are equal to 0), then taking the x -derivatives of the two sides according to Equation (F.6) and checking that they are equal (using when needed the previously established lower-weight formulae).

Another class of identities is obtained by integrating (F.4) by parts. These IBP identities read:

$$\begin{aligned} H(m_1, \dots, m_q; x) &= H(m_1; x)H(m_2, \dots, m_q; x) - H(m_2, m_1; x)H(m_3, \dots, m_q; x) \\ &\quad + \dots + (-1)^{q+1}H(m_q, \dots, m_1; x). \end{aligned} \quad (\text{F.14})$$

These identities are not fully linearly independent from the product identities.

A numerical implementation of the HPLs up to weight $w = 4$ is available [104].

F.2 Two-Dimensional Harmonic Polylogarithms

The 2dHPLs family is obtained by the repeated integration, in the variable y , of rational factors chosen, in any order, from the set $1/y$, $1/(y - 1)$, $1/(y + z - 1)$,

$1/(y+z)$, where z is another independent variable (hence the ‘two-dimensional’ in the name). In full generality, let us define the rational factor as

$$g(a; y) = \frac{1}{y-a}, \quad (\text{F.15})$$

where a is the *index*, which can depend on z , $a = a(z)$; the rational factors which we consider for the 2dHPLs are then

$$\begin{aligned} g(0; y) &= \frac{1}{y}, \\ g(1; y) &= \frac{1}{y-1}, \\ g(1-z; y) &= \frac{1}{y+z-1}, \\ g(-z; y) &= \frac{1}{y+z}. \end{aligned} \quad (\text{F.16})$$

With the above definitions the index takes one of the values $0, 1, (1-z)$ and $(-z)$.

Correspondingly, the 2dHPLs at weight $w = 1$ (i.e. depending, besides the variable y , on a single further argument, or *index*) are defined to be

$$\begin{aligned} G(0; y) &= \ln y, \\ G(1; y) &= \ln(1-y), \\ G(1-z; y) &= \ln \left(1 - \frac{y}{1-z} \right), \\ G(-z; y) &= \ln \left(1 + \frac{y}{z} \right). \end{aligned} \quad (\text{F.17})$$

The 2dHPLs of weight w larger than 1 depend on a set of w indices, which can be grouped into a w -dimensional *vector* of indices \vec{a} . By writing the vector as $\vec{a} = (a, \vec{b})$, where a is the leftmost component of \vec{a} and \vec{b} stands for the vector of the remaining $(w-1)$ components, the 2dHPLs are then defined as follows: if all the w components

of \vec{a} take the value 0, \vec{a} is written as $\vec{0}_w$ and

$$G(\vec{0}_w; y) = \frac{1}{w!} \ln^w y, \quad (\text{F.18})$$

while, if $\vec{a} \neq \vec{0}_w$,

$$G(\vec{a}; y) = \int_0^y dy' g(a; y') G(\vec{b}; y'). \quad (\text{F.19})$$

In any case the derivatives can be written in the compact form

$$\frac{d}{dy} G(\vec{a}; y) = g(a; y) G(\vec{b}; y), \quad (\text{F.20})$$

where, again, a is the leftmost component of \vec{a} and \vec{b} stands for the remaining $(w-1)$ components.

It should be noted that the notation for the 2dHPLs employed here is the notation of [105], which is different from the original definition proposed in [47, 48]. Detailed conversion rules between different notations, as well as relations to similar functions in the mathematical literature (hyperlogarithms and multiple polylogarithms) can be found in the appendix of [105].

Algebra and reduction equations of the 2dHPLs are the same as for the ordinary HPLs. The product of two 2dHPLs of a same argument y and weights p, q can be expressed as a combination of 2dHPLs of that argument and weight $r = p + q$, according to the product identity

$$G(\vec{p}; x) G(\vec{q}; x) = \sum_{\vec{r} = \vec{p} \uplus \vec{q}} G(\vec{r}; x), \quad (\text{F.21})$$

where \vec{p} and \vec{q} stand for the p and q components of the indices of the two 2dHPLs, while $\vec{p} \uplus \vec{q}$ represents all possible mergers of \vec{p} and \vec{q} into the vector \vec{r} with r components, in which the relative orders of the elements of \vec{p} and \vec{q} are preserved. The explicit product identities up to weight $w = 4$ are identical to those for the

HPLs (F.10)–(F.13), with all H replaced by G.

The IBP identities read:

$$\begin{aligned} G(m_1, \dots, m_q; x) = & G(m_1; x)G(m_2, \dots, m_q; x) - G(m_2, m_1; x)G(m_3, \dots, m_q; x) \\ & + \dots + (-1)^{q+1}G(m_q, \dots, m_1; x). \quad (\text{F.22}) \end{aligned}$$

A numerical implementation of the 2dHPLs up to weight $w = 4$ is available [105].

APPENDIX G

Weyl–van der Waerden Spinor Calculus

The basic quantity is the two-spinor ψ_A or ψ^A and its complex conjugate $\psi_{\dot{A}}$ or $\psi^{\dot{A}}$. Raising and lowering of indices is done with the antisymmetric tensor ε ,

$$\varepsilon_{AB} = \varepsilon^{AB} = \varepsilon_{\dot{A}\dot{B}} = \varepsilon^{\dot{A}\dot{B}} = \begin{pmatrix} 0 & 1 \\ -1 & 0 \end{pmatrix}. \quad (\text{G.1})$$

We define an antisymmetric spinorial “inner product”:

$$\langle \psi_1 \psi_2 \rangle = \psi_{1A} \varepsilon^{BA} \psi_{2B} = \psi_{1A} \psi_2^A = -\psi_1^A \psi_{2A} = -\langle \psi_2 \psi_1 \rangle, \quad (\text{G.2})$$

and

$$\langle \psi_1 \psi_2 \rangle^* = \psi_{1\dot{A}} \psi_2^{\dot{A}}. \quad (\text{G.3})$$

Any momentum vector k_μ gets a bispinor representation by contraction with σ^μ :

$$k_{\dot{A}B} = \sigma_{\dot{A}B}^\mu k_\mu = \begin{pmatrix} k_0 + k_3 & k_1 + ik_2 \\ k_1 - ik_2 & k_0 - k_3 \end{pmatrix}, \quad (\text{G.4})$$

where σ^0 is the unit matrix and σ_i are the Pauli matrices. Since

$$\sigma_{\dot{A}B}^{\mu} \sigma^{\nu \dot{A}B} = 2g^{\mu\nu}, \quad (\text{G.5})$$

we have

$$k_{\dot{A}B} p^{\dot{A}B} = 2k \cdot p. \quad (\text{G.6})$$

For light-like vectors one can show that

$$k_{\dot{A}B} = k_{\dot{A}} k_B, \quad (\text{G.7})$$

where

$$k_A = \begin{pmatrix} (k_1 - ik_2)/\sqrt{k_0 - k_3} \\ \sqrt{k_0 - k_3} \end{pmatrix}, \quad (\text{G.8})$$

so that for light-like vectors we have

$$2k \cdot p = \langle kp \rangle \langle kp \rangle^* = |\langle kp \rangle|^2. \quad (\text{G.9})$$

The following relation is often useful:

$$\sigma_{\dot{A}B}^{\mu} \sigma_{\mu}^{\dot{C}D} = 2\delta_{\dot{A}}^{\dot{C}} \delta_B^D. \quad (\text{G.10})$$

For massless spin- $\frac{1}{2}$ particles the four-spinors can be expressed in two-spinors as follows:

$$\begin{aligned} u_+(p) &= v_-(p) = \begin{pmatrix} p_B \\ 0 \end{pmatrix}, \\ u_-(p) &= v_+(p) = \begin{pmatrix} 0 \\ p^{\dot{B}} \end{pmatrix}, \end{aligned}$$

$$\begin{aligned}\bar{u}_+(q) &= \bar{v}_-(q) = \begin{pmatrix} 0, & -iq_{\dot{A}} \end{pmatrix}, \\ \bar{u}_-(q) &= \bar{v}_+(q) = \begin{pmatrix} iq^A, & 0 \end{pmatrix}.\end{aligned}\tag{G.11}$$

The Dirac γ matrices now become

$$\gamma^\mu = \begin{pmatrix} 0 & -i\sigma_{\dot{B}A}^\mu \\ i\sigma^{\mu\dot{A}B} & 0 \end{pmatrix},\tag{G.12}$$

so that, for example:

$$\bar{u}_+(q)\gamma^\mu v_-(p) = q_{\dot{A}}\sigma^{\mu\dot{A}B}p_B.\tag{G.13}$$

The general electroweak vertex for vector boson V coupling to two fermions is denoted by $ie\delta_{ij}\Gamma_\mu^{Vf_1f_2}$, where i and j are the colour labels associated with the fermions f_1 and f_2 respectively. The vertex contains left- and right-handed couplings,

$$\Gamma_\mu^{V,f_1f_2} = L_{f_1f_2}^V \gamma_\mu \left(\frac{1-\gamma_5}{2} \right) + R_{f_1f_2}^V \gamma_\mu \left(\frac{1+\gamma_5}{2} \right),\tag{G.14}$$

where for a photon,

$$L_{f_1f_2}^\gamma = R_{f_1f_2}^\gamma = -e_{f_1}\delta_{f_1f_2},\tag{G.15}$$

and for a Z -boson,

$$L_{f_1f_2}^Z = \frac{I_3^{f_1} - \sin^2\theta_W e_{f_1}}{\sin\theta_W \cos\theta_W} \delta_{f_1f_2}, \quad R_{f_1f_2}^Z = \frac{-\sin\theta_W e_{f_1}}{\cos\theta_W} \delta_{f_1f_2}.\tag{G.16}$$

Here, e_f represents the fractional electric charge, I_3^f the weak isospin and θ_W the weak mixing angle. In the Weyl-van der Waerden notation, the vertex Γ_μ^{V,f_1f_2} becomes,

$$\Gamma_\mu^{V,f_1f_2} = \begin{pmatrix} 0 & -iL_{f_1f_2}^V \sigma_{\mu\dot{B}A} \\ iR_{f_1f_2}^V \sigma_\mu^{\dot{A}B} & 0 \end{pmatrix}.\tag{G.17}$$

For the polarisation vectors of outgoing gluons and photons we use the spinorial

quantities

$$e_{\dot{A}B}^+(k) = \sqrt{2} \frac{k_A b_B}{\langle bk \rangle}, \quad (\text{G.18})$$

$$e_{\dot{A}B}^-(k) = \sqrt{2} \frac{b_A k_B}{\langle bk \rangle^*}. \quad (\text{G.19})$$

The gauge spinor b is arbitrary and can be chosen differently in each gauge-invariant expression. A suitable choice can often simplify the calculation.

Bibliography

- [1] M. E. Peskin and D. V. Schroeder, *An Introduction to Quantum Field Theory* (Addison–Wesley, 1995).
- [2] R. K. Ellis, W. J. Stirling, and B. R. Webber, *QCD and Collider Physics* (Cambridge University Press, 1996).
- [3] T. Muta, *Foundations of Quantum Chromodynamics* (World Scientific, 2000).
- [4] A. D. Martin and F. Halzen, *Quarks and Leptons: An Introductory Course in Modern Particle Physics* (Wiley, 1984).
- [5] L. H. Ryder, *Quantum Field Theory* (Cambridge University Press, 1996).
- [6] C. Itzyson and J. Zuber, *Quantum Field Theory* (McGraw–Hill, 1980).
- [7] Particle Data Group, K. Hagiwara *et al.*, Phys. Rev. **D66**, 010001 (2002).
- [8] M. Gell-Mann, Phys. Lett. **8**, 214 (1964).
- [9] G. Zweig, Preprint CERN-8182, 401, 1964.
- [10] M. Gell-Mann, Acta Phys. Austriaca Suppl. **9**, 733 (1972).
- [11] J. Siegrist *et al.*, Phys. Rev. **D26**, 969 (1982).
- [12] DASP, R. Brandelik *et al.*, Phys. Lett. **B76**, 361 (1978).
- [13] PLUTO, J. Burmester *et al.*, Phys. Lett. **B66**, 395 (1977).

- [14] T. Kinoshita, J. Math. Phys. **3**, 650 (1962).
- [15] T. D. Lee and M. Nauenberg, Phys. Rev. **133**, B1549 (1964).
- [16] F. Bloch and A. Nordsieck, Phys. Rev. **52**, 54 (1937).
- [17] G. 't Hooft and M. J. G. Veltman, Nucl. Phys. **B44**, 189 (1972).
- [18] C. G. Bollini and J. J. Giambiagi, Nuovo Cim. **B12**, 20 (1972).
- [19] G. M. Cicuta and E. Montaldi, Nuovo Cim. Lett. **4**, 329 (1972).
- [20] D. P. Barber *et al.*, Phys. Rev. Lett. **43**, 830 (1979).
- [21] J. R. Ellis, M. K. Gaillard, and G. G. Ross, Nucl. Phys. **B111**, 253 (1976).
- [22] S. Bethke, J. Phys. **G26**, R27 (2000), hep-ex/0004021.
- [23] R. K. Ellis, D. A. Ross, and A. E. Terrano, Nucl. Phys. **B178**, 421 (1981).
- [24] K. Fabricius, I. Schmitt, G. Kramer, and G. Schierholz, Zeit. Phys. **C11**, 315 (1981).
- [25] W. T. Giele and E. W. N. Glover, Phys. Rev. **D46**, 1980 (1992).
- [26] S. Catani and M. H. Seymour, Nucl. Phys. **B485**, 291 (1997), hep-ph/9605323.
- [27] ECFA/DESY LC Physics Working Group, J. A. Aguilar-Saavedra *et al.*, (2001), hep-ph/0106315.
- [28] Z. Kunst, Proceedings of the workshop on “New techniques for calculating higher order qcd corrections”, in *ETH-TH/93-01*, Zürich, 1992.
- [29] S. Catani, Phys. Lett. **B427**, 161 (1998), hep-ph/9802439.
- [30] Z. Bern, L. J. Dixon, and A. Ghinculov, Phys. Rev. **D63**, 053007 (2001), hep-ph/0010075.

- [31] C. Anastasiou, E. W. N. Glover, C. Oleari, and M. E. Tejeda-Yeomans, Nucl. Phys. **B601**, 318 (2001), hep-ph/0010212.
- [32] C. Anastasiou, E. W. N. Glover, C. Oleari, and M. E. Tejeda-Yeomans, Nucl. Phys. **B601**, 341 (2001), hep-ph/0011094.
- [33] C. Anastasiou, E. W. N. Glover, C. Oleari, and M. E. Tejeda-Yeomans, Nucl. Phys. **B605**, 486 (2001), hep-ph/0101304.
- [34] E. W. N. Glover, C. Oleari, and M. E. Tejeda-Yeomans, Nucl. Phys. **B605**, 467 (2001), hep-ph/0102201.
- [35] Z. Bern, A. De Freitas, and L. J. Dixon, JHEP **09**, 037 (2001), hep-ph/0109078.
- [36] Z. Bern, A. De Freitas, L. J. Dixon, A. Ghinculov, and H. L. Wong, JHEP **11**, 031 (2001), hep-ph/0109079.
- [37] F. V. Tkachov, Phys. Lett. **B100**, 65 (1981).
- [38] K. G. Chetyrkin and F. V. Tkachov, Nucl. Phys. **B192**, 159 (1981).
- [39] S. Laporta, Int. J. Mod. Phys. **A15**, 5087 (2000), hep-ph/0102033.
- [40] V. A. Smirnov, Phys. Lett. **B460**, 397 (1999), hep-ph/9905323.
- [41] J. B. Tausk, Phys. Lett. **B469**, 225 (1999), hep-ph/9909506.
- [42] V. A. Smirnov and O. L. Veretin, Nucl. Phys. **B566**, 469 (2000), hep-ph/9907385.
- [43] C. Anastasiou, E. W. N. Glover, and C. Oleari, Nucl. Phys. **B572**, 307 (2000), hep-ph/9907494.
- [44] C. Anastasiou, E. W. N. Glover, and C. Oleari, Nucl. Phys. **B565**, 445 (2000), hep-ph/9907523.

- [45] T. Gehrmann and E. Remiddi, Nucl. Phys. **B580**, 485 (2000), hep-ph/9912329.
- [46] T. Gehrmann and E. Remiddi, Nucl. Phys. Proc. Suppl. **89**, 251 (2000), hep-ph/0005232.
- [47] T. Gehrmann and E. Remiddi, Nucl. Phys. **B601**, 248 (2001), hep-ph/0008287.
- [48] T. Gehrmann and E. Remiddi, Nucl. Phys. **B601**, 287 (2001), hep-ph/0101124.
- [49] K. Hagiwara and D. Zeppenfeld, Nucl. Phys. **B313**, 560 (1989).
- [50] F. A. Berends, W. T. Giele, and H. Kuijf, Nucl. Phys. **B321**, 39 (1989).
- [51] N. K. Falck, D. Graudenz, and G. Kramer, Nucl. Phys. **B328**, 317 (1989).
- [52] Z. Bern, L. J. Dixon, D. A. Kosower, and S. Weinzierl, Nucl. Phys. **B489**, 3 (1997), hep-ph/9610370.
- [53] Z. Bern, L. J. Dixon, and D. A. Kosower, Nucl. Phys. **B513**, 3 (1998), hep-ph/9708239.
- [54] E. W. N. Glover and D. J. Miller, Phys. Lett. **B396**, 257 (1997), hep-ph/9609474.
- [55] J. M. Campbell, E. W. N. Glover, and D. J. Miller, Phys. Lett. **B409**, 503 (1997), hep-ph/9706297.
- [56] L. W. Garland, T. Gehrmann, E. W. N. Glover, A. Koukoutsakis, and E. Remiddi, Nucl. Phys. **B627**, 107 (2002), hep-ph/0112081.
- [57] V. N. Baier, E. A. Kurayev, and V. S. Fadin, Sov. J. Phys. **31**, 364 (1980).
- [58] J. J. van der Bij and E. W. N. Glover, Nucl. Phys. **B313**, 237 (1989).

- [59] R. J. Gonsalves, Phys. Rev. **D28**, 1542 (1983).
- [60] G. Kramer and B. Lampe, Z. Phys. **C34**, 497 (1987).
- [61] T. Matsuura and W. L. van Neerven, Z. Phys. **C38**, 623 (1988).
- [62] T. Matsuura, S. C. van der Marck, and W. L. van Neerven, Nucl. Phys. **B319**, 570 (1989).
- [63] P. Nogueira, J. Comput. Phys. **105**, 279 (1993).
- [64] J. A. M. Vermaseren, Symbolic manipulation with form, Version 2, 1991.
- [65] J. A. M. Vermaseren, New features of form, math-ph/0010025.
- [66] G. Passarino and M. J. G. Veltman, Nucl. Phys. **B160**, 151 (1979).
- [67] Waterloo Maple Inc, *Maple 7*, 2001.
- [68] L. W. Garland, T. Gehrmann, E. W. N. Glover, A. Koukoutsakis, and E. Remiddi, Nucl. Phys. **B642**, 227 (2002), hep-ph/0206067.
- [69] P. N. Burrows and P. Osland, Phys. Lett. **B400**, 385 (1997), hep-ph/9701424.
- [70] T. Binoth, E. W. N. Glover, P. Marquard, and J. J. van der Bij, JHEP **05**, 060 (2002), hep-ph/0202266.
- [71] Z. Bern, L. J. Dixon, and D. A. Kosower, JHEP **01**, 027 (2000), hep-ph/0001001.
- [72] Z. Bern, A. De Freitas, and L. Dixon, JHEP **03**, 018 (2002), hep-ph/0201161.
- [73] C. Anastasiou, T. Gehrmann, C. Oleari, E. Remiddi, and J. B. Tausk, Nucl. Phys. **B580**, 577 (2000), hep-ph/0003261.
- [74] C. Anastasiou, J. B. Tausk, and M. E. Tejeda-Yeomans, Nucl. Phys. Proc. Suppl. **89**, 262 (2000), hep-ph/0005328.

- [75] C. Anastasiou, E. W. N. Glover, and M. E. Tejeda-Yeomans, Nucl. Phys. **B629**, 255 (2002), hep-ph/0201274.
- [76] H. Weyl, *Gruppentheorie und Quantenmechanik* (Leipzig, 1928).
- [77] B. L. van der Waerden, Göttinger Nachrichten, 1929.
- [78] F. A. Berends and W. Giele, Nucl. Phys. **B294**, 700 (1987).
- [79] B. A. Kniehl and J. H. Kuhn, Phys. Lett. **B224**, 229 (1989).
- [80] A. Signer and L. J. Dixon, Phys. Rev. Lett. **78**, 811 (1997), hep-ph/9609460.
- [81] L. J. Dixon and A. Signer, Phys. Rev. **D56**, 4031 (1997), hep-ph/9706285.
- [82] Z. Bern, L. J. Dixon, D. C. Dunbar, and D. A. Kosower, Nucl. Phys. **B425**, 217 (1994), hep-ph/9403226.
- [83] D. A. Kosower, Nucl. Phys. **B552**, 319 (1999), hep-ph/9901201.
- [84] D. A. Kosower and P. Uwer, Nucl. Phys. **B563**, 477 (1999), hep-ph/9903515.
- [85] Z. Bern, V. Del Duca, and C. R. Schmidt, Phys. Lett. **B445**, 168 (1998), hep-ph/9810409.
- [86] Z. Bern, V. Del Duca, W. B. Kilgore, and C. R. Schmidt, Phys. Rev. **D60**, 116001 (1999), hep-ph/9903516.
- [87] S. Catani and M. Grazzini, Nucl. Phys. **B591**, 435 (2000), hep-ph/0007142.
- [88] J. M. Campbell and E. W. N. Glover, Nucl. Phys. **B527**, 264 (1998), hep-ph/9710255.
- [89] S. Catani and M. Grazzini, Phys. Lett. **B446**, 143 (1999), hep-ph/9810389.
- [90] S. Catani and M. Grazzini, Nucl. Phys. **B570**, 287 (2000), hep-ph/9908523.

- [91] F. A. Berends and W. T. Giele, Nucl. Phys. **B313**, 595 (1989).
- [92] S. Catani, in [?].
- [93] A. Gehrmann-De Ridder, T. Gehrmann, and E. W. N. Glover, Phys. Lett. **B414**, 354 (1997), hep-ph/9705305.
- [94] A. Gehrmann-De Ridder and E. W. N. Glover, Nucl. Phys. **B517**, 269 (1998), hep-ph/9707224.
- [95] Z. Nagy and Z. Trocsanyi, Phys. Rev. Lett. **79**, 3604 (1997), hep-ph/9707309.
- [96] J. M. Campbell, M. A. Cullen, and E. W. N. Glover, Eur. Phys. J. **C9**, 245 (1999), hep-ph/9809429.
- [97] S. Weinzierl and D. A. Kosower, Phys. Rev. **D60**, 054028 (1999), hep-ph/9901277.
- [98] T. Gehrmann and E. Remiddi, Nucl. Phys. **B640**, 379 (2002), hep-ph/0207020.
- [99] S. Moch, P. Uwer, and S. Weinzierl, J. Math. Phys. **43**, 3363 (2002), hep-ph/0110083.
- [100] S. Weinzierl, Comput. Phys. Commun. **145**, 357 (2002), math-ph/0201011.
- [101] S. Moch, P. Uwer, and S. Weinzierl, Phys. Rev. **D66**, 114001 (2002), hep-ph/0207043.
- [102] N. Nielsen, Nova Acta Leopoldina (Halle) **90**, 123 (1909).
- [103] E. Remiddi and J. A. M. Vermaseren, Int. J. Mod. Phys. **A15**, 725 (2000), hep-ph/9905237.
- [104] T. Gehrmann and E. Remiddi, Comput. Phys. Commun. **141**, 296 (2001), hep-ph/0107173.

BIBLIOGRAPHY

- [105] T. Gehrmann and E. Remiddi, *Comput. Phys. Commun.* **144**, 200 (2002), hep-ph/0111255.

